DEPARTMENT OF THE NAVY

HYDROMECHANICS

AERODYNAMICS

STRUCTURAL MECHANICS

APPLIED MATHEMATICS

ACOUSTICS AND VIBRATION

RUDDER-HULL VIBRATION AND FLUTTER ANALYSIS OF A HIGH-SPEED SHIP (PGM MOTOR GUNBOAT)

by

Ralph C. Leibowitz

Distribution of this Document is Unlimited

ACOUSTICS AND VIBRATION LABORATORY
RESEARCH AND DEVELOPMENT REPORT

October 1965

Report 1993

RUDDER-HULL VIBRATION AND FLUTTER ANALYSIS OF A HIGH-SPEED SHIP (PGM MOTOR GUNBOAT)

by

Ralph C. Leibowitz

October 1965

Report 1993

TABLE OF CONTENTS

Page

Page

LIST OF FIGURES

LIST OF TABLES

NOTATION

Symbol	Definition	Units
A	Area of rudder plan	ft^2
A_o, A_n	Amplitude of response	
AR	Aspect ratio (2 x rudder span squared divided by rudder area)	
a	Scale factor (impedance)	$ft^{\frac{1}{2}}$ (lb-sec-ohm)$^{-\frac{1}{2}}$
b,B	Dimensions of trapezoidal rudder (see Appendixes C and D and Figures 91 and 92)	ft
C	Dimension of trapezoidal rudder (see Figures 91, 92)	ft
C	Damping	lb-ft^{-1}-sec
C_c	Critical value of damping	lb-ft^{-1}-sec
$C_{L\gamma}$	Slope of lift coefficient for rigid rudder	
$C_{L\dot{\gamma}}$	Slope of coefficient of "unlagged" lift term for rigid rudder	
	Slope of moment coefficients for rigid rudder:	
$C_{M\alpha\dot{\alpha}}$	Roll moment due to roll velocity	
$C_{M\alpha\dot{\gamma}}$	Roll moment due to yaw velocity	
$C_{M\gamma\dot{\alpha}}$	Yaw moment due to roll velocity	
$C_{M\gamma\dot{\gamma}}$	Yaw moment due to yaw velocity	
c	Chord of rudder (function of spanwise location)	ft

Symbol	Definition	Units
$\bar{c}$	Geometric mean chord of rudder given by dividing rudder area by rudder span	ft
$c_{L\gamma}$, $c_{L\dot{\gamma}}$ $c_{M\gamma\dot{\gamma}}$	Same as $C_{L\gamma}$, $C_{L\dot{\gamma}}$, $C_{M\gamma\dot{\gamma}}$, except C's are for entire rigid rudder , and c's are for an incremental strip at a particular spanwise location. Thus, $c_{L\gamma}$, $c_{L\dot{\gamma}}$, $c_{M\gamma\dot{\gamma}}$ may be functions of z	
D	Dimension of a trapezoidal rudder (see Appendixes C and D and Figures 91 and 92)	ft
D_f	Coefficient of lateral viscous damping force	lb-sec-ft
D_m	Coefficient of yaw viscous damping moment	lb-sec-ft
E	Modulus of elasticity	$lb\text{-}ft^{-2}$
F_x , F_y or F_v , F_z	Force acting in x, y, z directions	lb
G	Shear modulus of elasticity	$lb\text{-}ft^{-2}$
I	Area moment of inertia	ft^4
I	Mass moment of inertia	$lb\text{-}sec^2\text{-}ft$
J	Area polar moment of inertia	ft^4
j	$\sqrt{-1}$	
k	Dimensionless frequency parameter, $\frac{\omega c}{2V}$	
$\bar{k}$	Dimensionless frequency parameter, $\frac{\omega \bar{c}}{2V}$	

Symbol	Definition	Units
M	Mass (see Table 1)	$lb\text{-}sec^2\text{-}ft^{-1}$
$M_\alpha, M_\beta, M_\gamma$	Moment acting about x,y,z, axes; M_γ is also generalized to allow its axis to be elsewhere than on the z-axis (see Appendix B)	lb-ft
N	Scale factor (time)	
P_{xz}	Product of inertia (see Tables 1 and 2)	$lb\text{-}sec^2\text{-}ft$
P_α, P_γ	Scale factor (distance) (see Appendix G)	ft
p	Differential operator, $\frac{d}{dt}$	sec^{-1}
T	Taper ratio (tip chord divided by root chord)	
t	Time	sec
u,v,w	Displacements in x,y,z directions	ft
V	Ship's forward speed relative to the fluid	$ft\text{-}sec^{-1}$
V_o	Reference value of V	$100\ ft\text{-}sec^{-1}$
$v_1, \bar{v}_1$	Lateral displacement of a rudder strip at $x = x_1$ and of the rudder strip at point $\bar{x}_1, z_o$, respectively	ft
x,y,z	Coordinate axes (see Figure 1)	ft
x_o	x-location of center of pressure on a chordwise strip of the rudder when $\dot{\alpha} = \dot{\gamma} = 0$. x_o is a function of z.	ft
$\bar{x}_o$	x-location of center of pressure on rigid rudder when $\dot{\alpha} = \dot{\gamma} = 0$	ft

Symbol	Definition	Units
x_1	Assumed x-location of rotation center of a chordwise strip of the rudder perhaps varying with z.	ft
$\bar{x}_1$	$=\int \frac{x_1 c_{L\gamma} c\, dz}{A C_{L\gamma}}$	ft
x_m	x-location of midchord	ft
x_r	x-location on a strip of the axis about which the moment is measured	ft
Δx_t	Length of tiller	ft
y_R	Dimension of rudder support (see Figure 3)	ft
z_b, z_{b1}, z_{b2}, z_e, z_p, z_R, z_t	Dimensions of rudder support (see Figure 3)	ft
z_o	z-location of center of pressure on rigid rudder when $\dot{\alpha} = \dot{\gamma} = 0$	ft
z_1	z-location of rotation center of rigid rudder	ft
α, β, γ	Rotational displacements about x, y, z, axes	rad
ζ	Per unit critical damping; the damping ratio, for a single degree of freedom system is $\zeta = \frac{C}{C_c}$ (see Section V.B. and Appendixes E and F)	
ζ, η, ξ	Normalizing constants	
λ	Angle of sweepback of the 1/4 chord	deg
ρ	Density of water	$lb\text{-}sec^2\text{-}ft^{-4}$

Symbol	Definition	Units
ω	Radian frequency of oscillation	$rad\text{-}sec^{-1}$
ν	Poisson's ratio	
	Subscript numbers refer to points at which forces act, or about which moments act, or at which displacements are measured.	
0	Center of pressure	
1	Rotation center	
2	Arbitrary reference axis (sometimes taken at the "rudder origin"- Intersection of rudder stock center line and rudder root chord)	
3	Center of area of rudder	
4	Intersection of node lines of first two rudder modes (three-degree-of-freedom model)	
e	Electrical (the analog system)	
m	Center of mass	
m	Midchord	
m	Mechanical (the physical system)	
r	Axis about which rotation is measured	

ABSTRACT

This report presents the results of a "flutter" analysis for a PGM Motor Gunboat. The results were obtained both by computing the rudder-hull vibrations (including flutter) on an analog computer and by numerical analysis. The analogs are based upon extensions of previously derived theories and methods for representing the vibrating system excited by hydrodynamic forces and for evaluating the rudder-hull structural and hydroelastic parameters and hydrodynamic parameters referenced in this report.

The results indicate that (assuming a minimum conceivable value of damping) for the PGM rudder-hull system, control-surface flutter will occur at approximately 90 knots. Moreover, the flutter characteristics of the entire rudder-hull system are more complex than classical flutter of simpler systems involving two vibration modes; hence conclusions concerning the classical or binary flutter of a two- or three-degree-of-freedom rudder do *not* apply to the entire rudder-hull combination.

ADMINISTRATIVE INFORMATION

The flutter analysis performed for a PGM Motor Gunboat was authorized by Bureau of Ships ltr PGM/9400 ser 442/235 of 4 January 1963.

I. INTRODUCTION

At the request of the Bureau of Ships, a flutter analysis has been performed for the rudders flexibly attached to the hull of a high-speed ship, the PGM Motor Gunboat. The analysis is intended to anticipate possible undesirable vibration characteristics (e.g., subcritical flutter) or classical flutter* for the control surfaces. The need for this undertaking is substantiated by recent evidence which indicates that with an increase in ship speeds, hydroelastic interactions will produce classical control surface and subcritical flutter within the operating speed range. This evidence is

1. The transmission of severe vibrations to the hull of USS FORREST SHERMAN (DD 931) by the rudders during a steady horizontal turn.[1,2]**

2. The occurrence of classical flutter for two different types of models tested in the TMB towing basin.[3,4,5]

The general objective of this investigation is to determine, within the limitations of current hydrodynamic theory, the speed range within which flutter may be expected to occur. If this speed range were to fall below the maximum design speed of the ship, design changes to eliminate the difficulty would be required.† The structural, hydroelastic, and hydrodynamic properties entering the analysis are varied within

*Subcritical flutter is a condition of barely stable vibration due to marked reduction in the overall damping. Such a condition greatly magnifies the sensitivity of the mechanical system to external sources of vibration. Classical flutter is a dynamically unstable, self-excited vibration of an oscillatory system immersed in a field of flow.

**References are listed on page 191.

†Fortunately, evaluation of the results obtained for the PGM Motor Gunboat indicate that no such difficulty will arise.

reasonable limits to ensure that uncertainty with regard to the exact values of these parameters is properly accounted for in the final recommendations and also to provide insight into the mechanism of flutter.

The specific objectives of the study are:

1. To analyze the flutter characteristics of the rudder-hull combination for the PGM Motor Gunboat.

2. To conduct a simplified numerical analysis* for the purpose of comparing it to the analog computer solution and to explore the possibility of using simplified methods to make an adequate flutter analysis of rudder-hull systems.

3. To determine, by studies of the effects of parameter variations, which hydrodynamic parameters are significant and which are not in influencing the flutter characteristics of a flexibly attached rudder.

The theoretical basis for the computation, type of input data required, structural models used in representing the entire or partial system, and other pertinent computational data are outlined in Section II and are discussed in detail at appropriate places in the report.

The results of this computation, obtained by means of an electric-analog computer** and by numerical analysis, are the natural frequencies, mode shapes, critical flutter

*"Numerical analysis" here refers to manual calculations as well as to digital computer solutions for the *special case* of the rudder attached through a flexible structure to a *rigid* hull.

**A similar computation can also be made on a digital computer for the complete rudder-hull system; for the rudder system alone see footnote above.

speeds, and damping of the control surface-hull system and/or parts of the system as well as certain other data of interest.

In addition to achieving these objectives, the present report, together with a companion report,[6] illustrates in detail, by way of application to specific ships, the *procedure* for making a flutter computation for a control surface-hull system. Thus the designer is provided with a concrete guide not only for making similar computations on high-speed ships but also for extending or modifying the present procedure, if necessary.

II. THEORETICAL ANALYSIS OF THE PROBLEM AND METHOD OF ATTACK

The solutions for the normal modes and flutter of a combined rudder-hull system in forward motion and subject to hydrodynamic forces are chiefly based upon the analytical methods and theories of References 7 through 11.*

Each control surface of the PGM Motor Gunboat was treated as a rigid body attached through a flexible stock and supporting structure to a flexible hull, and small vibration theory was assumed to be applicable;** the validity of treating such control surfaces as rigid bodies was experimentally demonstrated in Reference 12. The procedure requires evaluation of the inertias, elastic constants, damping constants, hydroelastic parameters, and (four classes of) hydrodynamic forces acting on the system.

*The inertial-elastic representation and method for evaluating the physical parameters of the rudder-hull system (including the virtual mass), are covered by References 7 and 8. The method for determining the hydroelastic parameters for the rudder is described in References 9 and 10. The derivation of the hydrodynamic forces for two-dimensional incompressible flow (i.e., Classical Theodorsen Equations) on the rudder is given in Reference 11; extension of this theory to a rigid three-degree-of-freedom lifting surface is presented in the present report.

**The analysis of motions for the PGM Motor Gunboat is given in Appendix A.

The equations for the hydrodynamic forces are based upon an *extension to three dimensions* of two-dimensional incompressible flow theory (i.e., Classical Theodorsen Theory)—see Appendix B. This two-dimensional theory assumes an untapered rudder, no sweepback, zero thickness, zero Mach number, and infinite aspect ratio.* Two different types of spanwise distribution of the hydrodynamic forces on the rudder, which are represented by equivalent trapezoidal planforms, are treated; see Appendixes C and D. The hydrodynamic forces are functions of certain hydrodynamic parameters which are varied to determine the effect of the variation on flutter; these parameters are the slope of lift and moment coefficients, center of pressure, rotation center, Theodorsen lag function, virtual mass, and viscous damping due to water.

The study was undertaken for the following increasingly complex representations of the structure: (a) two-, three-, and six-degree-of-freedom models (rudder and supporting structure), (b) twenty-degree-of-freedom model (hull only), and (c) twenty-three-degree-of-freedom model (rudder, supporting structure, and hull). In general, the vibrations considered include coupled torsion-horizontal bending motions of the hull (represented as a beam) and antisymmetric rudder motions with respect to the plane of symmetry of the ship; see Appendix A.

*Equations given in Appendix B permit the determination of hydrodynamic parameters for a rigid rudder of arbitrary plan shape, assuming that the forces and moments acting on each strip of the rudder are determinable from the motion of that strip, based on two-dimensional, incompressible flow. However, to accommodate (or incorporate) known characteristics of finite-aspect-ratio lifting surfaces, certain parameters in the expressions for the forces and moments on the strips are permitted to vary with spanwise position (see Appendixes B, C, and D).

The actual solutions for the natural frequencies, mode shapes, critical flutter speeds, and modal damping of the PGM rudder-hull system and/or parts of the system were obtained by means of electrical analogs which represent the equations of motion of the combined or partial system. In addition, by numerical analysis, normal mode and flutter solutions were obtained for the two degree-of-freedom system and normal mode solutions were obtained for the three degree-of-freedom system; see Appendix E. Measurement of damping parameters of a flutter root is discussed in Appendix F.

The actual electrical analogs used for the solution of the PGM Motor Gunboat motions and certain details pertinent to their development are given in Appendix G.

III. DESCRIPTION OF RUDDER-HULL SYSTEM

Figures 1 and 2 represent the hull and rudder-hull systems, respectively, for the PGM Motor Gunboat, and the positive sign convention for locating points and describing their displacements from the equilibrium position. For this coordinate system, the hull and appendages (i.e., two rudders) are symmetric with respect to an x-z plane through the center of the ship and only antisymmetric motions of the hull and rudder about this plane are treated (see Appendix A). Hence, only v, α, and γ displacements corresponding to lateral, roll, and yaw motions, respectively, are considered here. Because of symmetry of the rudder-hull system, only the properties of the complete port rudder and of one-half the hull are represented (i.e., one-half the total hull mass and twice the total hull beam flexibility). This simplifies the analysis and reduces the required number of analog computer components.

The structural system has been modeled and analyzed in four different ways. The amount of structure considered, the mass of the portion represented and the flexibilities associated with it vary from one model to the other.* These models, now described, are designated:

(1) Three-degree-of-freedom model (rudder and supporting structure)

(2) Two-degree-of-freedom model (rudder and supporting structure)

(3) Six-degree-of-freedom model (rudder and supporting structure)

(4) Twenty-degree-of-freedom model (hull only)

(5) Twenty-three-degree-of-freedom model (rudder, supporting structure, and hull)

A. THREE-DEGREE-OF-FREEDOM MODEL (RUDDER AND SUPPORTING STRUCTURE)

The three-degree-of-freedom model refers to the permissive motions v, α, γ for a rudder assumed to be completely rigid. All motions out of the plane of the rudder are represented by v, α, γ and, therefore, they are the only significant motions from the viewpoint of hydrodynamic forces. The hull is assumed to be rigid except as noted below (see Section III.A.2)

1. Mass and Inertia Terms

Table 1A shows a tabulation of the mass and inertia terms for v, α, γ motions of the rudder structure, including the virtual mass and inertias due to adjacent water, which must accelerate laterally when the rudder does. The center of mass of the structural and virtual mass are also given in the table. The designation "rudder support

*The *basic case* alludes to reference values of data presented in several tables or in the text (e.g. see Appendix B) and is so designated there. For a particular model the effects of variations in data from values for the basic case are determined in this report.

structure" refers to those portions of the steering mechanism and the hull which carry and distribute the forces acting on the rudder, and the elasticity of which contributes to the effective flexibility of the rudder relative to the hull. Specifically included are the rudder stock and rudder bearings; the bearing carrier and rudder trunk; the tiller, connecting rod, ram, and hydraulic system of the steering mechanism; and portions of the bottom and platform of the hull structure adjacent to the rudder trunk and bearing carrier (see Figures 2 and 3). Table 1B gives an estimate of the masses of the rudder support structure alone. Table 2 summarizes the combined mass and inertias for this system and also gives the center of mass of the system.

2. Flexibilities

For the three-degree-of-freedom model, the hull is treated as rigid (except for local deformation of portions of the hull constituting the rudder supporting structure) and clamped. Hence, rudder motion is assumed to be due to the deformation of the rudder supporting structure and not due to any motion of the hull acting as a beam. Representation of the flexibilities for the rudder supporting structure is necessary in order to accurately describe the elastic forces which oppose displacements of the rudder caused by the hydrodynamic and inertia forces acting on the rudder.

Table 3A lists the elastic properties of the rudder supporting structure* in terms of the types of loads carried by the various parts of this structure and, therefore, the mechanism by which strain energy is introduced. Table 3B shows the lumped flexibilities used in representing the rudder supporting structure. The pertinent geometrical dimensions, with respect to the hull baseline, associated with the rudder support structure are given in Figure 3.

*For an alternative method of description of these properties, in terms of influence coefficients, see Section VIII.

B. TWO-DEGREE-OF-FREEDOM MODEL (RUDDER AND SUPPORTING STRUCTURE)

The two-degree-of-freedom model is identical in every respect to the three-degree-of-freedom model except that the lateral displacement of a particular coordinate is constrained to a value of zero. The node lines in Figures 4 and 5 represent the modes for the constrained basic and modified basic three-degree-of-freedom models. These figures show a Point 4 on the rigid rudder located at x_4, z_4 measured forward and upward from the rudder root chord reference point, for which the lateral displacement v_4 is zero. (Actually, this point is geometrically not on the rudder, but a rigid extension of the rudder was imagined on which to locate Point 4. The basis for the selection of Point 4 is described in Section VIII.)

C. SIX-DEGREE-OF-FREEDOM MODEL (RUDDER AND SUPPORTING STRUCTURE)

The six-degree-of-freedom model is identical in every respect to the three-degree-of-freedom model except that three additional lumped masses, representing the distribution of the supporting structure, are located at points in the rudder supporting structure. Table 2 (column 3) shows the location and magnitudes of these masses, and Table 1B indicates the components contributing to each lumped mass.

D. TWENTY-DEGREE-OF-FREEDOM MODEL (HULL ONLY)

The twenty-degree-of-freedom model describes the inertial-elastic parameters of the hull (excluding the rudder and rudder support structure) represented as a free-free, continuous, nonuniform *ten-section beam* capable of simultaneously bending in the horizontal plane and twisting about a longitudinal axis; thus, coupled torsion-horizontal bending of the beam is permissible. The elastic axis is taken to be

at the centerline of the hull. The twenty degrees of freedom of the hull are represented by specifying the lateral motions of the hull elastic axis at ten stations (1, 3, 5 .....19), and the roll displacement of the hull at the same ten stations, Station 0 being at the bow and Station 20 at the stern.

Table 4 presents the magnitude of the lumped masses and lumped roll inertia elements, located at the 20 stations, which represent mass and inertial properties of the hull; the location of the center of mass at each station above or below the neutral axis, ship and section length, and rudder stock location are also given in this table. Table 4, column 3, shows that the mass coupling effect (first moment of mass with respect to the neutral axis) was relatively small, hence the entire effect was represented by coupling at only five stations: 5, 9, 11, 13, and 17. The analog representation for this effect is discussed in Appendix G.

Figure 6B and Table 5 show the distributed and corresponding lumped elastic parameters (I,J) of the hull, respectively, represented as a beam.* Determination of the side bending and torsional polar moments of inertia (I,J) is required at several hull cross sections (Figure 6B) to reduce the structural characteristics of the hull to equivalent elastic parameters of the beam (Table 5).** The general formula used to calculate

*In Figure 6B, $\bar{z}$, the height of the neutral axis of the bending material of the hull, measured above the baseline does not vary more than 1 ft over the aft 80 percent of the ship. Hence, it was deemed reasonable to apply beam theory and to assume that the neutral axis had a height of 8 ft above the baseline.

**Shear flexibility of the hull was *not* represented in the analysis; only bending and torsion flexibility of the hull was represented. If the hull were represented as flexible in shear, with the lumped properties derived from the actual cross section properties, there would be a tendency for the hull vibration modes to occur at somewhat lower frequencies (Reference 8). This effect on the general conclusions drawn in this report would, however, be negligible.

the lumped bending and twisting flexibilities from the I and J curves of Figure 6B are

$$\text{Flexibility} = \int \frac{dx}{EI \text{ or } GJ}$$

where EI or GJ are expressed as functions of x, longitudinal location, and the integration is carried out over a lumping interval of the beam. The computation of the lumped bending and twisting flexibilities for the hull given in Table 5 have been simplified by assuming EI and GJ to be linear with respect to x over a Δx section, but still adequately approximating the I, J curves of Figure 6B (multiplied by E and G, respectively).

E. TWENTY-THREE-DEGREE-OF-FREEDOM MODEL (RUDDER, SUPPORTING STRUCTURE, AND HULL)

The twenty-three-degree-of-freedom model is devised by attaching the rudder and supporting structure (three degrees of freedom) model to the beam (twenty degrees of freedom) model of the hull. The hull beam is free at both ends, and at any point may undergo roll (α), lateral (v), and yaw (γ) displacements. Hence, the rudder displacement is partially due to the displacement of the hull and partially due to the elastic deformation of the rudder supporting structure. The hydrodynamic forces described in Section IV act on the rudder in an identical manner in this model.

IV. HYDRODYNAMIC FORCES

The following four classes of hydrodynamic forces are represented in the analysis of all models (the form of representation is the same, but the values for the hydrodynamic parameters given below may vary in different instances):

1. Hydrodynamic forces proportional to the second (time) derivative of lateral

displacements* of the ship and independent of the forward velocity of the ship. These forces being inertial in form account for the virtual or added mass (or inertia) effects. For the *rudder* these effects are assumed to consist of a mass term for the lateral motion coordinate v, an inertia term for the roll coordinate α, an inertia term for the yaw coordinate γ, and a product of inertia term coupling the α and γ coordinates. In addition, the lateral motion of the hull causes hydrodynamic forces to exist due to the virtual mass associated with the *hull*. This class will not be fully described here, but it is described in connection with the mass and inertial terms due to the rudder structure, ship structure, and ship load.

2. Hydrodynamic forces on the rudder only, proportional to the velocity of the ship, and (for the basic case) to the first derivative of lateral displacements* of the rudder; see Items 5, 8, and Equation B-1 in Appendix B. These forces, which are associated with the circulation and lift forces of the water acting on the rudder, are based on an *extension of incompressible-flow theory in two dimensions to a rigid three-degree-of-freedom lifting surface*, and are treated in Appendix B; the developments of Appendix B lead to integral equations which may be used for calculating lift- and moment-coefficient

*"Lateral displacements" here include v, α, γ displacements. In general, the forces are not proportional to the first derivatives of the lateral displacement because the lag function $C_t(\bar{k})$ often causes these quantities to differ in phase. However, when $C_t(k)$ is real or equal to unity (basic case), the statement made in the text holds; see Items 5 and 8 of Appendix B.

slopes* based on spanwise integration over the rudder of effects on local chordwise strips of the rudder. And, for two different examples of the spanwise distribution of hydrodynamic forces on trapezoidal rudders, these integrations are carried out in Appendixes C and D. Alternative sources and values of theoretical and experimental hydrodynamic data; geometric data for the rudder; values of the hydrodynamic parameters (lift and moment coefficients, center of pressure, center of rotation, center of area, damping constants) used in calculations; and the effect of lag functions for infinite and finite aspect ratio are also described in Appendix B.

3. Hydrodynamic forces on the rudder only proportional to the square of the velocity of the ship and to γ, the yaw deflection of the rudder;* see Equation B-1 in Appendix B. These forces are associated with the circulation of the water acting on the rudder and are also based on an *extension of incompressible-flow theory in two dimensions to a rigid, three-degree-of-freedom lifting surface;* see footnote (*) to Item 2.

4. Hydrodynamic (viscous) forces on the rudder only which are independent of velocity and proportional to the first derivative of lateral displacements (see Appendix B, Item 7).

---

*The forces discussed in Item 3 are mathematically represented by the first term of the right-hand side of Equations (B-1), F_y equation only. Thus, actually the coefficients and other data discussed in Item 2 are also associated with the forces in Item 3; see Appendix B for details. In this report the word "forces" is used generically to include both forces and moments except where otherwise indicated.

V. RESULTS

A. MODES

Normal modes of vibration observed on the analog computer* for several different configurations (i.e., models) of the rudder and hull, are presented in three forms:

(1) Plot of the node lines for the cantilevered rudder (those points which have zero v motion).

(2) Tables of frequencies, mode shapes, and computer parasitic damping.

(3) Plots of hull deflection and twist.

Linear dimensions are given in feet, angles in radians, and frequencies in cycles per second. Only antisymmetric modes about the vertical plane of symmetry are treated.

1. Summary of Normal Mode Frequencies (Three-, Six-, Twenty-, and Twenty-Three-Degree-of-Freedom Models)

Table 6 summarizes the frequencies of all normal modes of vibration measured on the computer for the models with three, six, twenty, and twenty-three degrees of freedom; modes of the different models which are related in general characteristics (frequency, shape) are entered on the same line. For models with three, six, and twenty-three degrees of freedom, which include the simulation of the rudder, both

*These modes correspond to the natural frequencies of the undamped system. Modes are found by driving some *electrical* node (point on the structure) with a voltage of constant amplitude (velocity) and observing those frequencies for which the current (force) is a minimum. Usually several modes are tried to ensure that all frequencies are found. The normal damping associated with the passive elements of the computer was present in all cases where normal modes were studied, and the resulting damping of each mode was obtained by observing the sharpness of the resonance. Computer studies are reported in Reference 20.

the basic rudder and the variation in which bearing friction permits yaw moment to be transmitted from the stock to the hull are considered. For the twenty-degree-of-freedom model (hull only) both the basic case (i.e., mass coupling included) and the case with no mass coupling are treated.

2. Three-Degree-of-Freedom Model (Rudder and Supporting Structure)

Table 6 presents the mode frequencies of the three-degree-of-freedom model, determined analytically (see Appendix E) and by measurement. The mode shapes are indicated by plots of the node lines in Figure 4 (basic case, no yaw moment transmitted) and in Figure 5 (variation in which yaw moment is transmitted by bearing friction; i.e., yaw moment is exerted on stock by friction in bearings by which the stock is attached to the hull).

3. Six-Degree-of-Freedom Model (Rudder and Supporting Structure)

Table 7 presents the mode shapes of the six-degree-of-freedom model, determined by measurement. For each mode, the measured damping, due to parasitic effects in the computer passive elements, is listed (see Appendix F).

4. Twenty-Degree-of-Freedom Model (Hull Only)

With the rudder and supporting structure *disconnected* from the hull, the natural modes of vibration were measured for two variations of hull mass and inertia properties (i.e., two hull configurations); the flexibilities for both configurations are those given in Table 5.

For the first configuration of the hull, Table 8 and Figures 7-16 present the frequencies, measured damping, and shapes for the first ten vibration modes of the basic hull, with the exception that no mass coupling (and therefore no mechanism

for coupled bending torsion) exists. Hence, these modes consist of four pure bending modes and six pure torsion modes. Measured damping due to computer parasitics associated with the passive elements of the analog computer is recorded for each mode.

For the second configuration of the hull, Table 9 and Figures 17-26 present the frequencies, measured damping, and shapes for the first ten vibration modes of the basic hull including the mass coupling. Whereas the modes of Table 9 are normalized with respect to the same coordinates as those of Table 8, the modes of Figures 17-26 are not necessarily normalized to the same values as given in Table 9.

5. Twenty-Three-Degree-of-Freedom Model (Rudder, Supporting Structure, and Hull)

Table 10 presents a normal mode study of the entire basic structure, with the full twenty-three degrees of freedom. For each mode, the measured values for the frequency, damping, relative lateral and torsional displacement of each hull station, together with the lateral displacement, roll, and yaw of the rudder are presented. Where the modes of Table 10 are correlated with those of Tables 8 and 9, they are normalized at the same coordinate.

Figures 27-37 present mode shapes for the hull displacements v and α. The overall vertical scale is arbitrary and the normalizing factors selected for these curves are not necessarily the same as those of the corresponding columns of Table 10.

Figure 38 presents a plot of the node lines* of the rudder for the first eleven modes of the entire system. In addition, for purposes of comparison, dotted lines

*The node line for a mode locates points on the rudder which have no motion in that natural mode of vibration.

are added to show the node lines of the vibration modes of the three-degree-of-freedom system.

B. FLUTTER*

1. Two- and Three-Degree-of-Freedom Models (Rudder and Supporting Structure)

a. Flutter Effects of Damping (Viscous or Inertial)—Basic Case.** Figure 39 represents stability predictions obtained by numerical analysis (Appendix E) for the basic two-degree-of-freedom model. In this figure the calculated roots of the characteristic (quartic) equation of the fourth-order linear differential equation of motion of the system, with zero excitation, are plotted in the complex plane for different values of ship's velocity v (or velocity ratio).

In Figure 39 the dimensions of the roots of the characteristic equations are in sec^{-1}, so that the real part of S represents damping per unit time and the frequency of oscillation, determined from the imaginary part, is given in radians per second. Usually, the stability of a system is treated in terms of the decrement or damping of roots on a *per cycle* basis, which is dimensionless. Hence, in this report, the basic presentation of flutter data will be in terms of ζ, the per unit critical damping (i.e., damping per unit cycle) of an equivalent single-degree-of-freedom system. (For a *single-degree-of-freedom system*, ζ is the damping ratio C/C_c which is actual damping divided by critical damping.) The per unit critical damping ζ and the means of measuring it on an analog computer are discussed further in Appendixes E and F.

*Classical flutter is defined in the footnote on page 2.

**See footnote on page 7.

Figure 40 shows a plot of damping versus velocity for the basic case. This plot includes (in dotted lines) the results of the numerical analysis, which correspond to Figure 39 and three curves which present data taken from the analog computer for the corresponding case. (These three curves are valid both for the two- and three-degree-of-freedom systems, as no difference of behavior was discernible for the basic case.)

b. Variation of Hydrodynamic Parameters (Direct Analog Computer). Figures 41-51 are plots of contours of constant ζ with two dimensions consisting of the velocity ratio V/V_0 and the hydrodynamic parameter that is being varied. These plots were obtained by repeating the calculations described in Item a above for configurations of the rudder system in which one (or, in some instances, two) of the hydrodynamic parameters are varied from the basic values. Each of these curves is concerned with the variation of one hydrodynamic parameter, generally over a range above and below the basic value. On any plot, to keep the damping ratio of the solution constant, the slope of a particular contour line gives the sensitivity of the solution to the parameter under consideration in terms of the change in flutter speed corresponding to a given change in parameter. In all cases, these plots are made for the three-degree-of-freedom system for which all parameters are basic except the one indicated on the figure. The normal parasitic damping associated with the passive elements of the analog computer was present in each case and was not eliminated by compensation. Therefore, in every plot, the form of the solution along the line indicated by "basic" corresponds to the curve of Figure 40 labeled "computer damping present." Basic values for the hydrodynamic parameters are given in Item 8 of Appendix B.

Figures 41-45 show the effect of flutter characteristics of the rudder due to variations in the lift- and moment-coefficient slopes, $C_{L\gamma}$ to $C_{M\gamma\dot{\alpha}}$.*

Figure 46 shows the effects on flutter of moving the center of pressure $\bar{x}_o$ in a chordwise direction.

Figure 47 shows the effect on flutter of chordwise motion of the rotation center $\bar{x}_1$.

Figure 48 indicates the effect of moving the center of pressure and the rotation center in the spanwise direction. One family of curves in this figure shows the effect of changing z_o, spanwise location of the center of pressure, while holding z_1, spanwise location of rotation center, constant. A second family of curves in the figure shows the reverse effect; that is, varying z_1 while holding z_o constant at the basic value. A third family of curves illustrates the effects, due to a further variation, obtained by varying z_o and z_1 simultaneously.

Figures 49-51 show the effects on flutter of varying the coefficient $C_{L\dot{\gamma}}$, a coefficient relating to the portion of the lift force which is not subjected to the Theodorsen lag function (see Appendix B). For the curves of Figure 49, no lag function was imposed in the simulation of hydrodynamic forces. For Figures 50 and 51, the lag function C_t of Figure 52, for aspect ratio equal to 2.5 and ∞, respectively, was applied to the force and moment terms with coefficients $C_{L\gamma}$, $C_{M\alpha\dot{\alpha}}$, and $C_{M\gamma\dot{\alpha}}$.

*See Appendix B for definitions of the hydrodynamic parameters.

In all cases no lag was applied to the terms with coefficients $C_{M\alpha\dot{\gamma}}$, $C_{M\gamma\dot{\gamma}}$, and $C_{L\dot{\gamma}}$. (Note that for the basic case of these coefficients $C_{M\alpha\dot{\gamma}} = C_{M\gamma\dot{\alpha}} = 0$.) This treatment of the lag functions, although not in exact accord with the treatment in Appendix B, is a sufficiently close approximation to it.

Figure 53 illustrates the results of another variation in hydrodynamic parameters. In this case, the form of the hydrodynamic force representation is the same as that employed for the rudder in the hull-rudder system analyzed in Reference 6. In this representation, forces acting at the center of pressure are proportional to the effective angle of attack *at the center of pressure;* thus, the rotation center, as defined in Appendix B, must be considered located at the center of pressure. In addition, hydrodynamic moments due to angular velocity and based on fluid inertia forces (Item 2 of Section IV) are ignored. In the notation of this analysis, these conditions are met by $\bar{x}_1 = \bar{x}_0$, $z_1 = z_0$, and $C_{M\alpha\dot{\alpha}} = C_{M\alpha\dot{\gamma}} = C_{M\gamma\dot{\alpha}} = C_{M\gamma\dot{\gamma}} = 0$, other parameters being taken at their basic values.

For purposes of making accurate measurements and comparison with theory (in Figure 53), negative resistance elements were adjusted in the computer circuit to compensate for parasitic computer damping, so that neutral stability was achieved at zero ship's velocity for the first two normal modes of vibration. Thus, the curves of Figure 53 all correspond to the curve labeled "no damping present" in Figure 40. The curves labeled A,B,C are for three different locations (chordwise) of the center of pressure. In curve A the chordwise position is at the basic location. For all curves the spanwise location (z_0, z_1) is basic. Additional data were taken

for center of pressure location A but with viscous damping added to the rudder in the amount D_f = 18,860 lb-sec-ft; D_m = 665 lb-sec-ft (see DISCUSSION, Section VIII).

c. Variation of Hydrodynamic Parameters (Numerical Analysis). For a number of variations of hydrodynamic parameters as described in Item b, a numerical analysis (i.e., solutions of the characteristic equation) of the corresponding two-degree-of-freedom model was made by means of the digital computer. The equation is a frequency quartic. Table 11 lists and defines the cases so analyzed. For all cases (Item (4) below excepted):

(1) The rudder supporting structure flexibilities are those described as basic in Section III.A.2.

(2) No lag functions are employed.

(3) $C_{L\dot{\gamma}} = 0$.

(4) The rudder mass and inertia terms have the basic values described in Section III.A.1, except for Case 15 of Table 11. In the numerical analysis of Case 15, *all* mass and inertia terms are 1.25 times their basic value.* Thus, for all cases studied by numerical analysis, the normal mode shapes are the same, the node lines are the same, and the location of x_4, z_4, the point constrained to achieve the two-degree-of-freedom system, is the same.

*In the analog computer condition plotted as Case 15 on Figure 68 only the mass is 1.25 times basic. All moments of inertia about the center of mass remained basic. Thus, Case 15 does not exactly represent a true comparison.

The results of these numerical analyses are compared with the corresponding analog computer results in Figures 54-68.* These are all curves of ζ versus the velocity ratio V/V_o. The frequency of the flutter root is given by numbers in parentheses. In each case, the flutter root presented corresponds to the second vibration mode—this is the only mode with a possibility of fluttering; see Section VIII.

d. Variations in Mass and Inertia of Rudder. Figures 69-74 show the effect on flutter of varying the mass and inertia properties of the rudder In this study, the structural mass of the rudder and the virtual mass of the water associated with it were considered together as a unit.

Figure 69 shows the effect of changing the rudder mass. In this variation, the location of the mass is not changed, and the moments of inertia of the rudder mass about its own center of mass are not changed.

Figures 70, 71, and 72 show the effects of changes in roll moment of inertia, yaw moment of inertia, and product of inertia, respectively, all taken about axes through the center of mass of the rudder.

Figures 73 and 74 show the effect of changing the location of the center of mass. For these figures, the magnitude of the mass and its moments and products of inertia about axes through the center of mass are unchanged.

*See footnote on page 21.

In these variations, as well as in those in Item b, normal damping of the passive elements of the computer was present. And, as in Item b, all of the data presented are for the three-degree-of-freedom system and correspond to the flutter root associated with the second vibration mode (see Section VIII).

e. Variation of Flexibilities of the Rudder Supporting Structure. A limited* investigation was made of the effect of variations on flexibility of the rudder supporting structure on the flutter characteristics of the three-degree-of-freedom system. For *many* of the variations studied, the velocity was maintained constant at 6.0 V_o = 355 knots; it was felt that only variations in flexibility which would lead to instability at this velocity would be significant enough to warrant closer inspection.

Figures 75-78 all show the variation in ζ as certain changes are made in the flexibility of the supporting structure. These figures were obtained for V = 6.0 V_o and normal computer damping associated with the passive elements used. In all these figures, a point corresponding to the basic configuration exists at a damping ζ = 0.045 S (S means stable), and a frequency of oscillation of 34.4 cps.

In Figure 75 the flexibility which is varied is comprised of any and all flexibilities which affect only the $\gamma\gamma$ term in the deflection coefficient matrix; see Appendix E. This includes the flexibility of the rudder stock in torsion; the flexibility of the tiller, the connecting rod, and the hydraulic system; and the bending and shear flexibility of that portion of the rudder stock extending above the upper bearing.

Figure 76 shows the effect on ζ of the bending and shearing flexibility of the rudder stock. (Only the stock flexibility between the rudder root and the upper rudder bearing is varied.)

*These studies are less extensive than those of Items b and d.

Figure 77 shows the effect on stability of variations in the bending and shear flexibility of the rudder trunk and bearing carrier.

Figure 78 shows the effect on stability of varying three lumped flexibilities which act to distribute lateral force into the hull:

(1) The flexibility of the lower bearing in transmitting lateral force.

(2) The flexibility of the platform of the hull in carrying lateral force.

(3) The flexibility of the ship's bottom in carrying lateral force.

In each case, the abscissa of the graph is normalized to the basic value of the flexibility, which is being varied as reported in Table 3.

Figure 79 shows the variation of flutter speed with changes in diameter of the rudder stock, deduced from the data of Figures 75 and 76 and the basic flutter curve (ζ versus V/V_o) of Figure 40. Two curves are given, one showing flutter speed when no damping (other than velocity-dependent terms) is added, the other showing slightly higher flutter speeds when rudder viscous damping (D_f = 18,860 lb-sec-ft, D_m = 665 lb-sec-ft) is added. As noted on the figure, the value of the abscissa refers to the diameter of the rudder stock from 3.10 to 6.45 ft above the baseline. It is assumed that the diameter of the stock above 6.45 ft is changed a proportionate amount. (The portion of the rudder stock below 3.10 ft above the baseline is imbedded in the rudder hub casting and is assumed rigid in bending throughout this analysis.)

Another variation in the effect of the flexibility of the supporting structure was investigated. This variation consists of permitting yaw (twisting) moment to be

transmitted from the stock into the rudder trunk or bearing carrier by two rudder bearings. Figure 80 is a plot of ζ versus velocity for this variation.

2. Six-Degree-of-Freedom Model (Rudder and Supporting Structure)

Figure 81 illustrates the results of a flutter analysis of the six-degree-of-freedom model, conducted on the direct analog computer.

3. Twenty-Three-Degree-of-Freedom Model (Rudder, Supporting Structure, and Hull)

Figure 82 shows the results of the flutter analysis for the entire twenty-three-degree-of-freedom system. In this figure, the damping of each mode of response for the first eleven normal modes of vibration are plotted as functions of velocity, and the frequency of each point is given.

The basic curves (solid lines) in Figure 82 were taken with the normal damping associated with the passive elements of the computer present. Although it was possible, in the case of the three-degree-of-freedom model, to compensate for this damping by means of the negative resistance of active elements (at least to the extent of cancelling the damping at zero velocity for the first two modes), it was not practical to achieve a similar elimination of parasitic damping in the combined hull-rudder model because of the many degrees of freedom. However, rudder viscous damping (D_f = 18,860 lb-sec-ft, D_m = 665 lb-sec-ft) was added to the representation in addition to the computer damping already existing. The results are plotted in Figure 82 (dashed lines).

Table 12 lists calculated values for the initial slopes of the ζ versus V/V_o curves of the first eleven modes, based on the normal mode data for the twenty-three-degree-

of-freedom model (see Section V.A.5). The results for this table, as well as for Figure 82, are all for the basic twenty-three-degree-of-freedom model for which yaw moment *is not* diverted from the rudder stock via the bearings.

The data of Figure 83 recorded from the analog computer correspond to the variation in which yaw moment *is* transmitted through the bearings.

VI. THE ELECTRIC ANALOG

The development of electrical analogs for the mechanical and hydrodynamic models hitherto discussed is presented in Appendix G. Figures 84-87 illustrate these analogs for the PGM rudder, supporting structure, and hull, including the hydrodynamic forces.

VII. UNITS AND CONSTANTS

The units used in this analysis are the foot, pound, second in the physical system, and MKS units, volt, ampere, etc., in the analog system, except where otherwise noted. Unless mass is specified, lb means a pound of force. Angles are measured in radians, unless otherwise specified.

The following constants were used in this analysis:

1. Water density = $\frac{64.0 \text{ lb (mass)}}{\text{ft}^3} = \frac{1.9876 \text{ lb-sec}^2}{\text{ft}^4}$

2. Gravity = 32.2 ft/sec^2

3. Materials

Property	Aluminum	Steel	Micarta	Units
Modulus E	10.3×10^6	29×10^6	0.420×10^6	lb/in^2
Modulus G	3.9×10^6	11×10^6		lb/in^2
Poisson's Ratio ν	0.32	0.32		
Density ρ	0.0975	0.284		lb(mass)/in^3

4. V_0 = 100 ft/sec = 59.2 knots

Ship velocity is normalized with respect to V_0 in the presentation of data.

VIII. DISCUSSION

A. MODES

Normal modes of vibration were obtained from the analog computer for several different configurations of the rudder and hull. For the three-degree-of-freedom system, analog results confirmed the calculations that had been made with regard to both natural mode frequencies and mode shapes (Appendix E). For all configurations, the normal modes of measured vibration correspond to the values of the response taken at zero velocity of the ship. The normal damping associated with the passive elements of the computer was present in all cases where normal modes were studied, and the resulting damping of each mode was obtained by observing the sharpness of the resonance.

The purpose of the two-degree-of-freedom model is the creation of a simplified model for which numerical analytical methods are practical, so that the performance of the analog computer in similar models of equal or greater complexity can be verified. It was felt that the characteristics of the three-degree-of-freedom model, which were important from the viewpoint of flutter, were associated with the first and second modes of vibration. Therefore, the selection of a constraint to reduce the number of degrees of freedom from three to two was made in a way which, as shown in Appendix E, leaves the characteristics of the first and second vibration modes undisturbed, but necessarily suppresses the third mode completely. Such a

constraint is made by locating Point 4 at the intersection of the node lines of the first and second modes of vibration in the three-degree-of-freedom system (see Figures 4 and 5). Since Point 4 has no lateral displacement in either of the first two modes, constraining it to be equal to zero imposes no change on the first two modes.

The reasoning in the selection of this point as the one to be constrained to achieve a two-degree-of-freedom model is as follows: The rudder is assumed rigid in out-of-plane motion in the three-degree-of-freedom model. Thus, there are three normal modes of vibration, each one characterized by a mode shape which involves the rigid out-of-plane motion of the rudder. Such a mode shape can be defined by the existence of a node line, on which there is no lateral displacement of the rigid rudder.

In Figure 4, which shows the node lines of the three modes of the basic case superimposed on an outline of the rudder, it is a matter of apparent coincidence that the location of Point 4 turned out to be right on the centerline of the rudder stock.

It was verified on the analog computer that the imposition ot this constraint, reducing the number of degrees of freedom from three to two, had no effect whatever on the first two vibration modes and an almost negligible effect on the flutter characteristics. The only instances in which the effect of this constraint was appreciable,(i.e., observable), were variations in the elastic properties of the rudder supporting structure, which would naturally be expected to change the influence coefficient matrix (see Appendix E), and the characteristics of the first and second vibration modes. However, variations in these properties did not significantly affect these modes.*

*When hydrodynamic forces were added (except damping forces of any kind), the modes were unaffected. When mass or elastic changes were made, the modes were affected because v_4, the basic point, was made invariant. However, this effect was small, even for large changes. Hence, these results are not shown here.

For the variation of the rudder supporting structure in which it was assumed that, due to static friction in the bearing, yaw moment was transmitted through the bearings from the rudder stock to the rudder trunk or bearing carrier, a separate computation of the node lines of the three normal modes in the three-degree-of-freedom system was made. These node lines are plotted in the sketch of Figure 5. Note that the values given on that page for the location of the intersection of the node lines of the first and second modes, also by apparent coincidence lies within about 0.5 in. of Point 4 as located above for the basic case.

The six-degree-of-freedom model is identical to the three-degree-of-freedom model with the exception that three additional lumped masses were located at points in the rudder supporting structure. These masses represent the distributed inertia of the supporting structure. Although it is felt (and the results confirm this feeling; see Section VIII.B.2) that the flutter characteristics of the rudder with the hull rigid and clamped are adequately described by solutions of the two- and three-degree-of-freedom models (because the greatest masses and the most significant static deflections are associated with the rudder rather than the supporting structure), it was a relatively simple matter when using the analog computer to add the lumped masses which seemed to participate the most in the motion of the supporting structure.

The twenty-degree-of-freedom model was employed only in normal mode studies for the reason that no hydrodynamic forces were considered acting on the hull, except for virtual mass effects. (See footnote (*) to Table 4.) The purpose of this model is to determine vibration mode characteristics of the hull alone for comparison

with flutter and vibration mode characteristics of the hull-rudder combination described in Section V.A.5.

To identify the normal modes of vibration of the ship, one of the variations of the hull which was studied involved the hull with no rudder attached and with the twenty degrees of freedom as outlined above. Another variation, for the same purpose, also had the rudder disconnected from the hull, and represented the hull as detailed above, except that the height of the center of mass at each section above the neutral axis was assumed to be zero. In this latter variation, therefore, there is no coupling at all between the side bending and roll properties of the hull, and these normal modes are completely separated and uncoupled from each other. Thus, this variation is referred to as the hull with no mass coupling.

For the basic hull which includes the mass coupling, with the rudder and supporting structure disconnected, examination of Figures 17-26 and Table 9 leads to the following conclusion: Although none of the modes is pure bending or pure torsion, any of them may be easily correlated with a pure mode of the uncoupled system (see Figures 7-16) by virtue of both the dominant mode shape and the frequency of vibration of the mode.

The following observations may be made regarding the vibration modes of the twenty-three-degree-of-freedom model. (See Figures 27-37 and Tables 6 and 10.) Of the first eleven modes, the characteristics of the second mode are traceable to the first-mode behavior of the rudder and its supporting structure in the three-degree-of-freedom model; likewise, the tenth and eleventh modes are related to the second

mode of the three-degree-of-freedom system, involving substantial rudder motion. The first mode, and modes 3 to 9, are readily correlated with bending and torsion modes of the hull alone.

Some rudder motion is involved in all of the modes of vibration of the entire structure, however, and it seems appropriate to study the rudder motion by means of node lines. The plot of the node lines superimposed on an outline of the rudder shown in Figure 38 substantiates the correlations made above relating modes of the three-degree-of-freedom system to particular modes of the twenty-three-degree-of-freedom system.

B. FLUTTER

1. Two- and Three-Degree-of-Freedom Models

a. Effects of Damping on Flutter—Basic Case. For the basic two-degree-of-freedom model as described in Appendix E, the differential equation describing the motion of the system, when there is no excitation, is a linear, fourth-order equation. The form of solutions to this equation may be obtained by solving the characteristic equation, which is a quartic equation in terms of the differential operator. A numerical analysis has been made for the basic case and the roots of the characteristic equation, for different values of the ship's velocity V, are presented in a (Nyquist) plot in the complex plane in Figure 39. In this figure, roots with negative real parts correspond to solutions which are either exponentially monotonically decreasing, or exponentially damped oscillatory waves. Roots with zero real part correspond to the marginal stability of sinusoidal oscillations which neither increase nor decrease with

time. At velocity equal to zero, the lack of any damping causes the solution to consist of two pairs of imaginary roots, which correspond to the two normal modes of vibration. It is seen that for velocities greater than 6.25 V_o roots exist with a positive real part. Therefore, the solution of the equations of motion will contain terms which increase without limit with time. With the velocity between 6.25 V_o and approximately 30 V_o, this increasing form of the solution is oscillatory in nature and is referred to as flutter. Above approximately 30 V_o, the solution is nonoscillatory and is a form of instability known as divergence.

In terms of ζ, the critical damping parameter, it may be seen from Figures 39 and 40 that the first (or low-frequency) mode becomes stable very quickly and is not a factor in the flutter characteristics. The second mode initially becomes more stable as velocity is increased; eventually, however, the stability decreases, and it goes unstable (see Appendix E). The three solid curves of Figure 40 show the effects of different forms of damping that are not dependent on velocity in the analog computer solution. These three curves are more fully described in the note to Figure 40. With regard to the basic configuration of the three-degree-of-freedom system, Figure 40 illustrates that:

(1) The numerical analysis of the two-degree-of-freedom system validates the analog computer solution.

(2) Intentionally imposed viscous damping is comparable in effect and magnitude to normal computer damping in the passive elements.

(3) Viscous damping or computer damping (or generally any damping which is reasonable in size and not dependent on ship's velocity) has a minor effect on the essential flutter characteristics of the system, including the stability at moderate velocities, and the velocity at which flutter instability occurs.

It will be seen later, however, that the above conclusions do not necessarily apply to the more complex system consisting of the rudder, supporting structure, and elastic hull. Nor are these conclusions necessarily true for other ships.

Of course, the damping which is proportional to velocity (due to the second class of hydrodynamic force listed in Section IV.) is important and strongly affects the flutter characteristics.

b. Effects of Variation of Hydrodynamic Parameters (Direct Analog Computer). One of the purposes of undertaking this analysis is the determination of the sensitivity of the flutter characteristics of the rudder system to various hydrodynamic parameters (see INTRODUCTION).

Figures 41-45 show the effect of flutter characteristics of the rudder due to variations in the lift-and-moment-coefficient slopes, $C_{L\gamma}$ to $C_{M\dot{\gamma}_\alpha}$. It is concluded from these figures (not unexpectedly) that the flutter speed decreases as $C_{L\gamma}$ is increased, the flutter speed increases as any of the moment coefficients is increased, and that the effects of the cross-coupling terms, $C_{M\alpha\dot{\gamma}}$ and $C_{M\dot{\gamma}_\alpha}$, are very small for expected values of these terms.

Figure 46 shows the effects on flutter of moving the center of pressure, Point 0 ($x = \bar{x}_o$, $z = z_o$; see Item 5 of Appendix B), in a chordwise direction. It is observed that for center-of-pressure locations aft of the basic location, the solution is

generally more stable, whereas when the center of pressure is moved forward, the solution is less stable. Two different types of instabilities were observed on the computer and are indicated in Figure 46. A normal oscillatory instability occurs when the velocity is increased sufficiently. In addition, a nonoscillatory divergence, easily predictable from the static deflection influence coefficient matrix of the rudder supporting structure, is encountered at any velocity if the center of pressure is moved sufficiently far forward.* (At normal operating velocities of the ship, however, the amount the center of pressure would have to be moved to encounter this divergence instability is very large compared with the dimensions of the rudder.) Points at which this nonoscillatory divergence was observed on the computer are indicated by D on Figure 46.

Figure 47, which shows the effect on flutter of chordwise motion of the rotation center, Point 1 ($x = \bar{x}_1$, $z = z_1$; see Item 5 of Appendix B), is of interest for two reasons. First, it is noted that by moving the rotation center sufficiently far aft, it is possible to achieve flutter at very low velocities. In fact, the numerical analysis confirms that changing $\bar{x}_1$ from its basic value of -2.234 ft to a location of -3.093 ft or farther aft makes the two-degree-of-freedom rudder system unstable at any velocity other than zero. Secondly, the parameter $\bar{x}_1$ is difficult to measure in experimental tests of actual control surfaces, and theory is lacking for its calculation for low-aspect-ratio control surfaces.

*This can be shown by applying the Routh Criteria to the frequency quartic having the form $A_0S^4 + A_1S^3 + A_2S^2 + A_3S + A_4 = 0$. (This is a revision of the form given in Appendix E where the A_i are functions of the elements in the matrix, some of which are functions of velocity. The details of calculation are not given here.)

In Figure 48, the effects shown from moving the center of pressure and rotation center in the spanwise direction are opposite. The system is more stable when the center of pressure is raised or when the rotation center is lowered. It is a by-product of the theory expounded in Appendix B for the calculation of these hydrodynamic parameters that the spanwise location of the center of pressure and of the rotation center are the same; that is, that $z_o = z_1$ (see Item 8 of Appendix B). Therefore, a further variation, also shown in the third sketch of Figure 48, was to vary z_o and z_1 simultaneously. In this instance, the solution is more stable if z_o and z_1 are lowered below the basic position of 2.093 ft below the rudder root.* If z_o and z_1 are raised above the basic position, the solution first becomes less stable but eventually becomes more stable again.

Since the basic configuration studied in Figure 49 omits the lag function entirely (i.e., $C_t = 1$, a real quantity), there is no significance to a *separate* "unlagged" term, and inspection of Equations (B-1) of Appendix B will verify that any value assumed for $C_{L\dot{y}}$ can be accounted for by a variation in the parameter $\bar{x}_1$. In fact, a comparison of Figure 49 and that portion of Figure 47 lying to the left of the basic value of $\bar{x}_1$ shows that they are indeed equivalent (see Item 8 of Appendix B).

When the lift forces are subjected to a lag function, however, there is a mathematical significance attached to the existence of an unlagged term characterized

*Item 8 of Appendix B gives $z_o = z_1 = -2.060$ ft. Another value in Table 13 is $z_o = z_1 = -2.083$ ft. These discrepancies in z_o, z_1 are due to round off errors in simulating distances with available discrete transformer taps. The amount of error is insignificant.

by coefficient $C_{L\dot{\gamma}}$. By comparing Figures 50 (lag function for an aspect ratio of 2.5) and 51 (lag function for infinite aspect ratio) with Figure 49, it is concluded that the lag functions are somewhat stabilizing (i.e., they cause the instabilities to occur at higher velocities), and that the effect of the unlagged term $C_{L\dot{\gamma}}$ is not very different in the three cases.

It should be noted in all of the plots of Figures 41 to 51 that the oscillatory root corresponding to the second vibration mode is the only one described. In the two-degree-of-freedom system, the first mode quickly becomes very highly damped as the velocity is increased from zero and is never a significant factor in flutter (see Appendix E).* In the three-degree-of-freedom system, the first mode remains an insignificant factor in flutter; the third mode, although it does not become markedly stable at higher velocities, neither does it ever seem to change its stability. The third vibration mode of the three-degree-of-freedom system was always observed to be stable with ζ equal to 0.05 and 0.10; the results for this mode are therefore not plotted here.

The agreement between calculated and measured values of ζ in Figure 53 is not very good, and this discrepancy has not been accounted for. The curves of frequency versus velocity at the top of Figure 53 show very good agreement. However, a number of observations are made:

(1) It is the first mode which exhibits the critical flutter behavior. (In the basic cases and in all other variations reported previously,** the first mode becomes

*First mode damping obtained by numerical analysis and measured on the analog computer is shown in Figures 39 and 40, respectively.

**Using the form of the hydrodynamic force representation given in Appendix B rather than in Reference 6.

strongly damped as velocity increases, and the second mode is the only one which may flutter.) In this variation the second mode becomes very stable as V goes from 0 to $2V_o$.

(2) The numerical analysis corresponding to curve B indicates neutral damping at a constant frequency for any velocity. This is due to the center of pressure being located right on the node line of the first mode. Thus the first mode has no coupling with the hydrodynamic forces and is not affected by them.

(3) For curve C, when V is a little greater than $3V_o$, static (nonoscillatory) divergence occurs. This may account for the sudden deviation from "calculated" values, which are, themselves, only approximations at higher velocities.

(4) Additional data were taken for center of pressure location A but with viscous damping added to the rudder in the amount:

D_f = 18,860 lb-sec-ft

D_m = 665 lb-sec-ft

The resulting measured values of ζ give a curve which is more stable by 0.065 than curve A of Figure 53. Thus, even though the results of employing the hydrodynamic theory of Reference 6 do not correlate ideally with analytical results, the mode most critical in flutter is strongly damped by rudder viscous damping, and no flutter instabilities are expected below $V = 2V_o$.

In the study of the effect on flutter of the variation of hydrodynamic parameters, it is noted that the assumption of a "rotation center" distinct from the center of pressure has a large influence on the flutter characteristics, and the location of the

rotation center is significant. In addition, the hydrodynamic terms of Class 2, discussed in Section IV., have a pronounced effect on stability, particularly the self terms $C_{M\dot{\alpha}\dot{\alpha}}$ and $C_{M\dot{y}\dot{y}}$. Although flutter speeds by either form of hydrodynamic parameters are safely above operational speeds for the PGM design studied herein, it would appear desirable to have a research program directed toward achieving greater insight and confidence in the mechanism of hydrodynamic forces.

c. Effects of Variation of Hydrodynamic Parameters (Numerical Analysis). Comparison of the results of the numerical analysis* with the corresponding analog computer results (see Figures 54-68) indicates that in each case (see Table 11) the flutter root presented corresponds to the second vibration mode--as previously noted, this is the only mode with a possibility of fluttering. The analog results are uniformly somewhat more stable than the numerical analyses. As possible factors accounting for this discrepancy, note that:

(1) Parasitic computer damping was existing uncompensated in the analog computer. (An exception: In Case 7, the analog data were taken with computer damping reduced to zero at V = 0 by compensation. Only the intended viscous damping was present.)

(2) The analytical data are for two degrees of freedom. The analog data are for three degrees of freedom. This effect should be very small, because changing the analog computer simulation from three to two degrees of freedom had negligible effect.

*These results are solutions to the frequency quartic (Appendix E); the different curves correspond to different coefficients. The solutions here were obtained by use of a digital computer rather than manually.

(3) The data giving flutter root frequencies show excellent agreement.

It is felt that the results of Figures 54-68 generally validate the analog computer as exhibiting *satisfactory engineering accuracy, and faithfully indicating the trends* of the flutter characteristics.

d. Effects of Variation of Mass and Inertia of Rudder. A study of Figures 69-74 shows that of the six variations of mass and inertia properties of the rudder, only the magnitude of the mass and the x and z coordinates of its location have any significant effect on the flutter characteristics. The following changes tend to make the system more stable: decreasing the total amount of mass, moving the center of mass forward, and moving the center of mass upward. At low velocities, the effects of these changes are minor. However, at high velocities (V/V_o = 6 and above) the effects on flutter stability are very profound.

e. Effects of Variation of Flexibilities of Rudder Supporting Structure. A study of the effects of varying the flexibilities of the rudder supporting structure (Figures 75-80) leads to certain significant observations:

Figure 75 is important because it shows the effect of a change in the flexibility attributable to the hydraulic control system for the steering mechanism. (See Section V.B.1.e) As the value assumed for this flexibility (see Table 3 and Section III.A.2) was based on very incomplete information and rough assumptions, it is important to know what effect variations of this parameter can have. It is fortunate to see, by inspecting Figure 75, that variations in this parameter are not likely to make the system significantly less stable than the basic system which was analyzed. The significance of Figure 77 is indicated in the note to the figure.

It is concluded from an inspection of Figure 79 that (in the three-degree-of-freedom model) the flutter behavior is not critically affected by rudder stock diameter. This dimension presumably should be selected by other criteria; for example, strength.

Another variation in the effect of flexibility of the supporting structure was studied. This variation consists of permitting yaw moment (twisting moment) to be transmitted from the stock into the rudder trunk or bearing carrier by the two rudder bearings. Based on information contained in Reference 13, it seems possible that this condition of flexibility might exist under either of two conditions. In the first condition, the static position of the rudder entails a significant deflection to accomplish turning of the ship, in which case large static sideloads must be carried by the bearings, giving rise to a transmission of twisting moment because of frictional forces. The second condition corresponds to the limiting case of a large-amplitude vibration taking place, even with the intended position of the rudder straight ahead. In this condition the periodic lateral force imposed on the rudder would be large enough to (periodically) cause the bearings to carry lateral force, and therefore transmit yaw moment, during portions of the oscillation cycle. In this latter case, the system would actually be nonlinear, in that when the oscillation was passing through the neutral position, lateral force transmission through the bearings would be a minimum and yaw moment would not then be transmitted. But, at the extremes of the amplitude of oscillation, the bearings would effectively transmit yaw moment. The study of the variation in which yaw moment is transmitted through the bearings at all times is valuable in indicating what the possible limit cycle of the nonlinear

oscillation might be. However, it is felt that the first example above is the more important application of this variation of the structure.

In the variation in which yaw moment is transmitted through the rudder stock bearings, it was generally found the solution was considerably more stable than the basic case. A plot of ζ versus velocity for this variation is shown in Figure 80. Thus it appears that this variation is less susceptible to flutter than the basic case.

2. Six-Degree-of-Freedom Model

The results of the flutter analysis,* shown in Figure 81 for the six-degree-of-freedom model, show that this model is slightly more stable than the basic three-degree-of-freedom model. (Compare Figure 81 with the curve labeled "computer damping present" in Figure 40, the basic three-degree-of-freedom case.)

3. Twenty-Three-Degree-of-Freedom Model

With the entire system assembled on the computer, including the three degrees of freedom associated with the rudder and the supporting structure and the twenty degrees of freedom of the hull in lateral motion and in torsion, the resulting picture of the flutter characteristics is not as clear cut as in the simpler models discussed in earlier sections.

By observing the frequencies and shapes (see Figure 38) of the natural vibration modes, it is possible to see that the second mode of the hull-rudder combination is most closely associated with the first mode of the three-degree-of-freedom system, and the tenth mode of the hull-rudder combination is most closely associated with the second mode of the three-degree-of-freedom system. For the twenty-three-degree-of-freedom

*Conducted on the direct analog computer.

system, Figure 82 confirms that the flutter characteristics of Modes 2 and 10 do indeed approximate the flutter characteristics of the first two modes of the three-degree-of-freedom system.

For the PGM, therefore, the second rudder mode lies above the first eight *hull* vibration modes, whereas in a similar analysis for ALBACORE[6] the rudder flutter mode frequencies lie below the hull vibration mode frequencies. This probably accounts for the fact that a number of modes of doubtful stability exist for the PGM; i.e., whereas connection of the hull to the rudder did not affect the flutter mode (or characteristic) of ALBACORE, it does affect this mode for the PGM.

The other nine flutter roots shown in Figure 82 have varying behaviors ranging from the classical flutter appearance of the root associated with Mode 1 to the very slightly damped (but velocity-independent) behavior of Mode 9. In particular, Modes 4, 5, and 6 are associated with roots which eventually go unstable (at velocities of $4\,V_o$ to $6V_o$), but whose stability is never significantly greater than it is at zero velocity.

The results plotted in Figure 82 (dashed lines) show that the addition of viscous damping substantially affects the modes which involve rudder deflection to a large degree (Modes 2 and 10), and also Mode 1. However, the other modes, including those exhibiting uncertain flutter characteristics, are little affected by the addition of viscous damping at the rudder.

Because of the behavior of the flutter roots associated with Modes 3, 4, 5, and 6, in which damping indicates little increase in instability as velocity increases

and in which the instabilities which eventually occur are relatively gradual (i.e., the slope of the ζ versus V/V_0 curve is small), it is appropriate to give special attention to an accurate determination of the initial slope of the ζ versus V/V_0 curve at $V/V_0 = 0$. It is possible to make an analytical determination of this initial slope, provided the mode shapes and frequencies are known.*

Based on the normal mode data of Section V.A.5, the initial slopes of the ζ versus V/V_0 curves of the first eleven modes were calculated, and one is listed in Table 12. Realizing that these results apply only to the initial portion of the curve above $(V/V_0) = 0$, the correlation with the analog data of Figure 82 is satisfactory. It is significant that all eleven normal modes treated in Figure 82 and in Table 12 show a negative initial slope, indicating an increase in stability as velocity increases from zero. However, for several of the modes the value of the slope is not very large. But for all eleven modes, even if no damping (independent of velocity) exists, there will be no flutter instabilities for velocities under a finite flutter velocity of approximately $1.5\ V_0$.** If each mode has a zero-velocity damping of 0.01 times critical, the flutter velocity is approximately $2.9\ V_0$. If each mode has a zero-velocity damping of 0.02 times critical, the flutter velocity is approximately $3.5\ V_0$. (These flutter velocities are estimated by visual inspection of Figure 82.)

*The method of this determination is based on a comparison of the energy dissipated per unit time by the damping terms proportional to velocity and the total energy (potential and kinetic) of the natural vibration mode. The derivation is straightforward but lengthy and will not be presented here; see note 2 of Table 12.

**This can be seen by translating the vertical scale for ζ in all of the curves of Figure 82 by an amount such that $\zeta = 0$ at $\frac{V}{V_0} = 0$.

It is apparent that, although the design here analyzed appears safe from flutter at all operational speeds, the *actual flutter behavior is strongly dependent on the zero-velocity damping associated with each vibration mode.* For rudder motion, viscous damping estimated as outlined in Appendix B, Item 7, was represented and the effects noted. *However, damping associated with hull motion was not estimated or represented.* This damping might include (1) structural damping, (2) viscous damping, and (3) other hydrodynamic damping forces. Of these, the *first two would be accounted for by measurement of the decrement of vibrations experimentally induced in the hull at zero velocity.* For analysis of unbuilt ships, it is desirable to have a rule of thumb for estimating these sources of damping. Studies directed toward the establishment of reasonable and reliable values of damping of hull vibrations at zero velocity are recommended.

The results reported above (Table 12 and Figure 82) are all for the basic twenty-three-degree-of-freedom model in which yaw moment *is not* diverted from the rudder stock via the bearings. For the variation in which yaw moment *is* transmitted through the bearings, the data of Figure 83, recorded from the analog computer, show that no instabilities were encountered below $(V/V_o) = 8$. Thus, as in the three-degree-of-freedom model, this variation is less critical with respect to flutter than the basic case.

IX. SUMMARY OF RESULTS

The results of the analysis presented in this report are the normal mode and flutter data obtained for the rudder alone, with either two, three, or six degrees of freedom (the hull assumed clamped and rigid); for the flexible hull alone, with twenty degrees of freedom; and for the combination of the rudder, supporting structure, and hull, with twenty-three degrees of freedom.

The normal modes of vibration are described in terms of the natural vibration frequencies and their corresponding mode shapes; the results are given in Section V.A. The flutter characteristics are described in terms of the characteristic response of the system to transient excitations (see Appendix F); the results are given in Section V.B. This characteristic, for a particular configuration of the ship and assumed parameters at a given ship's velocity, consists of a damping, or logarithmic decrement of the free response and the frequency of this response. Here, flutter damping is measured either on a steady basis or on a transient basis, but it is always given in terms of the per unit critical damping of an equivalent single-degree-of-freedom system (Appendix F).

Extensive numerical analysis and calculations were conducted for the purpose of verifying the analog computer solution. The results are reported in Appendix E.

X. CONCLUSIONS

The principal conclusions supported by the results of this analysis are:

1. The PGM rudder-hull system (the particular design analyzed) is not expected to flutter. The flutter speed is difficult to predict because it is highly dependent on the viscous and structural damping associated with hull vibration modes,

and no quantitative estimate of this damping was available. However, assuming a minimum conceivable value of damping, the flutter speed of 90 knots should be more than twice the maximum operating speed of the PGM; thus, the general objective stated in the Introduction has been achieved.

2. In accordance with the first objective stated in the Introduction, the flutter characteristics of the entire rudder-hull system were analyzed and found to be more complex than classical flutter of simpler systems (for the rudder and supporting structure alone) involving two vibration modes. Flutter roots associated with six of the first eleven vibration modes show instabilities (at ship speeds considerably above operating speeds). This is probably due to the fact that the frequency of the second rudder vibration mode (the one which first flutters in a model of the rudder and supporting structure only) is greater than the frequencies of the first eight hull vibration modes. Hence, the conclusions concerning the classical flutter (or binary flutter) of a two- or three-degree-of-freedom rudder (Items 3 to 9 below) do *not* apply to the entire rudder-hull combination.

3. The excellent correlation between the numerical analysis of the two-degree-of-freedom model and the analog computer analysis of the three-degree-of-freedom model of the rudder and supporting structure validates the use of both the simplified numerical analysis and the analog computer; thus, the second objective stated in the introduction has been achieved.

4. By varying the hydrodynamic parameters, supporting structure flexibility, and rudder mass of the three-degree-of-freedom model consisting of the rudder and

its supporting structure, the significance both of the values and form (see (b) below) for these parameters in influencing the flutter characteristics of a flexibly attached rudder has been determined; thus, the third objective stated in the introduction has been achieved. Specifically, for this model:

(a) The flutter characteristics are most sensitive to the location of rotation center and center of pressure. They are moderately sensitive to the parameters describing the lift coefficient and the self-moment coefficients in roll and yaw, and least sensitive to the cross-coupling moment parameters, the lag functions, and viscous damping terms.

(b) There is considerable difference in the flutter characteristics between assuming the basic form of the hydrodynamic forces used in this analysis (i.e., rotation center located aft of the center of pressure,* minimum importance of viscous damping terms, hydrodynamic damping forces proportional to rate of yaw or roll and to ship's forward speed) and the form of the hydrodynamic forces used in Reference 6 (i.e., rotation center located at center of pressure, damping forces due to only (1) lift force at center of pressure which is dependent upon the angle of attack,** and (2) viscosity). In the former case, the first

*Rotation center and center of pressure have no direct connection.

**Effective angle of attack is due to γ (leading to lift proportional to V^2) and to v (leading to lift proportional V). Of these two components of lift, the first has the characteristics of an elastic spring, and the second has the characteristics of a damping force.

mode becomes highly damped, and the *second mode* exhibits the characteristics of classical flutter; as velocity increases, the damping first becomes greater, then less, and finally instability occurs. In the latter case, the *first mode* is critical and becomes unstable at a *relatively low velocity. Thus, flutter predictions will vary widely with the form of the analysis (or forces) used.* Although flutter speeds obtained by either form of the forces are safely above operational speeds for the PGM design studied here, it would appear desirable to have a research program directed toward achieving greater insight and confidence in the mechanism of hydrodynamic forces.

(c) Flutter is not extremely sensitive to the flexibilities of the supporting structure or of particular parts of the supporting structure.

(d) Flutter is sensitive to the total mass associated with the rudder, and the location of the center of mass. The following changes tend to make the system more stable: decreasing the total amount of mass, moving the center of mass forward, or moving the center of mass upwards. At low velocities, the effects of these changes are minor. At high velocities ($\frac{V}{V_o}$ = 6 or V = 355 knots) the effects on flutter stability are profound.

(e) Damping which is not dependent on ship's velocity, either computer parasitic damping or intentional viscous damping of the rudder, when present in reasonable amounts, has a small effect on the flutter characteristics, especially flutter speed of the PGM.

XI. RECOMMENDATIONS

The following recommendations are based on the present investigation and a consideration of its application to the design of naval vessels; the objective of these recommendations is to achieve a level of greater confidence in the prediction of the dynamic vibration characteristics of ships:

1. Further studies should be made to correlate the theory of hydrodynamic forces with model testing. Much work has been done to determine static lift coefficients and center of pressure. What is needed are experimental studies to verify the *form* of expressions for unsteady hydrodynamic forces, and the magnitude of the coefficients; see Item 4 (b) of CONCLUSIONS. These studies should be conducted with low aspect ratio control surfaces typical of rudders, hydrofoils, and diving planes.

2. Additional investigations should be conducted to explain the effect of the hull dynamic characteristics on rudder flutter. In the work of Reference 6, the hull elastic and inertia properties had little effect on rudder flutter characteristics. However, in the present analysis, the hull has a profound effect on rudder flutter characteristics.

3. Since flutter of the rudder-hull combination is very sensitive to zero-speed damping (composed, presumably, of structural damping and viscous and turbulent effects of the water) of the hull vibration modes, this damping should be investigated to achieve reliable quantitative predictions; for similar reasons, damping of the rudder vibration modes should also be studied.[18,19]

4. Investigation should be made of related phenomena which fall outside the present (linear, small-motion) theory and which may influence the dynamic

characteristics of ships. Specific examples of such phenomena are:

(a) the influence of ship maneuvering on vibration characteristics,*

(b) nonlinear hydrodynamic coefficients,*

(c) nonlinearities associated with friction and play in the rudder supporting structure, bearings, and steering mechanisms, and

(d) vibrations induced by periodic forces due to propellers, and the action of propeller downwash* on the rudder.

ACKNOWLEDGEMENTS

The author gratefully acknowledges the constructive criticism and suggestions of Dr. E.H. Kennard and Mr. G.J. Franz. The author is grateful also to Mr. E.F. Noonan, Jr., of DTMB, for his valuable administrative assistance and technical suggestions in establishing this study and for his continuing interest throughout the investigation. Acknowledgement is due to Dr. E. Buchmann and to Mr. A. Kilcullen of DTMB for their technical and administrative assistance at various stages of this study. Appreciation is expressed to Messrs. A. Taplin and A.J. Giddings, of Code 442 of the Bureau of Ships, for initiating the study, requesting the author's assistance in its execution, and providing significant technical information and advice for the author's guidance. Finally, the author wishes to acknowledge Dr. W.J. Dixon, formerly of Computer Engineering Associates, for his contribution[20] to the present report.

*This work is underway.

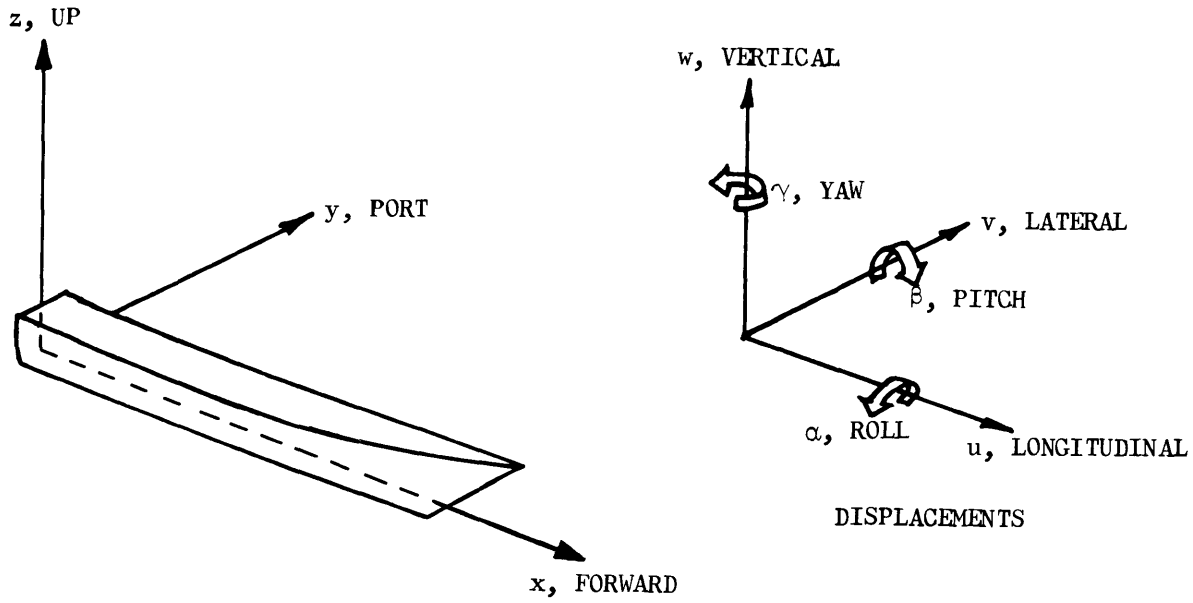

Figure 1 – Sign Conventions

All directions shown positive; symmetry is assumed about x-z plane. The elastic axis is along the centerline of the hull with origin at the stern.

The quantities x, y, and z are used to locate points on the hull and rudder (not shown here; see Figure 2). The quantities u, v, and w are used to indicate the displacements of points of the structure from the equilibrium position of these points. Similarly α, β, and γ indicate angular displacements from the equilibrium position of members of the structure. Motions of the hull (treated) are entirely antisymmetric. Thus only v, α, γ displacements are considered in this report; see Appendix A.

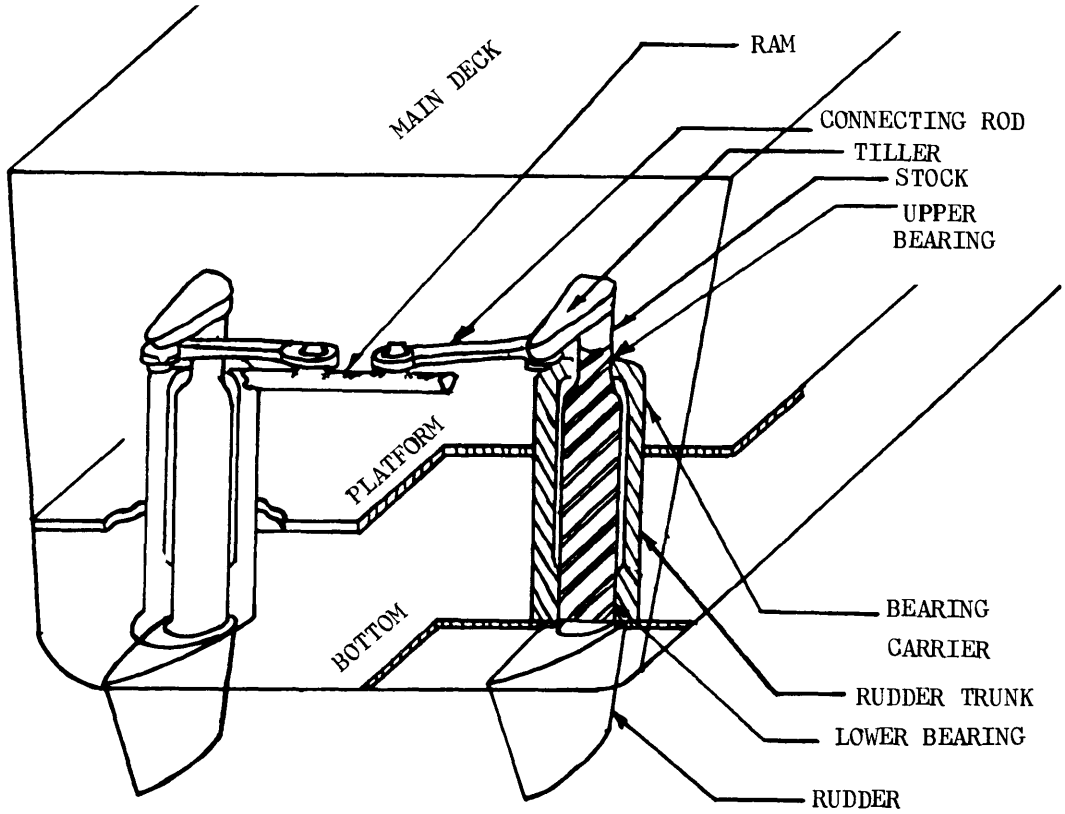

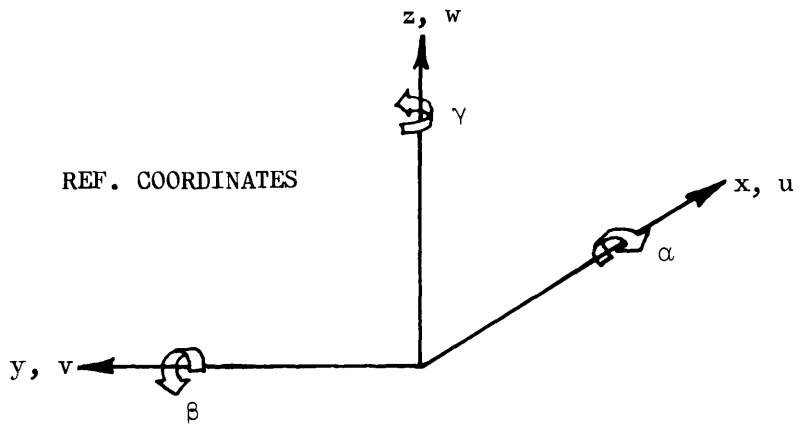

Figure 2 – Rudder Support and Control Mechanism

Data given by Notes 1 and 2 of Figure 1 are applicable here.

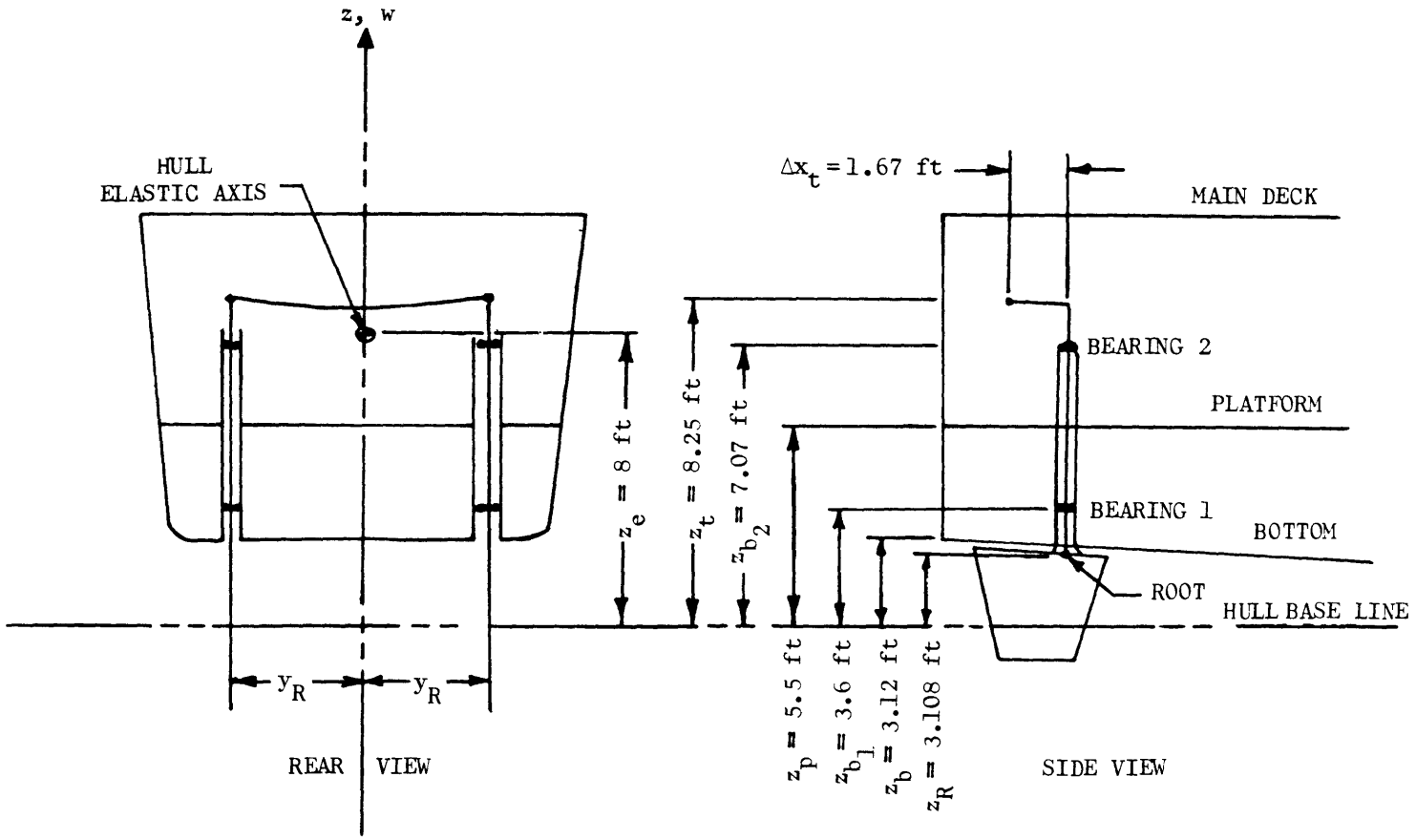

Figure 3 – Rudder Support and Control Mechanism–Location of Components

All dimensions are from Reference 13 except z_b which is from Reference 16.

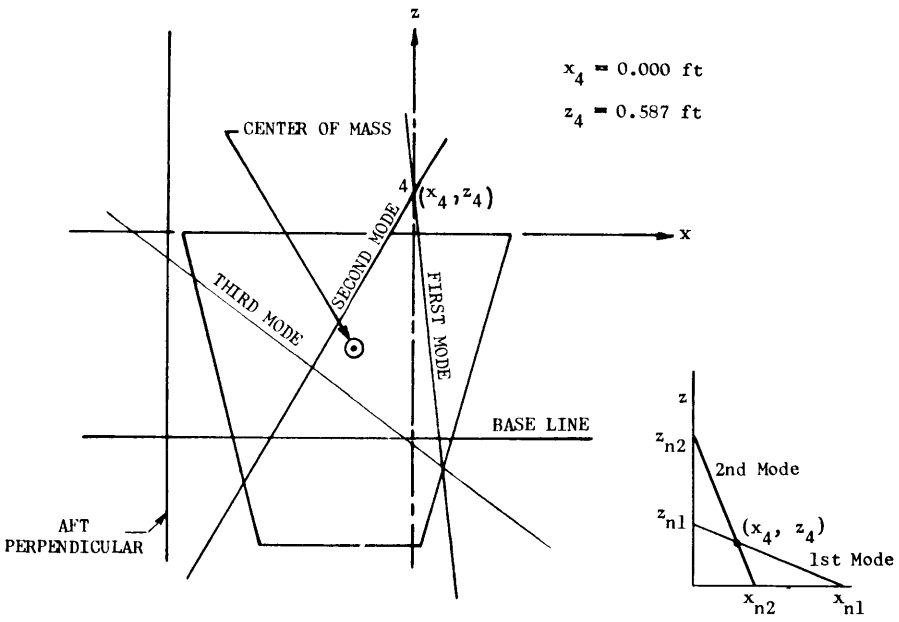

Figure 4 – Node Lines–Basic Case (Constrained Basic Model)–
Three Degrees of Freedom

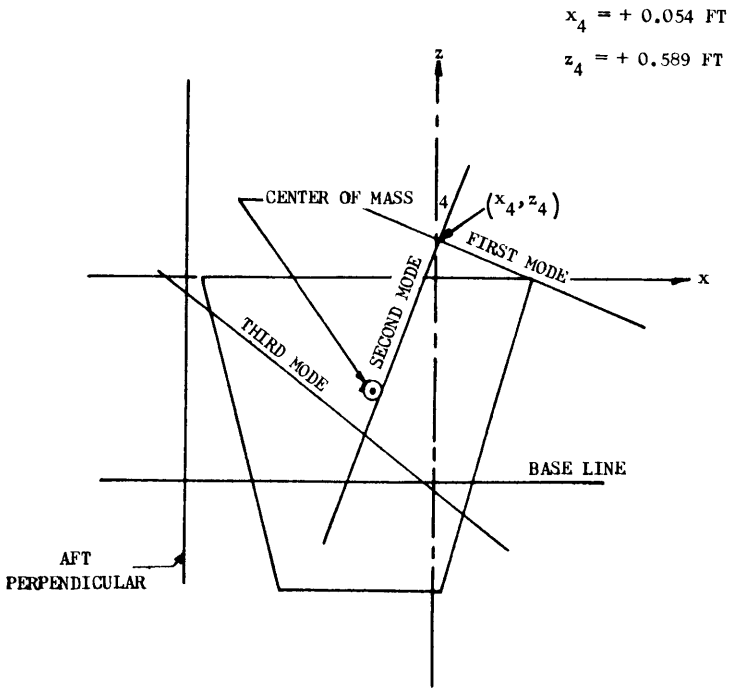

Figure 5 – Node Lines–Basic Case (Modified Basic Model) but with
Bearing Friction Present (Yaw Moment Transmitted through
Bearings)–Three Degrees of Freedom

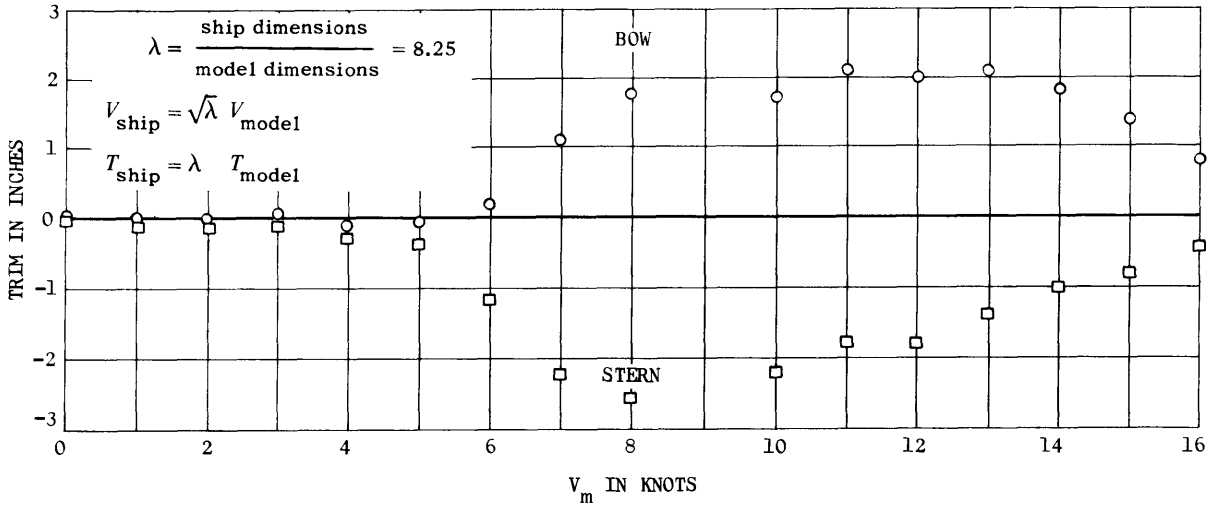

Figure 6A – PGM Trim Curve

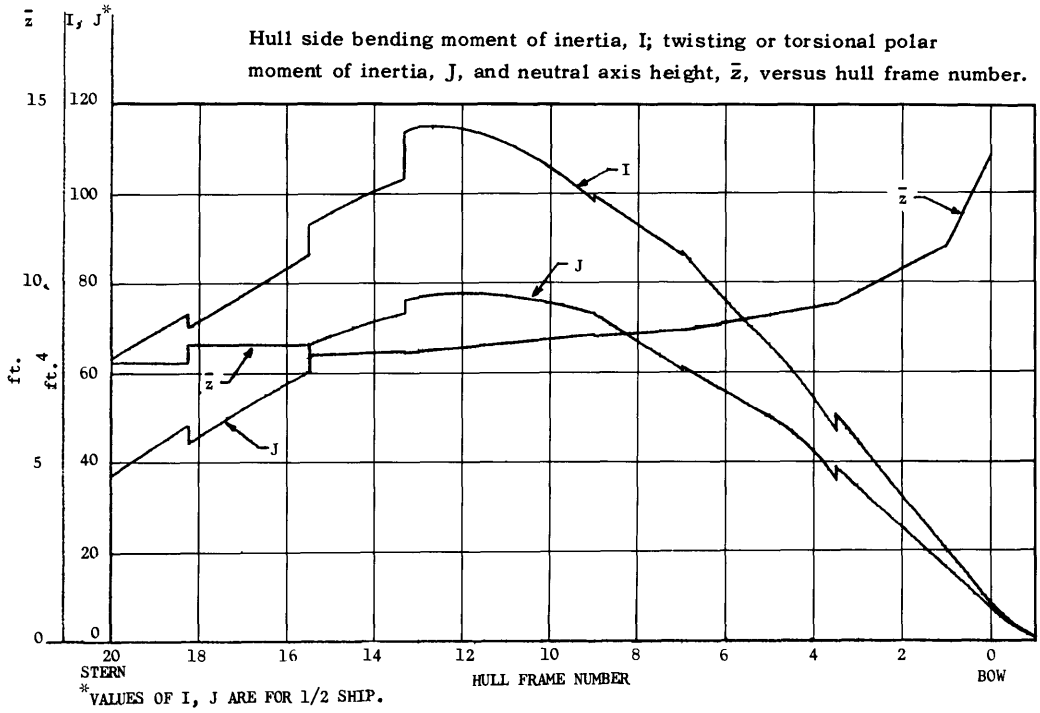

Figure 6B – Elastic Properties of the Hull Beam

For calculating I and J, plating dimensions were taken from References 16, 15 and 14 and longitudinal members dimensions and properties from References 15 and 14. Side bending moment was calculated from $I = \int y^2\, d\,A$ where y is the buttock line of each element of area $d\,A$, which carries longitudinal axial loads. J was determined according to the method of Reference 11, page 125.

Figures 7–16

Vibration Mode Shapes–Hull with No Mass Coupling– Rudder Disconnected

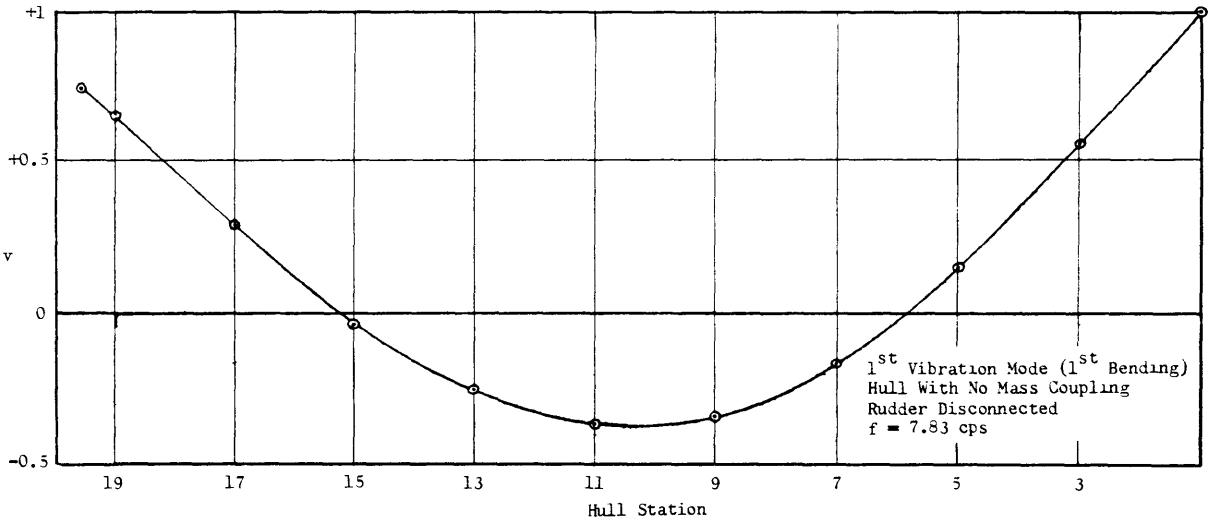

Figure 7

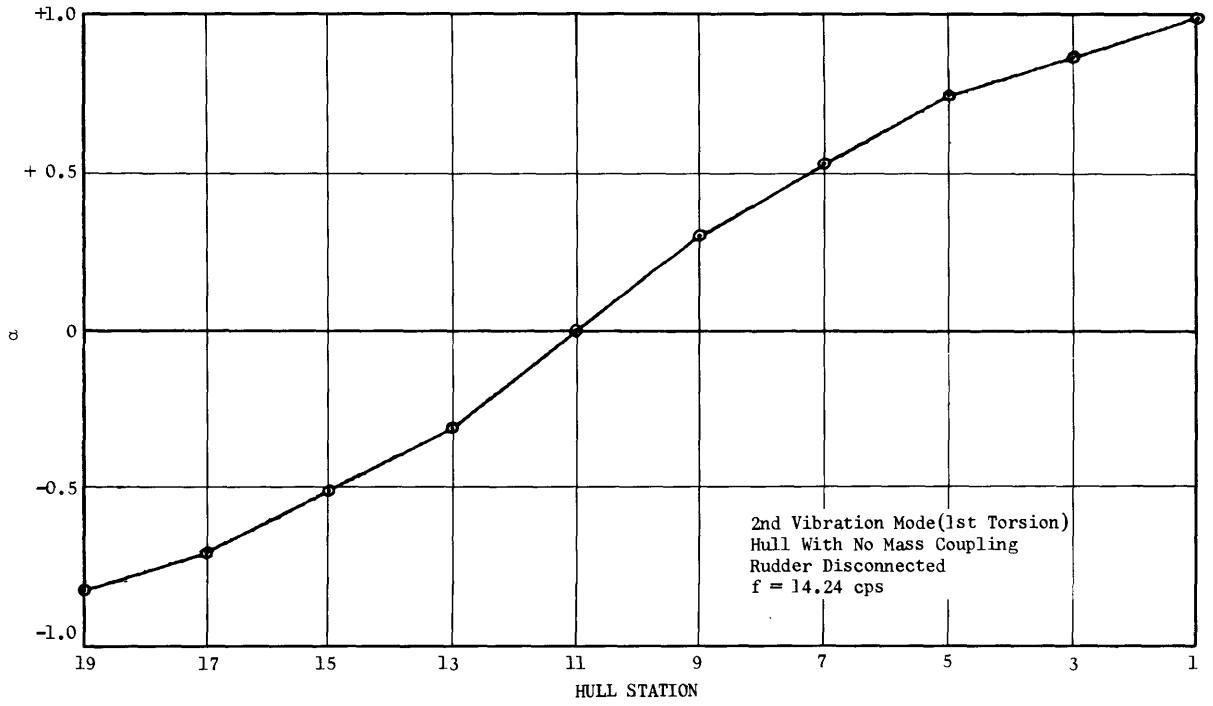

Figure 8

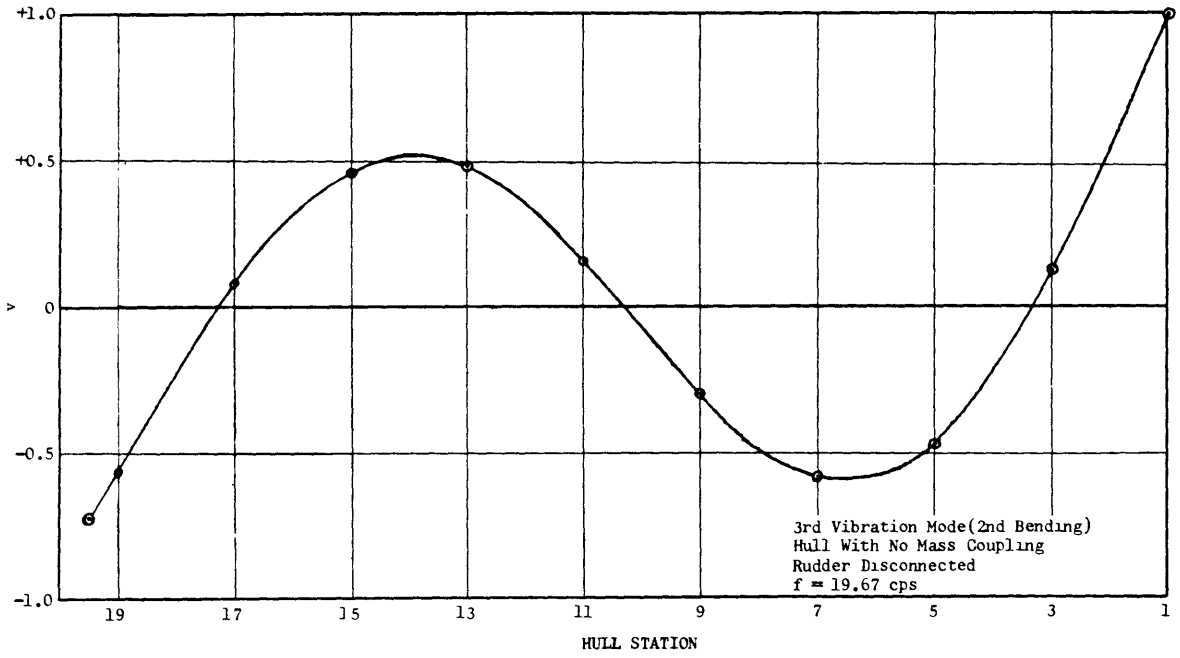

Figure 9

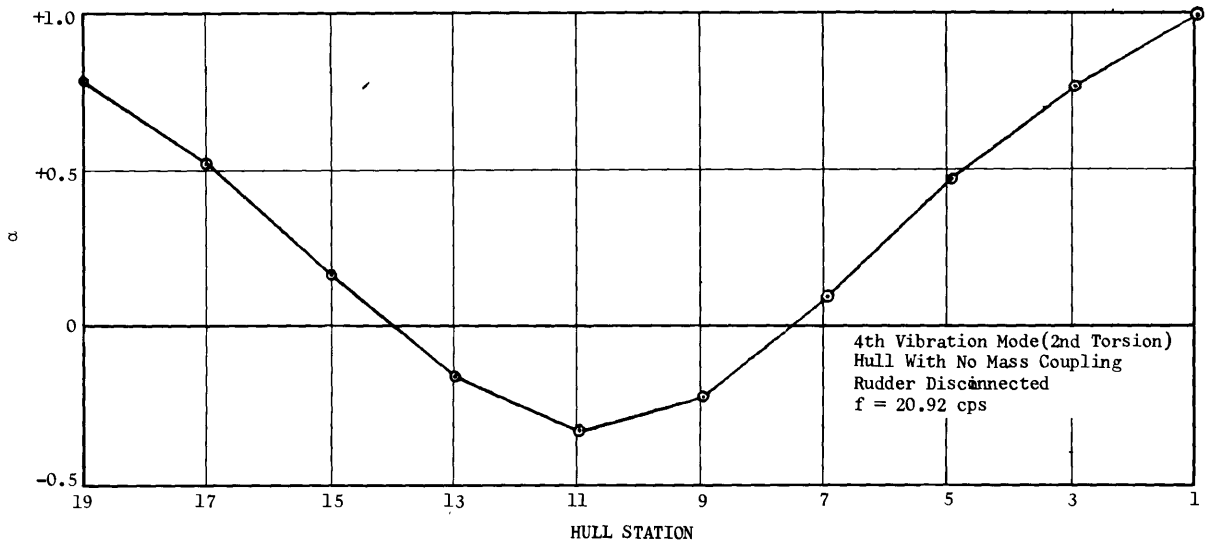

Figure 10

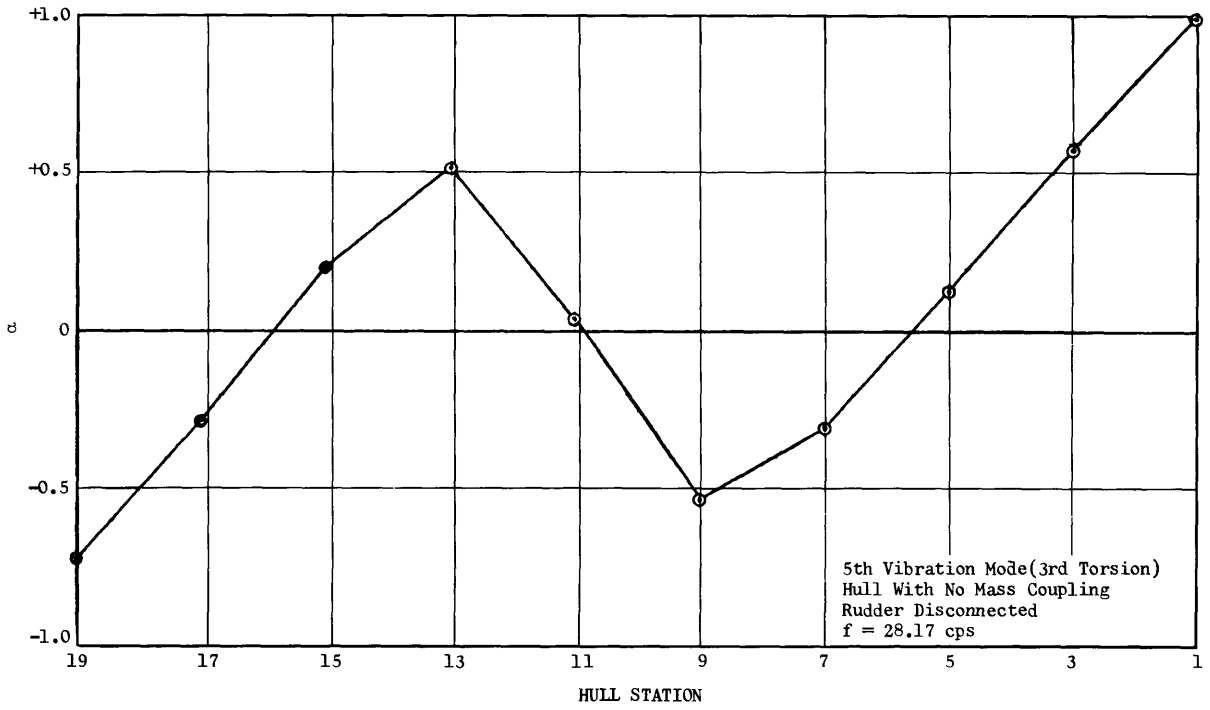

Figure 11

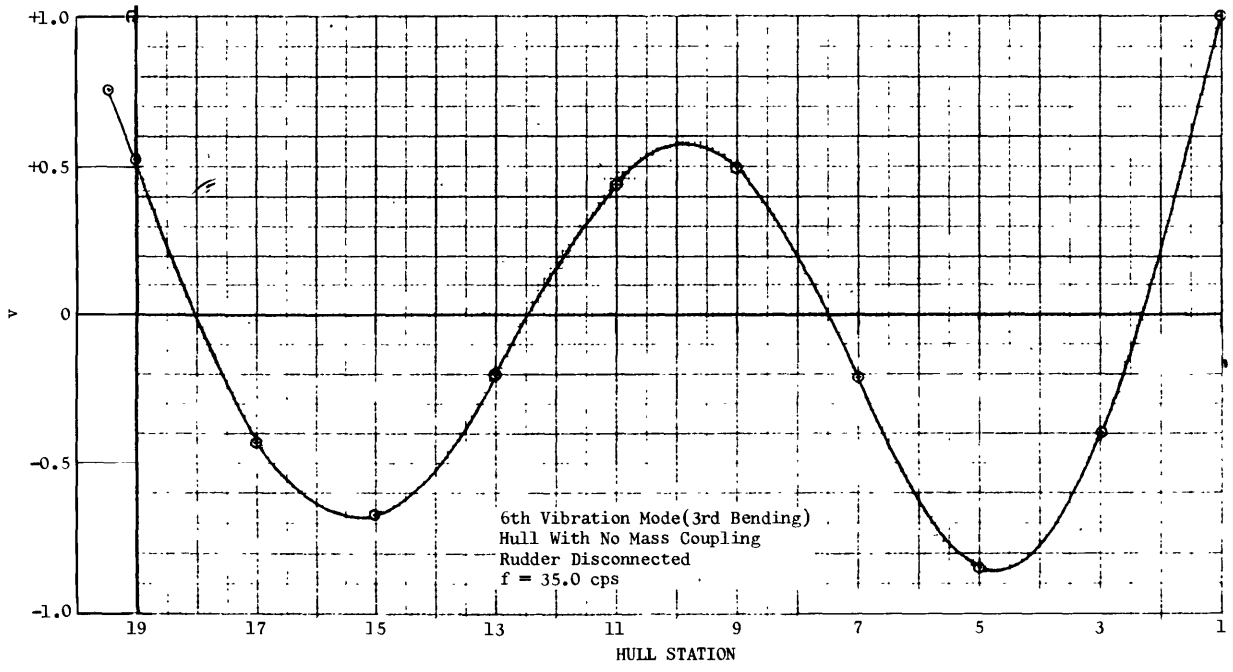

Figure 12

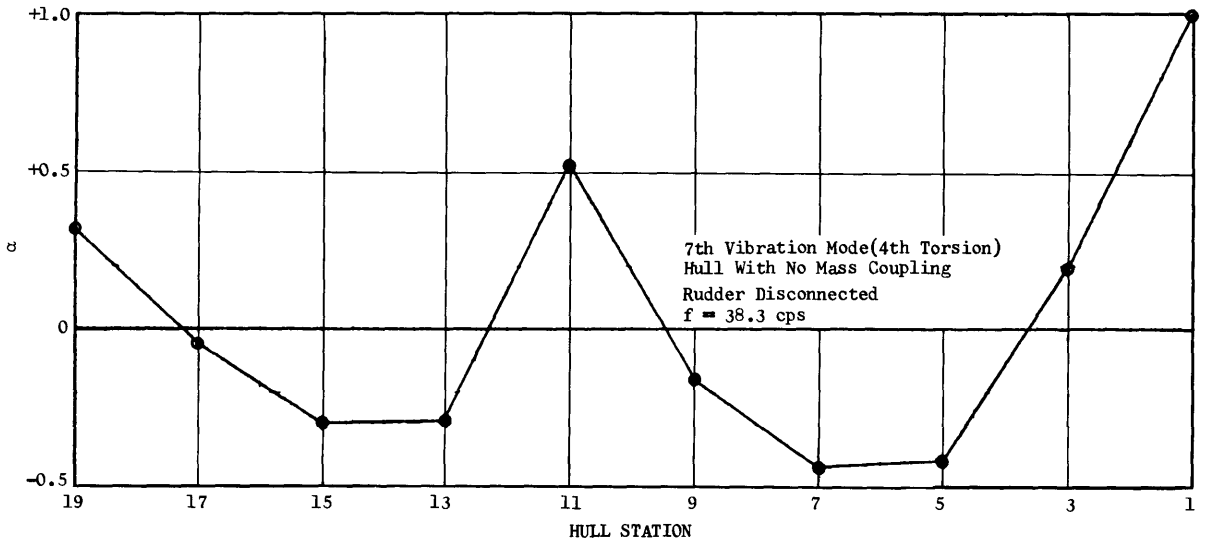

Figure 13

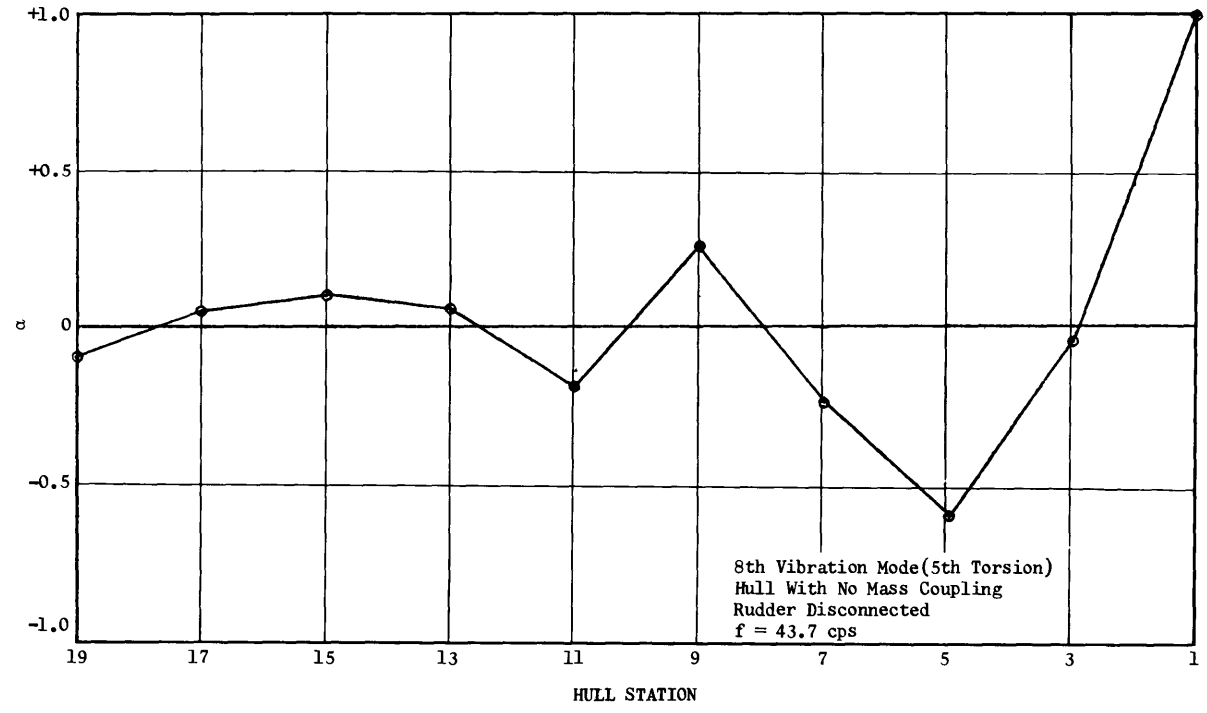

Figure 14

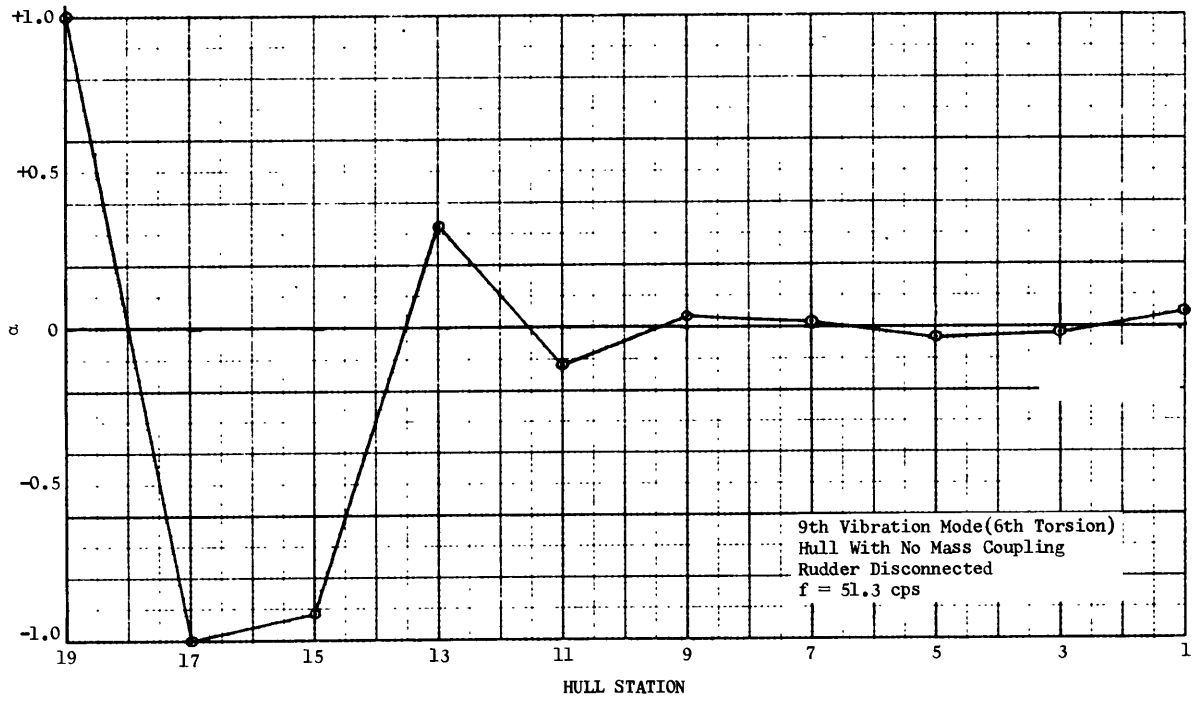

Figure 15

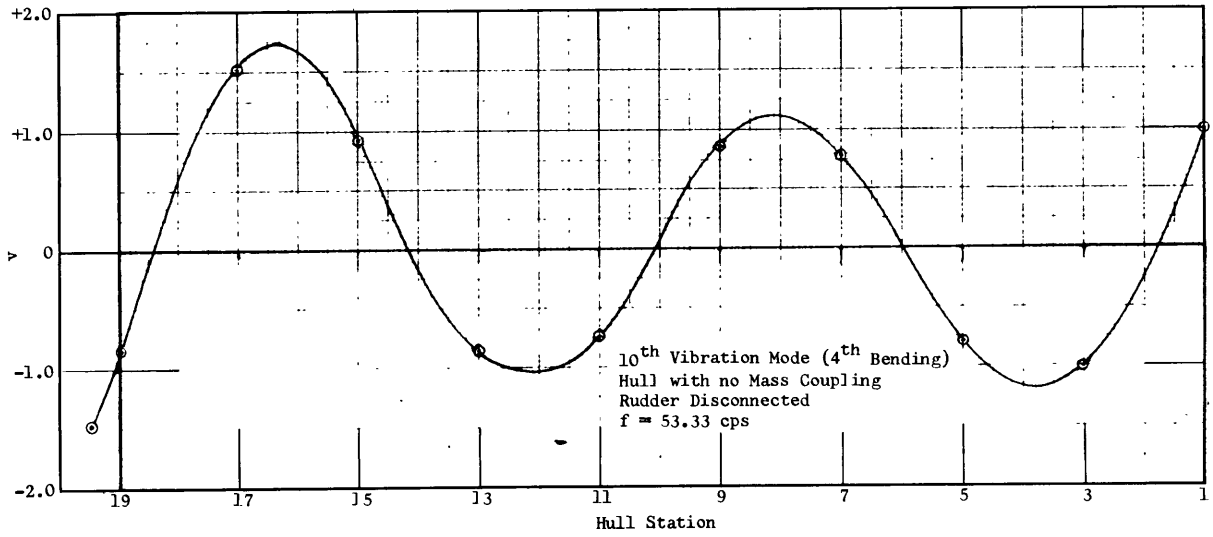

Figure 16

Figures 17–26

Vibration Mode Shapes–Basic Hull–Rudder Disconnected

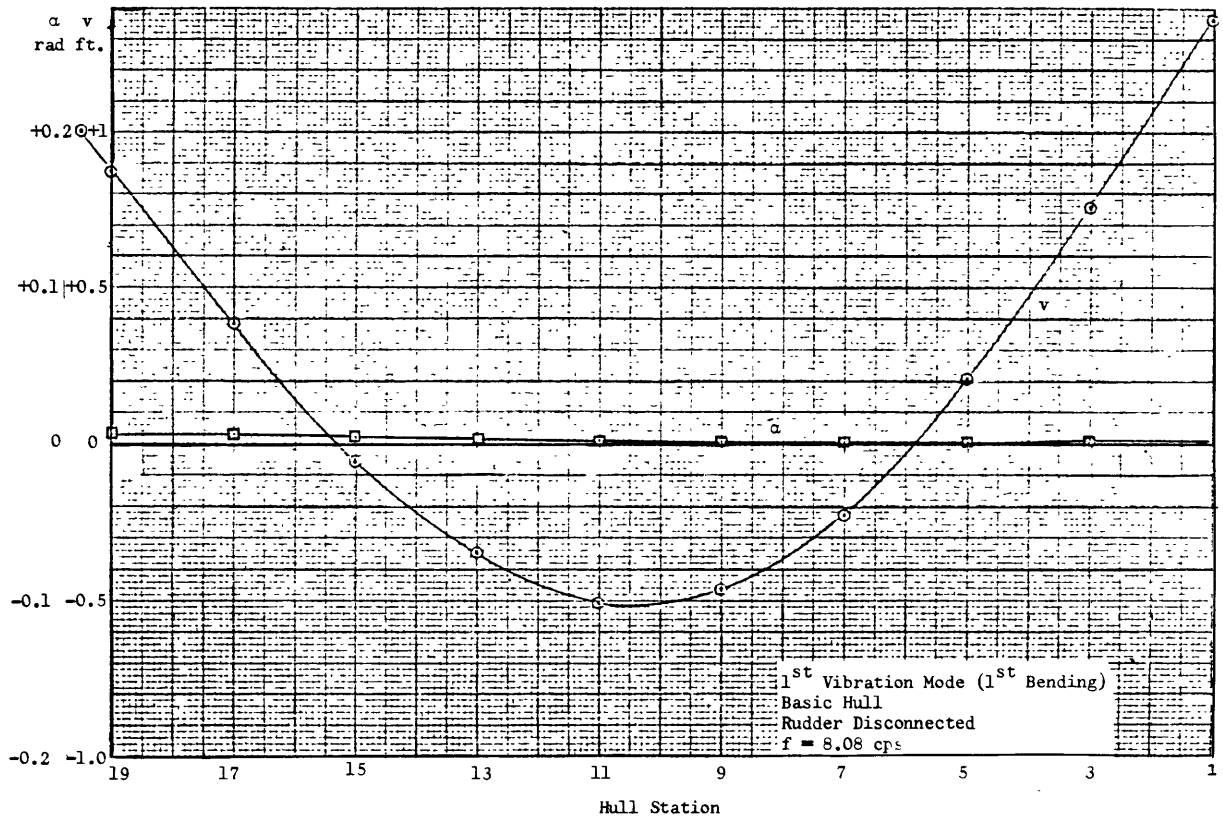

Figure 17

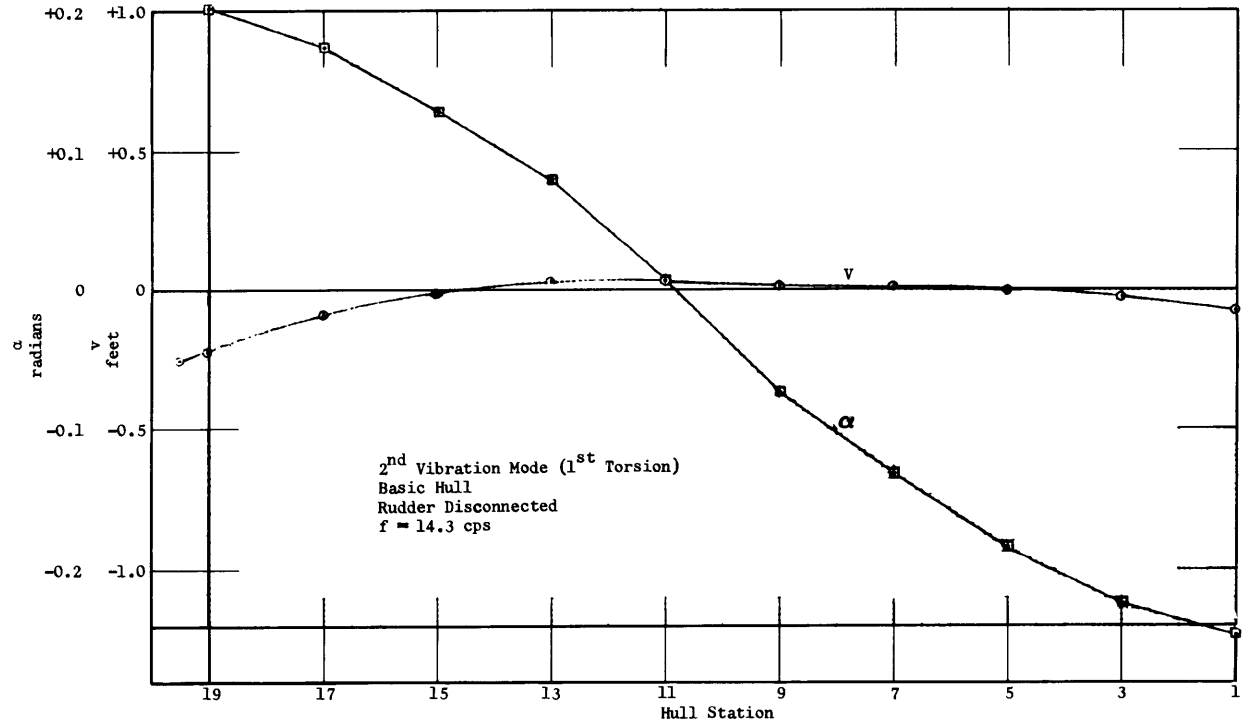

Figure 18

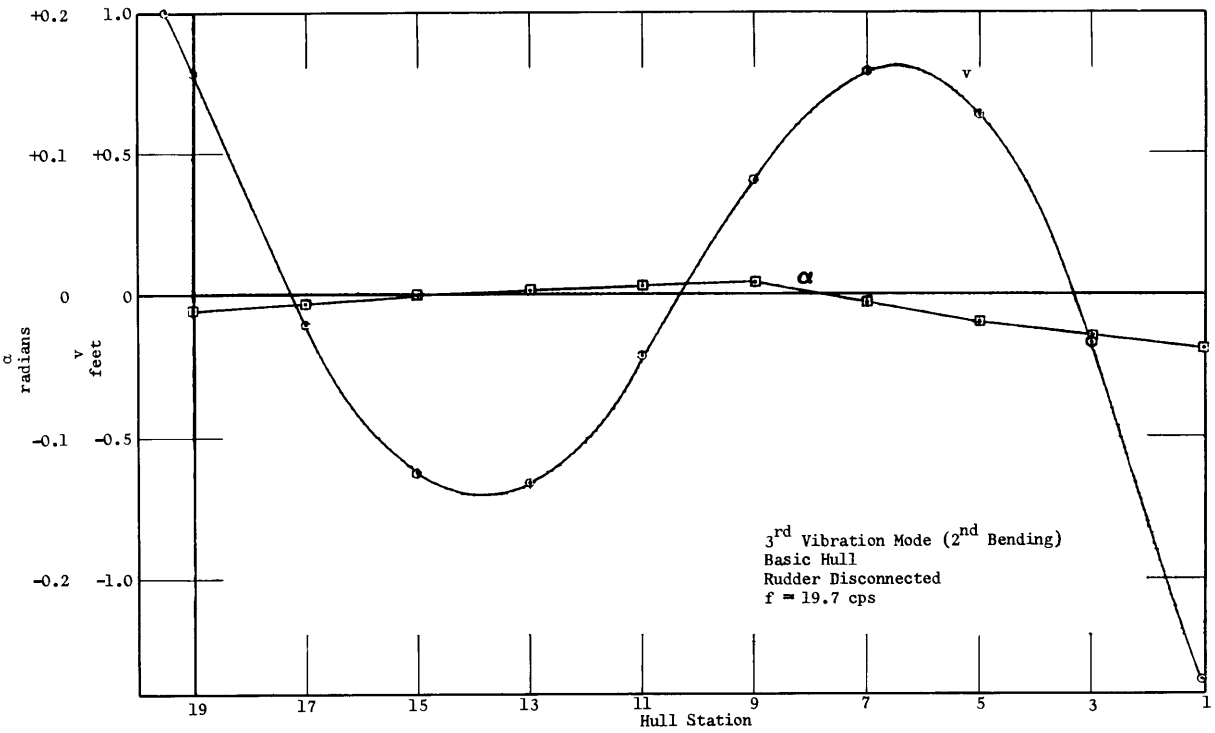

Figure 19

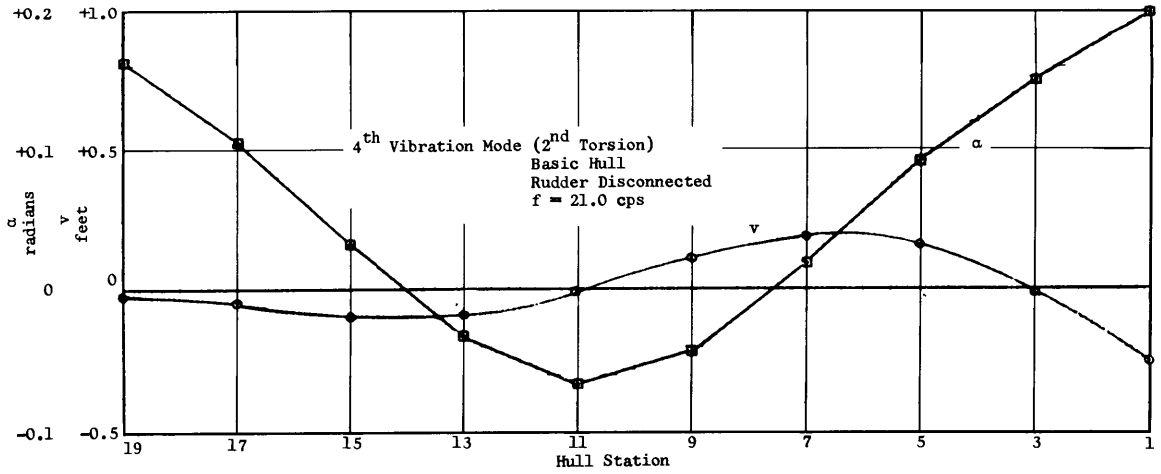

Figure 20

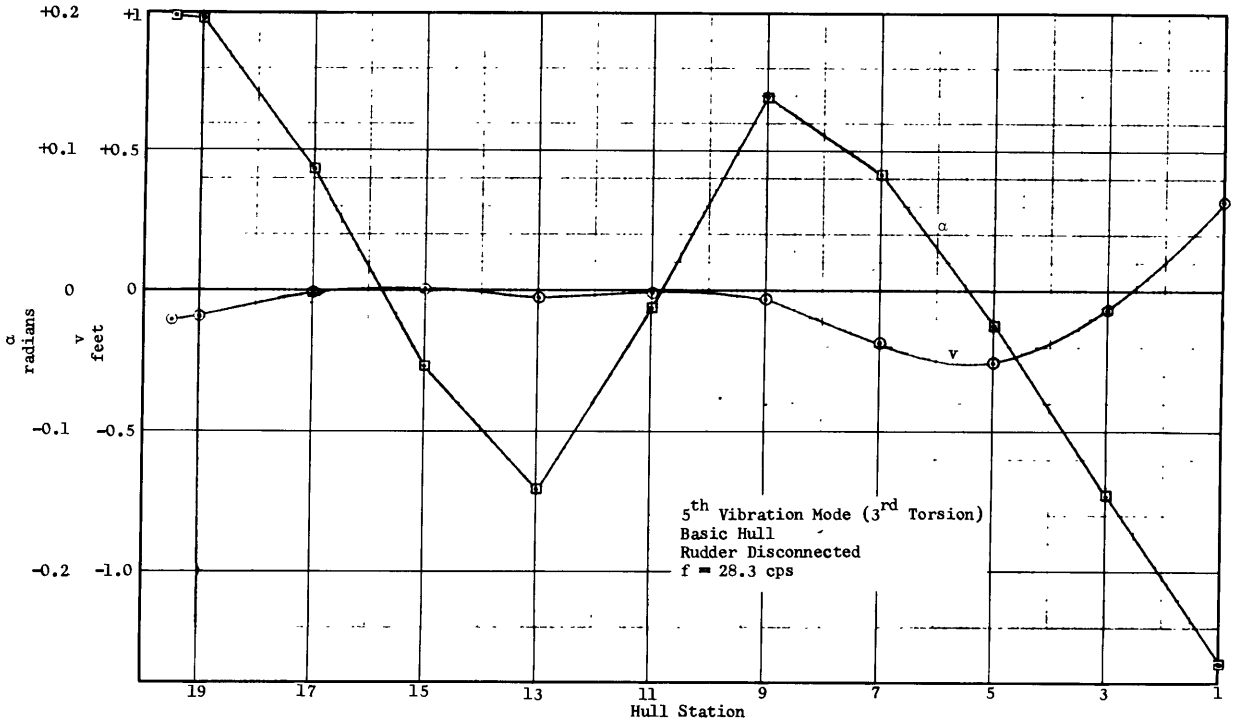

Figure 21

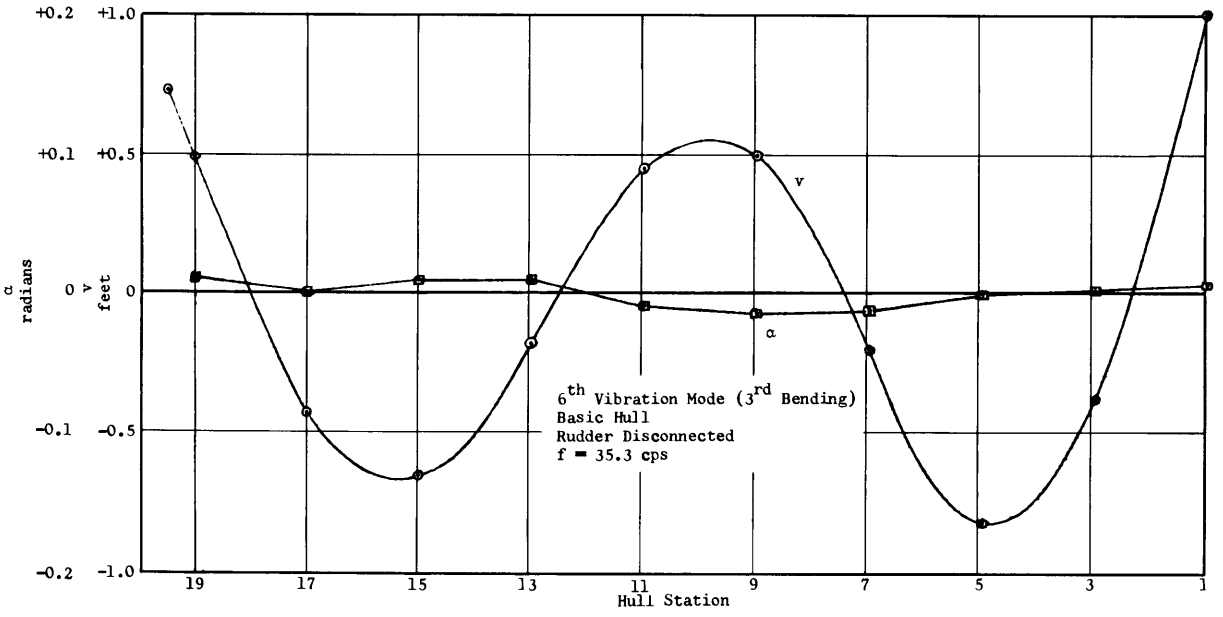

Figure 22

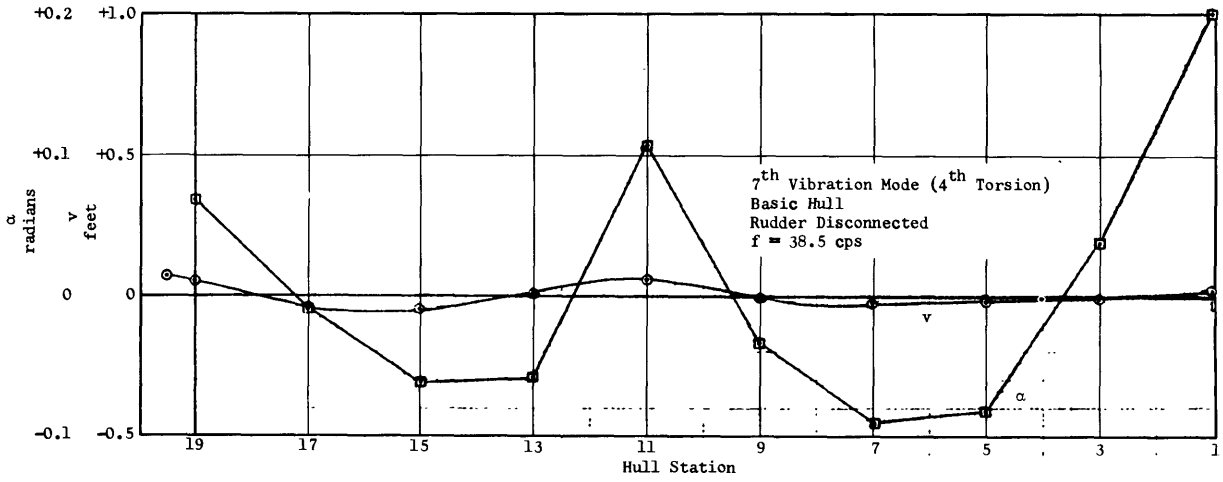

Figure 23

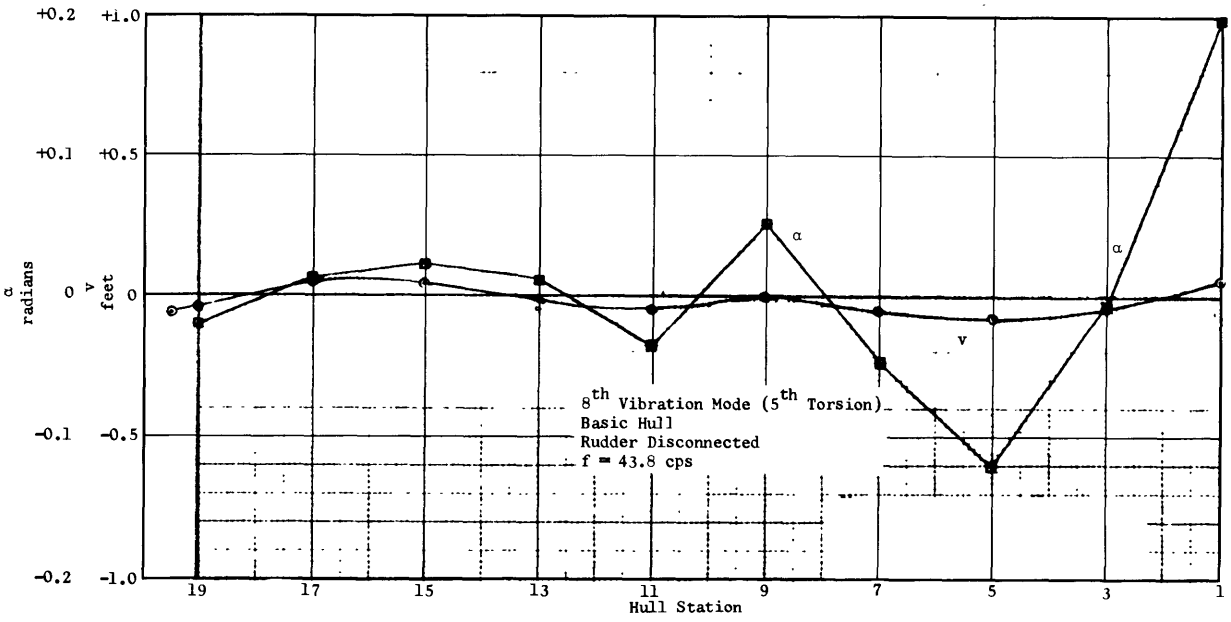

Figure 24

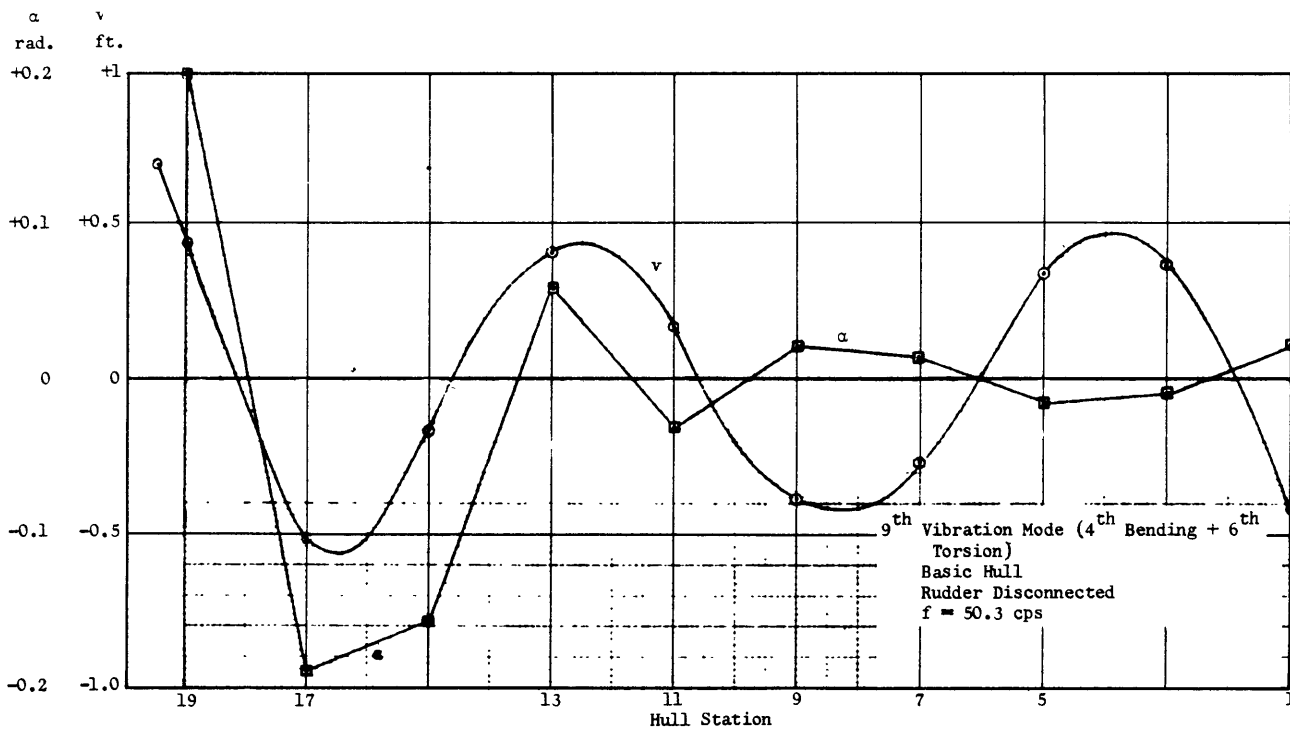

Figure 25

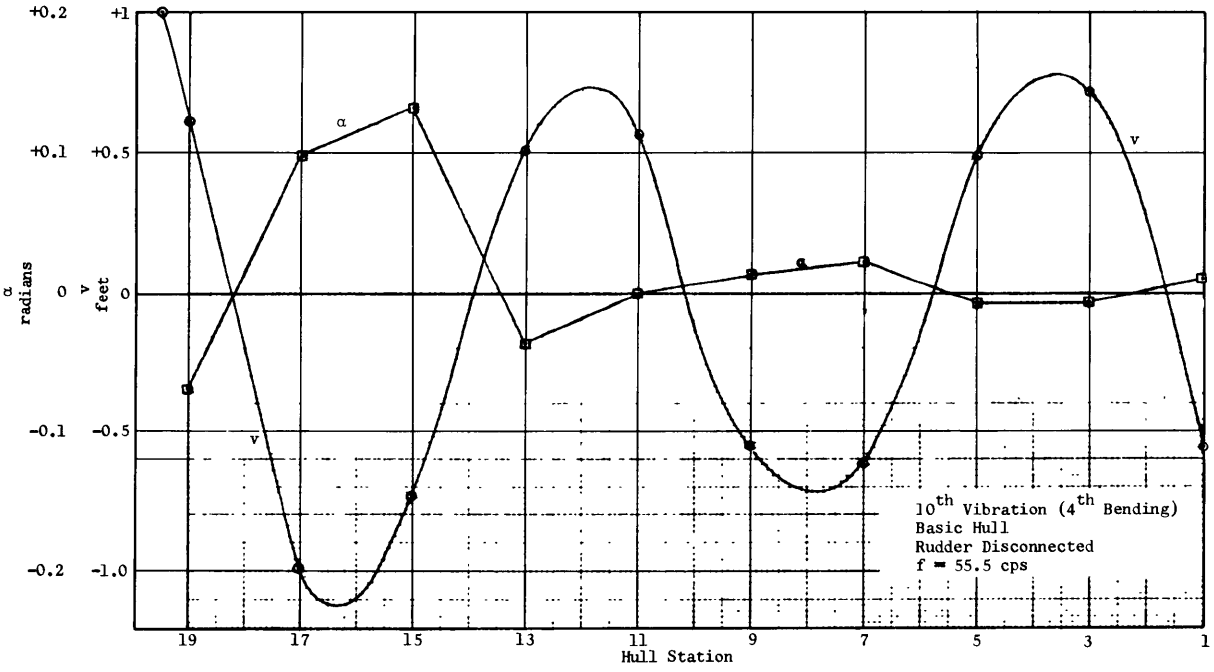

Figure 26

Figures 27–37

Vibration Mode Shapes–Basic Hull–Basic Rudder Connected

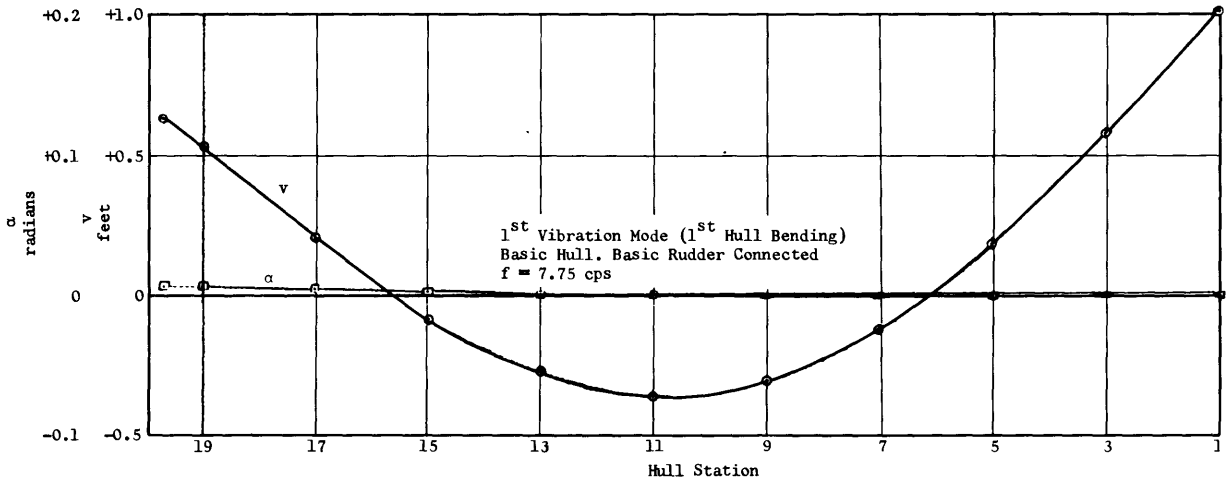

Figure 27

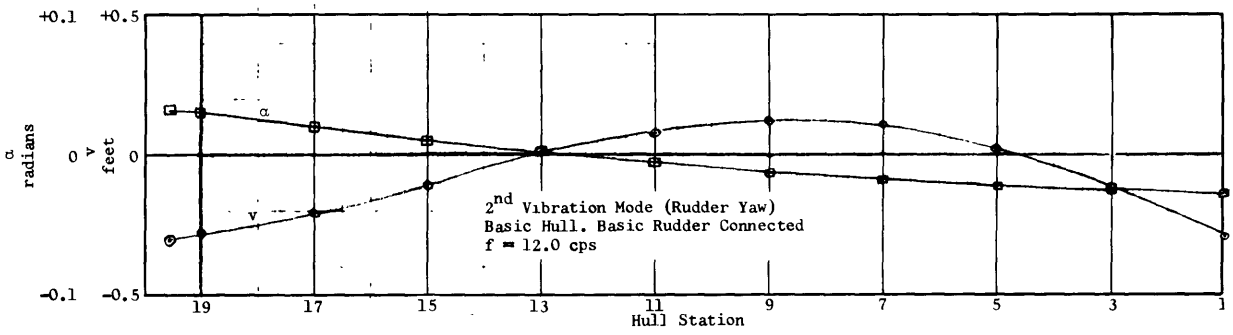

Figure 28

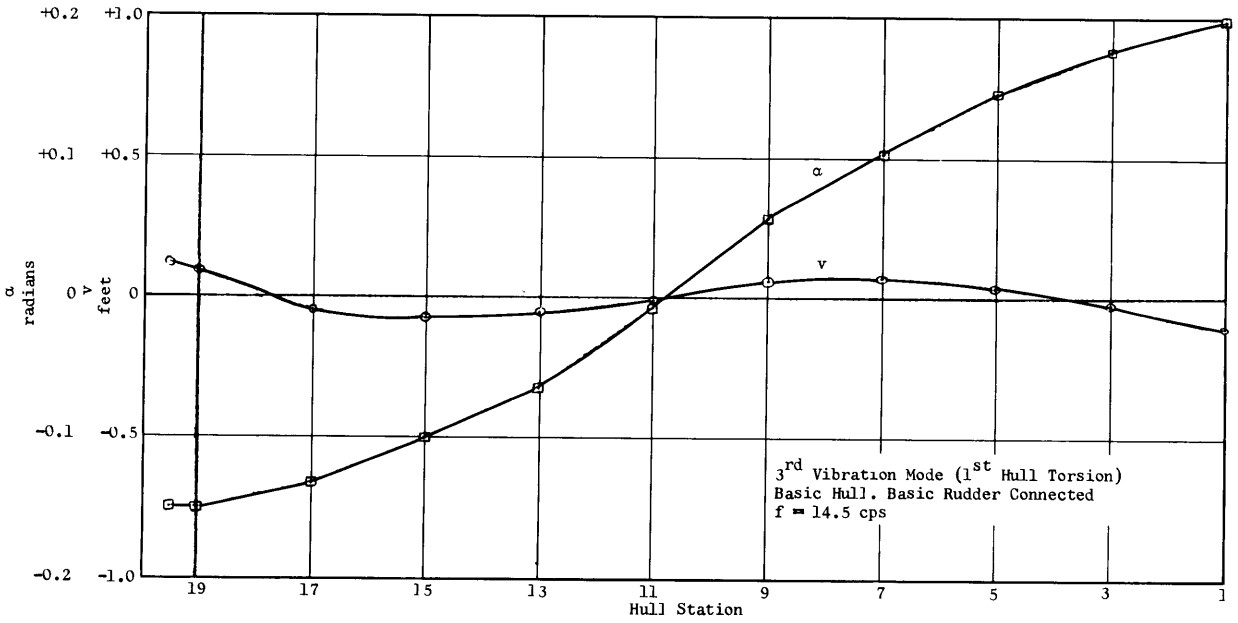

Figure 29

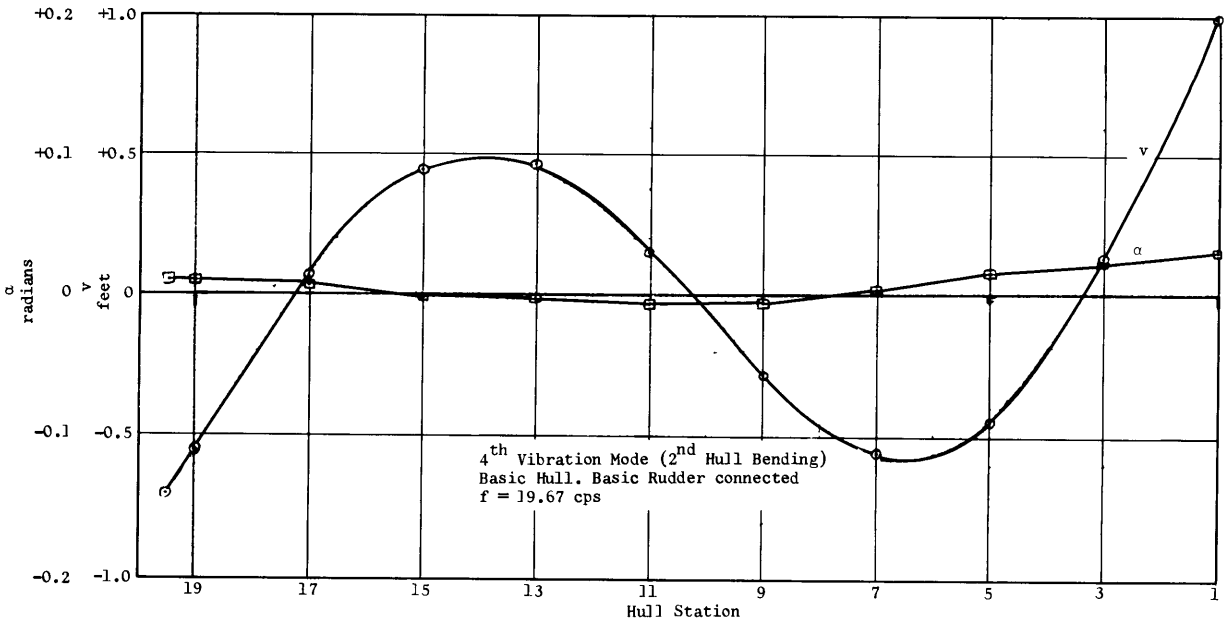

Figure 30

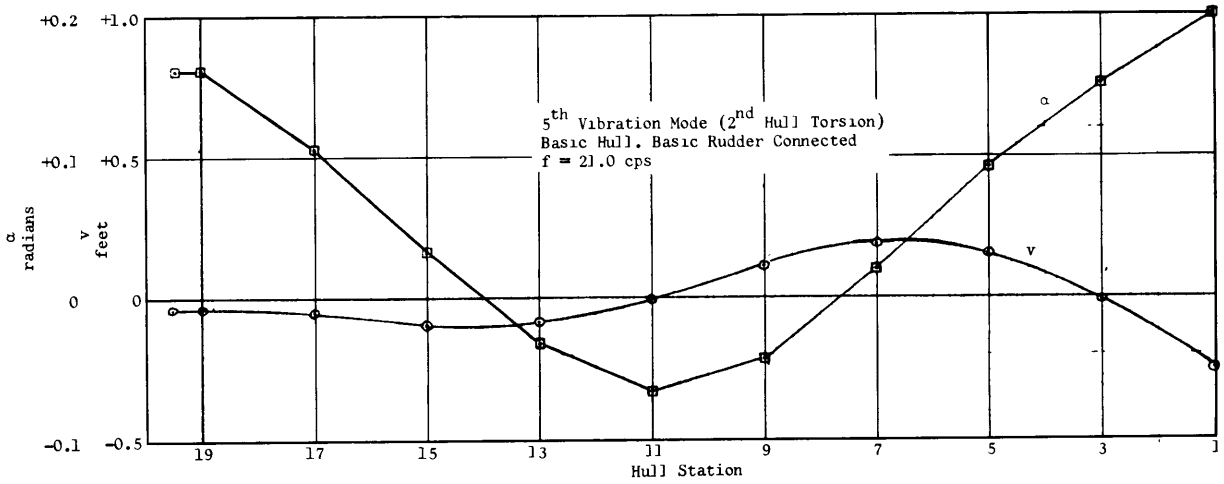

Figure 31

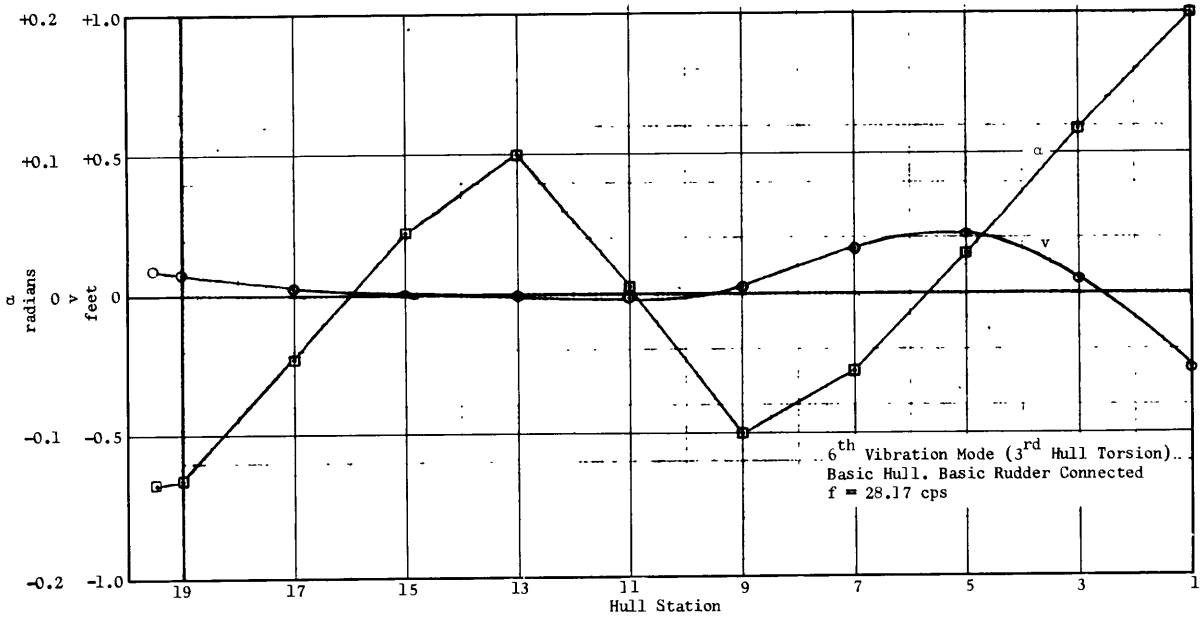

Figure 32

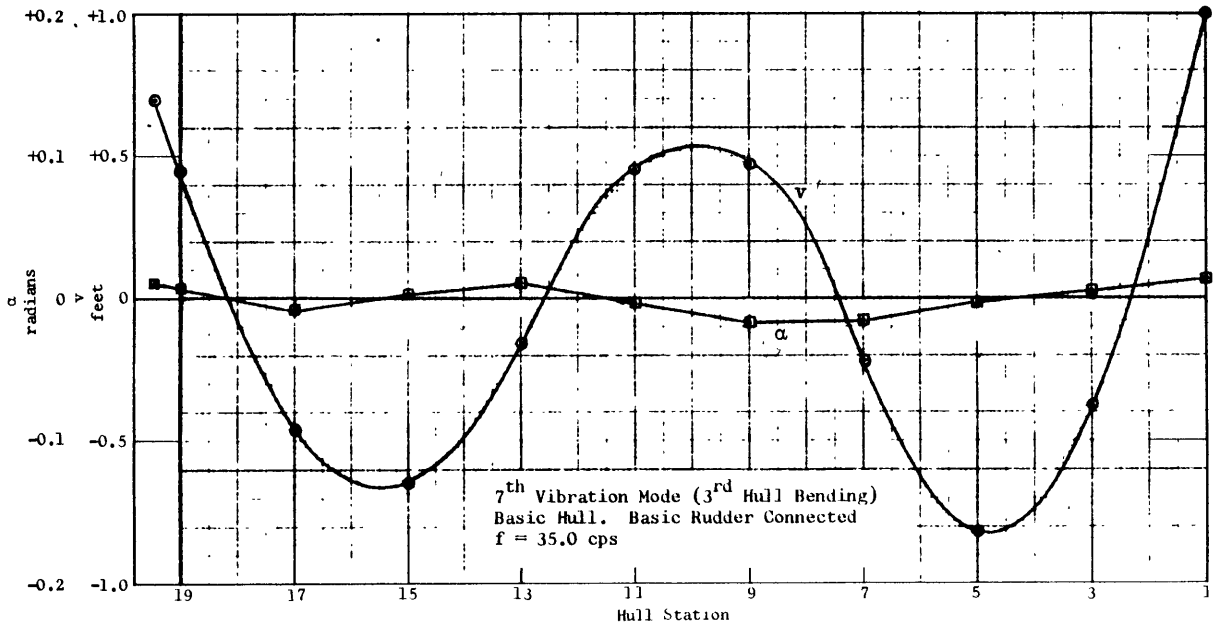

Figure 33

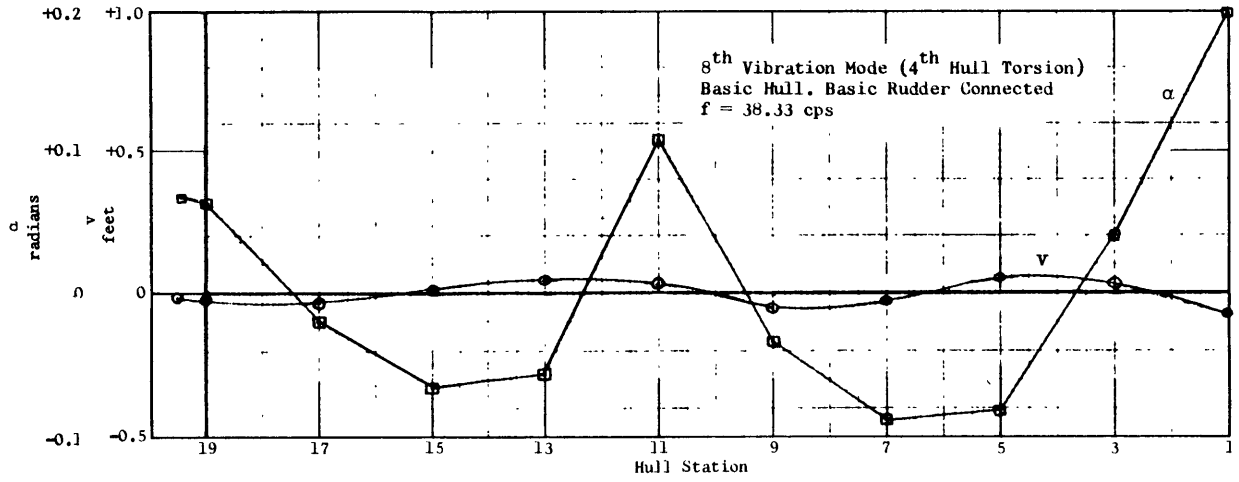

Figure 34

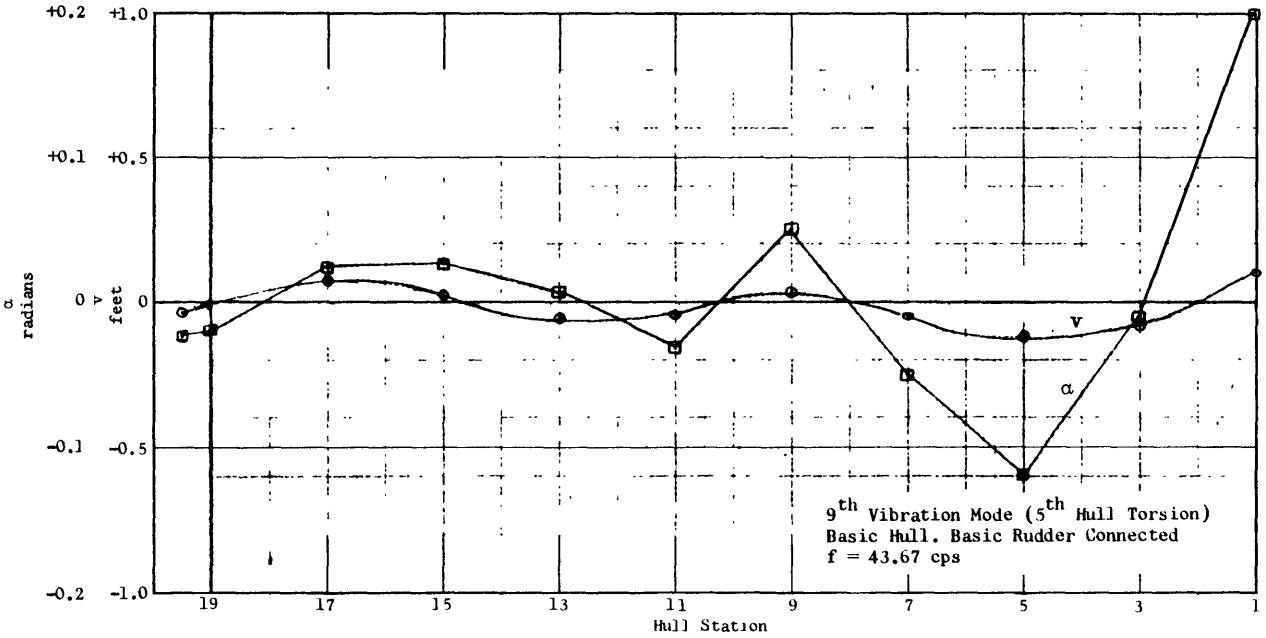

Figure 35

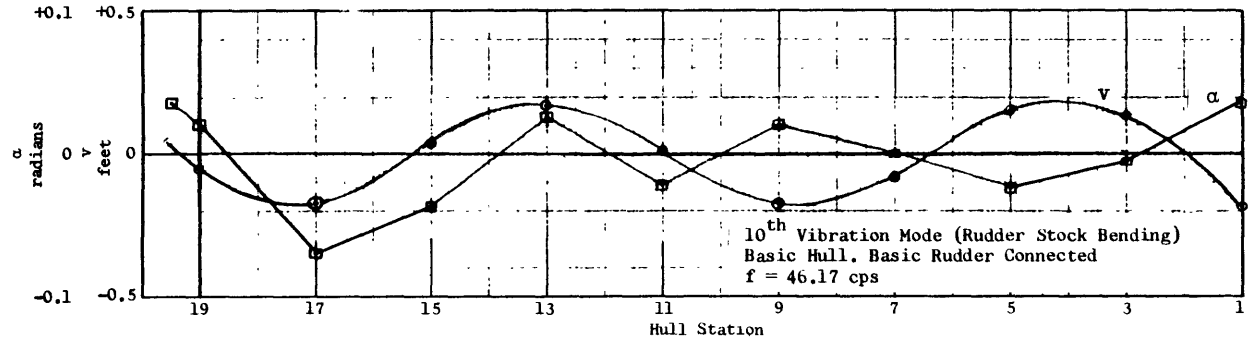

Figure 36

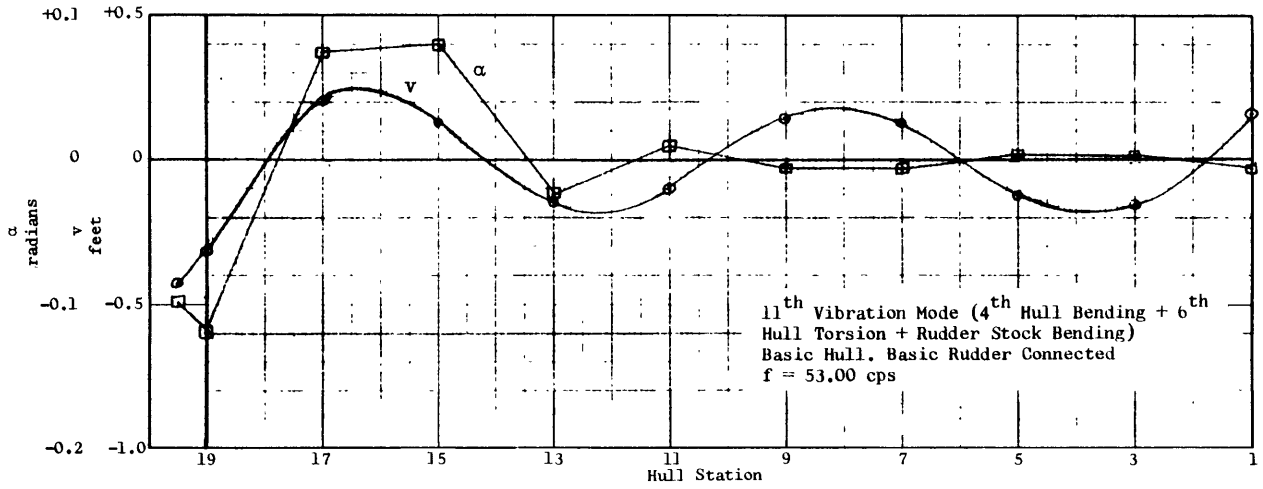
+0.1
+0.5
0
0
-0.1
-0.5
-0.2
-1.0
α
radians
v
feet
v
α
19
17
15
13
11
9
7
5
3
1
Hull Station
11th Vibration Mode (4th Hull Bending + 6th Hull Torsion + Rudder Stock Bending)
Basic Hull, Basic Rudder Connected
f = 53.00 cps

Figure 37

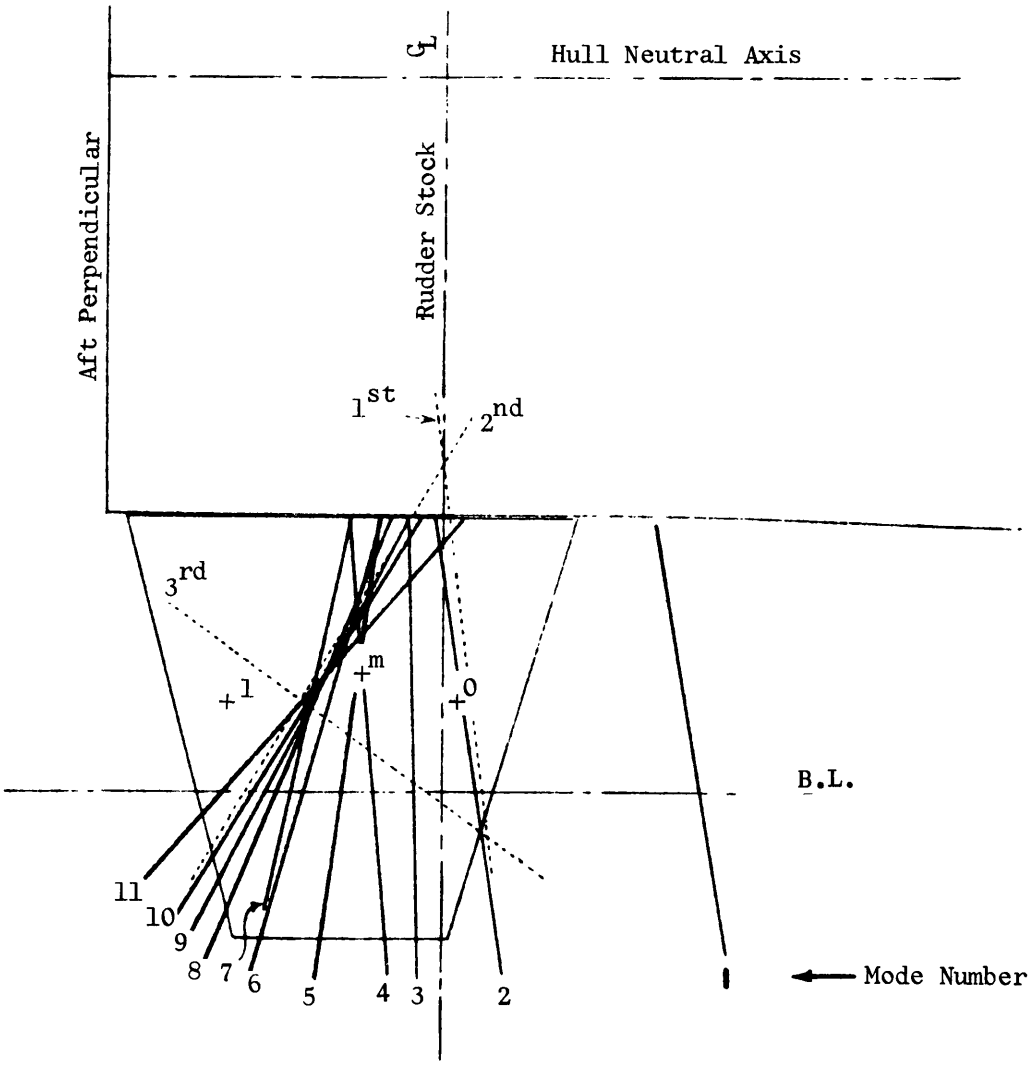

——— Node lines of first 11 modes, basic hull and rudder. (23 degrees of freedom)

--------- Node lines, hull rigid and clamped. (3 degrees of freedom)

$+^0$ Basic location, center of pressure

$+^1$ Basic location, rotation center

$+^m$ Basic location, center of mass

Figure 38 – Node Lines of the Rudder in Natural Vibration Modes

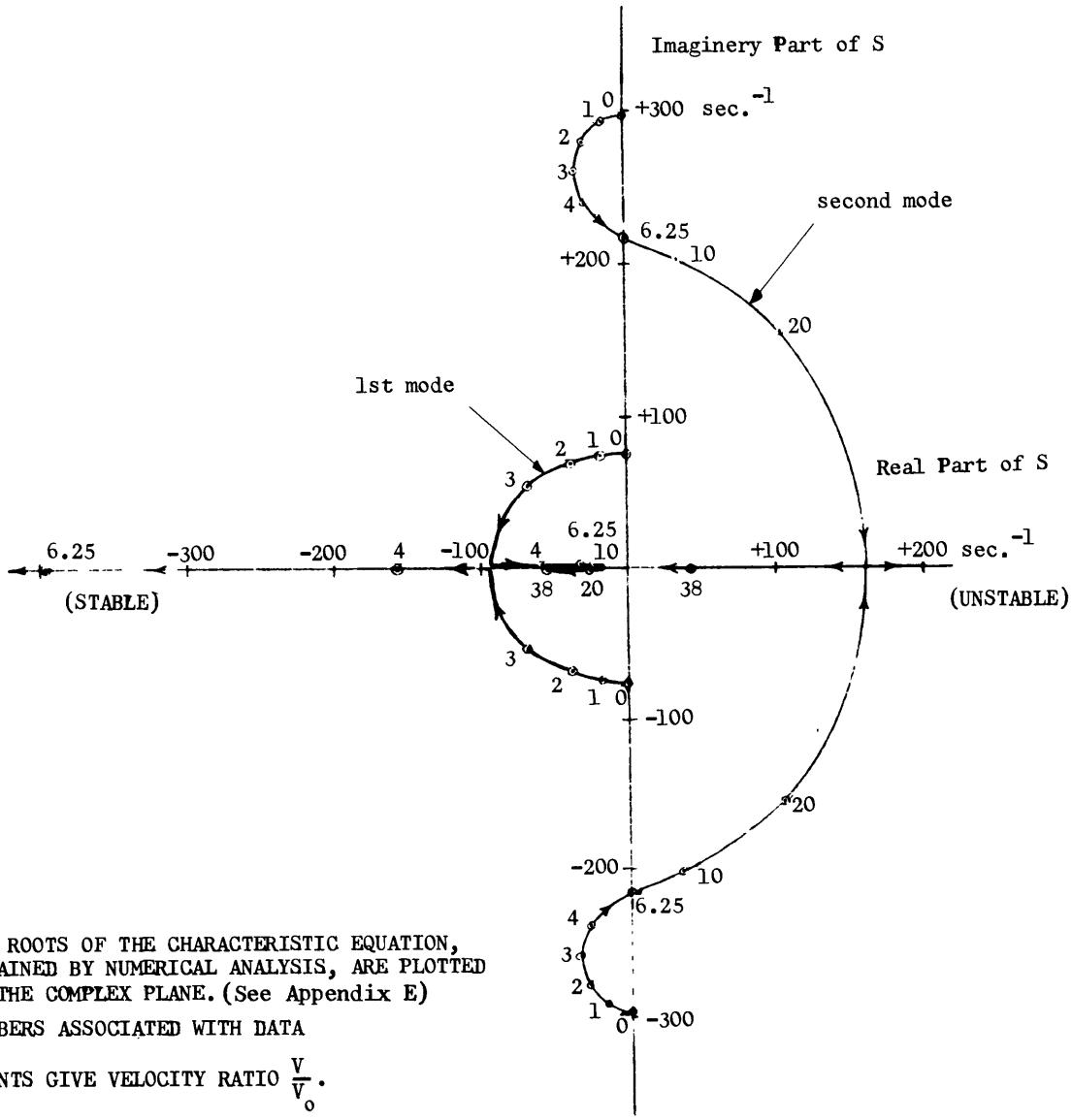

Figure 39 – Plot of Roots in Complex Plane–Basic Case (2 Degrees of Freedom)

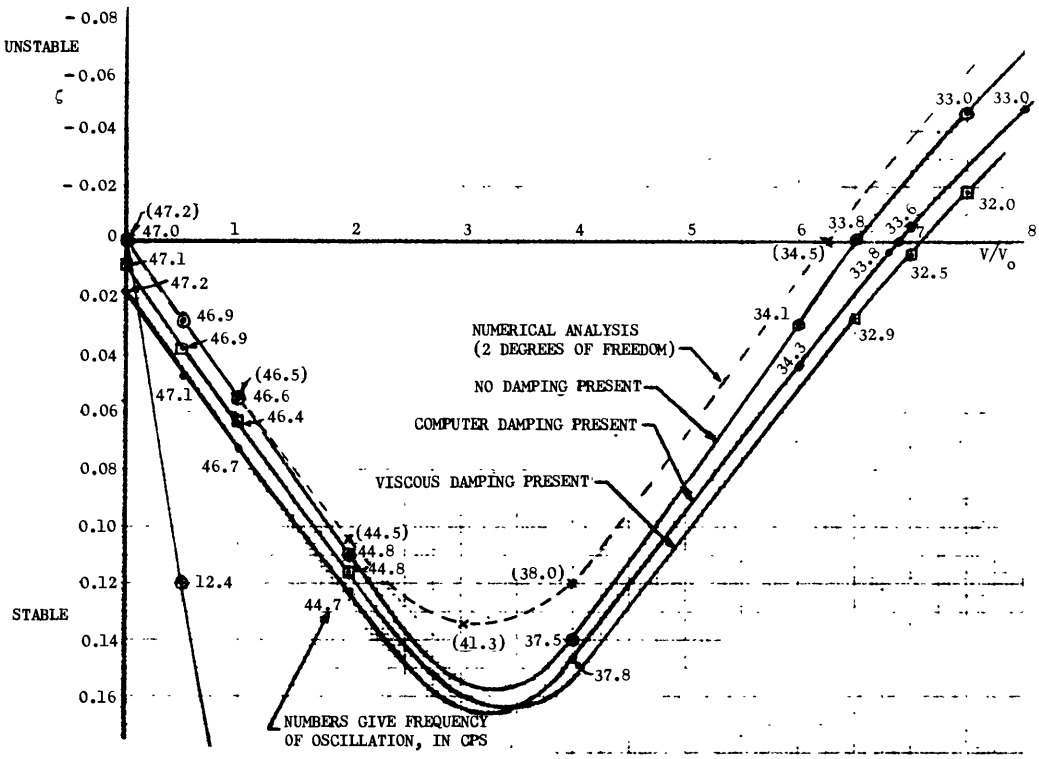

Figure 40 – Effects of Damping (Nonvelocity-Dependent) on ζ-V Curve– Three Degrees of Freedom

HEADING OF CURVE	EXPLANATION
No Damping Present	The basic analog circuit, with passive elements for the mass and inertia terms, and active elements representing the hydrodynamic forces (classes 2 and 3 in Section IV) was set up. In addition, negative resistance elements were carefully adjusted at coordinates v_o and γ to compensate for the effects of computer damping n ormally present in the passive elements in order to achieve neutral stability at zero ship's velocity for the first two vibration modes.
Computer Damping Present	Same as above, but with no negative resistance elements to com-ensate for the normal computer damping of the passive elements.
Viscous Damping Present	Identical to the situation "No Damping Present," except that the values of viscous damping parameters opposing rudder lateral motion $\dot{v}$ and yaw motion, $\dot{\gamma}$ were added to the following extent (see Appendix B, Item 7): D_f = 18,860 lb sec ft and D_m = 665 lb sec ft

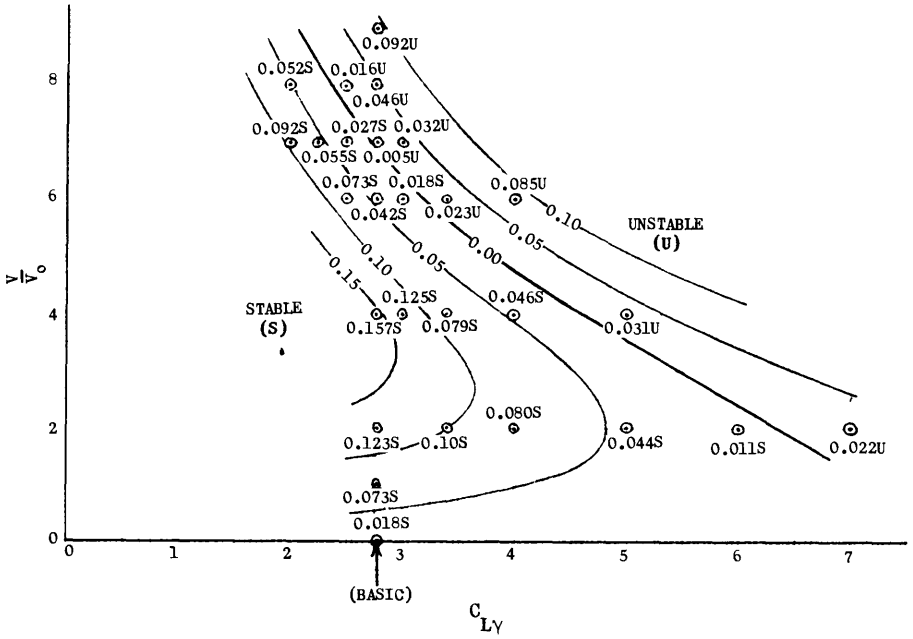

Figure 41 – Contours of Constant ζ–Lift Coefficient $C_{L\gamma}$ versus V/V_o– Three Degrees of Freedom

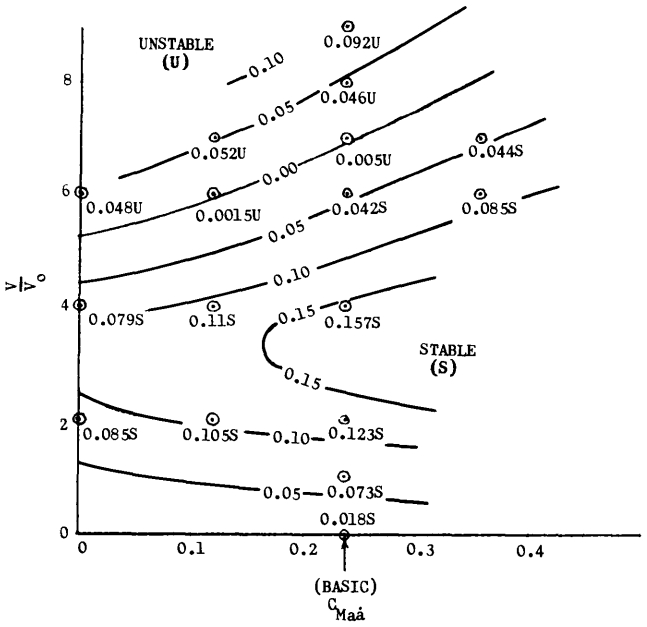

Figure 42 – Contours of Constant ζ–Moment Coefficient $C_{M\alpha\dot{\alpha}}$ versus V/V_o– Three Degrees of Freedom

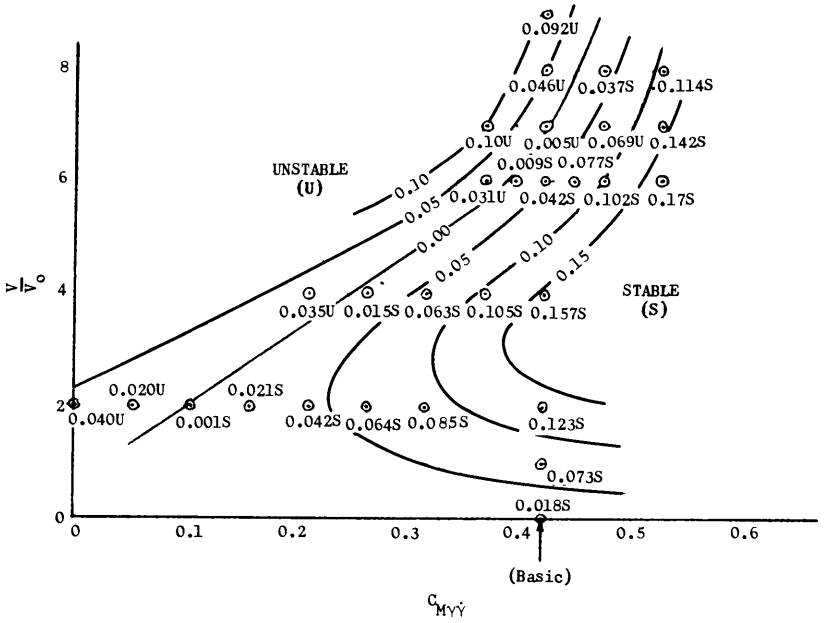

Figure 43 – Contours of Constant ζ–Moment Coefficient $C_{M\gamma\dot{\gamma}}$ versus V/V_o– Three Degrees of Freedom

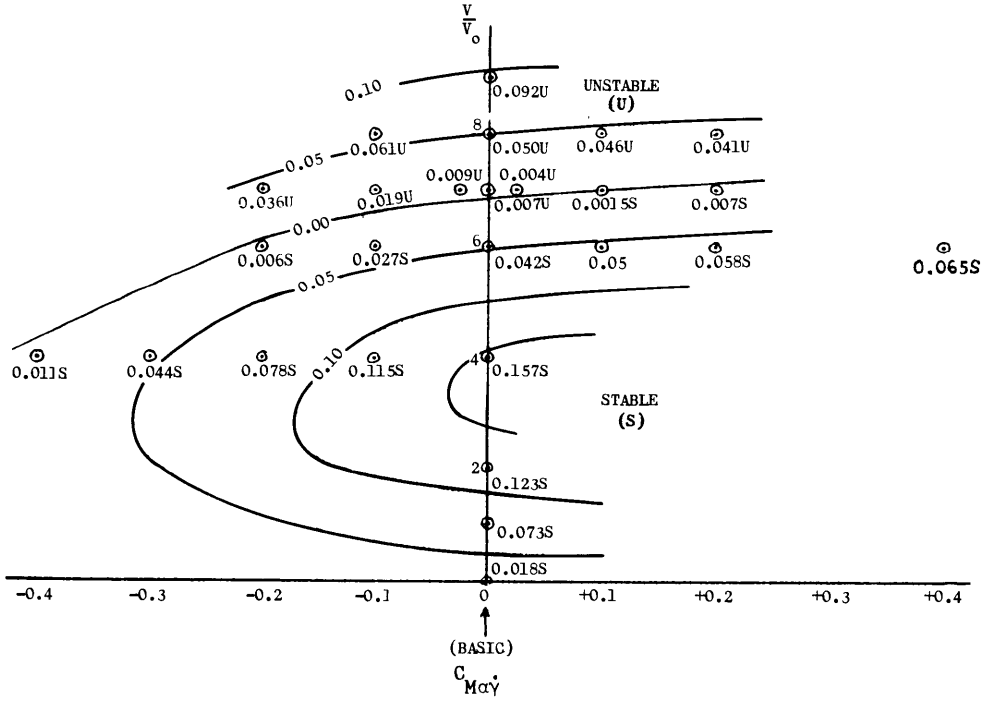

Figure 44 – Contours of Constant ζ–Moment Coefficient $C_{M\alpha\dot{\gamma}}$ versus V/V_o– Three Degrees of Freedom

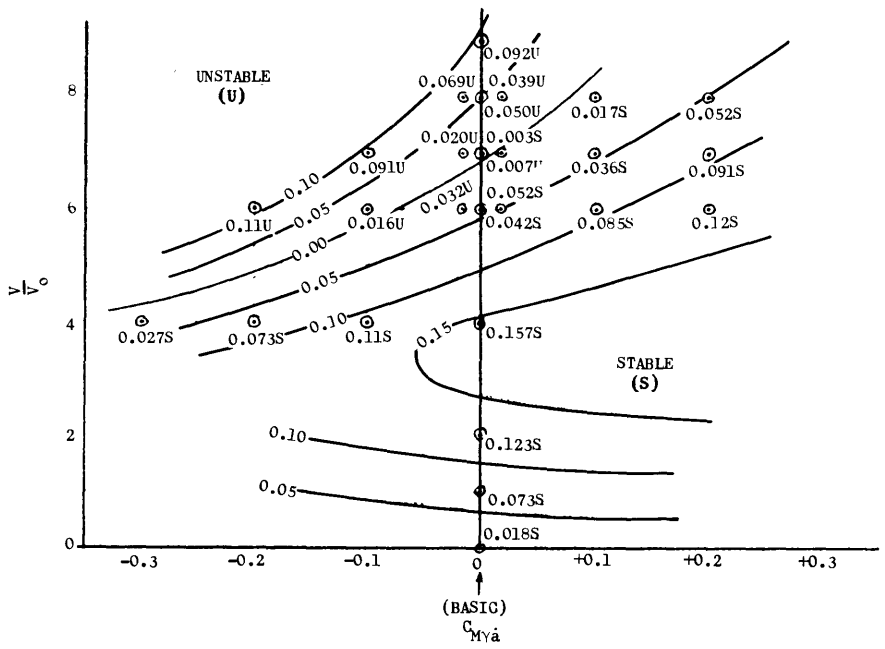

Figure 45 – Contours of Constant ζ–Moment Coefficient $C_{M\dot{\gamma}\dot{\alpha}}$ versus V/V_o– Three Degrees of Freedom

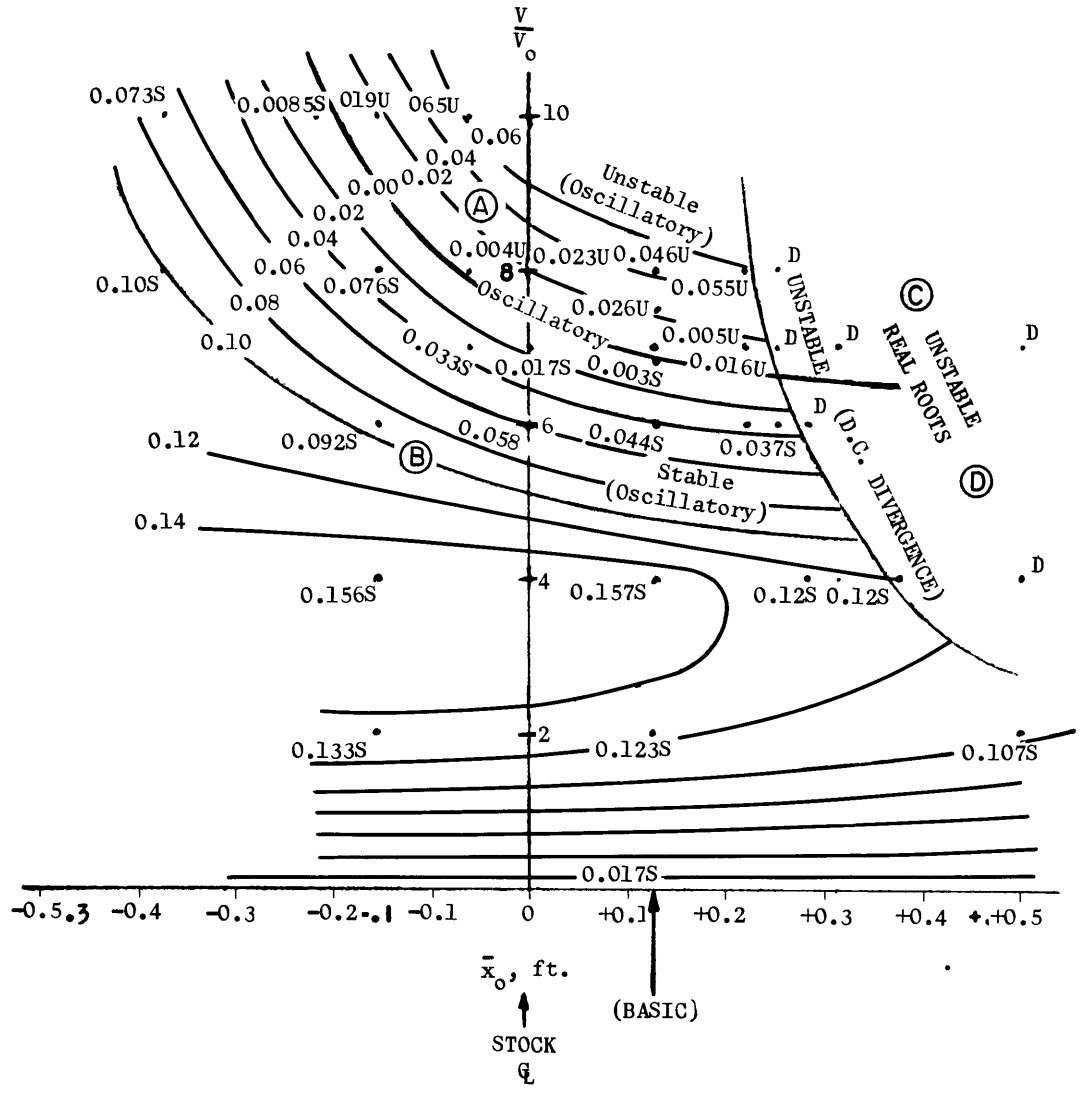

Figure 46 – Contours of Constant ζ–Fore and Aft Location of Center of Pressure, $\bar{x}_o$ versus V/V_o–Three Degrees of Freedom

NOTE:
FIGURE 46 IS DEVIDED INTO 4 QUADRANTS A, B, C, D AS DESIGNATED.

---- STABLE REAL ROOT
—— UNSTABLE OSCILLATORY ROOT

Ⓐ HAS STABLE REAL ROOTS BUT UNSTABLE OSCILLATORY ROOTS.

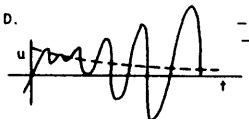

Ⓑ HAS BOTH STABLE REAL AND OSCILLATORY ROOTS.

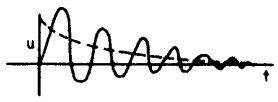

Ⓒ HAS BOTH UNSTABLE REAL AND OSCILLATORY ROOTS.

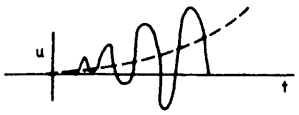

Ⓓ HAS UNSTABLE REAL ROOTS BUT STABLE OSCILLATORY ROOTS.

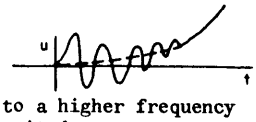

The third root was ignored since it corresponds to a higher frequency mode which was discriminated against by not being excited.

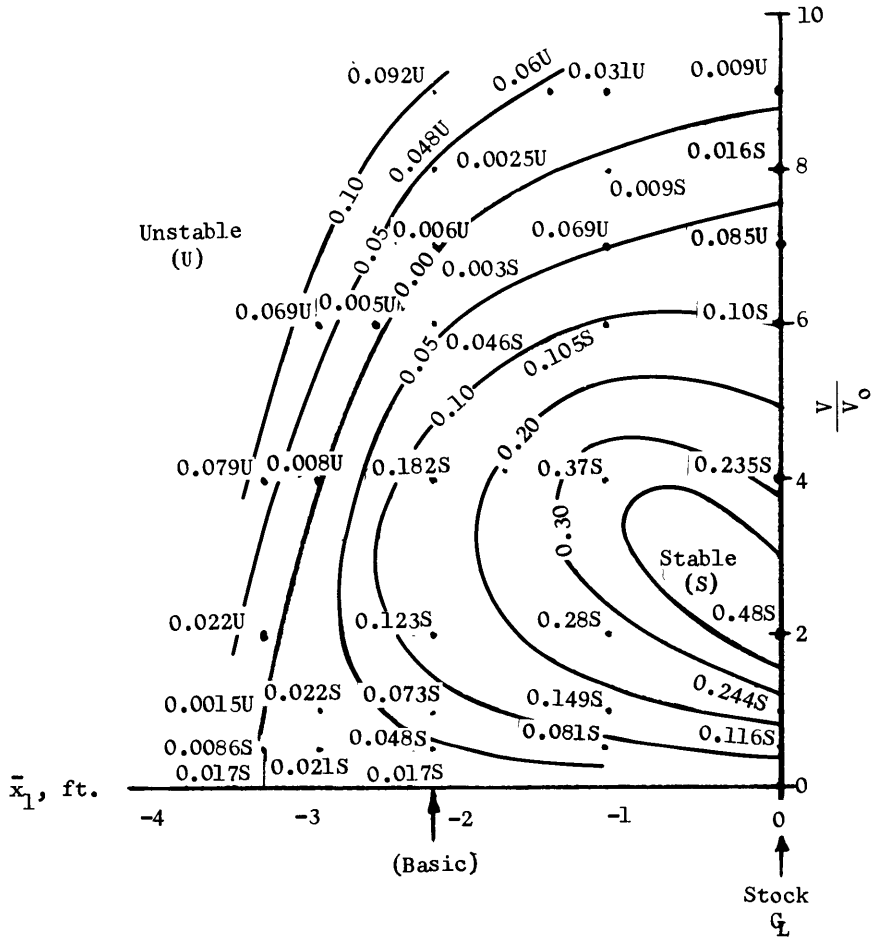

Figure 47 – Contours of Constant ζ–Fore and Aft Location of Rotation Center, $\bar{x}_1$ versus V/V_o–Three Degrees of Freedom

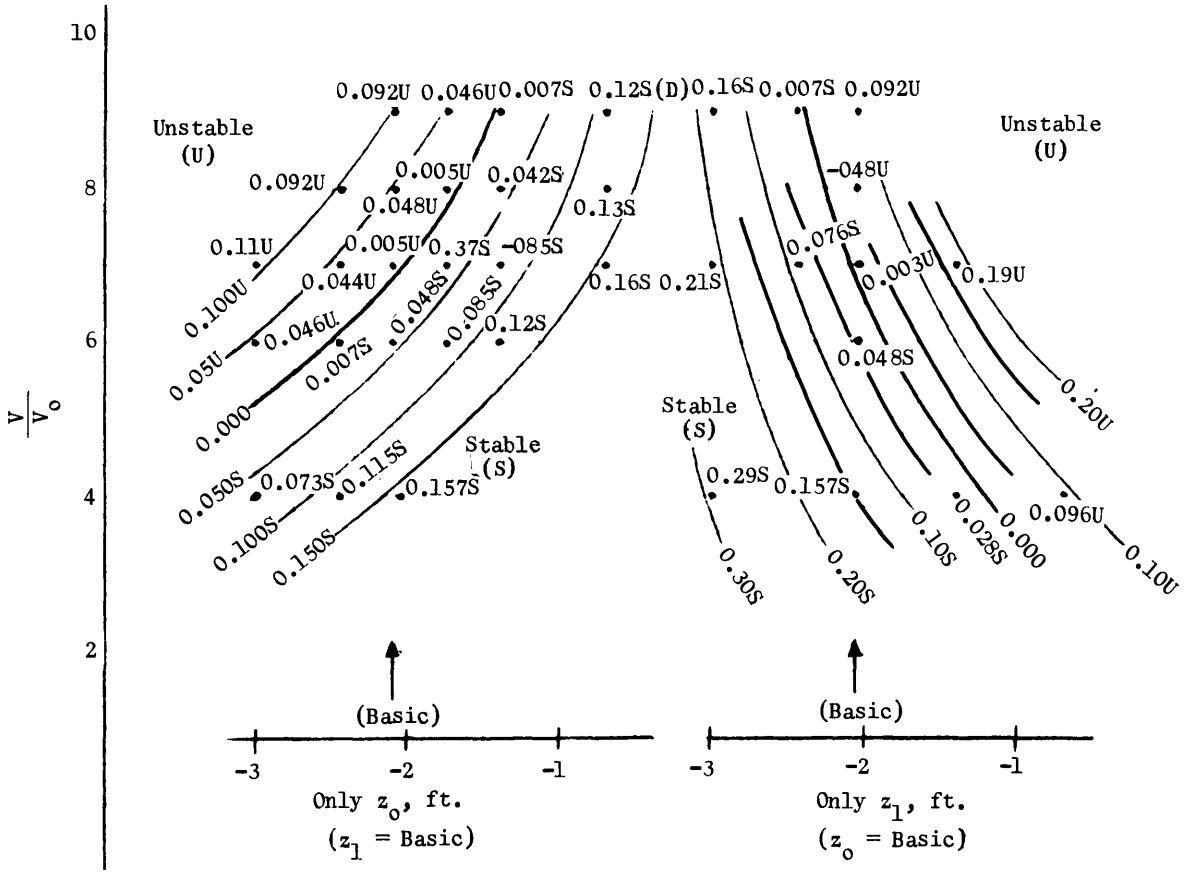

Figure 48a

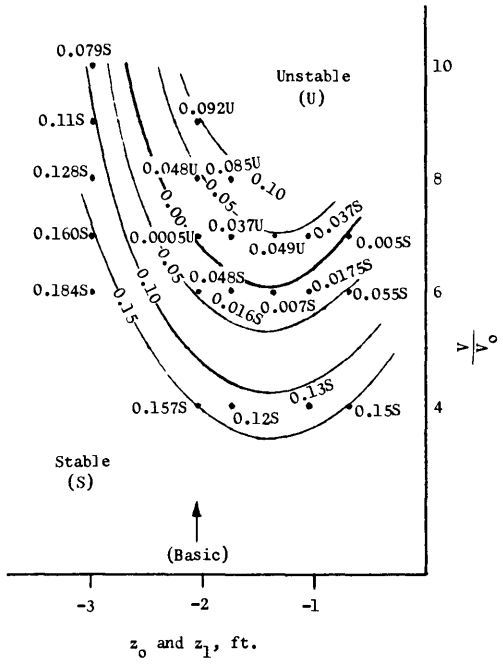

Figure 48b

Figure 48 – Contours of Constant ζ–Spanwise Location of Center of Pressure and Rotation Center–z_0, z_1 versus V/V_o–Three Degrees of Freedom

z_o and z_1 are taken relative to the rudder origin (point R in Figure 90).

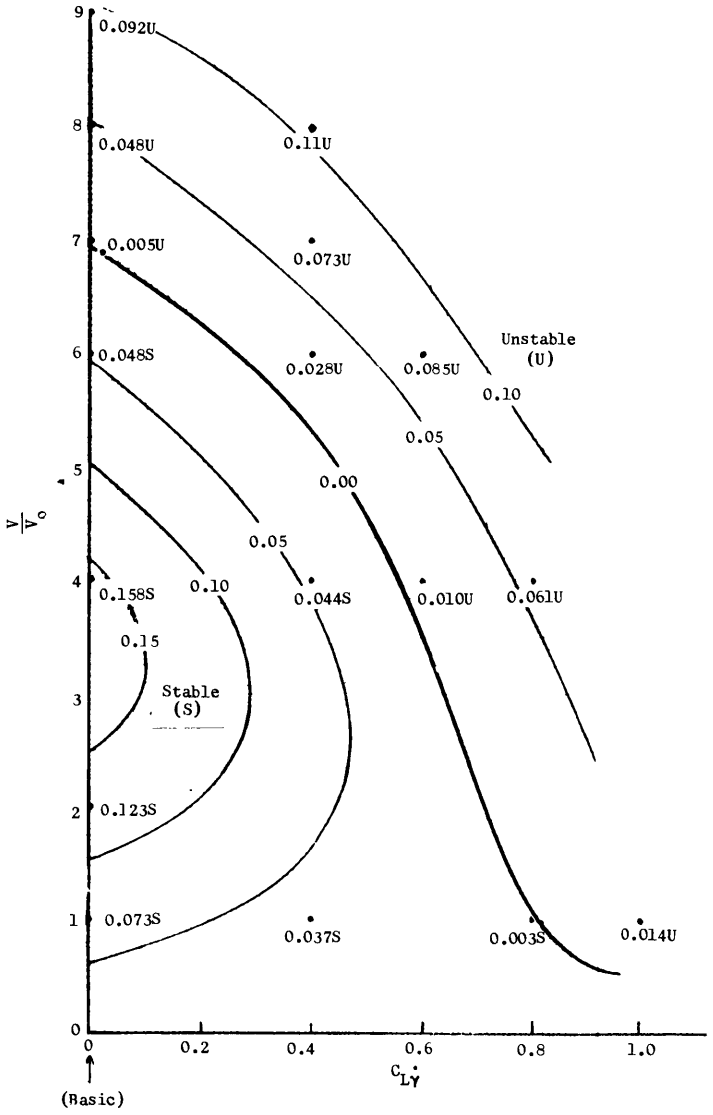

Figure 49 – Contours of Constant ζ–Coefficient $C_{L\dot{\gamma}}$ versus V/V_o– No Lag Function–Three Degrees of Freedom

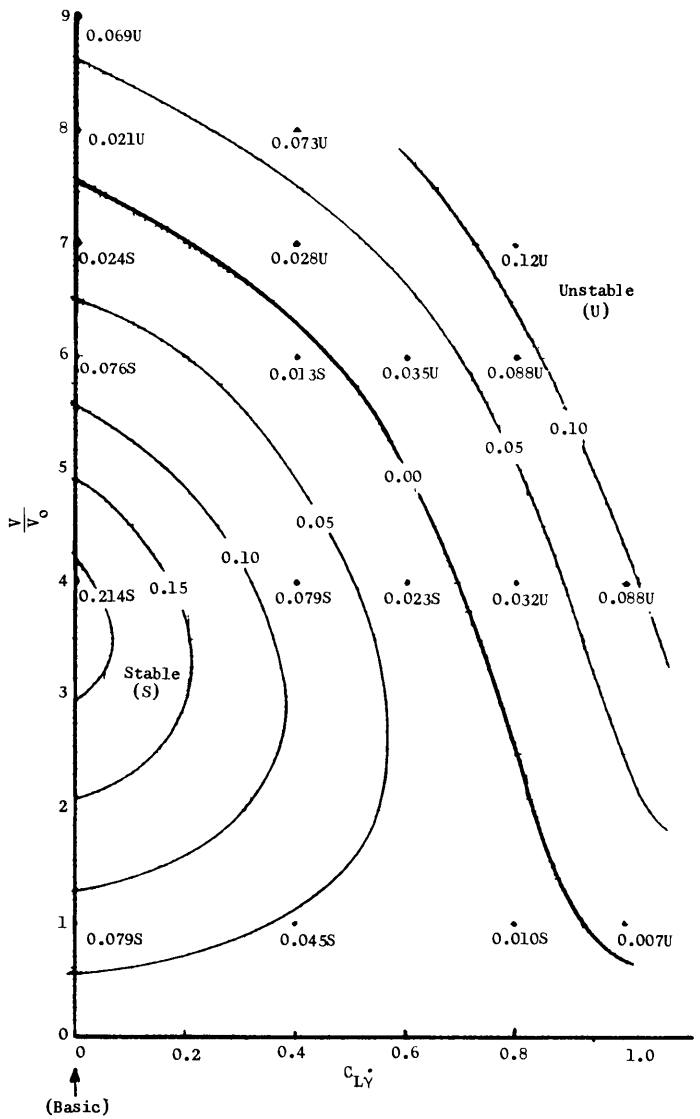

Figure 50 – Contours of Constant ζ–Coefficient $C_{L\dot{\gamma}}$ versus V/V_o– Lag Function for AR = 2.5–Three Degrees of Freedom

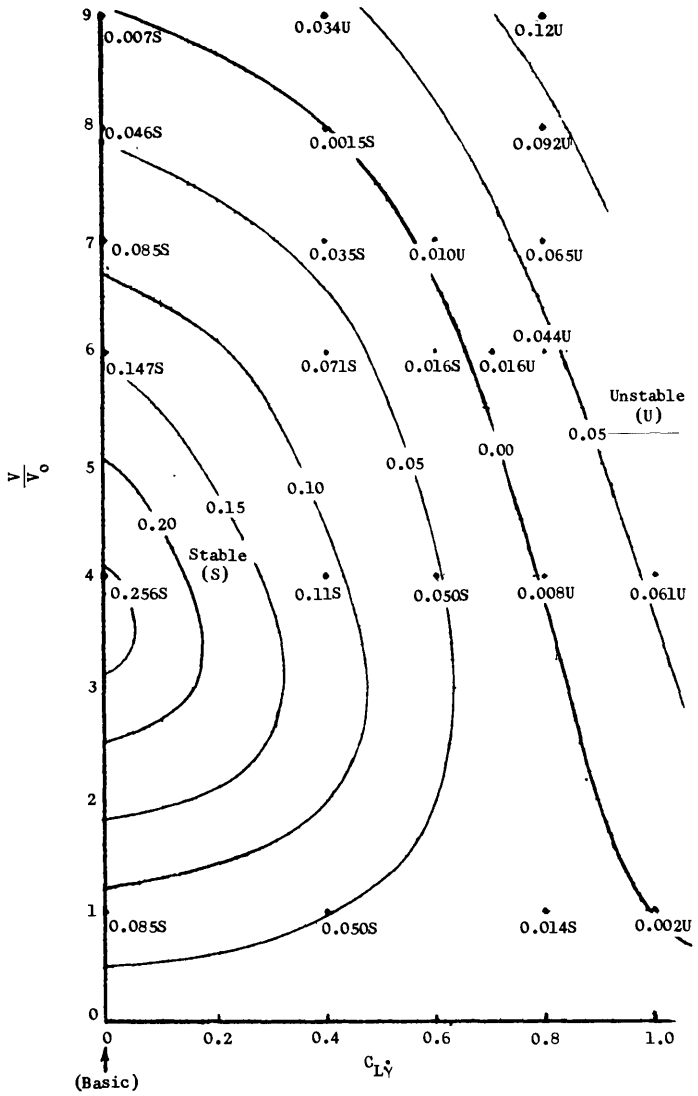

Figure 51 – Contours of Constant ζ– Coefficient $C_{L\dot{y}}$ versus V/V_o– Lag Function for AR = ∞–Three Degrees of Freedom

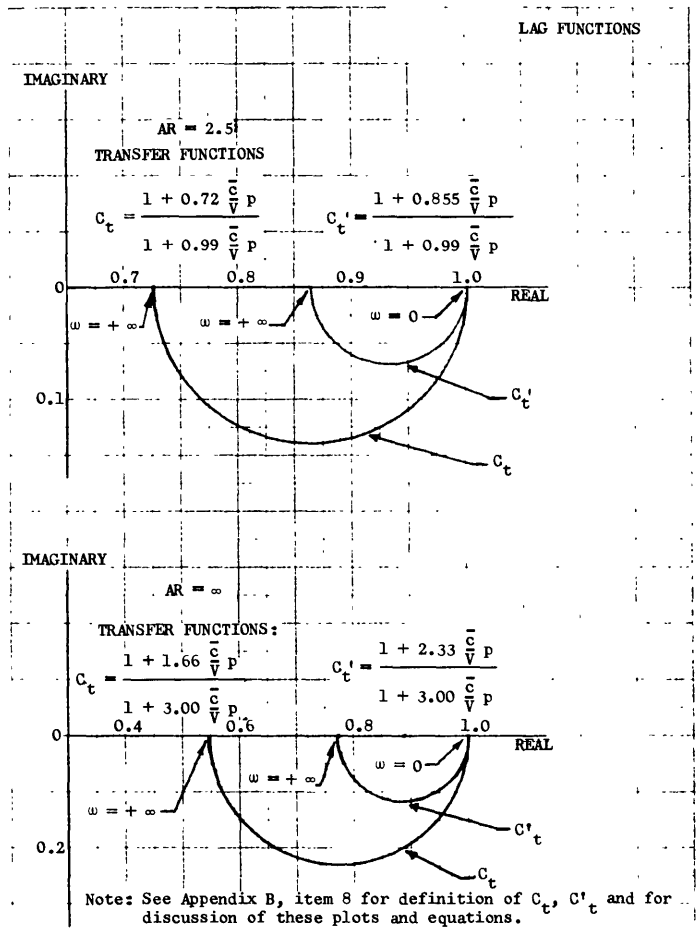

Note: See Appendix B, item 8 for definition of C_t, C'_t and for discussion of these plots and equations.

Figure 52 – Lag Functions

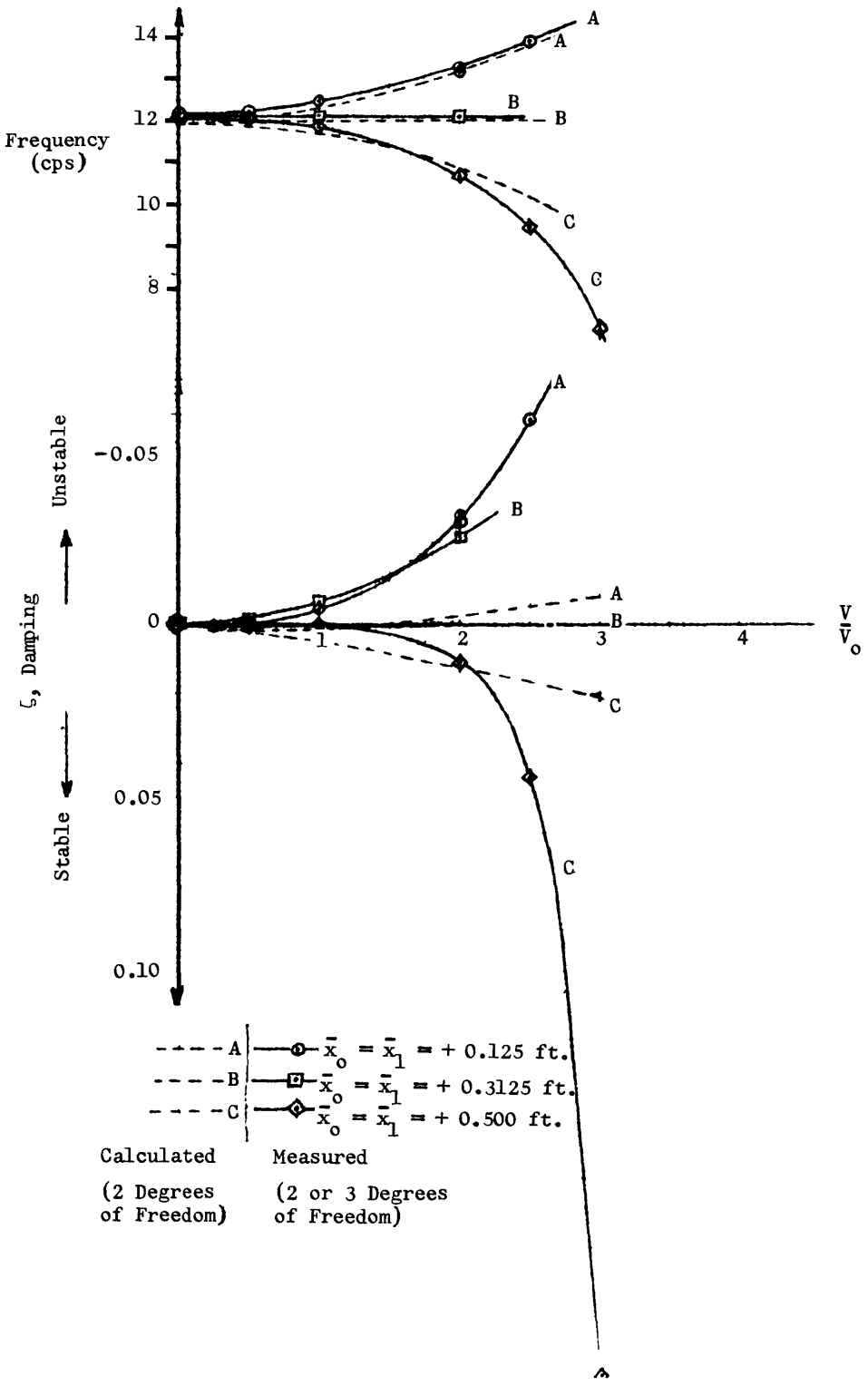

Figure 53 – Damping versus Velocity

Hydrodynamic forces of Reference 6 are used here. Damping which is not velocity dependent is removed.

Figures 54–68

Comparison of Analog Computer and Numerical Analysis Results– ζ versus V/V_o

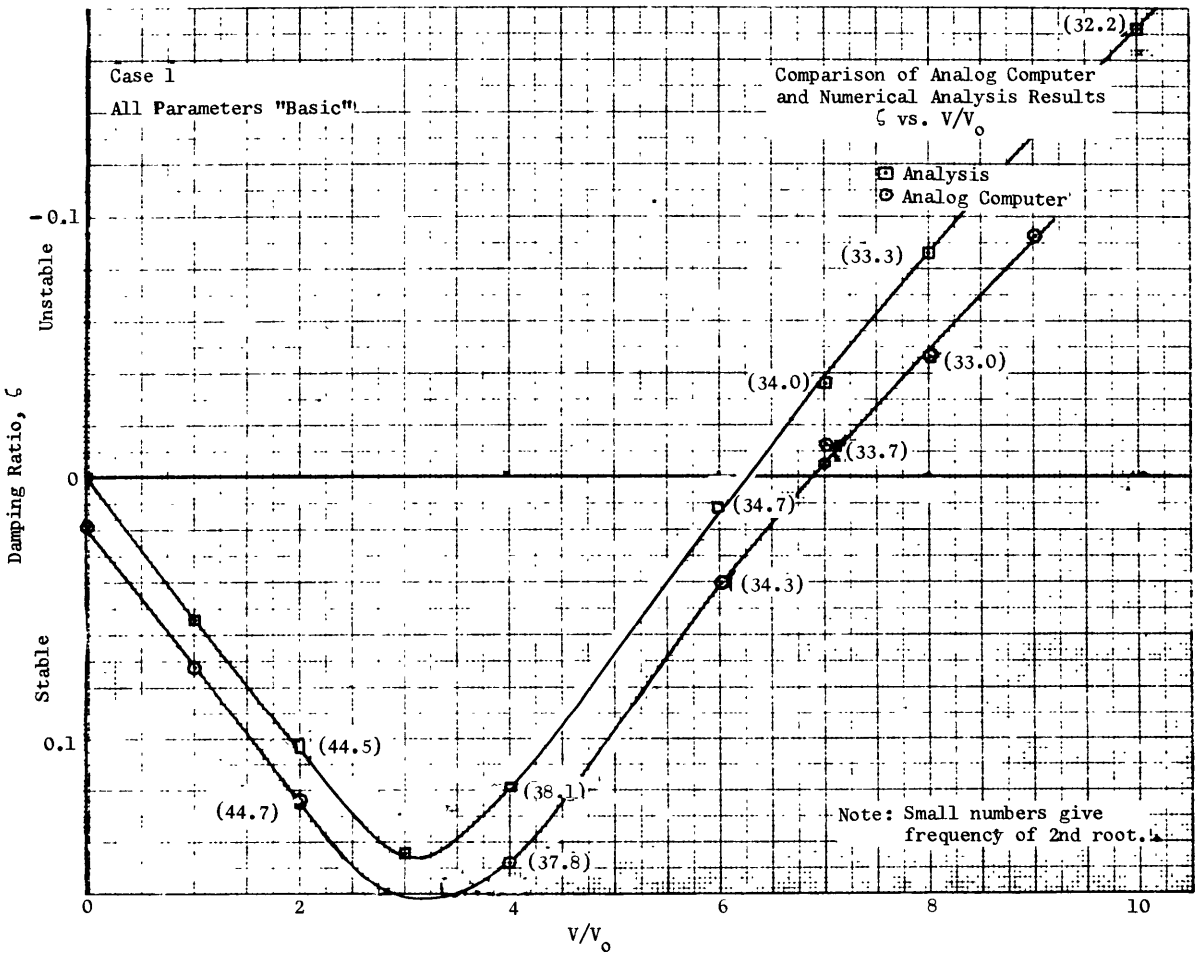
Case 1
All Parameters "Basic"
Comparison of Analog Computer and Numerical Analysis Results
ζ vs. V/Vo
Analysis
Analog Computer
(32.2)
(33.3)
(33.0)
(34.0)
(33.7)
(34.7)
(34.3)
(44.5)
(44.7)
(38.1)
(37.8)
Note: Small numbers give frequency of 2nd root.
Damping Ratio, ζ
Unstable
Stable
-0.1
0
0.1
0
2
4
6
8
10
V/Vo

Figure 54

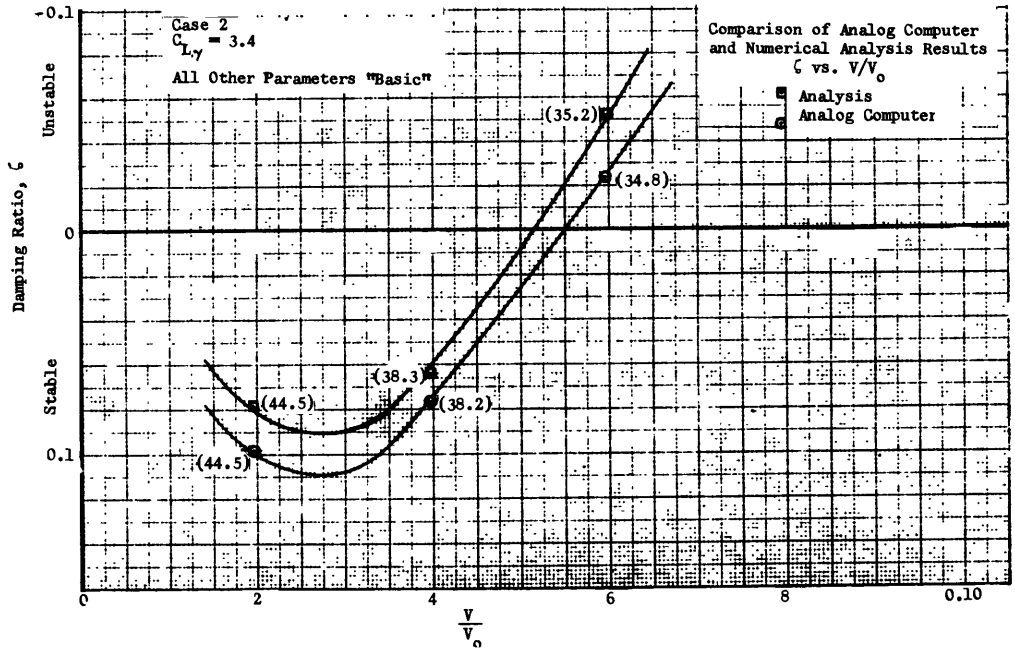

Figure 55

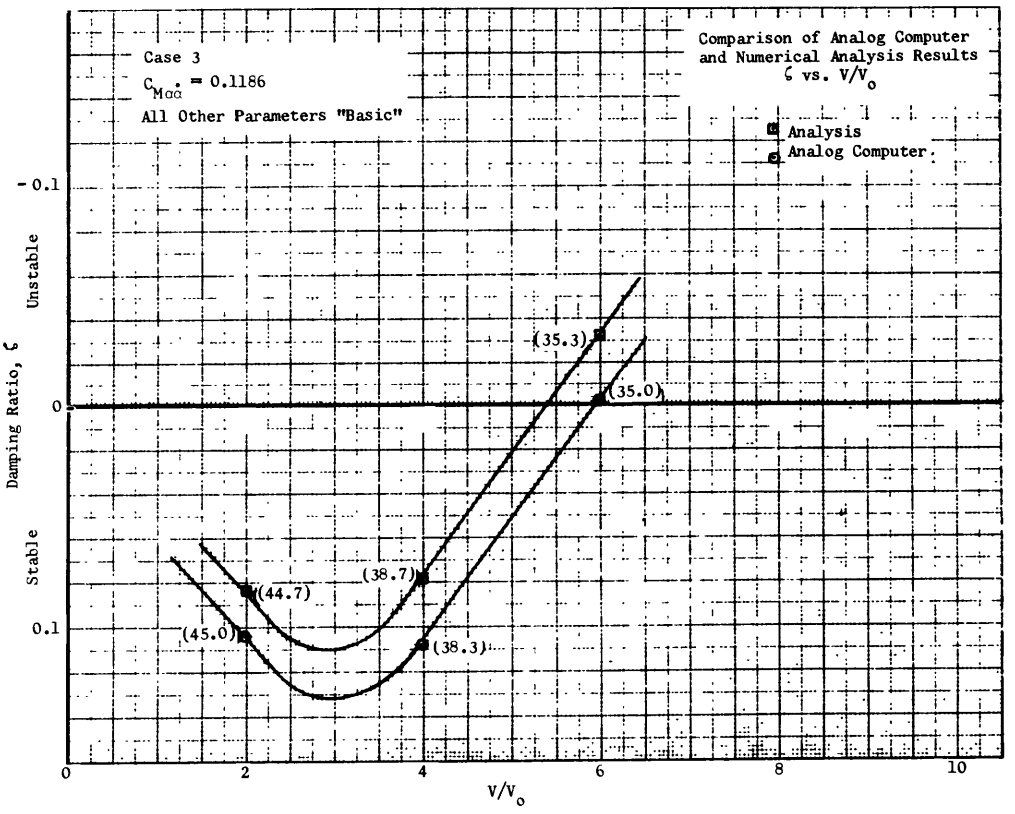

Figure 56

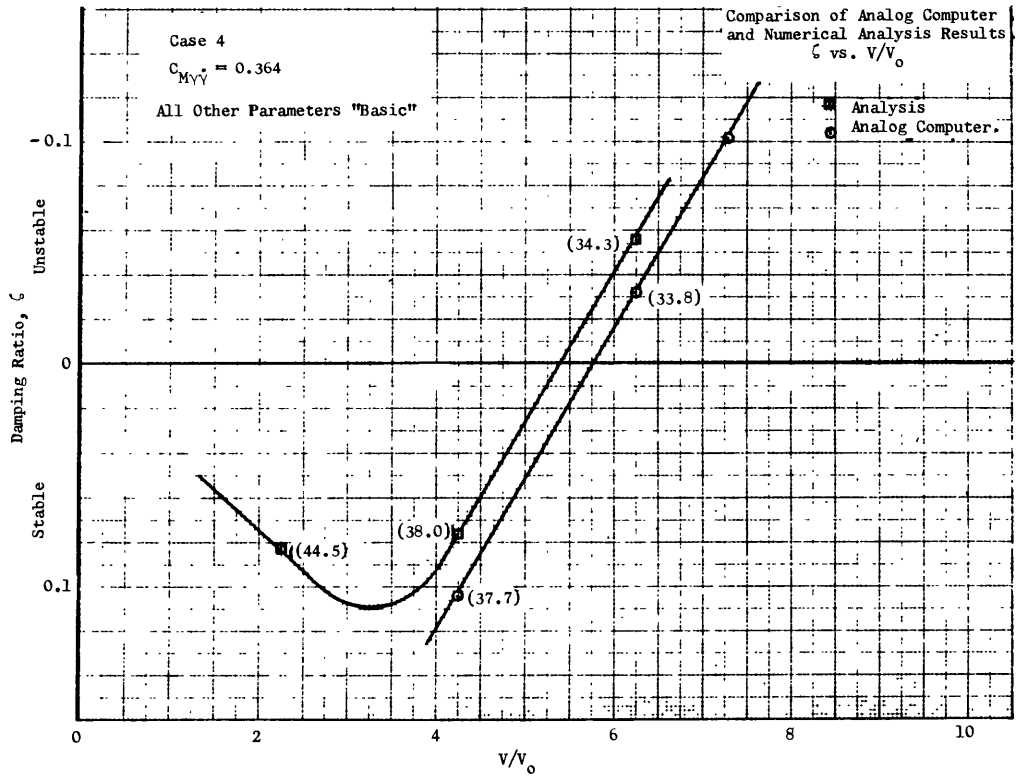

Figure 57

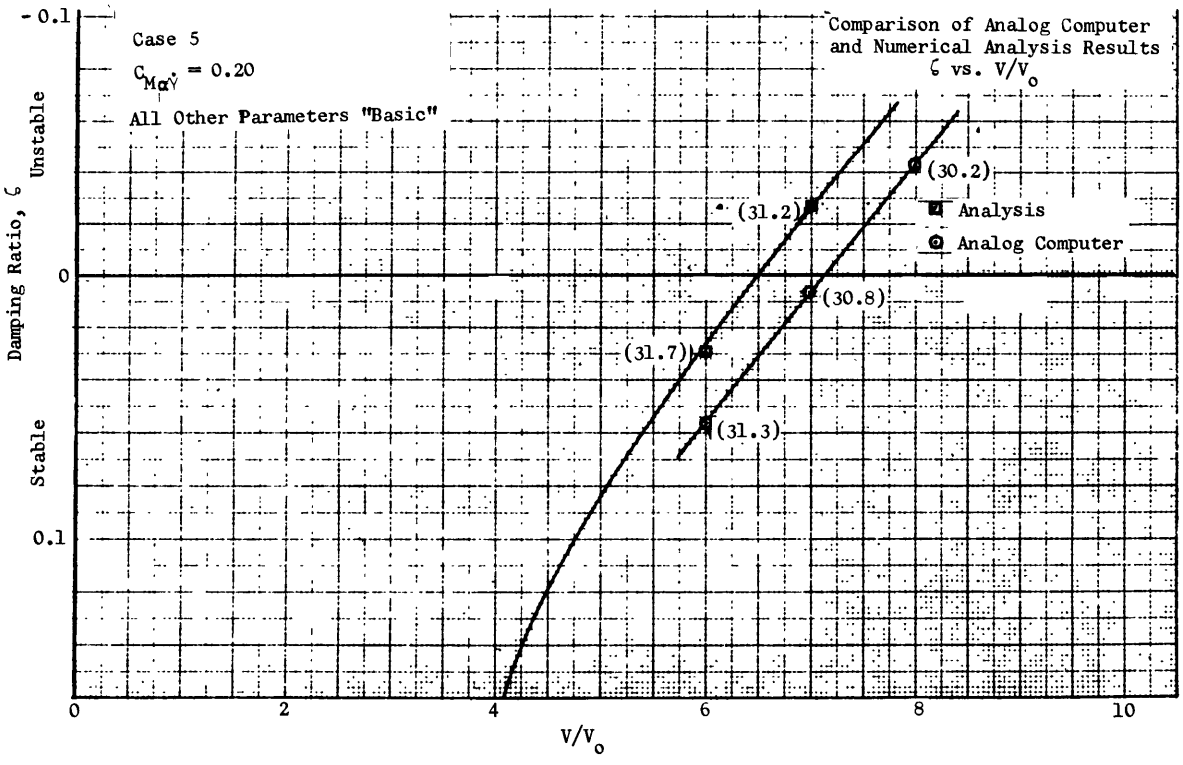

Figure 58

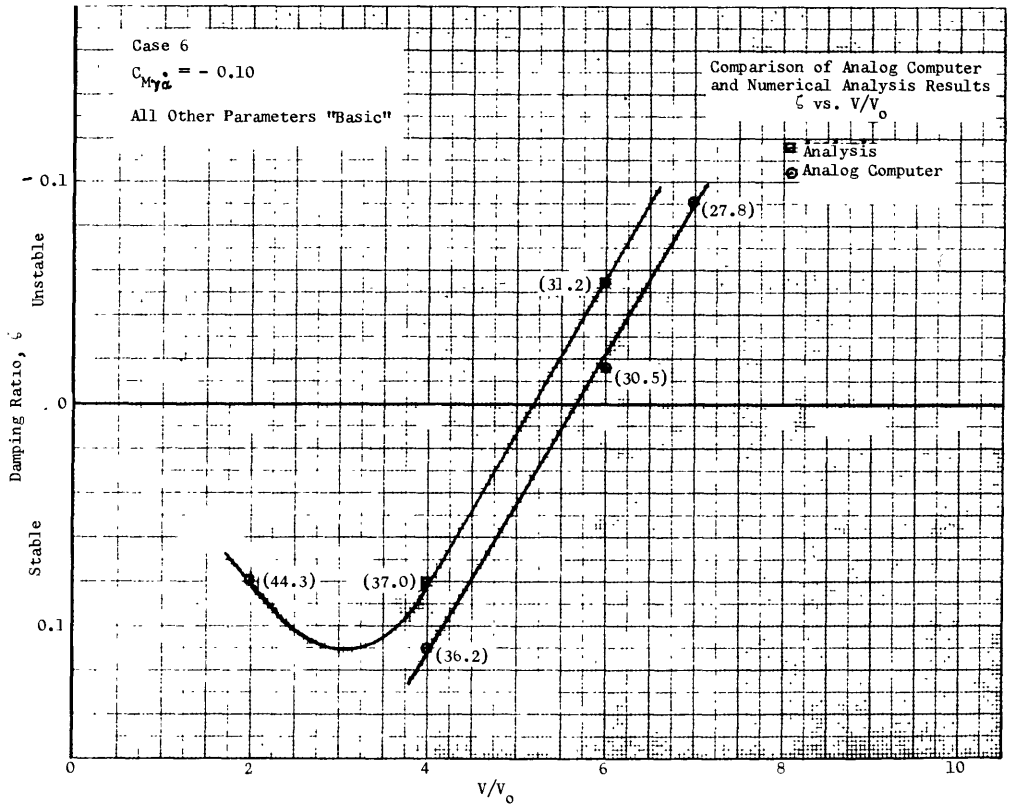

Figure 59

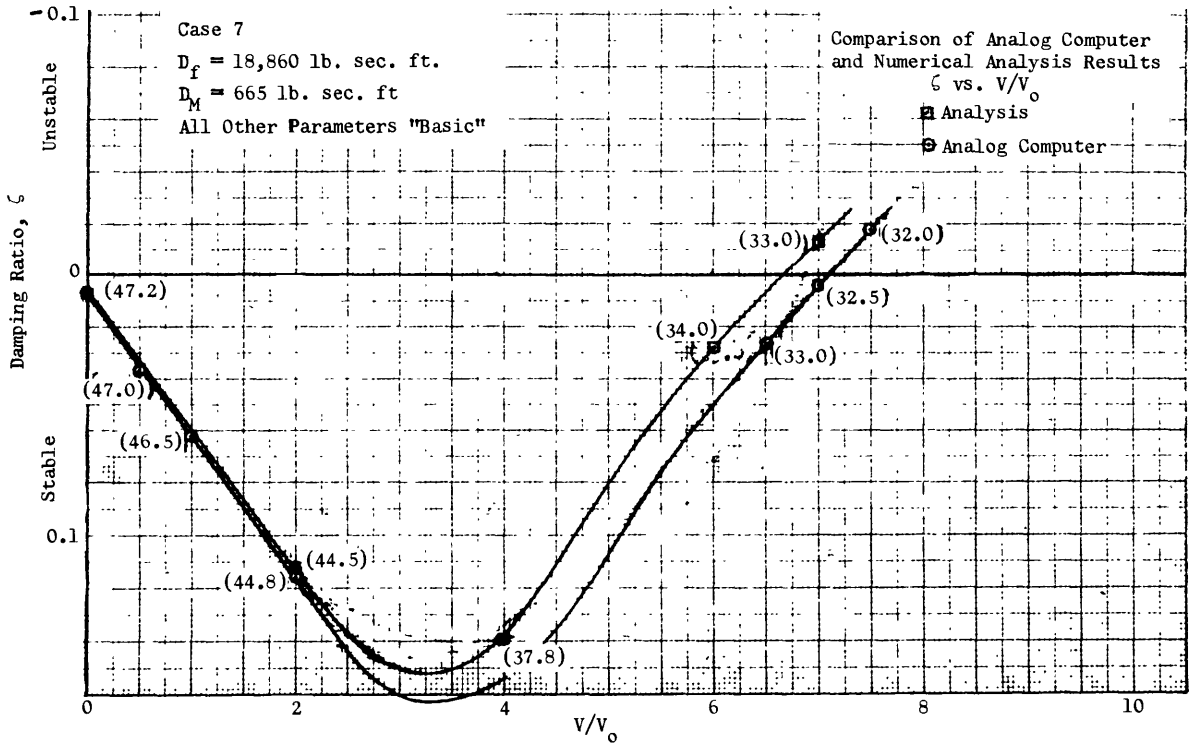

Figure 60

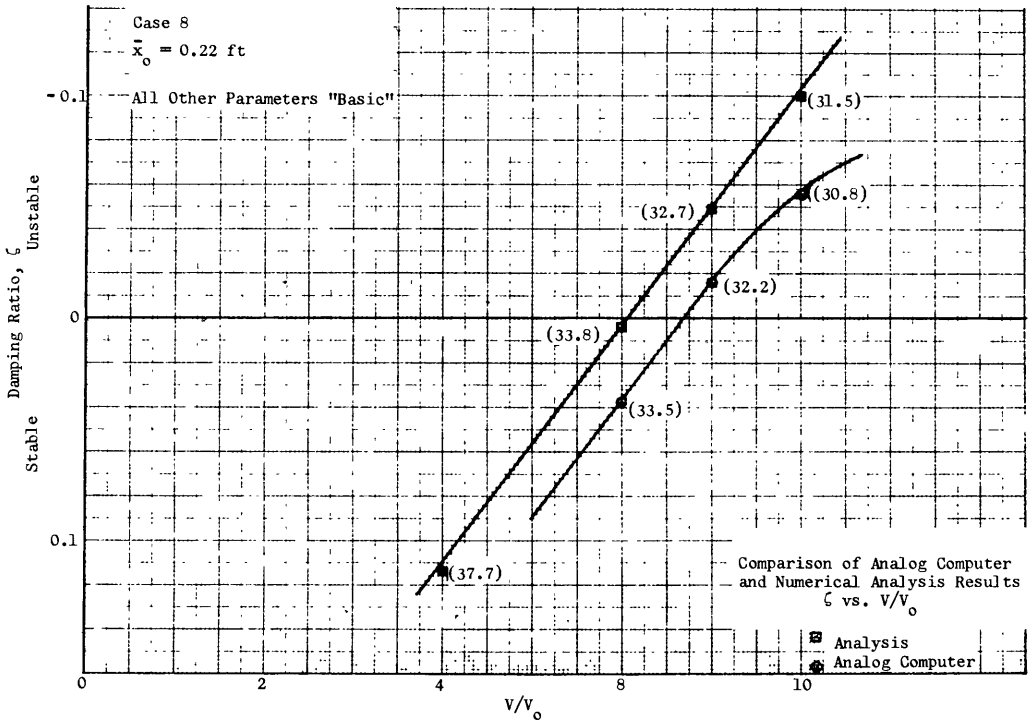

Figure 61

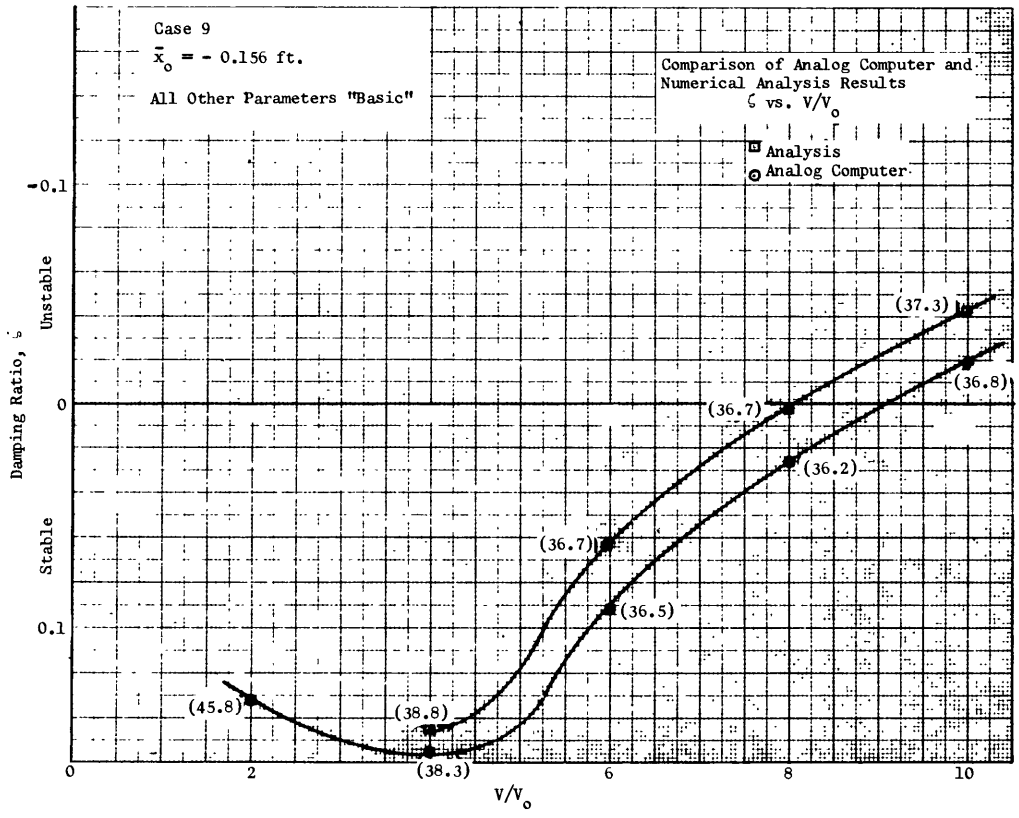

Figure 62

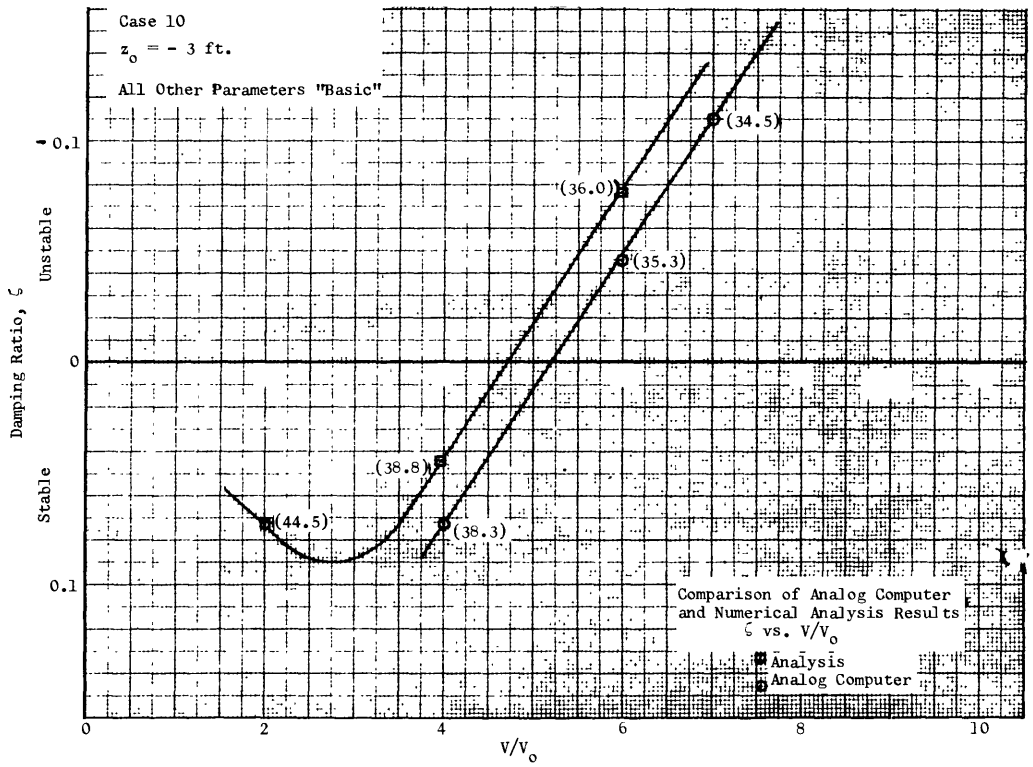

Figure 63

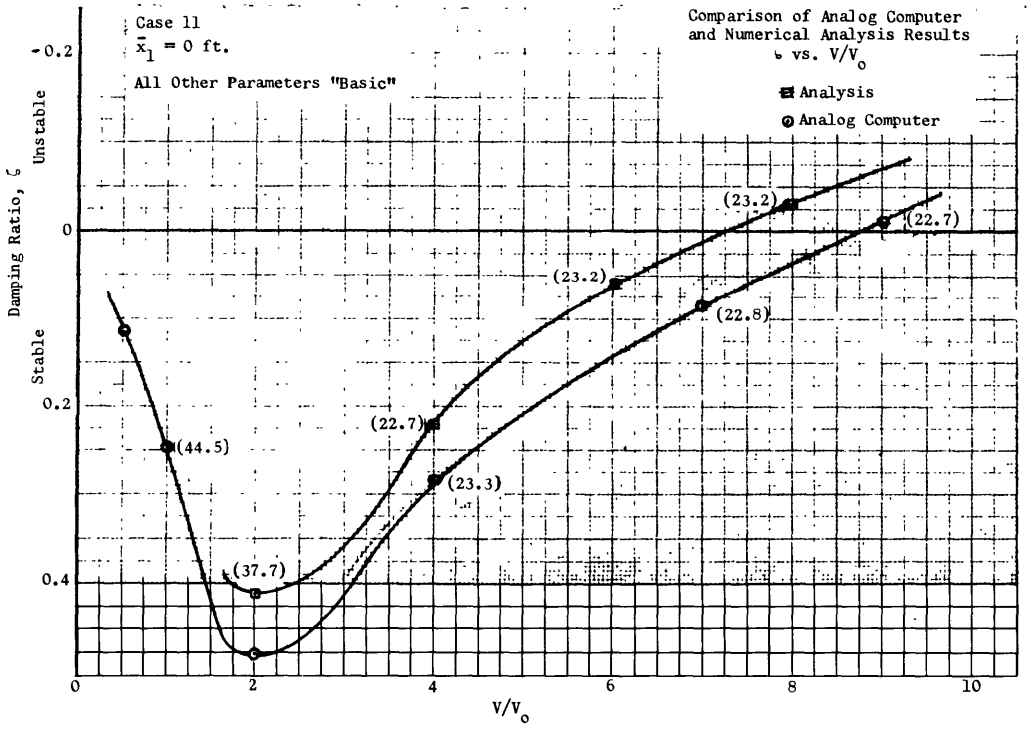

Figure 64

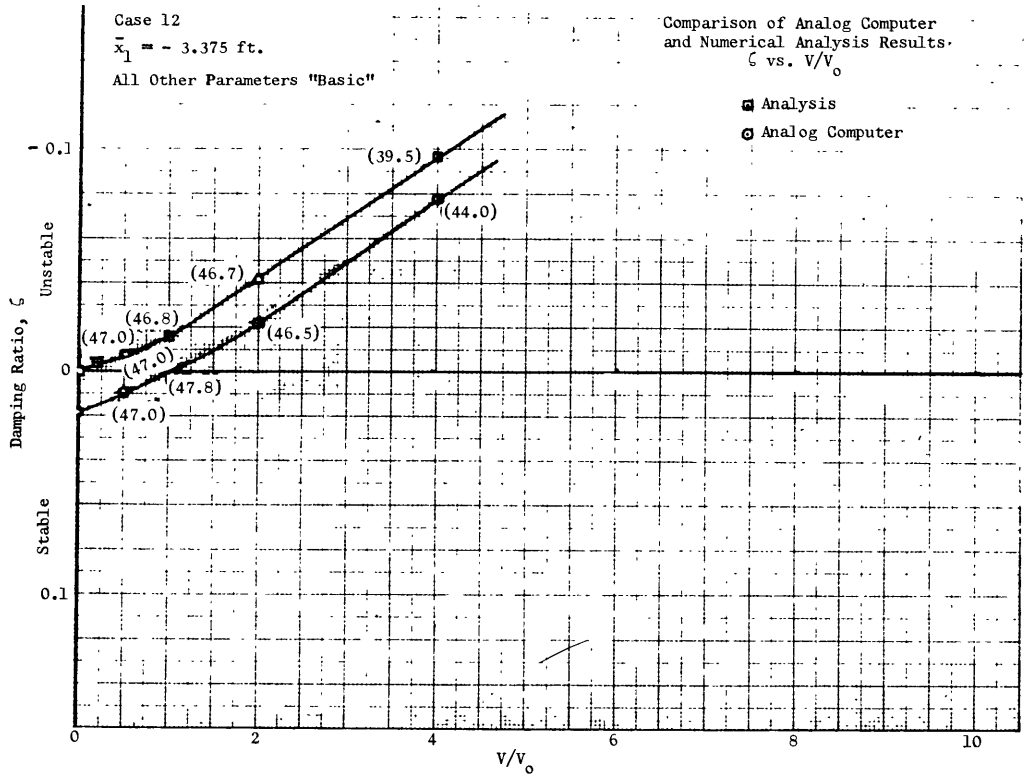

Figure 65

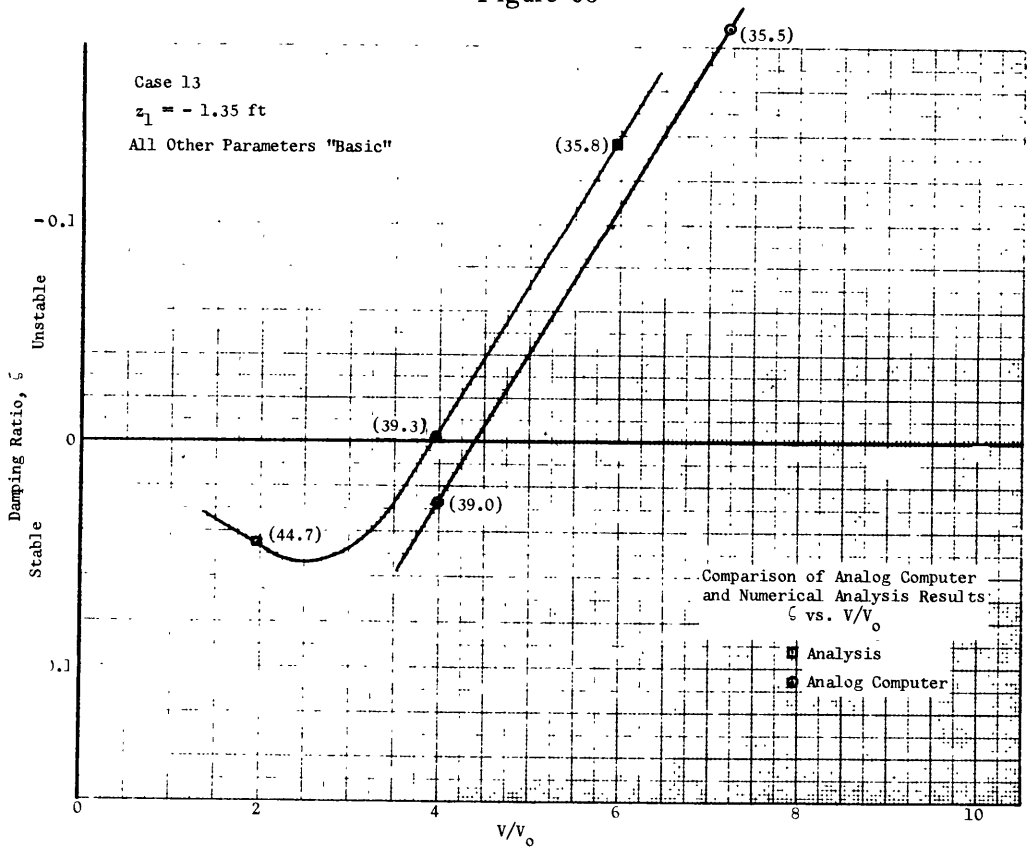

Figure 66

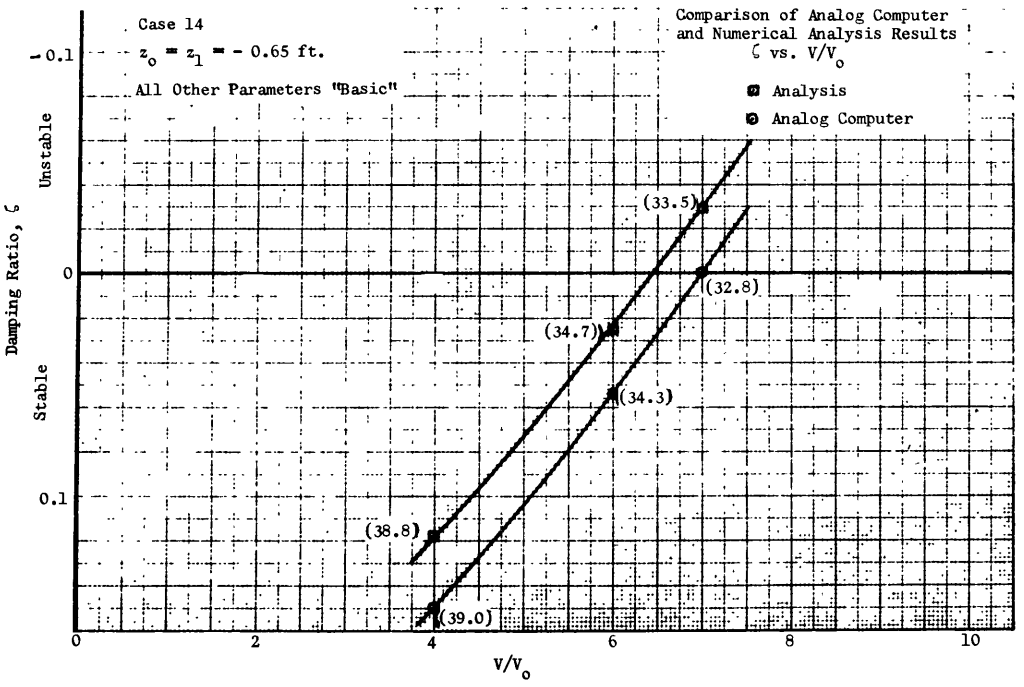

Figure 67

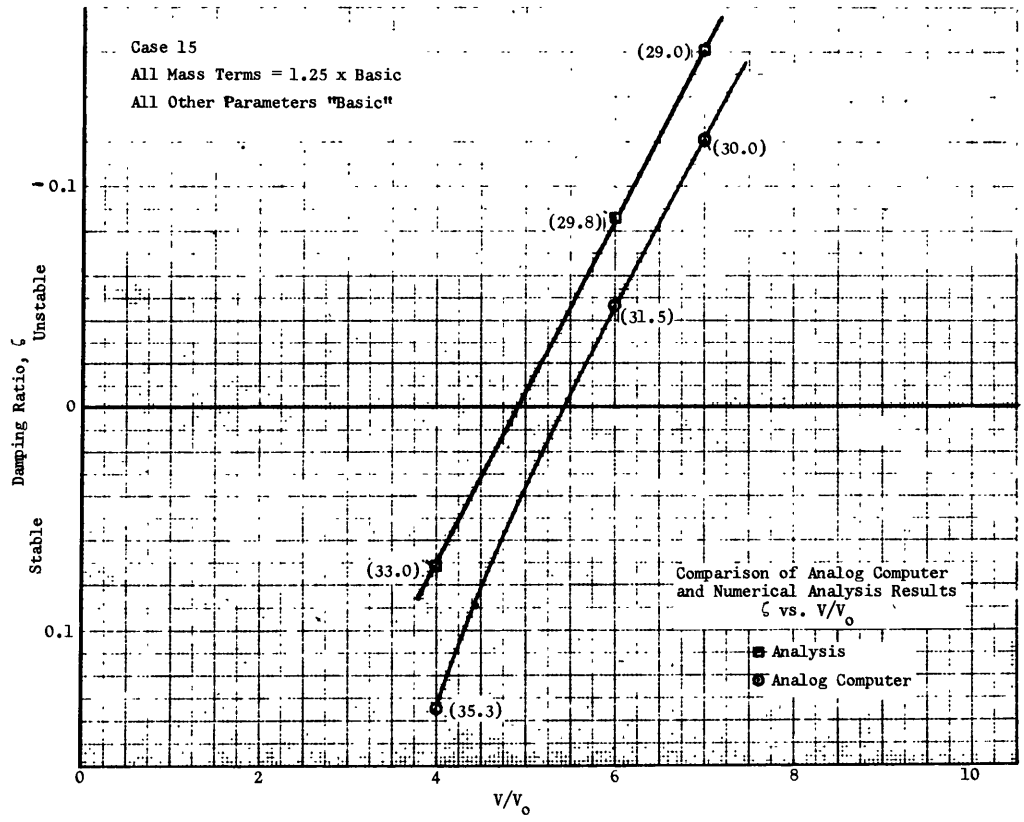

Figure 68

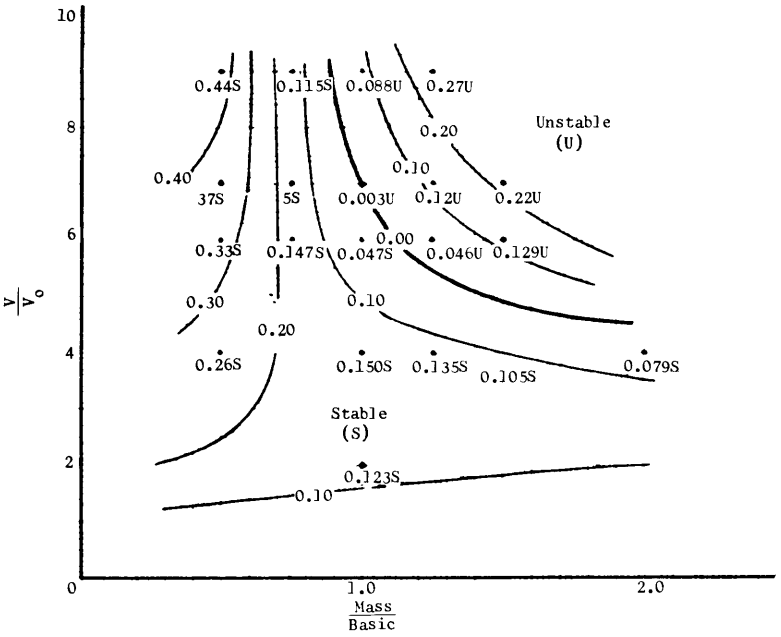

Figure 69 – Contours of Constant ζ–Rudder Mass versus V/V_o–Three Degrees of Freedom

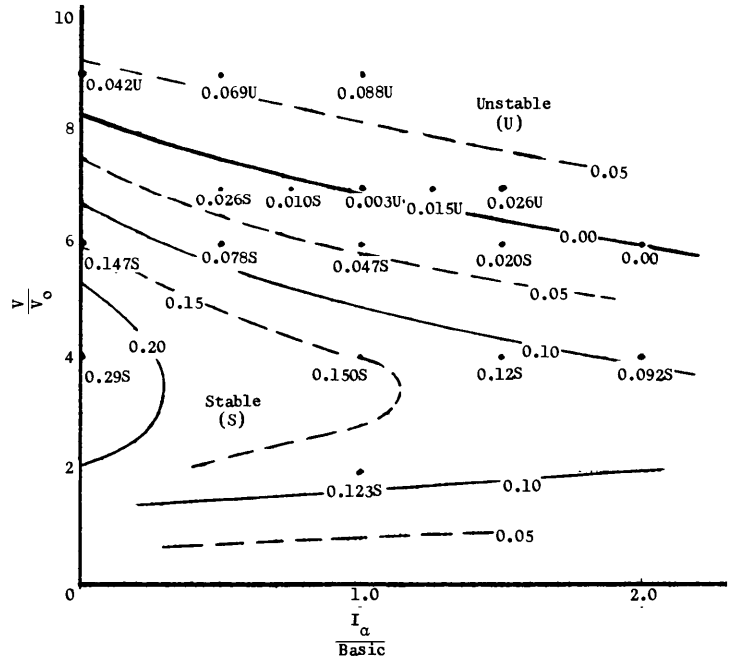

Figure 70 – Contours of Constant ζ–Roll Moment of Inertia I_α versus V/V_o–Three Degrees of Freedom

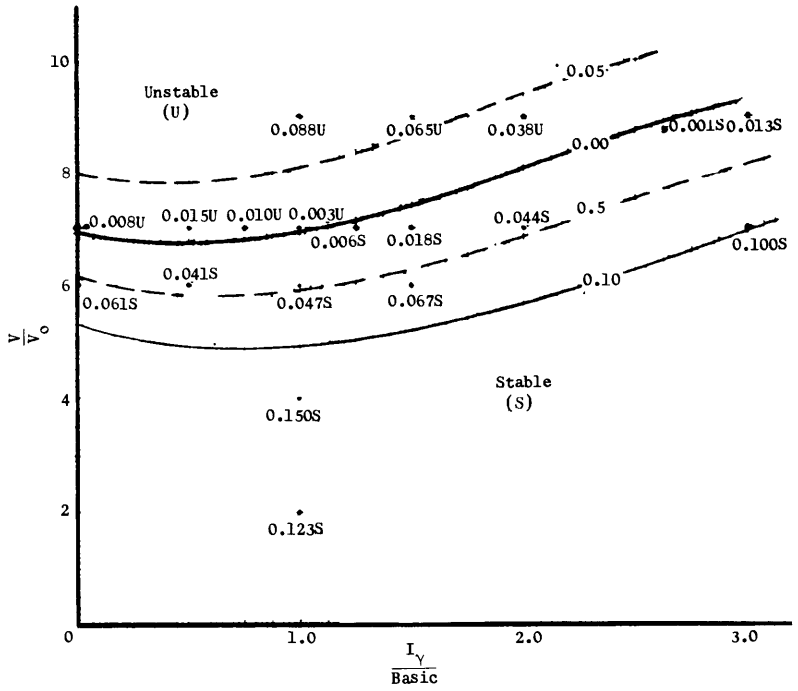

Figure 71 – Contours of Constant ζ–Yaw Moment of Inertia, I_y versus V/V_o– Three Degrees of Freedom

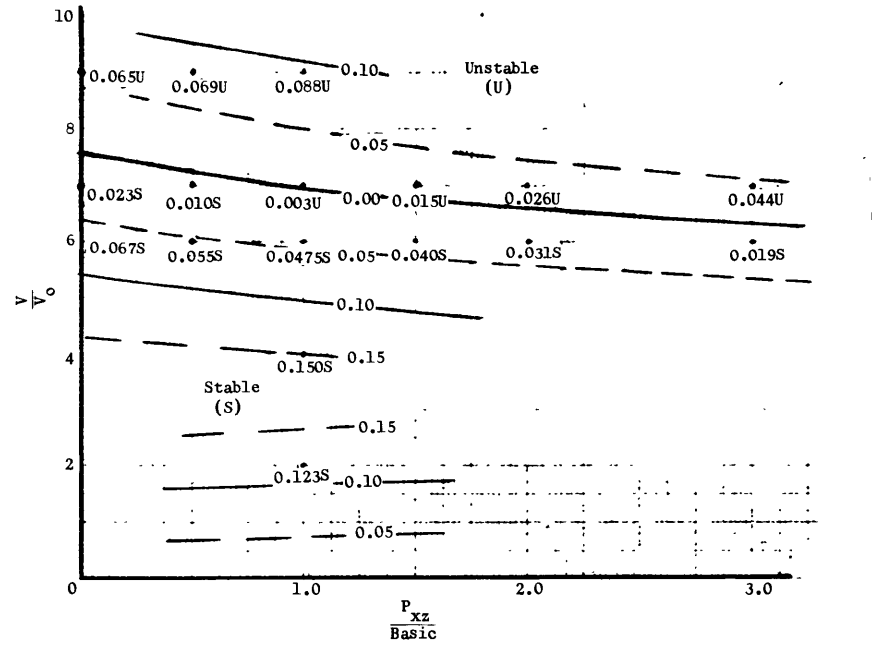

Figure 72 – Contours of Constant ζ–Product of Inertia P_{xz} versus V/V_o– Three Degrees of Freedom

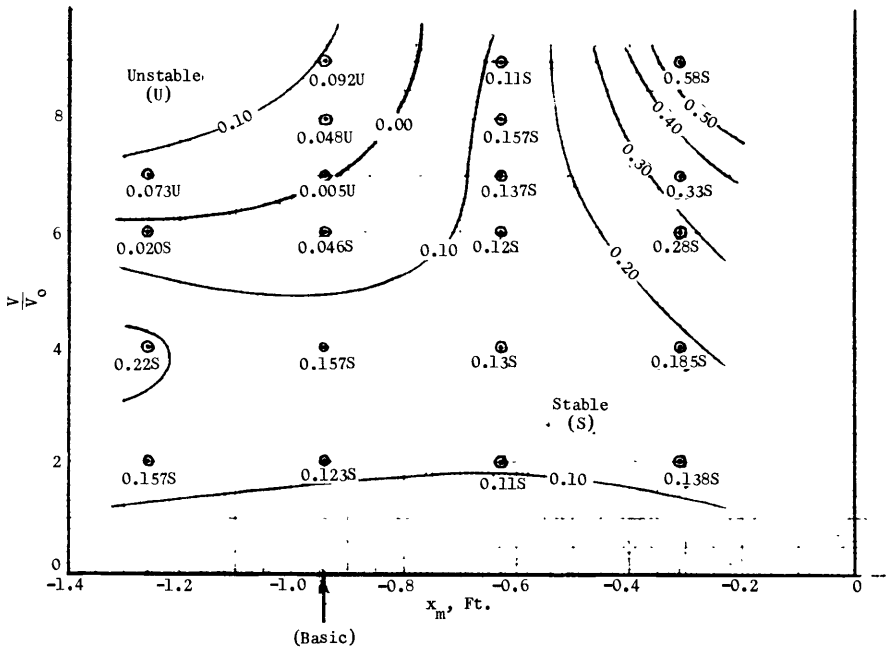

Figure 73 – Contours of Constant ζ–Chordwise Location of Center of Mass, x_m versus V/V_o–Three Degrees of Freedom

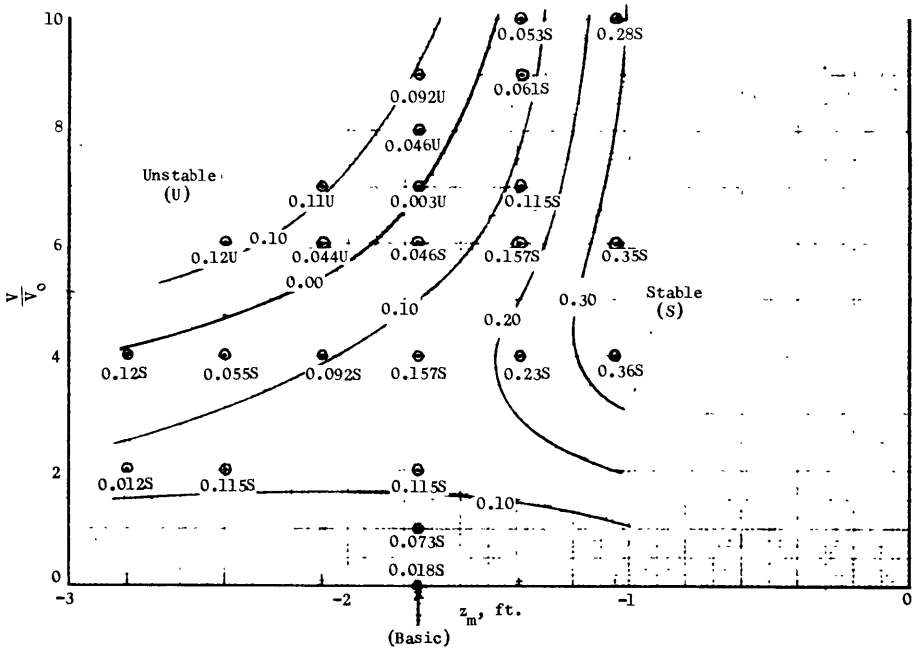

Figure 74 – Contours of Constant ζ–Vertical Location of Center of Mass, z_m versus V/V_o–Three Degrees of Freedom

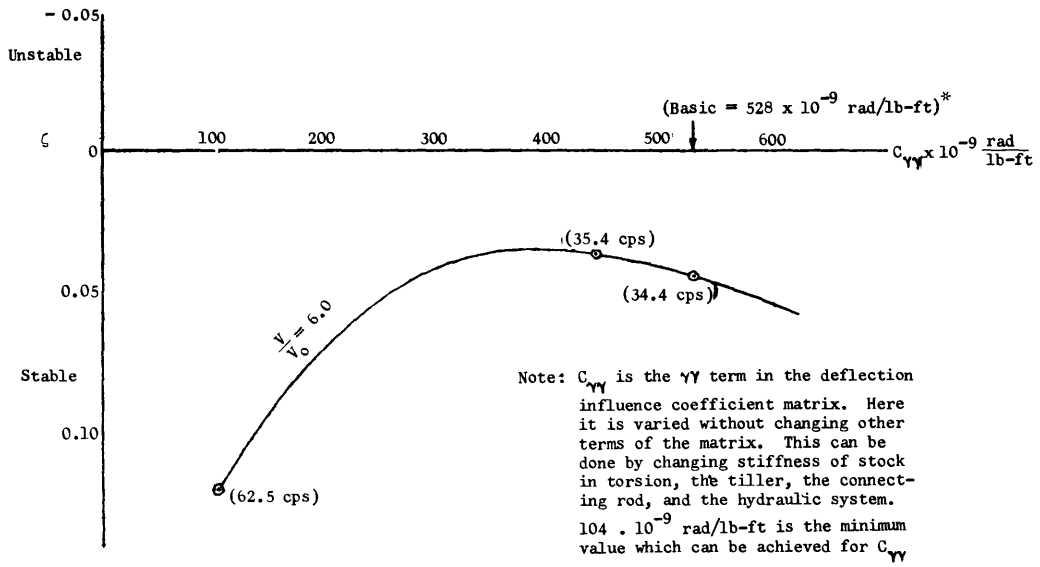

*The basic value of $C_{\gamma\gamma}$ is given in the influence Coefficient matrix; see Appendix E.

Figure 75 – Damping versus $C_{\gamma\gamma}$, V/V_o = 6.0–Three Degrees of Freedom

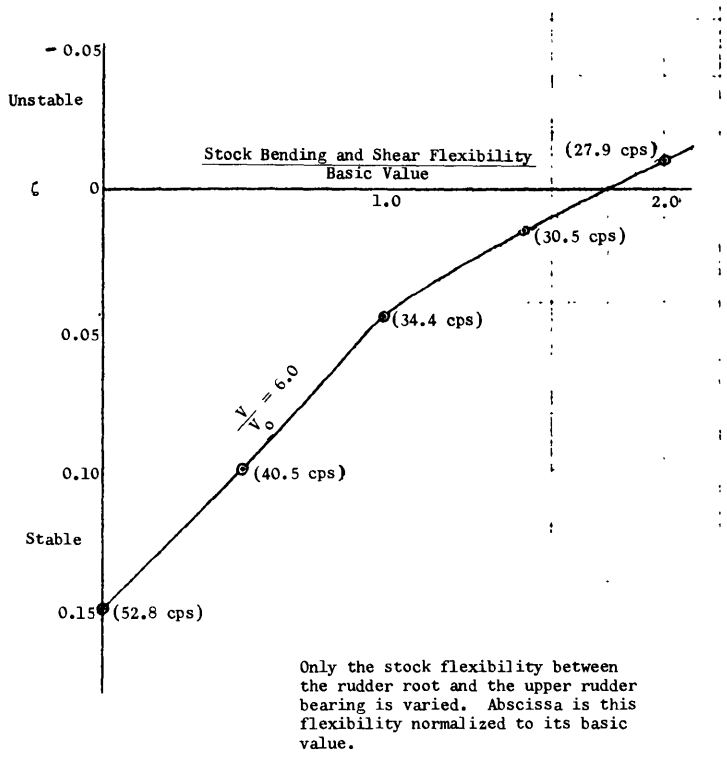

Figure 76 – Damping versus Stock Bending and Shear Flexibility, V/V_o = 6.0–Three Degrees of Freedom

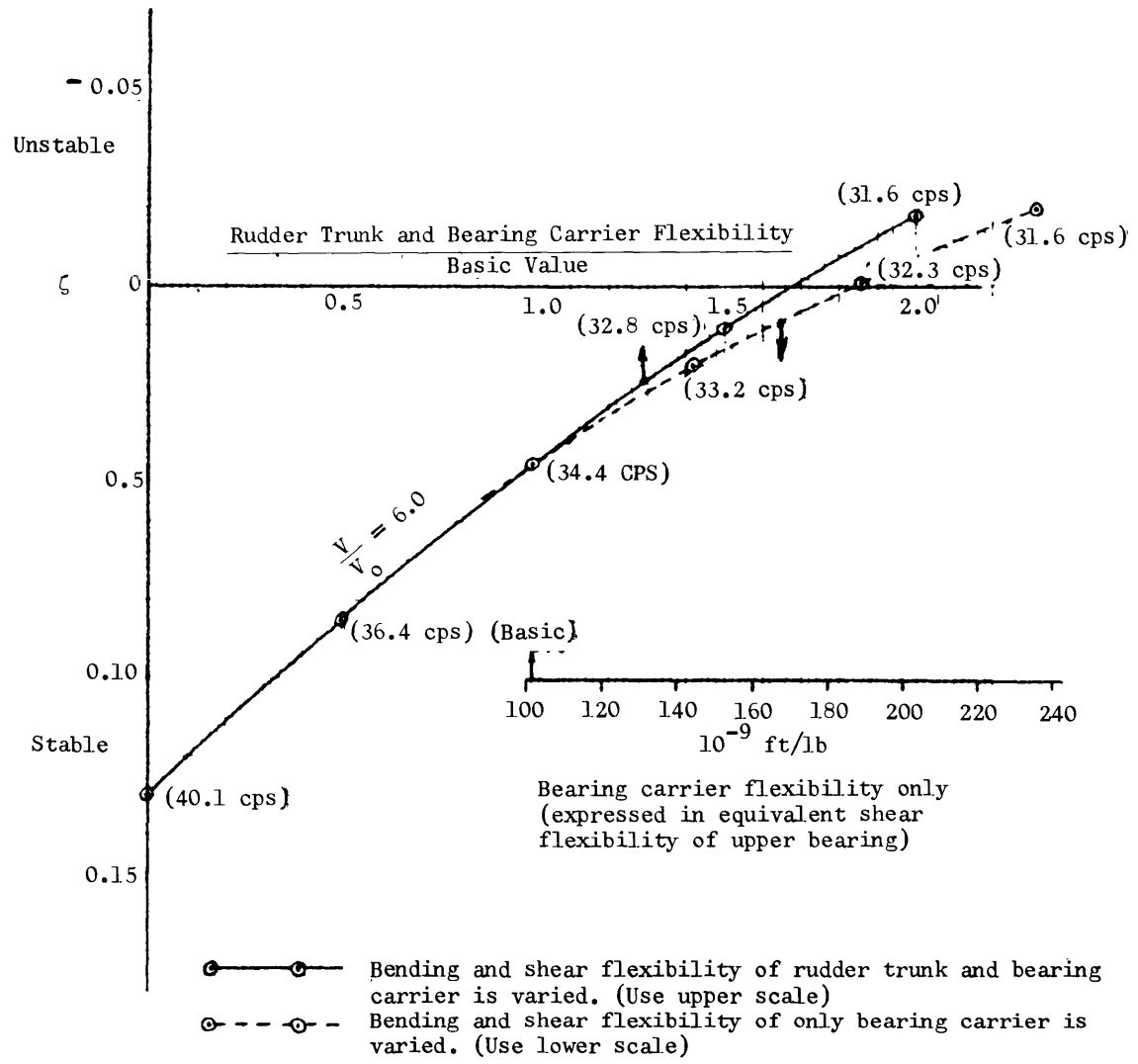

Figure 77 – Damping versus Rudder Trunk and Bearing Carrier Flexibility–V/V_o = 6.0– Three Degrees of Freedom

The solid curve, used with the upper scale, accounts for the flexibility of the rudder trunk and bearing carrier. This flexibility cannot be reduced to a number, i.e., it must be represented by a 2 × 2 matrix (as a minimum) or a larger matrix if any general set of changes are made to the system. In this figure also, the dashed curve, used with the lower scale, accounts for the flexibility of the *bearing carrier alone*. The flexibility for this case can be reduced to a single number. This number represents a spring acting in the shear direction since this bearing carrier system is pin ended. The spring which transmits lateral action only, above the pin, and represented by the dashed curve, is seen to account for most of the flexibility of the bearing carrier-rudder trunk system. In other words, the bending and shear flexibility of the bearing carrier system is expressed (and behaves) as an equivalent shear (i.e., lateral) flexibility of the upper bearing. The scale covers a range which indicates the requirements for increasing the stability, which is the subject of interest here; hence, the curve and scale for the bearing carrier alone are not explored beyond the basic carrier flexibility value for the stable region.

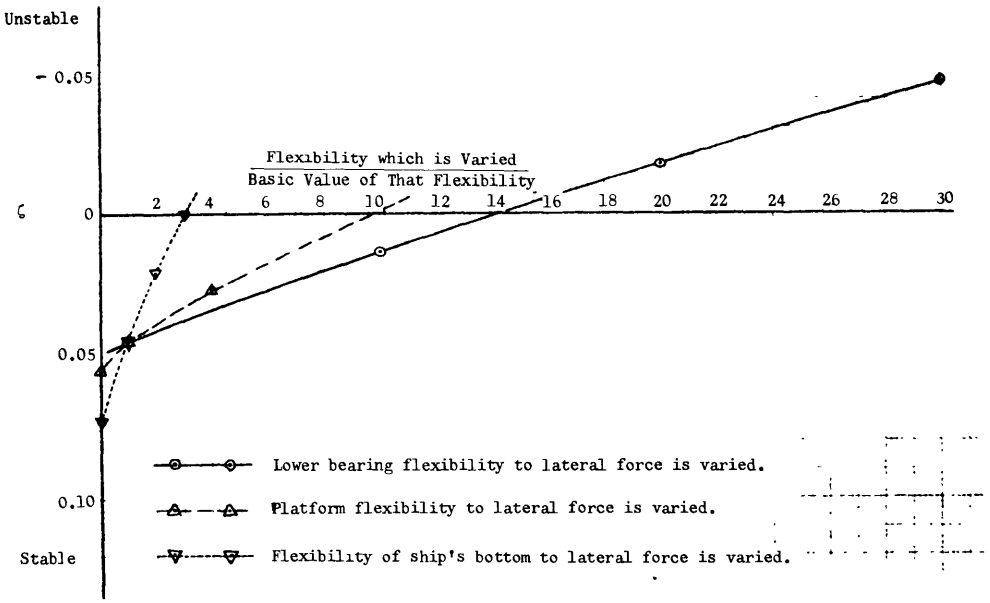

Figure 78 – Damping versus Flexibility to Lateral Force–V/V_o = 6.0– Three Degrees of Freedom

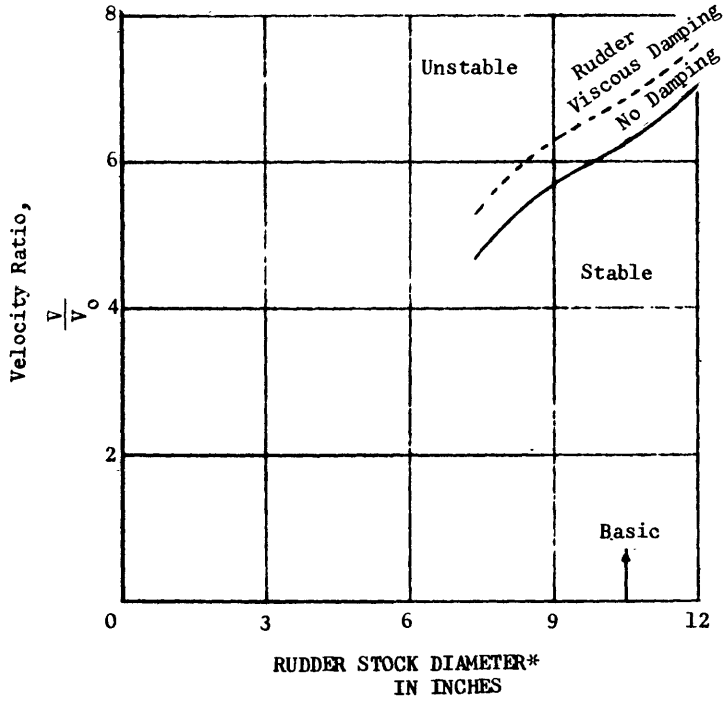

*The rudder stock diameter refers to the portion of the rudder stock between 3.10 ft and 6.45 ft above the baseline, the basic value of which is 10.5 in. It is assumed the diameter of the stock between 6.45 ft and 8.25 ft above the baseline (basic value = 6.88 in.) remains 0.655 times the indicated diameter. For torsion of the rudder stock $C_{\gamma\gamma}$ (see Figure 75)

$$= \int_{3.10}^{8.25} \frac{dz}{GJ} = 10^{-9} \left[\int_{3.10\ \text{ft}}^{6.45\ \text{ft}} \frac{dz}{13.12\ \text{lb in.}^2} + \int_{6.45\ \text{ft}}^{8.25\ \text{ft}} \frac{dz}{2.42\ \text{lb-in.}^2} \right]$$

$$= 144 \times 10^{-9}\ \frac{\text{rad}}{\text{lb ft}}$$

Figure 79 – Flutter Speed versus Rudder Stock Diameter–Three Degrees of Freedom

This figure is deduced as follows. For the basic point $\frac{V}{V_0} = 6.252$ at stock diameter d = 10.5 in. Suppose now that we wish to find $\frac{V}{V_0}$ at some other point, say, where the stock diameter d = 8.83 in. For this point the bending and twisting flexibilities are increased by a factor $\left(\frac{10.5}{8.83}\right)^4 \approx 2$ because I and J $\propto d^4$ on a cylindrical shaft (if the hole is neglected).

The change in damping is partly due to stock torsion. The calculation for $C_{\gamma\gamma}$ given above shows that doubling of the stock torsion flexibility will add 144×10^{-9} rad/lb ft to the basic value of $C_{\gamma\gamma}$ of 528×10^{-9}. Extrapolating Figure 75 shows a corresponding $\Delta\zeta$ of 0.021S (S means stable). The change in damping is partly due to bending and shear (shear enters as $f(d^2)$). If this flexibility is doubled, Figure 76 indicates a $\Delta\zeta$ of 0.055U (unstable).

Thus the net $\Delta\zeta$ (at $\frac{V}{V_0} = 6.0$) is 0.034U.

Now Figure 40 shows that $\frac{\partial \frac{V}{V_0}}{\partial \zeta}$ is about 18 in this region. Therefore, $\Delta\zeta$ of 0.034U is equivalent to a change in $\frac{V}{V_0}$ at flutter of $-19 \times 0.034 = -0.61$ and the dimensionless flutter velocity ratio $\frac{V}{V_0}$ (no damping) is $6.25 - 0.61 = 5.64$.

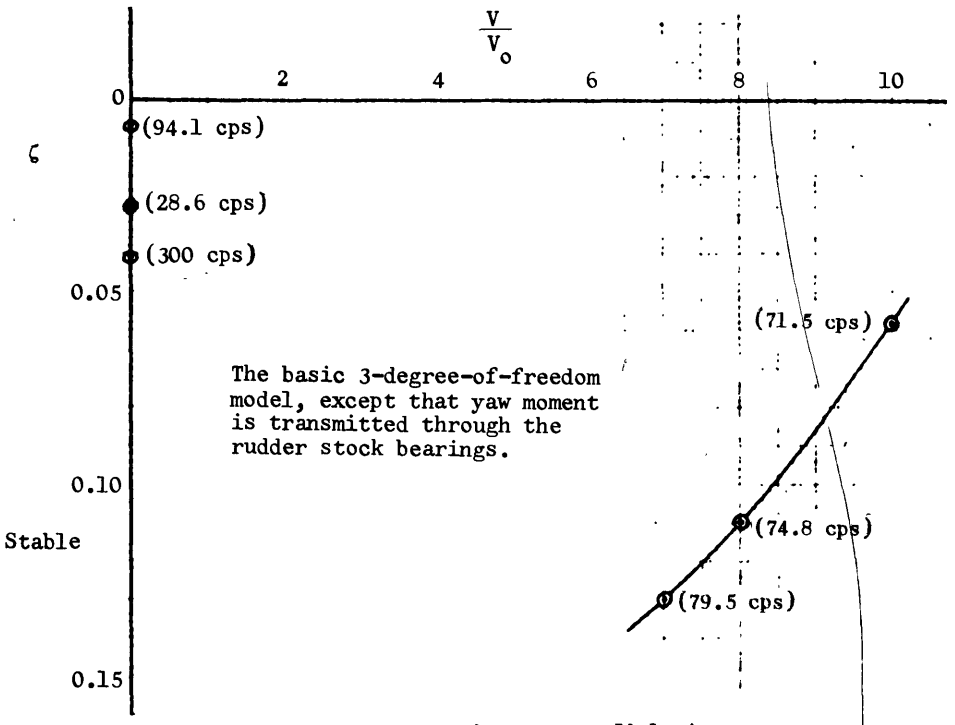

Figure 80 – Damping versus Velocity

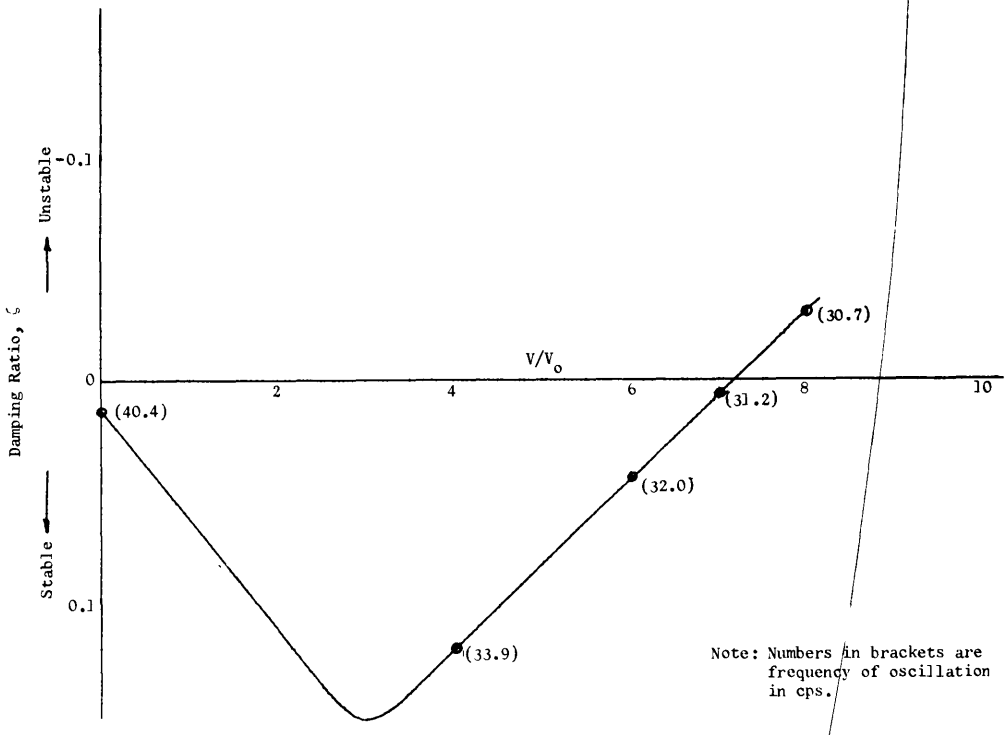

Figure 81 – Flutter of Six-Degree-of-Freedom Model, ζ versus V/V_o

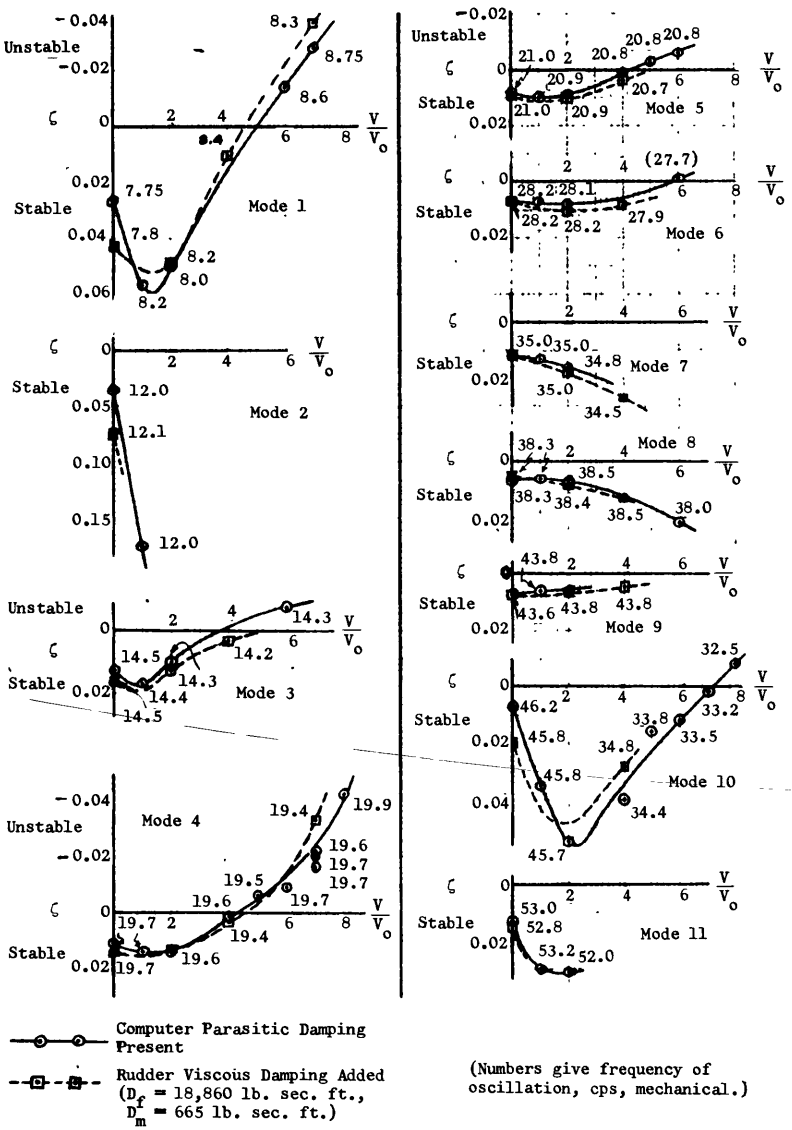

Figure 82 – Damping versus Velocity– Basic Hull–Rudder Connected

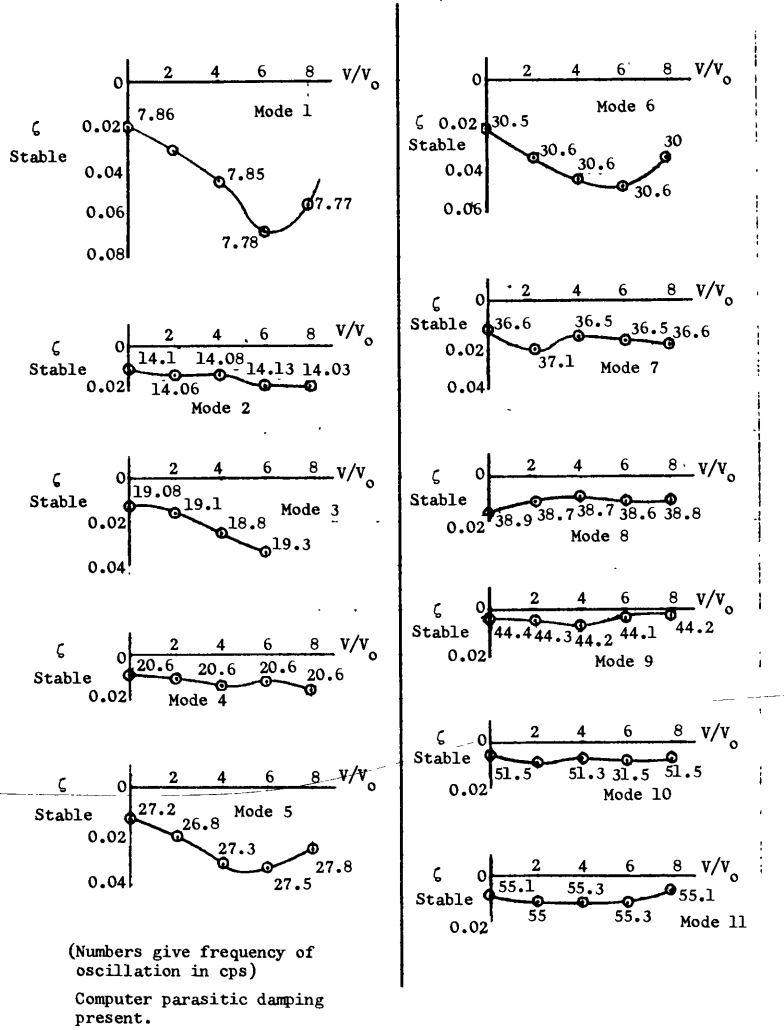

Figure 83 – Damping versus Velocity–Basic Hull– Rudder Connected– Yaw Moment Transmitted through Bearings

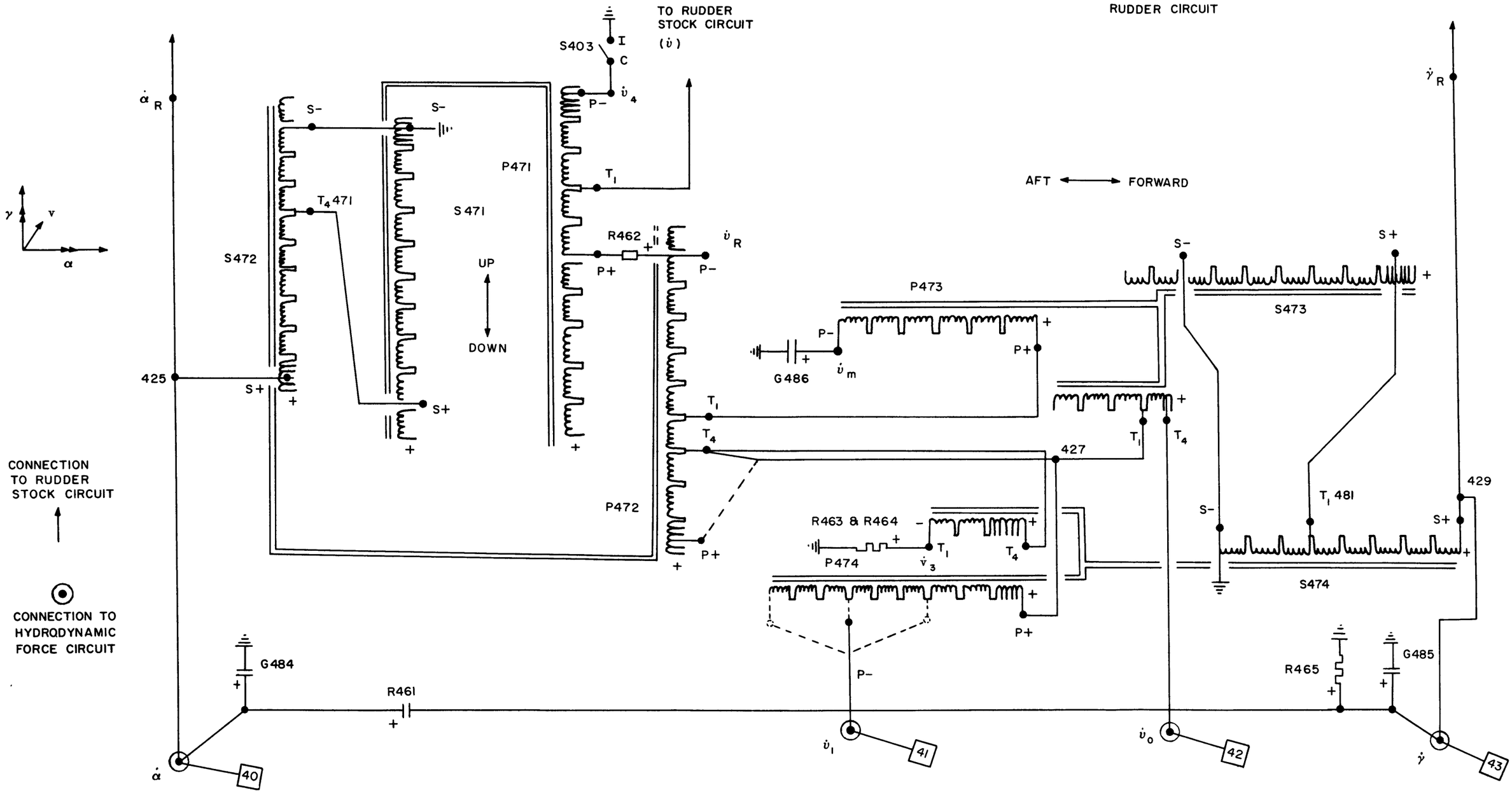

Figure 84 – Rudder Circuit (Mechanical Effects)

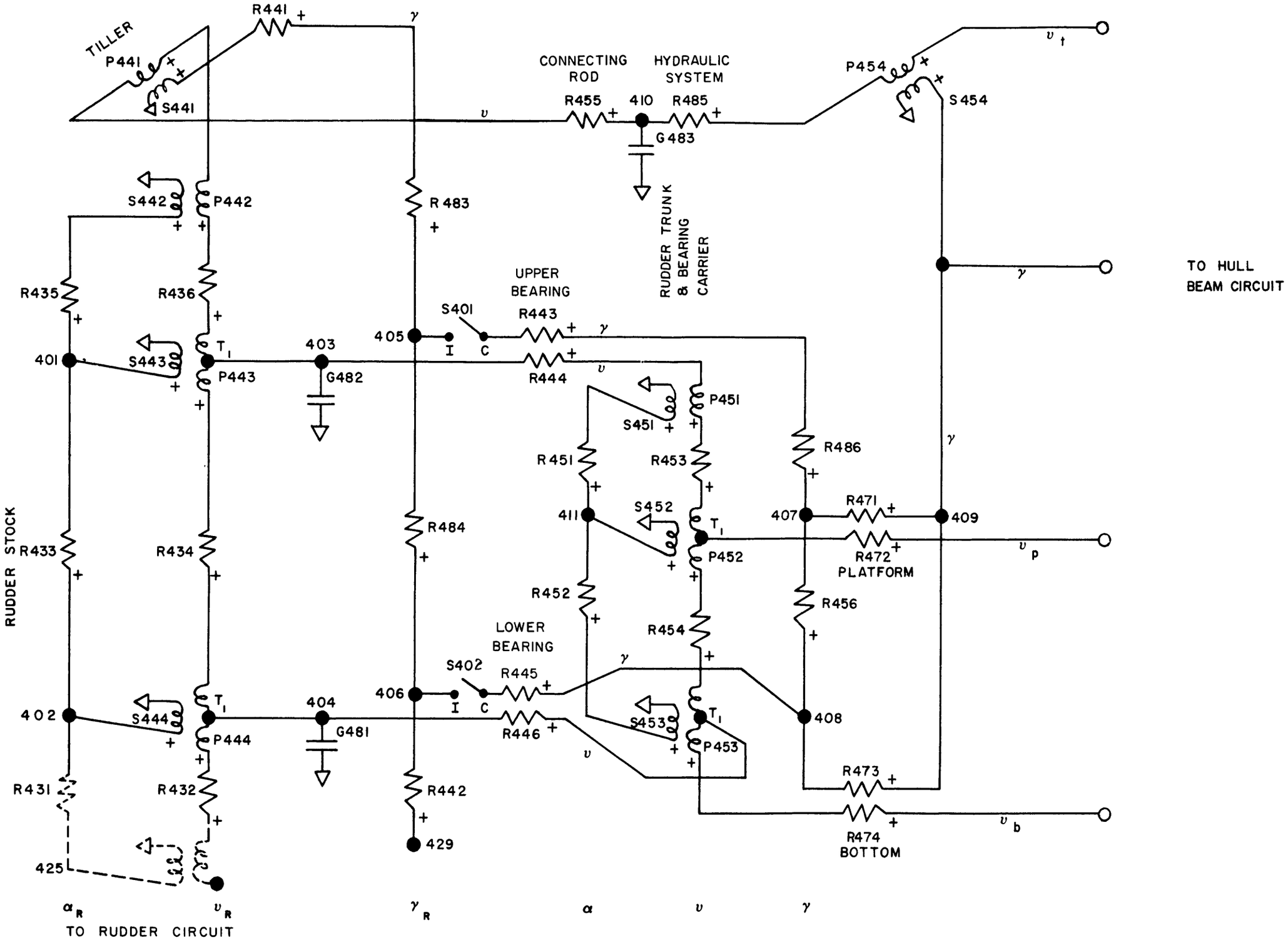

Figure 85 – Rudder Supporting Structure Circuit

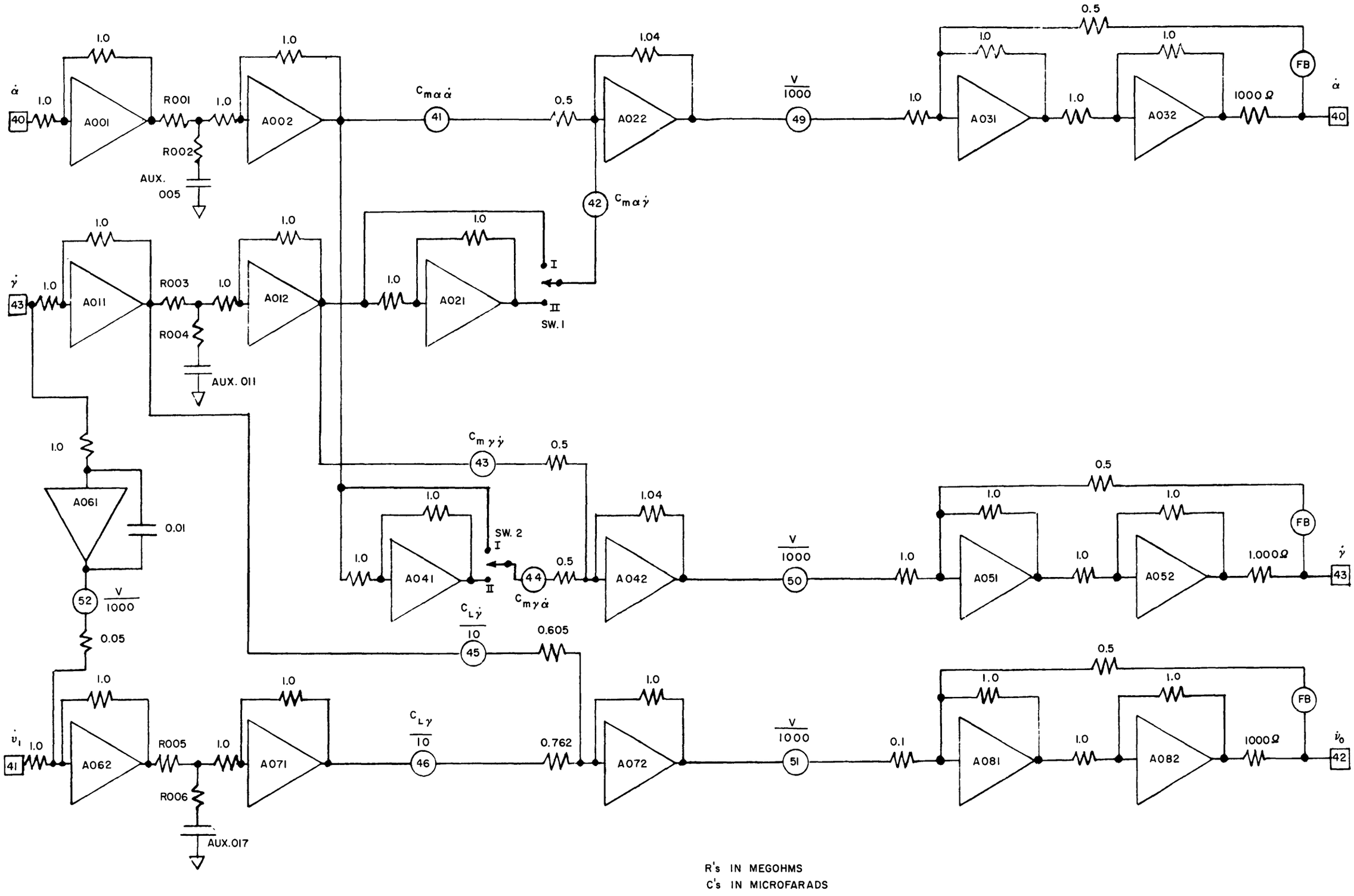

Figure 86 – Rudder Circuit (Hydrodynamic Forces)

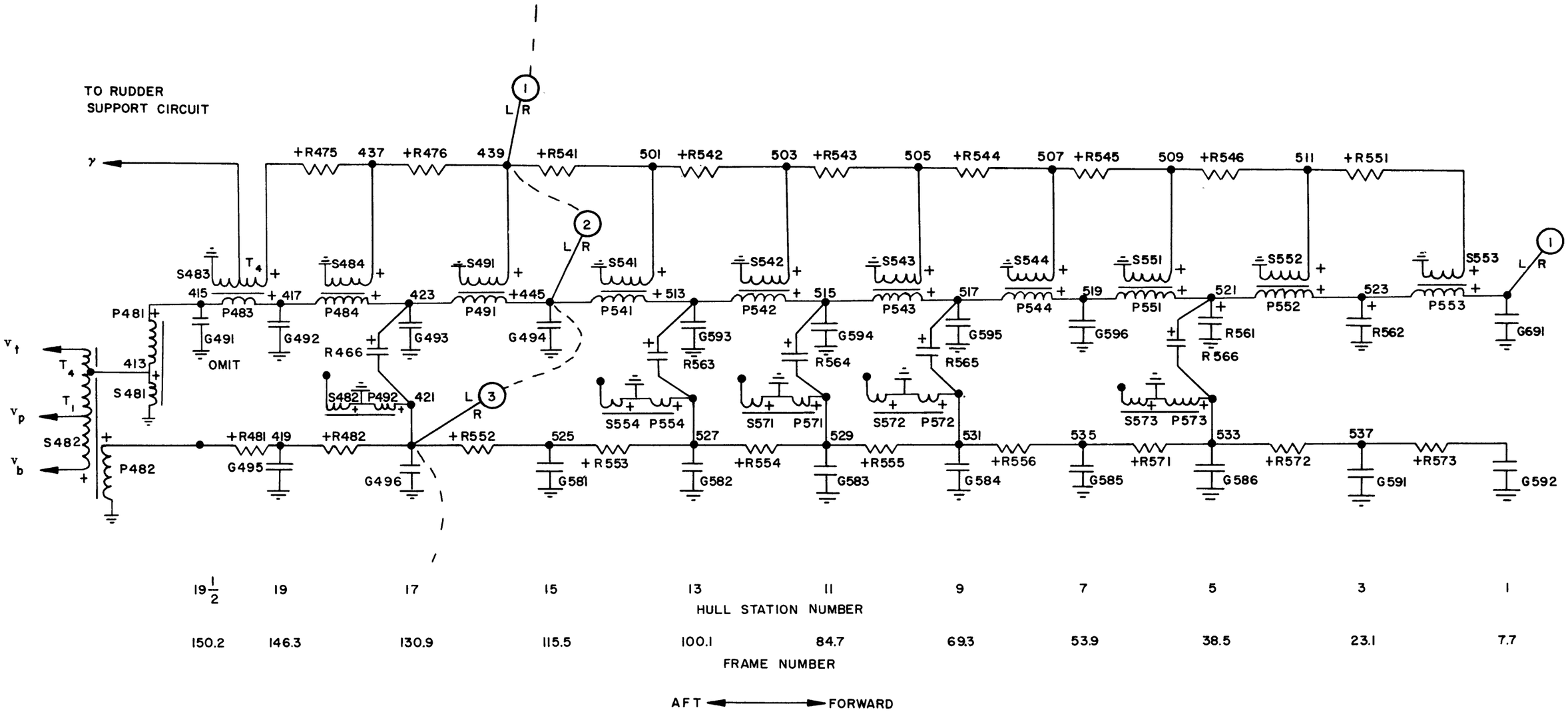

Figure 87 – Hull Circuit

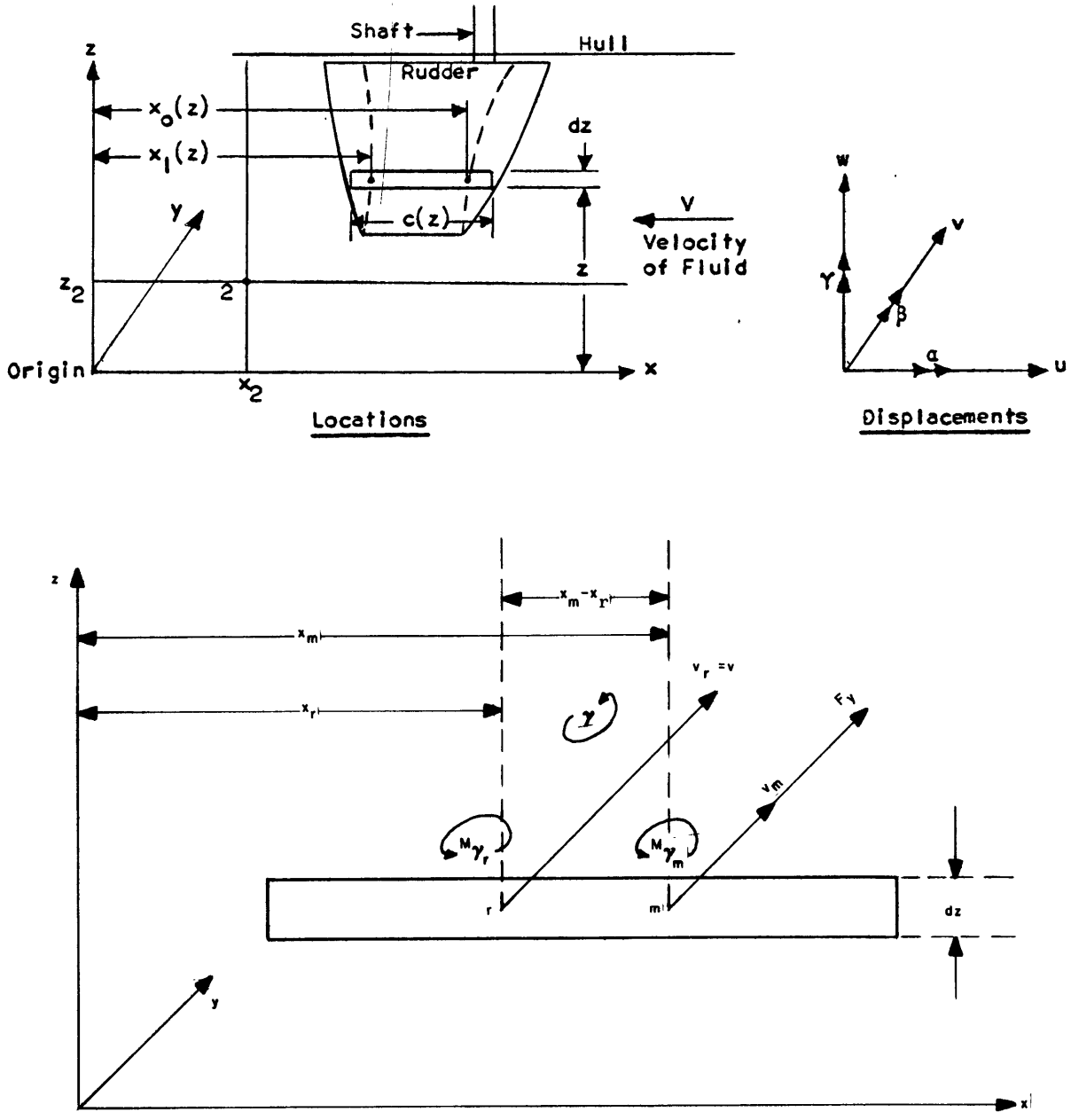

Sign connection for positive motions, forces and moments (The actual reaction of the water on the rudder representing the effects of the virtual mass and virtual inertia are opposite in direction to the directions convertically assumed positive here)

Figure 88 – Planform of a Rigid Rudder

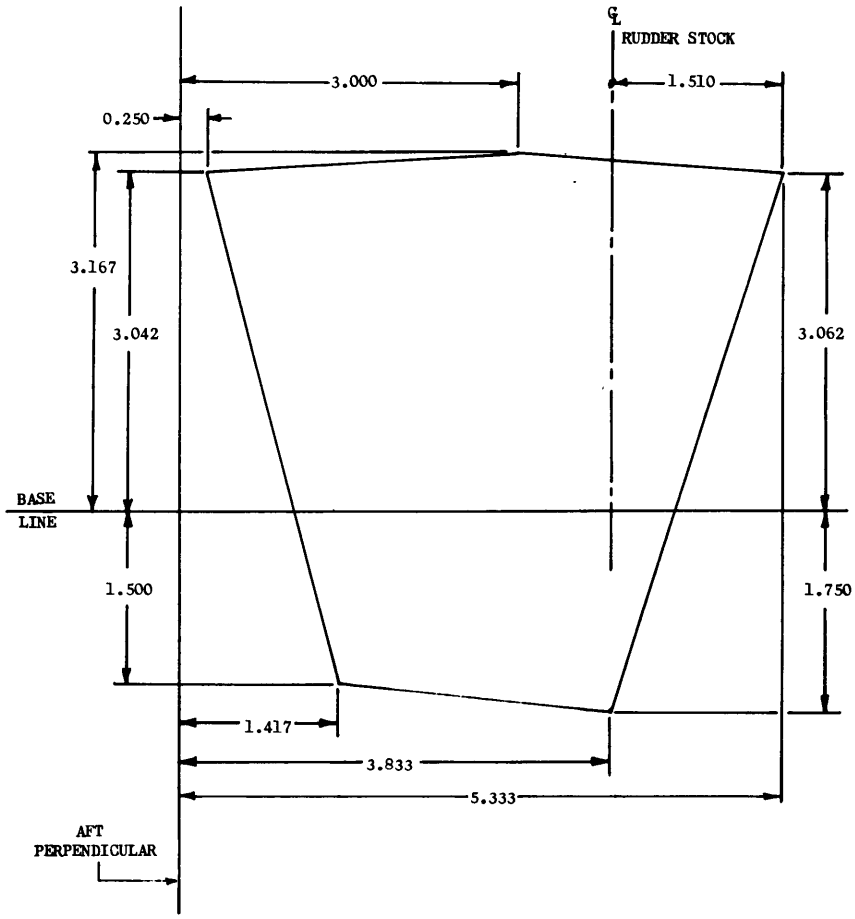

NOTE: ALL DIMENSIONS
IN FEET

Figure 89 – Rudder Planform

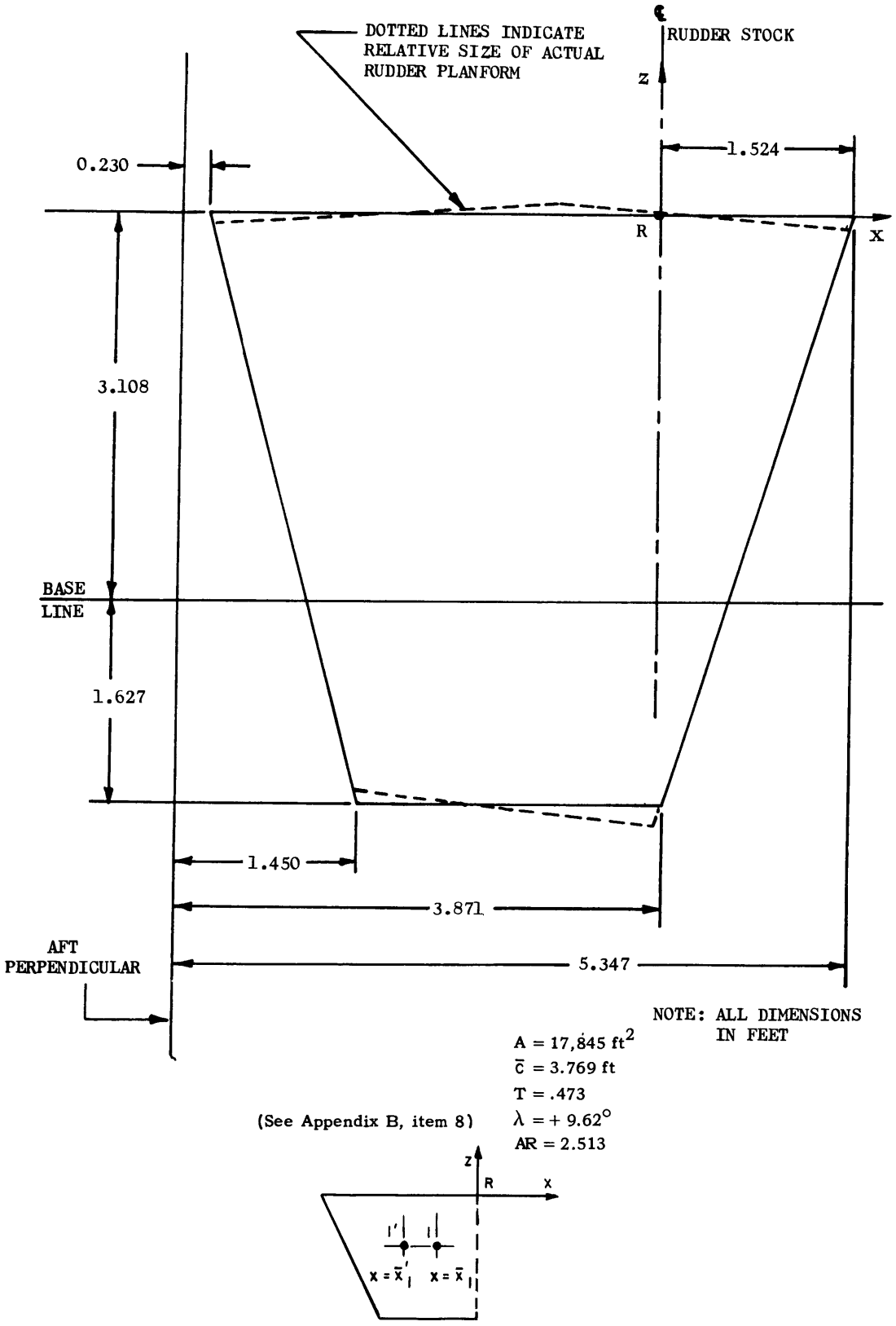

Figure 90 – Equivalent Trapezoidal Planform

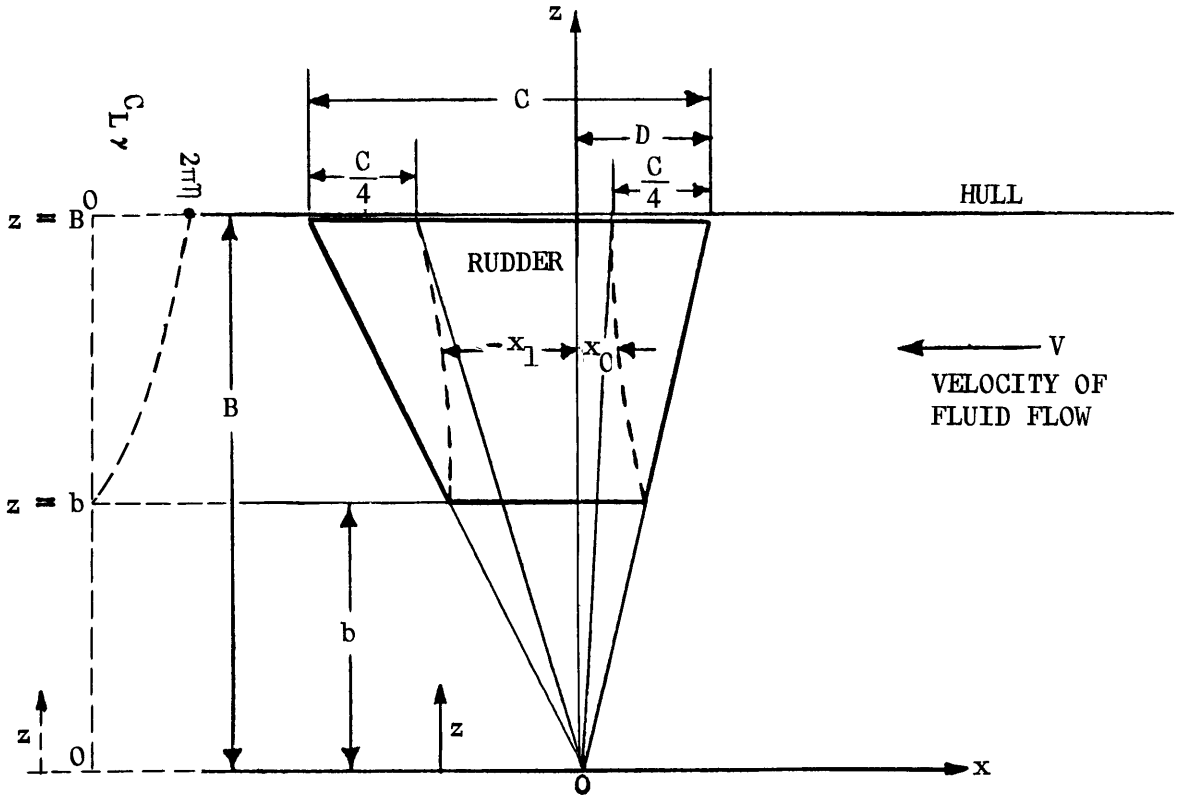

Figure 91 – Planform of Rigid Trapezoidal Rudder (Varying Lift Coefficient)

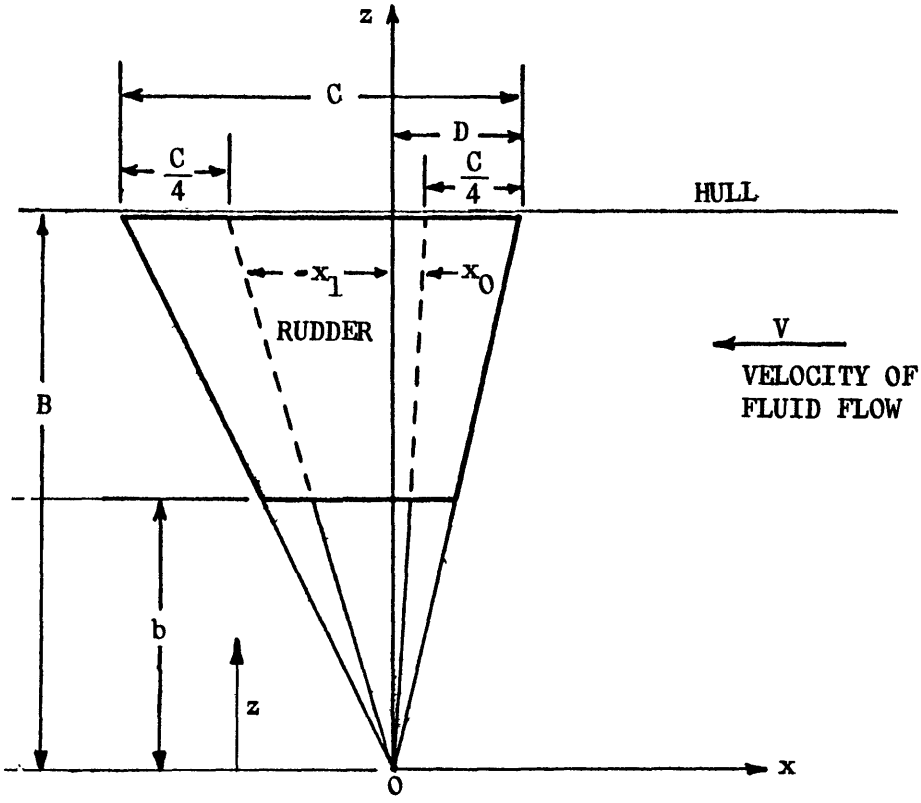

Figure 92 – Planform of Rigid Trapezoidal Rudder (Uniform Lift Coefficient)

Upper Trace: Response of System vs. Time (Used in measurement of ζ)

Second Trace: Response of System vs. Reference Sine Wave (Used in measurement of Frequency)

Third Trace: Excitation Force vs. Time

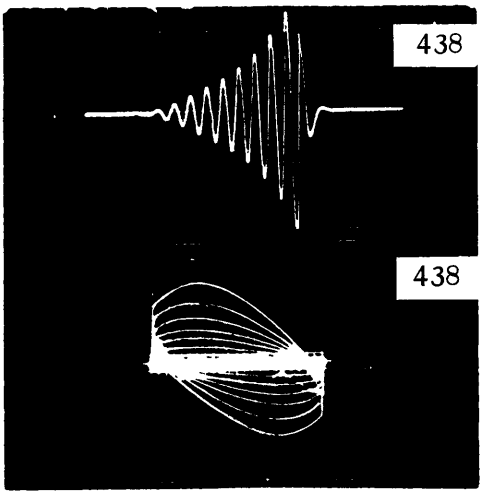

A. An Unstable Flutter Root

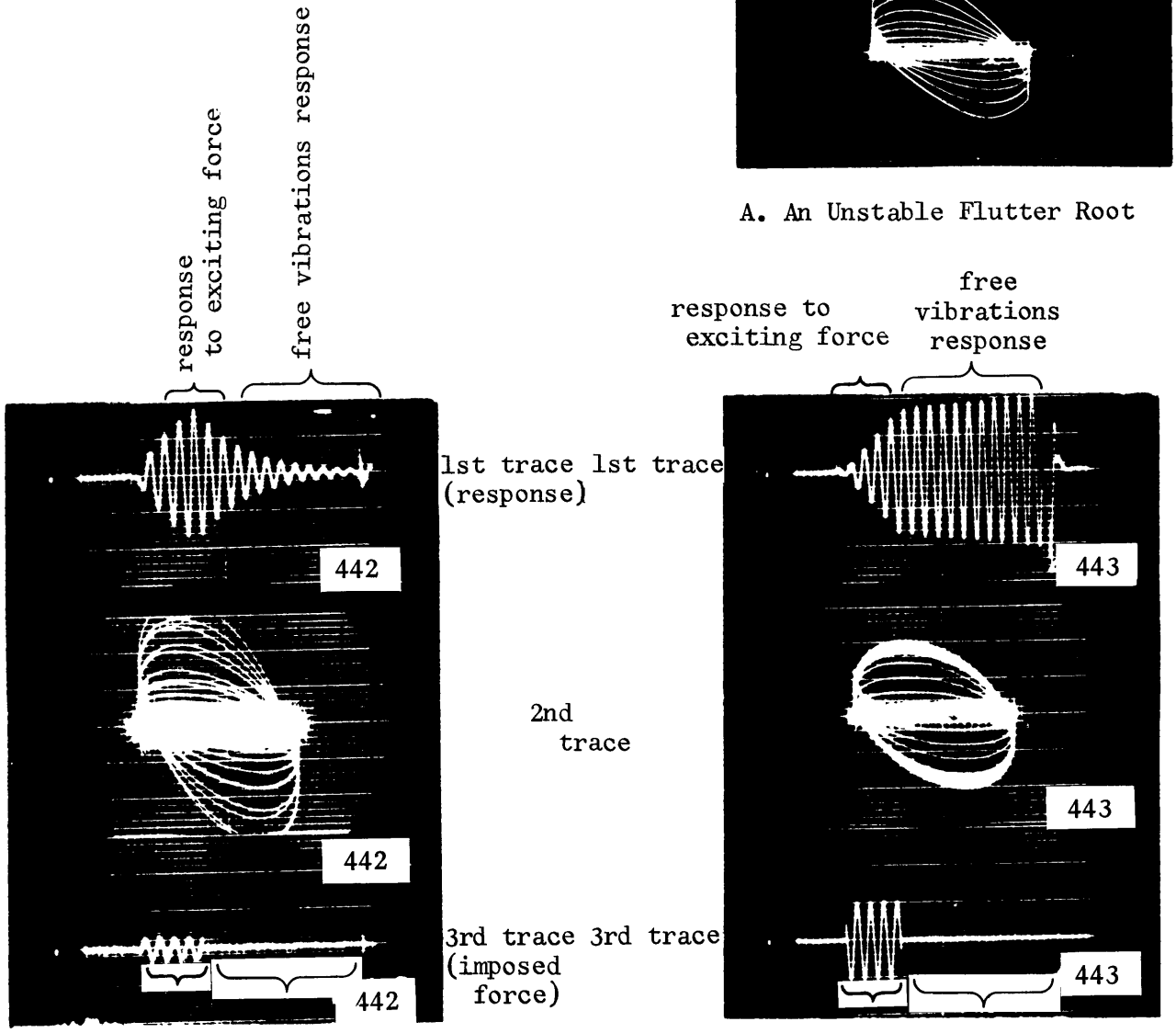

B. A Stable Flutter Root

C. A Slightly Unstable Flutter Root

Figure 93 – Photographs of Transient Records

Table 1
Computation of Structural and Virtual Mass and Inertia Terms of Rudder and Rudder Support Structure

A. Rudder

Parameter / Component	M lb	x_c ft	z_c ft	I_α lb-ft^2	I_γ lb-ft^2	P_{xz} lb-ft^2
Structure	1516	-0.609	-1.566	6309	2367	1978
Virtual Mass and Virtual Inertia	3525	-1.084	-1.826	17,523	6037	7134

B. Estimate of Masses of Rudder Support Structure

Location	Contributing Parts	Mass of Parts lb	Lumped Mass lb
Upper Bearing	Stock Carrier Tiller	603 39 91	733
Lower Bearing	Stock Trunk	663 297	960
Ram	Ram	513	513

Notes:

(1) x_c and z_c locate the center of mass of each component with respect to Point R, the "rudder origin" (intersection of centerline of rudder stock and root chord of the rudder).

(2) I_α, I_γ, and P_{xz} give moments and product of inertia with respect to axes through R, the "rudder origin".

(3) The source of information for the structural portion is a set of measurements taken from Reference 13.

(4) The virtual mass terms were determined by assuming two-dimensional, incompressible flow for each strip of the rudder. The magnitude of the term for each strip is determined from the items underlined thus in Appendix B. The entire virtual mass and moment of inertia for each strip of chord c and height dz is given by:
   (a) A mass of water giving inertia to lateral acceleration ($\dot{v}$) of amount $\frac{\pi}{4}\rho c^2 dz$, the location of this mass being at the mid-chord of the strip, and
   (b) A moment of inertia to yaw acceleration ($\dot{\gamma}$) of amount $\frac{\pi}{4}\rho c^2 dz \frac{c^2}{32}$.
   For the virtual mass and inertia of the entire rigid rudder, these differential expressions were integrated over the height of the rudder.

(5) In Table 1, lb refers to a pound of mass, not force.

(6) The rudder structure includes that portion of the rudder stock lying below the root chord of the rudder.

Table 2
Mass and Inertia Terms, Rudder and
Supporting Structure (Basic Case)

Location	Magnitude		Units
	Three-Degree-of-Freedom Model	Six-Degree-of-Freedom Model	
Rudder (Structural Plus Virtual Mass and Inertia)			
Mass (1)	156.6	156.6	$lb\text{-}sec^2\text{-}ft^{-1}$
I_α (2)	261.6	261.6	$lb\text{-}sec^2\text{-}ft$
I_γ (2)	122.3	122.3	$lb\text{-}sec^2\text{-}ft$
P_{xz} (2)	25.4	25.4	$lb\text{-}sec^2\text{-}ft$
Lumped Mass in Rudder Stock at Lower Bearing	0	29.8	$lb\text{-}sec^2\text{-}ft^{-1}$
Lumped Mass in Rudder Stock at Upper Bearing	0	22.8	$lb\text{-}sec^2\text{-}ft^{-1}$
Lumped Mass in Hydraulic Ram	0	15.9	$lb\text{-}sec^2\text{-}ft^{-1}$

Notes:

(1) Location of rudder center of mass is $x_m = -0.941$ ft, $z_m = -1.749$ ft. (Origin is rudder stock centerline at root chord of rudder.)

(2) Moments and products of inertia are about axes through the center of mass located as in Note 1.

TABLE 3

Elasticity of Rudder and Supporting Structure

TABLE 3A Elastic Properties of Rudder Supporting Structure

Structural Component	Material	Reference for Dimensions	Elastic Property
Connecting Rod	Steel (assumed)	13	Tension
Tiller	Steel (assumed)	13	Side Bending and Shear
Rudder Stock	Steel	13*	Side Bending, Shear and Torsion
Bearing Carrier and Rudder Trunk	Aluminum	13	Side Bending and Shear
Platform	Aluminum	14	Distribution of In-Plane Lateral Force
Bottom	Aluminum	15	Distribution of In-Plane Lateral Force
Rudder Stock Bearing**	Micarta	13	Compression of Micarta Bearing Materal
Hydraulic Rudder Control System	Hydraulic Fluid (Effective Bulk Modulus Estimated at 100,000 lb in^{-2})	13	Compression of Fluid and Expansion of Lines

*Except diameter (between 3.10 ft and 6.45 ft above baseline) is 10.5 in.(see Figure 79).

**As a later variation, it was assumed that yaw moment could be transmitted through the bearings. For this purpose strain energy in the torsion of the bearing carrier and rudder trunk, and in the distribution of yaw moments throughout the platform and bottom was also considered.

TABLE 3B Flexibility Terms, Rudder and Supporting Structure (Basic Case)

Location		Flexibility	
		$10^{-9}\ \frac{ft}{lb}$	$10^{-9}\ \frac{rad}{ft\text{-}lb}$
Rudder Stock:			
Shear	Top	9.305	
	Middle	60.63	
	Bottom	0.616	
Bending	Top		53.20
	Middle		51.70
	Bottom		4.09
Torsion	Top		70.20
	Middle		68.20
	Bottom		15.55*
Trunk and Bearing Carrier:			
Shear	Top	79.5	
	Bottom	9.85	
Bending	Top		33.75
	Bottom		11.69
Torsion	Top		135.20
	Bottom		15.45
Upper Bearing:			
	Shear	1.44	
	Torsion		20.98

*Includes $10.15 \cdot 10^{-9}\ \frac{rad}{ft\text{-}lb}$ to account for flexibility of the rudder stock below the rudder root.

TABLE 3B (Continued)

Location	Flexibility	
	$10^{-9}\ \frac{ft}{lb}$	$10^{-9}\ \frac{rad}{ft\text{-}lb}$
Lower Bearing:		
Shear	0.90	
Torsion		5.89
Platform:		
Shear	8.17	
Torsion		3.903
Bottom:		
Shear	5.32	
Torsion		3.206
Tiller:		
Bending		5.404
Connecting Rod:		
Tension	30.2	
Hydraulic System:	677.	

Notes:

(1) The dimensions and information on materials and cross sections used in obtaining these flexibilities are given in Figure 3 and Table 3A, respectively.

(2) For bending and shear of the rudder stock and of the rudder trunk and bearing carrier, some flexibilities are associated with the shear force and some with the bending moment. For these elements a Russell beam analogy was used and the lumped flexibility associated with the shear force accounts for a part of the bending strain energy, in addition to all of the shear strain energy. Reference 7 discusses in detail this division of strain energy for the Russell beam.

Table 4
Hull Mass and Inertia (Includes Virtual Mass)*
(Basic Case, 1/2 Ship)

Hull Station	Mass $lb\text{-}sec^2\text{-}ft^{-1}$	Height of Mass above Neutral Axis (1) ft	Radius of Gyration in Roll(3) ft
(Bow)			
1	360	+1.7	5.5
3	425	+0.5	6.5
5	815	+0.1	6.5
7	691	-0.6	6.5
9	1497	-1.9	9.0
11	1352	-0.7	10.0
13	1471	-0.6	9.5
15	754	-0.6	6.5
17	797	-0.2	6.5
19 (2)	892	-1.1	6.0
(Stern)			

Notes:

(1) Neutral axis is taken as 8.00 ft above Hull baseline (Figure 3).

(2) Excludes a total mass of 225 lb sec^2 ft^{-1} associated with the rudder and supporting structure.

(3) Relative to center of mass of section.

(4) Ship length at waterline is 154 ft. Thus each section of the 10 section beam is 14.14 ft long.

(5) The rudder stock centerline is almost exactly at Station 19½.

*The sources of information for this Table are: Column 2, Reference 17; Column 3, References 15, 17 and estimates; Column 4, Reference 16 and estimates. Of the total hull mass approximately 11 percent is due to virtual mass, which was calculated based on the method of Reference 8, the dimensions of Reference 16, and the immersion data of Figure 6A.

Table 5
Calculation of Hull Flexibilities

A. Side Bending

Station	Δx ft	*Moment of Inertia I, ft⁴ Forward End of Lumping Span, I_1	*Moment of Inertia I, ft⁴ Aft End of Lumping Span, I_2	$\Delta I = \lvert I_2 - I_1 \rvert$ ft⁴	$\log \frac{I_{max}}{I_{min}}$	B_I** ft^{-3}	Flexibility*** $C = B_I/E$ 10^{-9} $\frac{rad}{lb\text{-}ft}$
3	15.4	37.8	53.2	15.4	.342	.342	.230
5	↓	53.2	68.1	14.9	.2470	.2552	.1720
7		68.1	86.0	17.9	.2335	.2010	.1354
9		88.1	105.8	17.7	.1831	.1593	.1074
11		109.4	109.4	--	---	.1407	.0948
13		109.3	109.3	--	---	.1408	.0949
15		101.5	84.1	17.4	.1881	.1665	.1122
17	15.4	82.7	71.0	11.7	.1526	.2008	.1353
$18\frac{3}{4}$	11.55	69.7	69.7	--	---	.1657	.1117

B. Twisting

Station	Δx ft	*Moment of Inertia J, ft⁴ Forward End of Lumping Span, J_1	*Moment of Inertia J, ft⁴ Aft End of Lumping Span, J_2	$\Delta J = \lvert J_2 - J_1 \rvert$ ft⁴	$\log \frac{J_{max}}{J_{min}}$	B_J** ft^{-3}	Flexibility*** $C = B_J/G$ 10^{-9} $\frac{rad}{lb\text{-}ft}$
2	15.4	15.3	35.3	20.0	.836	.644	1.146
4	↓	35.3	48.7	13.4	.3217	.3697	.658
6		48.7	61.0	12.3	.2253	.2821	.502
8		60.2	73.7	13.5	.2022	.2307	.410
10		75.3	75.3	--	---	.2045	.364
12		76.8	76.8	--	---	.2005	.357
14		76.0	68.3	7.7	.1068	.2136	.380
16		64.2	51.1	13.1	.2280	.2681	.477
18	15.4	46.6	46.6	--	---	.3303	.588
$19\frac{1}{4}$	3.85	41.4	41.4	--	---	.0930	.1655

*I, J are 1/2 values for entire ship.

**$B_I = \int \frac{dx}{I} = \frac{\Delta x}{I}$ where I is constant over Δx and since d(log I) = Log I_{max} - Log I_{min} = Log $\frac{I_{max}}{I_{min}}$ then

$B_I = \frac{\Delta x}{|\Delta I|} \log \frac{I_{max}}{I_{min}}$ where I is linear between I_{max} and I_{min}. Similarly for B_J.

***$E = 10.3 \times 10^6$ $lb_f/in^2 = 1483 \times 10^6$ $lb_f\ ft^{-2}$; $G = 3.9 \times 10^6$ $lb_f/in^2 = 562 \times 10^6$ $lb_f ft^{-2}$
I_1 and I_2 are the extremes of an equivalent linear I versus x in the segment Δx. I_{min} = minimum of I_1, I_2 and I_{max} = maximum of I_1, I_2. Similarly for J.

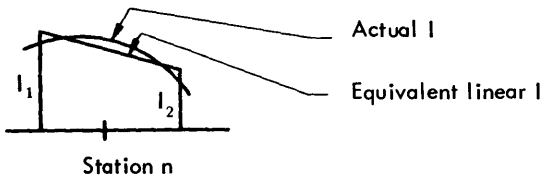

Table 6
Summary of Normal Mode Frequencies

Number of Degrees of Freedom of Model	3 (Basic) (Analysis)		3 (Basic) (Computer)		6 (Basic) (Computer)		20 (No Mass Coupling) (Computer)	20 (Basic) (Computer)	23 (Basic) (Computer)	
See Note (1)	A	B	A	B	A	B			A	B
							7.8 B	8.1	7.8	7.9
	11.968		12.2		12.1				12.0	
							14.2 T	14.3	14.5	14.1
							19.7 B	19.7	19.7	19.1
							20.9 T	21.0	21.0	20.7
							28.2 T	28.3	28.2	27.2
		29.415		28.6		28.0				30.5
							35.0 B	35.3	35.0	36.7
							38.3 T	38.5	38.3	39.1
							43.7 T	43.8	43.7	44.5
	47.154		47.1		40.4				46.2	
							51.3 T	50.3	53.0	51.5
							53.3 B	55.5		55.2
						62.5				
					71.7					
		93.107		94.2		95.2				
					132.0	138.3				
	352.619	354.816	298.3	300.0	257.5	258.3				
					X	X	X	X	X	X

Notes:

(1) A: No yaw moment diverted from rudder stock through rudder bearings.
B: Yaw moment is transmitted through rudder bearings.

(2) For twenty-degree-of-freedom model, rudder is disconnected, and only the hull participates.
B indicates hull bending mode, and T indicates hull torsion mode.

(3) Frequencies are in cycles per second.

(4) Related modes are entered on the same horizontal line.

(5) X indicates other modes exist with frequencies above those measured and listed.

Table 7
Normal Modes, Six-Degree-of-Freedom Model

Mode Number	1	2	3	4	5	Units
Frequency	12.18	40.4	71.7	132.0	257.5	cps
Measured Damping ζ	0.039	0.016	0.007	0.013	0.023	Per Unit Critical
Coordinate						
Rudder γ	+1.000	+1.000	+1.000	+1.000	+1.000	rad
Rudder α	-0.111	+0.636	+0.501	+0.365	-1.39	rad
v at Rudder Origin	-0.070	+0.363	+2.862	+1.811	+3.32	ft
v, Rudder Stock, Lower Bearing	-0.014	+0.075	+0.081	+2.078	+3.72	ft
v, Rudder Stock, Upper Bearing	+0.298	-1.017	+0.479	+25.38	-0.326	ft
v, Hydraulic Ram	-0.729	-2.46	+4.34	-5.54	-0.028	ft

Table 8
Mode Shapes—Twenty-Degree-of-Freedom Model—
Hull with No Mass Coupling—Rudder Disconnected

Mode Number	1		2		3		4		5		6		7		8		9		10	
Frequency (cps)	7.83		14.24		19.67		20.92		28.17		35.00		38.3		43.7		51.3		53.33	
Measured damping, ζ	0.053		0.012		0.013		0.008		0.007		0.010		0.007		0.008		0.006		0.008	
Hull Station	v	α	v	α	v	α	v	α	v	α	v	α	v	α	v	α	v	α	v	α
1	+1.000		+1.000		+1.000		+1.000		+1.000		+1.000		+1.000		+1.000		+0.045		+1.000	
3	+0.559		+0.875		+0.123		+0.763		+0.578		-0.402		+0.187		-0.049		-0.020		-1.007	
5	+0.151		+0.754		-0.475		+0.468		+0.130		-0.855		-0.421		-0.601		-0.032		-0.788	
7	-0.163		+0.537		-0.585		+0.096		-0.308		-0.214		-0.445		-0.240		+0.017		+0.806	
9	-0.339		+0.307		-0.301		-0.222		-0.529		+0.501		-0.162		+0.264		+0.035		+0.870	
11	-0.364		0.000		+0.154		-0.325		+0.040		+0.443		+0.523		-0.193		-0.120		-0.743	
13	-0.251		-0.311		+0.478		-0.156		+0.523		-0.201		-0.287		+0.059		+0.323		-0.857	
15	-0.039		-0.513		+0.459		+0.167		+0.211		-0.668		-0.297		+0.104		-0.920		+0.930	
17	+0.289		-0.703		+0.079		+0.524		-0.276		-0.427		-0.046		+0.046		-1.002		+1.537	
19	+0.647		-0.829		-0.563		+0.791		-0.717		+0.524		+0.323		-0.099		+1.000		-0.881	
19$\frac{1}{2}$	+0.739		-0.829		-0.722		+0.791		-0.717		+0.760		+0.323		-0.099		+1.000		-1.488	

Table 9
Mode Shapes—Twenty-Degree-of-Freedom Model—Basic Hull—Rudder Disconnected

Mode Number	1		2		3		4		5		6		7		8		9		10	
Frequency (cps)	8.08		14.3		19.7		21.0		28.3		35.3		38.5		43.8		50.3		55.5	
Measured Damping, ζ	.028		.012		.013		.008		.006		.012		.006		.005		.012		.014	
Hull Station	v	α	v	α	v	α	v	α	v	α	v	α	v	α	v	α	v	α	v	α
1	+1.000	+0.001	+0.298	+1.000	+1.000	+0.027	-1.279	+1.000	-1.187	+1.000	+1.000	+0.005	+0.070	+1.000	+0.276	+1.000	-2.09	+0.106	+1.000	-0.016
3	+0.555	+0.001	+0.125	+0.882	+0.126	+0.021	-0.041	+0.757	+0.256	+0.567	-0.391	+0.002	-0.066	+0.185	-0.268	-0.050	+1.86	-0.042	-1.088	+0.011
5	+0.150	+0.001	0.000	+0.732	-0.471	+0.014	+0.792	+0.461	+0.966	+0.097	-0.831	-0.001	-0.122	-0.414	-0.405	-0.602	+1.72	-0.078	-0.737	+0.010
7	-0.162	+0.001	-0.039	+0.520	-0.579	+0.003	+0.948	+0.097	+0.709	-0.309	-0.208	-0.012	-0.159	-0.448	-0.282	-0.245	-1.34	+0.073	+0.939	-0.035
9	-0.336	+0.001	-0.056	+0.294	-0.296	-0.006	+0.552	-0.221	+0.131	-0.519	+0.492	-0.014	-0.048	-0.164	-0.069	+0.259	-1.95	+0.105	+0.845	-0.021
11	-0.363	+0.002	-0.106	-0.020	+0.159	-0.006	-0.025	-0.332	+0.021	+0.049	+0.446	-0.009	+0.282	+0.535	-0.252	-0.183	+0.86	-0.152	-0.857	0.000
13	-0.252	+0.003	-0.093	-0.312	+0.483	-0.002	-0.423	-0.160	+0.049	+0.529	-0.183	+0.010	+0.040	-0.292	-0.101	+0.054	+2.04	+0.297	-0.769	+0.056
15	-0.041	+0.003	+0.061	-0.498	+0.460	+0.001	-0.475	+0.166	-0.024	+0.201	-0.659	+0.009	-0.217	-0.304	+0.193	+0.103	-0.85	-0.794	+1.111	-0.200
17	+0.283	+0.004	+0.372	-0.677	+0.076	+0.005	-0.240	+0.532	+0.016	-0.322	-0.435	+0.001	-0.189	-0.050	+0.230	+0.052	-2.60	-0.951	+1.507	-0.148
19	+0.637	+0.005	+0.874	-0.787	-0.574	+0.007	-0.123	+0.809	+0.338	-0.742	+0.492	+0.010	+0.230	+0.340	-0.220	-0.109	+2.22	+1.000	-0.924	+0.106
19½	+0.726	+0.005	+0.992	-0.787	-0.733	+0.007	0.000	+0.809	+0.425	-0.742	+0.730	+0.010	+0.336	+0.340	-0.335	-0.109	+3.45	+1.000	-1.514	+0.106
Units	ft	rad	ft	rad	ft	rad	ft	rad	ft	rad	ft	rad	ft	rad	ft	rad	ft	rad	ft	rad

Table 10
Mode Shapes—Twenty-Three-Degree-of-Freedom Model—Basic Hull—Basic Rudder Connected

Mode Number	1		2		3		4		5		6		7		8		9		10		11	
Frequency (cps)	7.75		12.0		14.5		19.7		21.0		28.2		35.0		38.3		43.7		46.2		53.0	
Measured Damping, ζ	.027		.035		.014		.011		.008		.007		.012		.007		.007		.007		.013	
Hull Station	v	α	v	α	v	α	v	α	v	α	v	α	v	α	v	α	v	α	v	α	v	α
1	+1.000	-0.003	+0.184	+0.017	-0.532	+1.000	+1.000	+0.031	-1.272	+1.000	-1.338	+1.000	+1.000	+0.013	-0.382	+1.000	+0.513	+1.000	-0.097	+0.019	-1 60	+0.058
3	+0.568	-0.002	+0.074	+0.016	-0.137	+0.889	+0.136	+0.025	-0.055	+0.759	+0.276	+0.592	-0.380	+0.005	+0.161	+0.198	-0.427	-0.048	+0.071	-0 003	+1 57	-0.032
5	+0.176	-0.002	-0.016	+0.014	+0.187	+0.737	-0.456	+0.016	+0.787	+0.461	+1.078	+0.145	-0.823	-0.003	+0.271	-0.413	-0.613	-0.599	+0.081	-0.013	+1.24	-0.040
7	-0.132	-0.002	-0.068	+0.011	+0.365	+0.516	-0.565	+0.004	+0.948	+0.097	+0.807	-0.284	-0.220	-0.016	-0.136	-0.445	-0.231	-0.256	-0.044	0.000	-1.27	+0.066
9	-0.313	-0.002	-0.078	+0.008	+0.304	+0.288	-0.288	-0.007	+0.557	-0.219	+0.125	-0.508	+0.478	-0.017	-0.271	-0.172	+0.151	+0.247	-0.093	+0.010	-1.43	+0.064
11	-0.359	0.000	-0.049	+0.004	-0.056	-0.037	+0.152	-0.007	-0.040	-0.330	-0.075	+0.024	+0.455	-0.004	+0.151	+0.546	-0.221	-0.163	+0.005	-0.012	+1.00	-0.100
13	-0.278	+0.001	+0.006	-0.001	-0.279	-0.328	+0.471	-0.003	-0.426	-0.162	-0.030	+0.503	-0.160	+0.011	+0.226	-0 285	-0.292	+0.031	+0.090	+0.014	+1.45	+0.238
15	-0.083	+0.003	+0.072	-0.006	-0.385	-0.508	+0.451	-0.002	-0.476	+0.165	+0.025	+0.223	-0.655	+0.003	+0.055	-0 333	+0.095	+0.134	+0.020	-0.020	-1.27	-0.796
17	+0.201	+0.005	+0.134	-0.012	-0.233	-0.672	+0.067	+0.006	-0.241	+0.532	+0.130	-0.232	-0.467	-0.010	-0.176	-0.100	+0.372	+0.121	-0.089	-0 037	-2.02	-0.745
19	+0.530	+0.007	+0.179	-0.019	+0.456	-0.763	-0.549	+0.009	-0.181	+0.808	+0.406	-0.663	+0.451	+0.006	-0.116	+0 318	-0.055	-0.103	-0.029	+0.011	+3.18	+1.198
19*	+0.618	+0.007	+0.188	-0.020	+0.608	-0 755	-0.707	+0.010	-0.221	+0.806	+0.466	-0.667	+0.691	+0.010	-0.090	+0.335	-0.186	-0.124	0.000	+0.019	+4.34	+1.000
Rudder																						
v_R	+0.670		+0.021		-2.768		-0.634		+4.01		-3.098		+0.802		+2.160		-1.552		+0.408		+1.271	
α	+0.043		-0.142		+0.025		+0.056		+0.643		-0.958		+0.123		+1.277		-1.425		+0.561		-13.74	
γ	-0.277		+1.000		-8 .17		-0.592		+5.21		-3.875		+0.745		+3.226		-2.932		+1.000		-16.56	

Notes:

(1) Units are feet for all lateral displacements (v hull; v_r) and radians for all angular displacements.

(2) v_R is the lateral displacement of the rudder origin (Point R, Figure 90).

Table 11
Definition of Cases for Numerical Analysis

Case No.	Parameters											
	$C_{L\gamma}$	$C_{M\alpha\dot{\alpha}}$	$C_{M\alpha\dot{\gamma}}$	$C_{M\gamma\dot{\alpha}}$	$C_{M\gamma\dot{\gamma}}$	D_f lb_f sec ft	D_m lb_f sec ft	$\frac{x_4 - \bar{x}_o}{\bar{c}}$	$\frac{x_4 - \bar{x}_1}{\bar{c}}$	$\frac{z_4 - \bar{z}_o}{\bar{c}}$	$\frac{z_4 - \bar{z}_1}{\bar{c}}$	All Mass Terms
(B) Basic Case	2.77	0.2373	0	0	0.416	0	0	-0.0334	0.5427	0.7023	0.7023	Table 1 Column 2
1 (Basic)	B	B	B	B	B	B	B	B	B	B	B	B
2	3.40	B	↓	↓	B	↓	↓	↓	↓	↓	↓	↓
3	B	0.1186	↓	↓	B	↓	↓	↓	↓	↓	↓	↓
4	↓	B	B	↓	0.364	↓	↓	↓	↓	↓	↓	↓
5	↓	↓	0.200	B	B	↓	↓	↓	↓	↓	↓	↓
6	↓	↓	B	-0.100	↓	B	B	↓	↓	↓	↓	↓
7	↓	↓	↓	B	↓	18,860	665	B	↓	↓	↓	↓
8	↓	↓	↓	↓	↓	B	B	-0.0580	↓	↓	↓	↓
9	↓	↓	↓	↓	↓	↓	↓	0.0415	↓	B	↓	↓
10	↓	↓	↓	↓	↓	↓	↓	B	B	0.9429	↓	↓
11	↓	↓	↓	↓	↓	↓	↓	↓	0	B	↓	↓
12	↓	↓	↓	↓	↓	↓	↓	↓	0.896	B	B	↓
13	↓	↓	↓	↓	↓	↓	↓	↓	B	B	0.5171	↓
14	↓	↓	↓	↓	↓	↓	↓	↓	B	0.3322	0.3322	B
15	B	B	B	B	B	B	B	B	B	B	B	1.25×B

Table 12
Initial Slope of ζ versus V/V_o Curve

Mode No.	Initial Slope*
1	-.041
2	-.180
3	-.017
4	-.0019
5	-.0044
6	-.0017
7	-.0022
8	-.0013
9	-.0029
10	-.030
11	-.019

*Initial slope is $$-\left.\frac{\partial \zeta}{\partial\left(\frac{V}{V_o}\right)}\right|_{\frac{V}{V_o}=0}$$

Notes:

(1) *Negative* values of initial slope correspond to a solution which becomes *more* stable as velocity V increases from zero.

(2) Above values are calculated analytically based on mode shapes recorded in Section V.A.5. The frequency of Mode 1 given as 8.08 cps in Table 9 corresponds to point $\frac{V}{V_o} = 0$, in Figure 82 (heavy lined curve), on the curve for Mode 1, etc. From the mode shapes given in Table 9, and knowing the theoretical form of the hydrodynamic forces, the values for the initial slopes corresponding to a given mode were determined by energy methods.

(3) Calculations are for the basic twenty-three-degree-of-freedom model described in Section III E. Yaw moment is not transmitted through the rudder stock bearings.

Table 13
Summary of Hydrodynamic Parameters

Source	Hydrodynamic Parameters									
	$C_{L\gamma}$	$C_{M\alpha\dot{\alpha}}$	$C_{M\alpha\dot{\gamma}}$	$C_{M\gamma\dot{\alpha}}$	$C_{M\gamma\dot{\gamma}}$	$\bar{x}_o$ (ft) *	$\bar{x}_1$ (ft) *	z_o, z_1 (ft) **	D_f lb-sec-ft	D_m lb-sec-ft
A1	2.77#	0.2373	+0.00248	-0.01664	0.416	+0.213	-2.234	-1.591		
A2	2.77#	0.3485	+0.0402	-0.0591	0.383	-0.146	-2.069	-2.083		
B	2.77					+0.126		-2.060		
C	3.02					+0.058				
D	2.57					+0.156				
E									18,860	665
Basic Value Chosen for Numerical Analysis	2.77	0.2373	0	0	0.416	+0.126	-2.234	-2.060	0	0

Source Code:

A1 - Quasi-Strip Theory - Parabolic Lift Distribution (See Appendixes B and C).
A2 - Same as A1, except lift distribution assumed constant over span (See Appendixes B and D).
B - TMB Report 933 - Results of Wind Tunnel Tests (See Reference 9).
C - TMB Report 933 - Theoretical Formulas (See Reference 9).
E - TMB Report 1508 - Notes 4, 5 of Table 1 (See Reference 10).
* - Measured positive forward from rudder stock centerline.
** - Measured positive upward from root of rudder.
\# - Chosen to match experiment (Source B). This establishes the normalizing factor, η; and the remaining parameters in each row.

Table 14
Definition of Scale Factors for Conversion of
Physical Quantities to Computer Parameters

Time: $t_m = N\, t_e$

$\omega_m = \frac{1}{N}\, \omega_e$

Dependent Variables:

	Velocity	Force	Displacement
A. Linear	$\frac{dv}{dt_m} = \frac{Ka}{N} e_v$	$F_v = \frac{K}{a} i_v$	$v = Ka \frac{1}{P_e} e_v$
B. Angular	$\frac{d\alpha}{dt_m} = \frac{Ka}{NP_\alpha} e_\alpha$	$M_\alpha = \frac{KP_\alpha}{a} i_\alpha$	$\alpha = \frac{Ka}{P_\alpha} \frac{1}{P_e} e_\alpha$

Where $e \equiv$ Voltage

$i \equiv$ Current

$t \equiv$ Time

$v \equiv$ Lateral Displacements

$\alpha \equiv$ An Angular Displacement

$F_v \equiv$ Lateral Force

$M_\alpha \equiv$ A Moment

Subscripts:

m, mechanical (the ship)

e, electrical (the computer)

$P_e \equiv \frac{d}{dt_e}$

K, a, N, P_α are the scale factors defined by the above relations.

Table 15
List of Computer Conversion Scale Factors

A. Rudder

Scale Factor	Value	Units
N	6	---
a	$\frac{2}{3} \times 10^{-3}$	$\left(\frac{\text{ft}}{\text{lb-ohm-sec}}\right)^{\frac{1}{2}}$
a^2	$\frac{4}{9} \times 10^{-6}$	$\frac{\text{ft}}{\text{lb-ohm-sec}}$
P_α	3	ft
P_γ	3	ft
$\frac{1}{a^2}$	$\frac{9}{4} \times 10^{6}$	$\frac{\text{hy-lb}}{\text{ft}}$
$\frac{P_\alpha^2}{a^2}$	$\frac{81}{4} \times 10^{6}$	hy-lb-ft
$\frac{P_\gamma^2}{a^2}$	$\frac{81}{4} \times 10^{6}$	hy-lb-ft
$\frac{a^2}{N^2}$	$\frac{1}{81}$	$\frac{\mu\text{fd} - \text{ft}}{\text{lb-sec}^2}$
$\frac{a^2}{N^2 P_\alpha^2}$	$\frac{1}{729}$	$\frac{\mu\text{fd}}{\text{lb-sec}^2\text{-ft}}$
$\frac{a^2}{N^2 P_\gamma^2}$	$\frac{1}{729}$	$\frac{\mu\text{fd}}{\text{lb-sec}^2\text{-ft}}$
$\frac{a^2}{N}$	$\frac{2}{27} \times 10^{-6}$	$\frac{\text{ft}}{\text{lb-ohm-sec}}$
$\frac{a^2}{N P_\alpha^2}$	$\frac{2}{243} \times 10^{-6}$	$\frac{\text{mho}}{\text{lb-ft-sec}}$
$\frac{a^2}{N P_\alpha P_\gamma}$	$\frac{2}{243} \times 10^{-6}$	$\frac{\text{mho}}{\text{lb-ft-sec}}$
$\frac{a^2}{N P_\gamma^2}$	$\frac{2}{243} \times 10^{-6}$	$\frac{\text{mho}}{\text{lb-ft-sec}}$

B. Hull

Scale Factor	Value	Units
N	6	---
a	$\frac{1}{6} \times 10^{-3}$	$\left(\frac{\text{ft}}{\text{lb-ohm-sec}}\right)^{\frac{1}{2}}$
a^2	$\frac{1}{36} \times 10^{-6}$	$\frac{\text{ft}}{\text{lb-ohm-sec}}$
P_α	5	ft
P_γ	9.240	ft
$\frac{P_\alpha^2}{a^2}$	900×10^{6}	hy-lb-ft
$\frac{P_\gamma^2}{a^2}$	3074×10^{6}	hy-lb-ft
$\frac{a^2}{N^2}$	$\frac{1}{1296}$	$\frac{\mu\text{fd} - \text{ft}}{\text{lb-sec}^2}$

Table 16
Calculation of Computer Element Settings

A. Inductors (Basic Rudder Supporting Structure)

Element No.	Flexibility		Scale Factor(3)		Inductance
(See Figure 85)	$10^{-9}\ \frac{ft}{lb}$	$10^{-9}\ \frac{rad}{lb\text{-}ft}$	$10^{6}\ \frac{hy\text{-}lb}{ft}$	10^{6} hy-lb-ft	henry
R436	9.305		2.25		0.020 (1)
R434	60.63		2.25		0.133 (1)
R432	0.616		2.25		0.000 (1)
R435		53.2		20.25	1.077
R433		51.70		20.25	1.047
R431		4.09		20.25	.083
R483		70.2		20.25	1.42
R484		68.2		20.25	1.38
R442		15.55		20.25	0.315
R453	79.5		2.25		0.179
R454	9.85		2.25		0.021 (1)
R451		33.75		20.25	0.683
R452		11.69		20.25	0.237
R486		135.2		20.25	2.74
R456		15.45		20.25	0.313
R444	1.44		2.25		0.003
R443		20.98		20.25	0.425
R446	0.90		2.25		0.002
R445		5.89		20.25	0.119
R472	8.17		2.25		0.018
R471		3.903		20.25	0.079
R474	5.32		2.25		0.012
R473		3.206		20.25	0.065
R441		5.404		20.25	0.109
R455	30.2		2.25		0.068
R485	677.		2.25		1.88 (2)

Notes:

(1) After correction for series parasitic inductance.

(2) After correction for shunt parasitic inductance.

(3) $\frac{1}{a^2}$ in first column. $\frac{P^2}{a^2}$ in second column.

B. Inductors (Basic Hull)

Element No. (See Figure 87)	Flexibility 10^{-9} $\frac{\text{rad}}{\text{lb-ft}}$	Scale Factor (1) 10^{9} hy-lb-ft	Inductance henry
Bending:			
R551	0.230	3.074	0.707
R546	0.1720		0.529
R545	0.1354		0.416
R544	0.1074		0.330
R543	0.0948		0.291
R542	0.0949		0.292
R541	0.1122		0.345
R476	0.1353		0.416
R475	0.1117	3.074	0.343
Torsion:			
R573	1.146	0.900	1.031
R572	0.658		0.592
R571	0.502		0.452
R556	0.410		0.369
R555	0.364		0.328
R554	0.357		0.321
R553	0.380		0.342
R552	0.477		0.429
R482	0.588		0.529
R481	0.1655	0.900	0.149

Note:
(1) $\frac{P_\gamma^2}{a^2}$, $\frac{P_\alpha^2}{a^2}$

C. Capacitors (Rudder and Supporting Structure)

Element No.	Identification	Mass or Inertia		Scale Factor (2)		Capacitance, μfd			
		lb-sec²-ft⁻¹	lb sec²-ft	$\frac{\mu fd\ ft}{lb\text{-}sec^2}$	$\frac{\mu fd}{lb\text{-}sec^2\text{-}ft}$	Total	Mutual	Self	Set
	Rudder								
G486	M	156.6		1/81		1.933		1.933	1.916(1)
G484	I_α		261.6		1/729	0.3585	0.0348	0.3237	0.317(1)
G485	I_γ		122.3		1/729	0.1679	0.0348	0.1331	0.114(1)
R461	P_{xz}		25.4		1/729	0.0348	0.0348		0.035
G482	Stock Upper Bearing	22.8		1/81		0.282		0.282	0.273(1)
G481	Stock Lower Bearing	29.8		1/81		0.368		0.368	0.359(1)
G483	Ram	15.9		1/81		0.196		0.196	0.196

(1) After correction for shunt parasitic capacitance.

(2) $\frac{a^2}{N^2}$ in first column. $\frac{a^2}{N^2p^2}$ in second column.

D. Capacitors (Hull)

Hull Sta.	Mass	$\bar{z}$ (1)	r (2)	Scale Factor $\frac{a^2}{N^2}$	M Capacitor Element No.	M Capacitor Capacitance (3), (5)	I_α- Capacitor Element No.	I_α- Capacitor Capacitance (4), (5)	Coupling Capacitor Element No.	Coupling Capacitor Capacitance (6), (7), (8)
	lb-sec²-ft⁻¹	ft	ft	$\frac{\mu fd\ ft}{lb\text{-}sec^2}$		μfd		μfd		μfd
1	360	+1.7	5.5	1/1296	G691	0.278	G592	0.369		
3	425	+0.5	6.5		R562	0.328	G591	0.557		
5	815	+0.1	6.5		R561	0.629	G586	1.063	R566	(+)0.076
7	691	-0.6	6.5		G596	0.533	G585	0.906		
9	1497	-1.9	9.0		G595	1.155	G584	3.905	R565	(-)0.439
11	1352	-0.7	10.0		G594	1.043	G583	4.196	R564	(-)0.146
13	1471	-0.6	9.5		G593	1.135	G582	4.110	R563	(-)0.136
15	754	-0.6	6.5		G494	0.582	G581	0.990		
17	797	-0.2	6.5		G493	0.615	G496	1.039	R466	(-)0.246
19	892	-1.1	6.0	1/1296	G492	0.688	G495	1.017		

(1) $\bar{z}$ = height of center of mass above neutral axis.

(2) r = radius of gyration of mass in roll about its center of mass.

(3) Capacitance = $\frac{a^2}{N^2}$ · Mass

(4) Capacitance = $\frac{a^2}{N^2}\ \frac{r^2 + \bar{z}^2}{P_\alpha{}^2}$ Mass, where P_α = 5 ft.

(5) Values are correct for variation with no mass coupling. For basic case subtract from these values the coupling capacitance appearing in the final column.

(6) Coupling capacitance = $\frac{a^2}{N^2 P_\alpha} \sum (\bar{z} \cdot \text{Mass})$, where the summation is indicated by the brace: }

(7) Values are correct for basic case. For the variation in which no mass coupling exists, set all capacitors to zero.

(8) (-) and (+) indicates negative terminal of capacitor connected to (-α) or (+α) node, respectively.

E. Resistors (Rudder Viscous Damping)

Function	v Circuit	γ Circuit
Element Number	R463 + R464	R465
Formula	$R = \frac{N \bar{c}^2}{a^2 D_f}$	$\frac{N P_\gamma^2}{a^2 D_m}$
Scale Factors	$\frac{a^2}{N} = \frac{2}{27} \cdot 10^{-6}$	$\frac{a^2}{N P_\gamma^2} = \frac{2}{243} \cdot 10^{-6}$
Physical Parameters	$\bar{c} = 3.769$ $D_f = 18,860$	$D_m = 665$
Resistance (1)	R = 10,170 ohms	R = 182,500 ohms

(1) These values are for the variation in which rudder viscous damping exists. For the basic case (no viscous damping) set R's to infinite.

F. Transformers

Transformer ratio calculations are not presented here (see Figure 84).

G. Active Element Section

Resistance and capacitance calculations for the elements of Figure 86 are not presented here.

APPENDIX A

ANALYSIS OF MOTIONS FOR PGM MOTOR GUNBOAT

The reader is referred to Appendix B of Reference 6 for background material on symmetry conditions applicable to the analysis of motions of the PGM Motor Gunboat.

In this analysis, the following conditions of symmetry were used:

1. Motion of the hull and rudders is entirely antisymmetric* with respect to the vertical (x-z) centerplane of the ship. Only displacements v, α,γ are represented.

2. The complete port rudder is represented in v, α, γ motion.

3. Properties of one-half the hull are represented, i.e., twice total hull beam flexibilities and half total hull masses.

The structural properties for symmetric motions of the two rudders of PGM are identical to those simulated in antisymmetric motion for the two- , three- , or six-degree-of-freedom system, even if the vibration characteristics of the rudders are different when they execute symmetric motions than when they execute antisymmetric motion. This follows from the fact that the hull, acting as a beam, does not significantly contribute to the symmetric behavior of the rudders.

*Any motion (of a structure which is symmetric about the x-z plane) can be resolved into the sum of a symmetric and an antisymmetric part[6]. For the symmetric part of the motion, motions at mirror image points on two sides of the plane will have the same value for components in the x, z, and β directions and the opposite values for components in the y, α and γ directions (see Figure 1). For the antisymmetric part of the motion, corresponding points will have opposite components in the x, z, and β directions and the same components in the y, α, and γ directions.

There may be an interaction, however, between the two rudders due to hydrodynamic properties which are somewhat different for symmetric and antisymmetric motions. No theory has been found to warrant the use of different basic hydrodynamic parameters for symmetric motion than for the antisymmetric analysis described here. However, it is believed that if such differences do exist, the range of variation of hydrodynamic parameters studied in this analysis would enable one to deduce the performance of any symmetric configuration for which the hydrodynamic parameters could be assumed or measured.

APPENDIX B

DERIVATION OF HYDRODYNAMIC FORCES ON A RIGID RUDDER

Four classes of hydrodynamic forces were discussed in Section IV. The first class, accounting for the added inertia effect, is discussed in the text (Section III.A.1) in connection with the mass and inertial terms due to the rudder structure, ship structure, and ship load. The second, third, and fourth classes will be treated in this Appendix. A summary of the results obtained in this Appendix and certain practical data are given in Item 8 below.

First, consider the steps leading to the derivation of equations for the second and third class of forces. Refer to Figures 1 and 88 for the positive direction of the coordinates x, z, v, α, γ, etc.

1. The rigid rudder is capable of motion out of its plane, characterized by three degrees of freedom, v (the lateral displacement of some point), α (roll), and γ (yaw). (See Figure 88.)

2. The *form* of the equations for hydrodynamic forces is derived based on the theory of two-dimensional potential flow* assuming an untapered rudder, no sweep-back, zero thickness, zero Mach number, and infinite aspect ratio. The *magnitude* of the constants will be taken from experimental values, where applicable data exist, and from the above theory or from judicious assumption otherwise.

*That is, the *form* is based on an extension of incompressible-flow theory in two dimensions to a rigid, three-degree-of-freedom lifting surface (rudder).

3. From Reference 11, p. 393, et seq., we can write the hydrodynamic forces per unit length on the strip (setting $\beta = 0$):

$$P = -2\pi\rho V^2 b C_t(k) \left[\alpha + \frac{\dot{h}}{V} + b\left(\frac{1}{2} - a\right)\frac{\dot{\alpha}}{V} \right] - \pi\rho b^2 \left[V\dot{\alpha} + \ddot{h} - ba\ddot{\alpha} \right]$$

$$M_\alpha = 2\pi\rho V^2 b^2 \left(\frac{1}{2} + a\right) C_t(k) \left[\alpha + \frac{\dot{h}}{V} + b\left(\frac{1}{2} - a\right)\frac{\dot{\alpha}}{V} \right]$$

$$- \pi\rho b^2 \left[Vb\left(\frac{1}{2} - a\right)\dot{\alpha} - ba\ddot{h} + b^2\left(\frac{1}{8} + a^2\right)\ddot{\alpha} \right]$$

To write these equations in terms of the notation of this analysis (see Figure 88) replace h by v, Pdz by dF_y, α by $-\gamma$, $M_\alpha dz$ by $-dM_\gamma$, 2b by c, and ab by $x_m - x_r$, where x_m locates the mid-chord and x_r locates the rotation axis where v is measured. Then

$$dF_y = \pi\rho V^2 c\,dz\, C_t(k) \left[\gamma - \frac{\dot{v}}{V} + \left\langle \frac{c}{4} - (x_m - x_r) \right\rangle \frac{\dot{\gamma}}{V} \right] + \frac{\pi}{4}\rho V^2 c^2\, dz \frac{\dot{\gamma}}{V}$$

$$- \frac{\pi}{4}\rho c^2\, dz\, \ddot{v} - \frac{\pi}{4}\rho c^2 (x_m - x_r)\, dz\, \ddot{\gamma}$$

$$dM_\gamma = \pi\rho V^2\, c\,dz \left\langle \frac{c}{4} + (x_m - x_r) \right\rangle C_t(k) \left[\gamma - \frac{\dot{v}}{V} + \left\langle \frac{c}{4} - (x_m - x_r) \right\rangle \frac{\dot{\gamma}}{V} \right]$$

$$- \frac{\pi}{4}\rho V^2 c^2 \left\langle \frac{c}{4} - (x_m - x_r) \right\rangle dz \frac{\dot{\gamma}}{V}$$

$$- \frac{\pi}{4}\rho c^2 (x_m - x_r)\, dz\, \ddot{v}$$

$$- \frac{\pi}{4}\rho c^2 \left\langle \frac{c^2}{32} + (x_m - x_r)^2 \right\rangle dz\, \ddot{\gamma}$$

The preceding terms underlined thus represent inertia terms which are independent of velocity and symmetric with respect to the midchord. As just stated, they are treated in Section III.A.1 (see Table 1) and will not be retained further here.

It only remains to show that these virtual mass forces are equivalent to those given by the equations in Table 2. Consideration of the motions of and the forces and moments on the strip of span width dz, shown in Figure 88, yields the relationships

$$v_m = v_r + (x_m - x_r)\,\gamma$$

and

$$M_{\gamma_r} = M_{\gamma_m} + F_y\,(x_m - x_r)$$

hence

$$F_y = ma_{c.m.} = \left(\frac{\pi}{4}\rho c^2\,dz\right)\ddot{v}_m = \left(\frac{\pi}{4}\rho c^2 dz\right)\left(\ddot{v}_r + (x_m - x_r)\,\ddot{\gamma}\right)$$

and

$$M_{\gamma_r} = \frac{\pi}{4}\rho c^2 dz\,\frac{c^2}{32}\,\ddot{\gamma} + \frac{\pi}{4}\rho c^2\,dz\left[(x_m - x_r)\,\ddot{v}_r + (x_m - x_r)^2\,\ddot{\gamma}\right]$$

$$= \frac{\pi}{4}\rho c^2 dz\,(x_m - x_r)\,\ddot{v}_r + \frac{\pi}{4}\rho c^2\left[\frac{c^2}{32} + (x_m - x_r)^2\right]\,dz\,\ddot{\gamma}$$

where

$$m = \frac{\pi}{4}\rho c^2 dz$$

$$I_\gamma = \frac{\pi}{4}\rho c^2 dz\,\frac{c^2}{32}$$

Letting $v_r = v$, it is evident that the virtual mass terms given here match those given in Table 2 (note that F_y, M_{γ_r} are the force and moment, respectively, exerted

by the rudder on the water whereas the negatives of these quantities are the reactions of the water on the rudder, which represent the effects of the virtual mass and virtual inertia.

The remaining forces are:

$$dF_y = (2\pi)\left(\frac{1}{2}\rho V^2\right)(cdz)\, C_t(k)\left[\gamma - \frac{\dot{v}}{V} + \left\langle \frac{c}{4} - (x_m - x_r)\right\rangle \frac{\dot{\gamma}}{V}\right] + \left(\frac{\pi}{2}\right)\left(\frac{1}{2}\rho V^2\right)(cdz)\left(c\frac{\dot{\gamma}}{V}\right)$$

$$dM_\gamma = (2\pi)\left(\frac{1}{2}\rho V^2\right)(cdz)\left\langle \frac{c}{4} + (x_m - x_r)\right\rangle C_t(k)\left[\gamma - \frac{\dot{v}}{V} + \left\langle \frac{c}{4} - (x_m - x_r)\right\rangle \frac{\dot{\gamma}}{V}\right] + \left(\frac{\pi}{2}\right)\left(\frac{1}{2}\rho V^2\right)(cdz)\left\langle \frac{c}{4} + (x_m - x_r)\right\rangle \left(\frac{c\dot{\gamma}}{V}\right) - \left(\frac{\pi}{2}\right)\left(\frac{1}{2}\rho V^2\right)(cdz)\frac{c}{2}\left(\frac{c\dot{\gamma}}{V}\right)$$

Thus

$$dM_\gamma = \left\langle \frac{c}{4} + (x_m - x_r)\right\rangle dF_y - \left(\frac{\pi}{4}\right)\left(\frac{1}{2}\rho V^2\right)(cdz)\, c\left(\frac{c\dot{\gamma}}{V}\right)$$

In the above expressions,

dF_y is the lateral force acting on the strip c(z) by dz,

dM_γ is the yaw moment about the reference $x = x_r$ due to pressure on the foil,

ρ = fluid density,

V = ship's forward speed relative to the fluid,

v = lateral displacement at $x = x_r$,

γ = yaw displacement,

c = c(z) = chord

x_m = location of midchord, and

$C_t(k) = C_t\left(\frac{c\omega}{2V}\right)$ = Theodorsen lag function;* see Item 8 of this Appendix.

To simplify the equations, locate x_r so that $x_m - x_r = \frac{c}{4}$, thus x_r is at the 3/4 chord point on the strip (measured from the leading edge). Denote x_r so located by x_1 and the lateral displacement v measured at x_1 by v_1. It will be more convenient, however, to use the moment about the 1/4 chord point, denoted by x_o, so that $x_o - x_m = \frac{c}{4}$. Then $x_o - x_r = \frac{c}{2}$ and denoting the moment about x_o by $M_{\gamma o}$, $dM_{\gamma o} = dM_\gamma - (\frac{c}{2})\, dF_y$. Then the simplified expressions for the force and moment acting on a single chordwise strip of an infinite aspect ratio wing are

$$dF_y = 2\pi\left(\frac{1}{2}\rho V^2\right)(cdz)\, C_t(k)\left(\gamma - \frac{\dot{v}_1}{V}\right) + \frac{\pi}{2}\left(\frac{1}{2}\rho V^2\right)(cdz)\left(\frac{c\dot{\gamma}}{V}\right)$$

$$dM_{\gamma o} = -\frac{\pi}{4}\left(\frac{1}{2}\rho V^2\right)(cdz)\, c\left(\frac{c\dot{\gamma}}{V}\right)$$

Thus, if $\dot{\gamma} = 0$, then $dM_{\gamma o} = 0$ and the center of pressure is at x_o. If $\dot{\gamma} \neq 0$, the

---

*The lag function term is used to describe the fact that for sinusoidal motions, the lift force changes with respect to the angle of attack both in amplitude and phase as a function of frequency. It is equivalent to the statement that for a step change in angle of attack, the lift does not reach a new steady value instantly, but grows rapidly toward this value. Note that $C_t(k) = F + jG$ where values of F and G for $k \leqq 40$ can be obtained from Figure A.3 of Reference 11. Other sources are given in Item 8 of this Appendix.

center of pressure is shifted in position.* Note that the center of pressure is a point on the rudder (x_o, z_o) about which there is no change in moment due to change of angle of attack provided that changing the angle of attack does not shift the center of pressure.

4. The preceding *form* of hydrodynamic equation is retained for application to the rudder of this analysis, but terms known to differ from the corresponding terms of the above expressions will be permitted to do so. This refers to the fact that certain hydrodynamic forces acting on the surfaces of small aspect ratio are known to differ from the corresponding forces on infinite-aspect-ratio surfaces; for example, see Reference 9. The expressions of Items 1, 2, and 3 of this Appendix are based on infinite aspect ratio.

The magnitude of the total lift and the location of the center of pressure on small aspect ratio surfaces differ, and the distribution of pressure is such that the local center of pressure (for each chordwise strip) is not uniform over the span.[9] Thus x_o

*The center of pressure on a plane is a point so located that the moment about any axis lying on the plane would not be changed if, instead of the distributed forces acting on the plane, a single force equal to their sum acted at the center of pressure. The moment due to these forces about any axis in the plane is therefore zero if, and only if, the axis passes through the center of pressure; it does not vanish about any other axis unless the resultant force is equal to zero. For an airfoil of infinite aspect ratio and zero thickness at Mach zero, the center of pressure is one-fourth of the distance from the leading edge to the trailing edge. For a rudder, see Appendix D.

In Reference 21 the rotation center was chosen to be at the center of pressure. In general, for describing the motion of a rigid plane the coordinates of the rotation center can be arbitrarily chosen. For a given choice of the location, the motion is automatically resolved into a translation at a velocity equal to the velocity $\dot{v}$ of the rotation center plus a rotation or rotations about an axis or axes through the assumed rotation center. If the rotation center is shifted, correction is made automatically by the resulting change in $\dot{v}$. Thus the position of the rotation center *is not fixed* by the properties of the rudder or of a strip and the motion thereof; i.e., it is not a point (on a rigid rudder or an imaginary extension of it) that stands still while the rudder turns around it because at such a point $\dot{v} = 0$.

and the lift coefficient are known (from wind-tunnel tests) to differ from the infinite-aspect-ratio case and to vary with spanwise position, i.e., with z. It is reasonable to surmise (lacking experimental evidence) that the corresponding quantities x_1, $c_{L\dot{\gamma}}$, and $c_{M\gamma\dot{\gamma}}$ vary similarly with spanwise position.

Hence, we generalize the preceding equations to those given below, replacing certain constants by coefficients which are permitted to vary. In Appendixes C and D, these coefficients will be represented by specific functions.

The expressions for dF_y and dM_{γ_0} are written

$$dF_y = (c_{L\gamma}) \left(\frac{1}{2}\rho V^2\right) (cdz) C_t(k) \left(\gamma - \frac{\dot{v}_1}{V}\right) + (c_{L\dot{\gamma}}) \left(\frac{1}{2}\rho V^2\right) (cdz) \left(\frac{c\dot{\gamma}}{V}\right)$$

$$dM_{\gamma_0} = -(c_{M\gamma\dot{\gamma}}) \left(\frac{1}{2}\rho V^2\right) (cdz) \; c \left(\frac{c\dot{\gamma}}{V}\right)$$

where v_1 is measured at $x = x_1 = x_1(z)$, the assumed local rotation center* at a particular spanwise position and *not* necessarily the 3/4 chord; dM_{γ_0} is moment about $x = x_0 = x_0(z)$, the local center of pressure, when $\dot{\gamma} = 0$, *not* necessarily the 1/4 chord, and $c_{L\gamma}$, $c_{L\dot{\gamma}}$, and $c_{M\gamma\dot{\gamma}}$ are lift coefficient slopes which may be functions of z.

These equations are now to be generalized so as to include the effects of a roll rotation through an angle α, and the equations are then to be integrated over an *entire rigid rudder*. Let a set of rudder axes be introduced; for example, an axis parallel to x at $z = z_2$ and an axis parallel to z at $x = x_2$, as indicated in Figure 88. It turns out to be convenient, however, to choose $x_2 = \bar{x}_0$ and $z_2 = z_0$ where the

*The local center of rotation must be so located that the coefficient of $\dot{\gamma}$ in dF_y does not involve C_t.

point $(\bar{x}_o, z_o)$ is the location of the center of pressure on the rudder when $\dot{\alpha} = \dot{\gamma} = 0$.*

Denote the roll moment *on the rudder* about an axis parallel to x at $z = z_o$ by $M_{\alpha o}$, and the yaw moment about an axis parallel to z at $x = \bar{x}_o$ by $M_{\gamma o}$. Denote the contributions to these moments *due to forces acting on a strip* by $d(M_{\alpha o})$ and $d(M_{\gamma o})$. Then for a strip at height z it is easily seen that

$$d(M_{\alpha o}) = -(z - z_o)\, dF_y, \quad d(M_{\gamma o}) = dM_{\gamma o} + (x_o - \bar{x}_o)\, dF_y$$

Here $dM_{\gamma o}$ continues to denote the moment acting *on the strip* about an axis at $x = x_o$.

Denote the lateral *rudder* displacement at $(\bar{x}_o, z_o)$ by v_o. Then the lateral displacement v_1 at $x = x_1$ on a strip at height z has the magnitude

$$v_1 = v_o - (z - z_o)\,\alpha + (x_1 - \bar{x}_o)\,\gamma$$

Substitution of this expression for v_1 and of the expression for dF_y in the preceding formulas gives

$$d(M_{\alpha o}) = (\tfrac{1}{2}\rho V^2)(c_{L\gamma} c\,dz)\, C_t(k) \left[-(z - z_o)\left(\gamma - \frac{\dot{v}_o}{V}\right) - (z - z_o)^2 \frac{\dot{\alpha}}{V} + (z - z_o)(x_1 - \bar{x}_o)\frac{\dot{\gamma}}{V} \right] - (\tfrac{1}{2}\rho V^2)(c_{L\dot{\gamma}} c^2 dz)(z - z_o)\frac{\dot{\gamma}}{V}$$

$$d(M_{\gamma o}) = (\tfrac{1}{2}\rho V^2)(c_{L\gamma} c\,dz)\, C_t(k) \left[(x_o - \bar{x}_o)\left(\gamma - \frac{\dot{v}_o}{V}\right) + (x_o - \bar{x}_o)(z - z_o)\frac{\dot{\alpha}}{V} - (x_o - \bar{x}_o)(x_1 - \bar{x}_o)\frac{\dot{\gamma}}{V} \right] + (\tfrac{1}{2}\rho V^2)(c_{L\dot{\gamma}} c^2 dz)(x_o - \bar{x}_o)\frac{\dot{\gamma}}{V} - (\tfrac{1}{2}\rho V^2)(c_{M\gamma\dot{\gamma}} c^3 dz)\frac{\dot{\gamma}}{V}$$

*Nonzero $\dot{\alpha}$ or $\dot{\gamma}$ will usually shift the center of pressure somewhat.

Here α and γ are uniform over the rudder because of its assumed rigidity. Also, in integrating, $C_t(k)$ will be replaced by the constant quantity $C_t(\bar{k}) = C_t\left(\frac{\bar{c}\omega}{2V}\right)$ where $\bar{c}$ denotes the geometric mean chord of the rudder. Only the following may be functions of z because of the finite aspect-ratio of the rudder (see Item 8): $c_{L\gamma}$, $c_{L\dot{\gamma}}$, $c_{M\gamma\dot{\gamma}}$, c, x_1, and x_0. Hence, integration of dF_y, $d(M_{\alpha o})$, and $d(M_{\gamma o})$ gives as the total force and moments on the rudder:

Unreduced Formulas

$$F_y = (\tfrac{1}{2}\rho V^2)\left\{ C_t(\bar{k}) \left[\gamma \int c_{L\gamma} c\,dz - \frac{1}{\nabla}\int \dot{v}_1 c_{L\gamma} c\,dz \right] + \frac{\dot{\gamma}}{\nabla}\int c_{L\dot{\gamma}} c^2 dz \right\}$$

$$M_{\alpha o} = (\tfrac{1}{2}\rho V^2)\left\{ C_t(\bar{k}) \left[-\left(\gamma - \frac{\dot{v}_o}{V}\right)\int (z - z_o)\, c_{L\gamma} c\,dz \right.\right.$$
$$\left. -\frac{\dot{\alpha}}{V}\int (z - z_o)^2 c_{L\gamma} c\,dz + \frac{\dot{\gamma}}{V}\int (z - z_o)(x_1 - \bar{x}_o) c_{L\gamma} c\,dz \right]$$
$$\left. -\frac{\dot{\gamma}}{V}\int (z - z_o)\, c_{L\dot{\gamma}}\, c^2 dz \right\}$$

$$M_{\gamma o} = (\tfrac{1}{2}\rho V^2)\left\{ C_t(\bar{k}) \left[\left(\gamma - \frac{\dot{v}_o}{V}\right)\int (x_o - \bar{x}_o)\, c_{L\gamma} c\,dz \right.\right.$$
$$\left. +\frac{\dot{\alpha}}{V}\int (x_o - \bar{x}_o)(z - z_o)\, c_{L\gamma} c\,dz - \frac{\dot{\gamma}}{V}\int (x_o - \bar{x}_o)(x_1 - \bar{x}_o) c_{L\gamma} c\,dz \right]$$
$$\left. +\frac{\dot{\gamma}}{V}\int (x_o - \bar{x}_o)\, c_{L\dot{\gamma}}\, c^2 dz - \frac{\dot{\gamma}}{V}\int c_{M\gamma\dot{\gamma}}\, c^3 dz \right\}$$

These formulas would remain valid if $\bar{x}_o$, z_o, and $\dot{v}_o$ were replaced by x_2, z_2, and $\dot{v}_2$, respectively, where (x_2, z_2) is any point on the rudder and v_2 the displacement there.

Since, however, the point $(\bar{x}_o, z_o)$ on the rudder has been located at the center of pressure when $\dot{\alpha} = \dot{\gamma} = 0$, it follows that $M_{\alpha o}$ and $M_{\gamma o}$ must vanish when

$\dot{\alpha} = \dot{\gamma} = 0$. This requires that*

$$\int (x_o - \bar{x}_o)\, c_{L\gamma}\, c\, dz = 0 \quad \text{or} \quad \bar{x}_o = \left(\int x_o c_{L\gamma}\, c\, dz\right) / \left(\int c_{L\gamma}\, c\, dz\right)$$

$$\int (z - z_o)\, c_{L\gamma}\, c\, dz = 0 \quad \text{or} \quad z_o = \left(\int z c_{L\gamma}\, c\, dz\right) / \left(\int c_{L\gamma}\, c\, dz\right)$$

These formulas fix the location of the center of pressure for $\dot{\alpha} = \dot{\gamma} = 0$. They also effect several simplifications in the formulas for the force and moments on the rudder.

F_y contains an integral in $\dot{v}_1$. Write

$$\bar{v}_1 = \left(\int v_1 c_{L\gamma}\, c\, dz\right) / \left(\int c_{L\gamma}\, c\, dz\right)$$

Inserting here $v_1 = v_o - (z - z_o)\,\alpha + (x_1 - \bar{x}_o)\,\gamma$, and noting that v_o and $\bar{x}_o$ are independent of z, and that $\int (z - z_o)\, c_{L\gamma}\, c\, dz = 0$, it is seen that

$$\bar{v}_1 = v_o + \gamma\,(\bar{x}_1 - \bar{x}_o)$$

where

$$\bar{x}_1 = \left(\int x_1 c_{L\gamma}\, c\, dz\right) / \left(\int c_{L\gamma}\, c\, dz\right)$$

Thus $\bar{v}_1$ is the displacement of the rudder at the point $(\bar{x}_1, z_o)$. *This is the assumed center of rotation for the rudder as a whole.*

In $M_{\alpha o}$ and $M_{\gamma o}$, the integrals multiplying $\gamma - (\dot{v}_o/V)$ are now seen to vanish, likewise any part of other integrals containing the constant $\bar{x}_o$ multiplied by $(z - z_o)$ or $(x_o - \bar{x}_o)$. Finally, $(z - z_o)^2$ may be replaced by $z^2 - z_o^2$, since $(z - z_o)^2 = z^2 - z_o^2 - 2z_o\,(z - z_o)$ and the integral of $(z - z_o)$ vanishes.

*Note that $\bar{x}_o$ and z_o, the resultant center of pressure of the entire rudder, are constants. We recall that x_o is the chordwise coordinate of the center of pressure of a single strip. Because x_o varies with spanwise location of the strip in the rudder, it is a function of z.

The force formulas thus reduce to the following:

Simplified Force Formulas

$$F_y = (\tfrac{1}{2}\rho V^2) \left\{ C_t(\bar{k}) \left[\gamma - \dot{\bar{v}}_1/V \right] \int c_{L\gamma}\, c\, dz + \frac{\dot{\gamma}}{V} \int c_{L\dot{\gamma}}\, c^2 dz \right\}$$

$$M_{\alpha o} = (\tfrac{1}{2}\rho V^2) \left\{ C_t(\bar{k}) \left[-\frac{\dot{\alpha}}{V} \int (z^2 - z_o^2)\, c_{L\gamma}\, c\, dz + \frac{\dot{\gamma}}{V} \int x_1 (z - z_o)\, c_{L\gamma}\, c\, dz \right] - \frac{\dot{\gamma}}{V} \int (z - z_o)\, c_{L\dot{\gamma}}\, c^2 dz \right\}$$

$$M_{\gamma o} = (\tfrac{1}{2}\rho V^2) \left\{ C_t(\bar{k}) \left[\frac{\dot{\alpha}}{V} \int x_o (z - z_o)\, c_{L\gamma}\, c\, dz - \frac{\dot{\gamma}}{V} \int x_1 (x_o - \bar{x}_o)\, c_{L\gamma}\, c\, dz \right] + \frac{\dot{\gamma}}{V} \int (x_o - \bar{x}_o)\, c_{L\dot{\gamma}}\, c^2 dz - \frac{\dot{\gamma}}{V} \int c_{M\gamma\dot{\gamma}}\, c^3 dz \right\}$$

5. *Force coefficients of the usual kind* for the rudder may now be introduced by writing the following equations* suggested by the simplified force formulas given at the beginning of Item 4:

$$\begin{aligned} F_y &= (\tfrac{1}{2}\rho V^2) \left[A C_{L\gamma} C_t(\bar{k}) \left(\gamma - \frac{\dot{\bar{v}}_1}{V} \right) + A C_{L\dot{\gamma}} \left(\frac{\bar{c}\dot{\gamma}}{V} \right) \right] \\ M_{\alpha o} &= -(\tfrac{1}{2}\rho V^2)\, A\bar{c} \left[C_{M\alpha\dot{\alpha}} \left(\frac{\bar{c}\dot{\alpha}}{V} \right) + C_{M\alpha\dot{\gamma}} \left(\frac{\bar{c}\dot{\gamma}}{V} \right) \right] \qquad [B\text{-}1] \\ M_{\gamma o} &= -(\tfrac{1}{2}\rho V^2)\, A\bar{c} \left[C_{M\gamma\dot{\alpha}} \left(\frac{\bar{c}\dot{\alpha}}{V} \right) + C_{M\gamma\dot{\gamma}} \left(\frac{\bar{c}\dot{\gamma}}{V} \right) \right] \end{aligned}$$

*This is an extension of the form of the equations given at the beginning of Item 4 for a one-dimensional strip to a two-dimensional surface (complete rudder planform) including a postulation of the coefficients; note $C_t(\bar{k}) = 1$ in the basic case.

The form of Equations [B-1] differs from that given by the equations at the beginning of Item 4 because the postulation of Equations [B-1] assumes that if the common set of axes $x = x_2$, $z = z_2$ were introduced they would give rise to an $M_{\alpha o}$ term and that $M_{\alpha o}$ and $M_{\gamma o}$ will both contain items in $\dot{\alpha}$ and $\dot{\gamma}$. The coefficients in Equations [B-1] are chosen to match the form of the equation at the beginning of Item 4. It should be noted that the equations at the beginning of Item 4 are for a strip of a finite-aspect-ratio surface and each strip has two degrees of freedom v and γ. Equations [B-1], on the other hand, pertain to the entire rigid rudder which has three degrees of freedom, v, γ, α.

Here $\bar{c} = (\int c\,dz) / (\int dz)$ and represents the geometric mean chord of the rudder whose planform area is $A = \int c\,dz$. F_y is the total lateral force on the rudder* and $M_{\alpha o}$ and $M_{\gamma o}$ are roll and yaw moments about respective axes parallel to x at $z = z_o$ and parallel to z at $x = \bar{x}_o$, $(\bar{x}_o, z_o)$ being the center of pressure on the rudder when $\dot{\alpha} = \dot{\gamma} = 0$. $\bar{v}_1$ is the lateral displacement of the rudder at the assumed center of rotation $(\bar{x}_1, z_o)$ as defined in the analysis.

These Equations [B-1] are equivalent to the last set obtained for F_y, $M_{\alpha o}$, and $M_{\gamma o}$ provided:

$$AC_{L\gamma} = \int c_{L\gamma} c\,dz$$

$$\bar{c}AC_{L\dot{\gamma}} = \int c_{L\dot{\gamma}} c^2 dz$$

$$\bar{c}^2 AC_{M\alpha\dot{\alpha}} = C_t(\bar{k}) \int (z^2 - z_o^2)\, c_{L\gamma} c\,dz$$

$$\bar{c}^2 AC_{M\alpha\dot{\gamma}} = -C_t(\bar{k}) \int x_1 (z - z_o)\, c_{L\gamma} c\,dz + \int (z - z_o)\, c_{L\dot{\gamma}} c^2 dz$$

$$\bar{c}^2 AC_{M\gamma\dot{\alpha}} = -C_t(\bar{k}) \int x_o (z - z_o)\, c_{L\gamma} c\,dz$$

$$\bar{c}^2 AC_{M\gamma\dot{\gamma}} = C_t(\bar{k}) \int x_1 (x_o - \bar{x}_o)\, c_{L\gamma} c\,dz - \int (x_o - \bar{x}_o)\, c_{L\dot{\gamma}} c^2 dz + \int c_{M\gamma\dot{\gamma}} c^3 dz$$

For some purposes, however, it may be preferable to shift the constants $\bar{x}_o$ and z_o from under the integral sign. The definitions of $\bar{x}_1$ and $\bar{x}_o$ may be rewritten thus:

$$AC_{L\gamma}\,\bar{x}_1 = \int x_1\, c_{L\gamma} c\,dz; \quad AC_{L\gamma}\,\bar{x}_o = \int x_o\, c_{L\gamma}\, c\,dz$$

*F_y is the total lateral force acting on the rudder. More precisely, it is the lateral component of the vector integral $\int p\,dA$, (i.e., $F_y = [\int p\,dA]_{y\ \text{component}}$) where p is the hydrodynamic pressure on the surface and the integration is carried out over the entire wetted surface of the rudder. It doesn't actually act at just a single point.

Then the equations for the four C_M coefficients may take the form

$$\bar{c}^2 AC_{M\alpha\dot{\alpha}} = C_t(\bar{k}) \left(\int z^2 c_{L\gamma} c\,dz - z_o^2 AC_{L\gamma}\right)$$

$$\bar{c}^2 AC_{M\alpha\dot{\gamma}} = -C_t(\bar{k}) \left(\int x_1 z c_{L\gamma} c\,dz - z_o \bar{x}_1 AC_{L\gamma}\right) + \int (z - z_o) c_{L\dot{\gamma}} c^2 dz$$

$$\bar{c}^2 AC_{M\gamma\dot{\alpha}} = -C_t(\bar{k}) \left(\int x_o z c_{L\gamma} c\,dz - \bar{x}_o z_o AC_{L\gamma}\right)$$

$$\bar{c}^2 AC_{M\gamma\dot{\gamma}} = C_t(\bar{k}) \left(\int x_1 x_o c_{L\gamma} c\,dz - \bar{x}_1 \bar{x}_o AC_{L\gamma}\right)$$
$$- \int x_o c_{L\dot{\gamma}} c^2 dz + \bar{x}_o \int c_{L\dot{\gamma}} c^2 dz + \int c_{M\gamma\dot{\gamma}} c^3 dz$$

It will be noted that all four of these coefficients contain terms in $C_t(\bar{k})$, but only $C_{M\alpha\dot{\gamma}}$ and $C_{M\gamma\dot{\gamma}}$ contain additional terms.

In these formulas:

$C_{L\gamma}$ is the steady slope of lift coefficient ($C_{L\alpha}$ in aircraft usage),

$C_{L\dot{\gamma}}$ is the additional slope of lift coefficient due to yaw velocity,

$C_{M\alpha\dot{\alpha}}$ is the slope of roll moment coefficient due to roll velocity,

$C_{M\alpha\dot{\gamma}}$ is the slope of roll moment coefficient due to yaw velocity,

$C_{M\gamma\dot{\alpha}}$ is the slope of yaw moment coefficient due to roll velocity,

$C_{M\gamma\dot{\gamma}}$ is the slope of yaw moment coefficient due to yaw velocity (C_{Mq} in aircraft usage),

x_1, x_o are functions of z, x_1 denoting the location on a *strip* of the assumed rotation center and x_o the location of the center of pressure on the *strip* when $\dot{\gamma} = 0$.

v_1 is the lateral displacement of the strip at $x = x_1$,

$(\bar{x}_1, z_o)$ and $(\bar{x}_o, z_o)$ are locations of corresponding rotation center and center of pressure when $\dot{\alpha} = \dot{\gamma} = 0$, for the *entire rudder*

$\bar{v}_1$ is the lateral displacement of the rudder at the point $(\bar{x}_1, z_o)$.

(z_1 may be written for z_o in specifying the rudder rotation center, but $z_1 = z_o$.)

The significant parameters, then, are the C's and the values of $\bar{x}_1$, z_o and $\bar{x}_o$, z_o. Formulas for calculating these coefficients based upon the above developments are summarized in Item 6.

6. The equations derived in Item 5 yield the following relations*

$$C_{L\gamma} = \frac{1}{A}\int c_{L\gamma}\, cdz \qquad C_{L\dot{\gamma}} = \frac{1}{\bar{c}A}\int c_{L\dot{\gamma}} c^2 dz$$

$$z_o = z_1 = \frac{1}{AC_{L\gamma}}\int z\, c_{L\gamma} cdz = \frac{\int z c_{L\gamma}\, cdz}{\int c_{L\gamma}\, cdz}$$

$$\bar{x}_1 = \frac{1}{AC_{L\gamma}}\int x_1 c_{L\gamma} cdz = \frac{\int x_1 c_{L\gamma} cdz}{\int c_{L\gamma}\, cdz}$$

$$\bar{x}_o = \frac{1}{AC_{L\gamma}}\int x_o c_{L\gamma} cdz = \frac{\int x_o c_{L\gamma} cdz}{\int c_{L\gamma}\, cdz}$$

$$C_{M\alpha\dot{\alpha}} = C_t(\bar{k})\,\frac{\int z^2 c_{L\gamma} cdz - z_o^2\, AC_{L\gamma}}{\bar{c}^2\, A}$$

$$C_{M\gamma\dot{\alpha}} = -C_t(\bar{k})\,\frac{\int x_o z c_{L\gamma} cdz - \bar{x}_o z_o\, AC_{L\gamma}}{\bar{c}^2\, A}$$

*The relationship between $c_{L\gamma}$ and $C_{L\gamma}$ is given by these equations and their definitions are obtained from Equations [B-1]. The large C's are required in order to mechanize the equations on the analog computer. An element of the computer uses an integral of f (z). The large C's are equivalent to these integrals; i.e., they are specific numbers which are fed to the computer.

$$C_{M\alpha\dot{\gamma}} = \frac{1}{\bar{c}^2 A}\left\{ -C_t(\bar{k}) \left[\int x_1 z c_{L\gamma} cdz - \bar{x}_1 z_o AC_{L\gamma}\right] + \left[\int z c_{L\dot{\gamma}} c^2 dz - z_o \bar{c} AC_{L\dot{\gamma}}\right]\right\}$$

$$C_{M\gamma\dot{\gamma}} = \frac{1}{\bar{c}^2 A}\left\{ C_t(\bar{k}) \left[\int x_o x_1 c_{L\gamma} cdz - \bar{x}_o \bar{x}_1 AC_{L\gamma}\right] - \left[\int x_o c_{L\dot{\gamma}} c^2 dz - \bar{x}_o \bar{c} AC_{L\dot{\gamma}}\right] + \int c_{M\gamma\dot{\gamma}} c^3 dz\right\}$$

This indicates that the $C_{M\alpha\dot{\gamma}}$ and $C_{M\gamma\dot{\gamma}}$ terms each have a lagged portion and an unlagged portion.

7. The fourth class of hydrodynamic forces mentioned in Item 4 of Section IV. can be referred to as viscous forces, and the following expressions are adopted:*

$$F_y = -\frac{D_f}{\bar{c}^2}\dot{v}_3$$

$$M_{\gamma_3} = -D_m\dot{\gamma}$$

in which F_y is the lateral force on the rudder (acting at the center of area), M_{γ_3} is the damping moment (yaw) acting about a vertical axis through the center of

*The damping terms mentioned in Item 2 of Section IV. are dependent upon ship speed. Here the terms are independent of speed, and hence will exist at zero speed. Such terms are discussed in Reference 21. The form of the equations for D_f and D_m were chosen to give the same dimensions for these quantities.

area* of the rudder, D_f and D_m are damping constants (with dimensions lb-sec-ft), $\bar{c}$ is the geometric mean chord of the rudder, v_3 is the lateral motion of the rudder, and γ is the yaw displacement of the rudder. For the PGM MOTOR GUNBOAT, two sets of damping constants D_f and D_m were used. In the basic case, $D_f = D_m = 0$, omitting entirely this class of viscous damping force. In the other instances, D_f = 18,860 lb-sec-ft and D_m = 665 lb-sec-ft. These latter values were obtained by scaling the damping terms presented in Reference10, Table 1, Notes 4 and 5, to account for the smaller area of the rudder of the PGM.

8. Summary

The information required for applying (and extending) the above analysis to the case of an actual rudder and certain basic data obtained for the PGM rudder are summarized here.

The equations of Item 6 enable one to determine the hydrodynamic parameters of a rigid rudder of arbitrary plan shape, assuming that the forces and moments acting on each strip of the rudder are determinable from the motion of that strip, based on two-dimensional, incompressible flow. However, to accommodate known characteristics of finite-aspect-ratio lifting surfaces, certain parameters in the expressions for the forces and moments *on the strips* may be permitted to vary with spanwise position (i.e., with z), namely:

c	rudder chord
x_o	chordwise location of center of pressure

*It was considered more rational to relate these forces to the rudder center of area rather then to the center of pressure.

x_1 chordwise location of rotation center

$c_{L\gamma}$ slope of lift coefficient

$c_{L\dot{\gamma}}$ slope of lift coefficient (unlagged portion)

$c_{M\gamma\dot{\gamma}}$ slope of moment coefficient

For two different examples of the spanwise distribution of hydrodynamic forces on trapezoidal rudders, the integrations required (Item 6) in determining the hydrodynamic parameters are carried out in Appendixes C and D. However, for many of the terms, there are other sources of theoretical and experimental data which can be used in making an intelligent estimate of the most probable values of the parameters and of the possible deviation from these values. Table 13 summarizes the values and corresponding sources for the above parameters. For purposes of describing the PGM rudder in terms amenable to the above sources, the actual planform of the rudder was altered slightly to give the closest equivalent trapezoidal planform. This evolution of the PGM rudder shape is shown in detail on Figures 89 and 90. For this equivalent trapezoidal rudder, the following parameters were calculated:[9, 10]

A = area = 17,845 ft^2

$\bar{c}$ = geometric mean chord = 3.769 ft

T = taper ratio = 0.473

λ = angle of sweepback of the 1/4 chord = +9.62 deg

AR = aspect ratio = 2.513

For the data presented in this report for PGM, the following values of the hydrodynamic parameters represent the basic values and were employed unless otherwise stated:

Parameter*	Basic Value
$C_{L\gamma}$	2.77
$C_{M\alpha\dot{\alpha}}$	0.2373
$C_{M\alpha\dot{\gamma}}$	0
$C_{M\gamma\dot{\alpha}}$	0
$C_{M\gamma\dot{\gamma}}$	0.416
$\bar{x}_0$	0.126 ft
z_0	-2.060 ft
$\bar{x}_1$	-2.234 ft
z_1	-2.060 ft
x_3	-1.091 ft
z_3	-2.085 ft
D_f	0
D_m	0
$C_{L\dot{\gamma}}$	0

Values of x are measured forward from the rudder stock centerline and values of z are measured upwards from the root of the rudder. In terms of the ship coordinates, this origin for locating points on the rudder is located 3.108 ft above the baseline of the hull (Figure 3) and 3.823 ft (almost exactly 1/2 station) forward of the aft perpendicular. It will be referred to herein as the "rudder origin," and is shown

*$\bar{x}_0$ and $\bar{x}_1$ are for the entire rudder rather than for a strip, hence they are independent of z; note $\bar{x}_0 \neq \bar{x}_1$. $C_{L\dot{\gamma}}$ given here is an arbitrary value which is chosen as a convenient reference level. The approximate values of $C_{L\dot{\gamma}}$ for the PGM Boat are obtained by computation using the equations for $C_{L\dot{\gamma}}$ given in Appendixes C and D in accordance with the assumptions regarding the nature of the lift coefficient given there.

in Figure 90 as point R. x_3, z_3 locate the center of area of the rudder, at which it is presumed the viscous damping force acts when a value of D_f other than the basic value of zero is employed.

An additional variation of hydrodynamic parameters that was studied is the introduction of Theodorsen's lag functions $C_t(\bar{k})$, which account for the delay in buildup of the hydrodynamic forces and moments, in comparison with the displacements and velocities which give rise to these forces and moments. In the basic case, no lag functions were employed. The electrical analog circuit used to represent these functions permitted lag functions to modify the five lift-coefficient slope terms ($C_{L\gamma}$ to $C_{M\gamma\dot{\gamma}}$) either individually or collectively. Lag functions corresponding to infinite aspect ratio and 2.5 aspect ratio were employed. These lag functions are described in Figure 52. They are defined by transfer functions of p; (here $pe^{j\omega t} = \frac{d}{dt} e^{j\omega t} = j\omega e^{j\omega t}$ or $p = j\omega$). In addition, they are described in Figure 52 by curves in the complex plane showing the locus of values of the lag function as p takes imaginary values $j\omega$ with ω varying from 0 to $+\infty$. For each aspect ratio (AR = 2.5, AR = ∞), the function C_t defined is the best known first approximation* of the actual

*By "first approximation" it is meant that the actual lag function $C_t(\bar{k})$ is approximated by a fraction of binomials, so that both numerator and denominator are first order in the variable $\bar{k}$; e.g., see equations given on Figure 52 where $k = \frac{c\omega}{2V}$ for a strip and $\bar{k} = \frac{\bar{c}\omega}{2V}$ for the entire rudder so that $j\bar{k} = \frac{\bar{c}(j\omega)}{2V} = \frac{\bar{c}p}{2V}$. Also $C_t(\bar{k}) = C\left(\frac{\bar{c}\omega}{2V}\right)$ is the analytic continuation of Theodorsen's function, related to the Wagner function. Theodorsen's functions C_t can be expressed[11, 22] in terms of Hankel functions (Bessel functions of the third kind) or in terms of standard Bessel functions of the first and second kinds of argument $\bar{k}$. This $\bar{k}$ is called the *reduced frequency* or *Strouhal number*. For simulation by an electrical circuit, C_t must be represented by the ratio of two polynomials. A comparison of the approximation for C_t given by Figure 52 with accurate values of Theodorsen's function shows good agreement; see, for example, Figure 8.15 of Reference 23 which, although using a somewhat different approximation for the polynomials, graphically illustrates the validity of using polynomial approximations. For additional information on this subject the reader is referred to Reference 24.

aerodynamic lag function that exists. For AR = ∞, this aerodynamic lag function is the Theodorsen lag function. (See Reference 11, pp. 393, 396.) Figure 52 also shows lag functions C_t' for each aspect ratio. These functions are just halfway between the lag functions C_t and no lag at all (i.e., $C_t = 1$). The functions C_t' were not employed for any calculations reported in this report. The effect of employing lag functions is to impose, at oscillation frequencies greater than zero, both a reduction in the magnitude and a lag in the phase of the aerodynamic force relative to the displacement or velocity which gives rise to that force. Whenever a lag function is employed in the calculations cited in this report, the value (usually the basic value) of the lift-coefficient slope listed always refers to the limit of the value as the frequency approaches zero.

If in the first of Equations [B-1] C_t is *real*, then the first term on the right-hand side makes no *separate* contribution to the unlagged term which is a function of $\dot{\gamma}$. Moreover, if the lagged function is omitted, i.e., $C_t = 1$, then the force acting on the rudder is

$$F_y = \tfrac{1}{2}\rho V^2 A \left[C_{L\gamma}\gamma - \frac{C_{L\gamma}}{V}\left(\dot{\bar{v}}_1 - \frac{\bar{c} C_{L\dot{\gamma}}}{C_{L\gamma}} \dot{\gamma} \right) \right]$$

where $\dot{\bar{v}}_1$ is the lateral velocity measured at $x = \bar{x}_1$, $z = z_o$. Let (see Figure 90 for location of $\bar{x}_1$, $\bar{x}_1'$ where $\bar{x}_1' = \bar{x}_1 + \Delta\bar{x}_1'$, $\Delta\bar{x}_1'$ being an increment of $\bar{x}_1$)

$$\bar{v}_1' = \bar{v}_1 - \gamma (\bar{x}_1 - \bar{x}_1')$$

or transposing

$$\dot{\bar{v}}_1 = \dot{\bar{v}}_1' + \dot{\gamma} (\bar{x}_1 - \bar{x}_1')$$

Then

$$F_y = \tfrac{1}{2}\rho V^2 A C_{L\gamma}\left[\gamma - \frac{1}{V}\left(\dot{\bar{v}}_1' + \dot{\gamma}(\bar{x}_1 - \bar{x}_1') - \frac{\bar{c}C_{L\dot{\gamma}}}{C_{L\gamma}}\dot{\gamma}\right)\right]$$

There is a direct relationship between the terms $\dot{\gamma}(\bar{x}_1 - \bar{x}_1')$ and $\frac{\bar{c}C_{L\dot{\gamma}}}{C_{L\gamma}}\dot{\gamma}$ because both of the coefficients of $\dot{\gamma}$ in these terms affect the total value of the $\dot{\gamma}$ term. Hence, the effect of the $C_{L\dot{\gamma}}$ term can be accounted for by a variation in the parameter $\bar{x}_1$. In fact, a comparison of Figure 49 and that portion of Figure 47 lying to the left of the basic value of $\bar{x}_1$ shows that they are equivalent. This is most easily seen from a comparison of the basic points where $C_{L\dot{\gamma}} = 0$; note that in Figure 47, $C_{L\dot{\gamma}} = 0$ (the basic value) and $\bar{x}_1$ is variable whereas in Figure 49, $\bar{x}_1 = -2.234$ ft (the basic value) and $C_{L\dot{\gamma}}$ is variable.

To account for the effect of the $C_{L\dot{\gamma}}$ term by a variation in the parameter $\bar{x}_1$ we move the rotation center from $\bar{x}_1$ to $\bar{x}_1'$.

$$\bar{x}_1' = \bar{x}_1 - \frac{\bar{c}C_{L\dot{\gamma}}}{C_{L\gamma}}$$

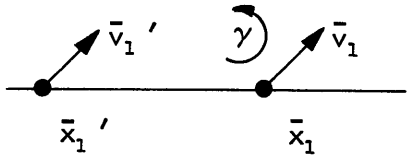

Then, the velocity $\dot{\bar{v}}_1'$ at $\bar{x}_1'$ is related to $\dot{\bar{v}}_1$ at $\bar{x}_1$ by

$$\dot{\bar{v}}_1 = \dot{\bar{v}}_1' + \left(\frac{\bar{c}C_{L\dot{\gamma}}}{C_{L\gamma}}\right)\dot{\gamma}$$

and substituting this for $\dot{\bar{v}}_1$ in the equation for F_y given on page 148.

$$F_y = \tfrac{1}{2}\rho V^2 A C_{L\gamma}\left(\gamma - \frac{\dot{\bar{v}}_1'}{V}\right)$$

Thus we have eliminated $C_{L\dot{\gamma}}$ from F_y and included it in $\bar{x}_1'$ and $\bar{v}_1'$. (There would be no change if $C_{L\dot{\gamma}}$ were zero).

APPENDIX C

HYDRODYNAMIC PARAMETERS FOR A TRAPEZOIDAL RUDDER (VARYING LIFT COEFFICIENT)

The results of Appendix B are applied to a rigid trapezoidal rudder as shown in Figure 91. The origin is taken at the apex 0 of the trapezoid, and the root chord at z = B is assumed to coincide with the horizontal bottom of the hull.

The lift coefficients are assumed to drop off parabolically with span from root to tip, as follows:

$$c_{L\gamma} = 2\pi\eta \left[1 - \left(\frac{B - z}{B - b}\right)\right]^2$$

$$c_{L\dot{\gamma}} = \frac{\pi}{2}\xi \left[1 - \left(\frac{B - z}{B - b}\right)\right]^2$$

$$c_{M\nu\dot{\gamma}} = \frac{\pi}{4}\zeta \left[1 - \left(\frac{B - z}{B - b}\right)\right]^2$$

in which η, ξ, ζ are normalizing factors to be selected later.

The reasoning underlying the development of these equations is as follows. For a rudder of infinite aspect ratio in two-dimensional incompressible flow, $c_{L\gamma} = 2\pi$. η is introduced as a normalizing factor to indicate the variation in values of $c_{L\gamma}$ along the span from the value for two-dimensional incompressible flow. Note that in Appendixes B and D, $c_{L\gamma}$ was taken as constant over the span. When η is set equal to unity, it yields a value for $c_{L\gamma}$ at the root corresponding to the infinite aspect ratio case (i.e., $c_{L\gamma} = 2\pi$ for z = B, $\eta = 1$. Actually, η was chosen to agree with wind-tunnel data (see Note # in Table 13). Based on Reference 9 and the first of Equations [B - 1] here, we obtain η from the relationship

$$\eta = \frac{1}{2\pi}\left(\frac{dc_L}{d\gamma_{rad}}\right) = \frac{c_{L\gamma}}{2\pi} = \frac{F_y}{2\pi\left(\frac{1}{2}\rho V^2\right) A\gamma}$$

using the static value for F_y, and for the static case setting $C_t(k) = 1$. η was determined by taking for $c_{L\gamma}$ a value of 2.77 interpolated from wind-tunnel data which fit this rigid lifting surface; the data are found in Reference 9. The quantity in brackets has the form of a parabola and is such as to yield for $c_{L\gamma}$ a value that agrees roughly with wind-tunnel data.

Similar relationships and data are not known for $c_{L\dot{\gamma}}$ and $c_{M\gamma\dot{\gamma}}$, which depend upon the vibrations (variations in γ), whereas $c_{L\gamma}$ was obtained from static considerations. However, we will assume that similar relationships exist for these quantities; the constants $\frac{\pi}{2}$ and $\frac{\pi}{4}$ in the equations for $c_{L\dot{\gamma}}$ and $c_{M\gamma\dot{\gamma}}$, respectively, are taken from corresponding terms in the equations for dF_y and $dM_{\gamma o}$ at the end of Item 3 here and ξ and ζ are taken equal to η. The values for the normalizing factors are not shown, but the results of their choice are shown in Table 13.

The values of x_o and x_1, which locate the position of the center of pressure and the rotation center, respectively, at any spanwise position, are assumed to be

$$x_o = \left(D - \frac{1}{4}C\right)\frac{z}{B} + \frac{C}{4}\frac{b}{B}\left(\frac{B-z}{B-b}\right)^2$$

$$x_1 = \left(D - \frac{3}{4}C\right)\frac{z}{B} - \frac{C}{4}\frac{b}{B}\left(\frac{B-z}{B-b}\right)^2$$

The resulting curves of x_o and x_1 are shown in Figure 91 (dotted lines). These expressions provide that x_o and x_1 are on the 1/4 and 3/4 chord, respectively, at

the rudder root, and curve parabolically to the leading and trailing edge, respectively, at the rudder tip.*

Because of the trapezoidal shape for the rudder, from similar triangles we obtain the local value of the chord c; namely

$$c = \frac{C}{B} z$$

and the tip value of the chord is therefore

$$c_{tip} = \frac{bC}{B}$$

The integrations indicated in Appendix B are carried out over the interval

$$b < z < B$$

Before performing these integrations, however, the following substitutions are made in order to use dimensionless ratios to the greatest possible extent; these equations for B, b, C, D follow from their definitions:

$$B = \bar{c} \frac{AR}{2(1 - T)}$$

$$b = \bar{c} \frac{T \ AR}{2(1 - T)}$$

$$C = \bar{c} \frac{2}{1 + T}$$

$$D = \bar{c} \left[\frac{AR \tan \lambda}{2(1 - T)} + \frac{1}{2(1 + T)} \right]$$

*In Figure 92 the values of x_0 and x_1 would occur on the 1/4 and 3/4 chords, respectively, for incompressible flow and infinite aspect ratio. However, for finite aspect ratio, wind-tunnel pressure distributions show that x_0 increases from the 1/4 chord toward the leading edge. A similar assumption was made for x_1. These assumptions are not critical, as can be seen from Figures 46 and 47, which show the effects of variations in these values.

The new variables introduced are:

$\bar{c}$ geometric mean chord of rudder, given by dividing rudder area by rudder span $\left(\text{equal to } \frac{C\,(B + b)}{2B} \right)$

T taper ratio of rudder, given by dividing tip chord by root chord $\left(\text{equal to } \frac{b}{B} \right)$

AR aspect ratio, given by twice the square of the rudder span, divided by rudder area $\left(\text{equal to } \frac{4B\,(B - b)}{C\,(B + b)} \right)$

λ sweepback angle of the rudder 1/4 chord $\left(\text{equal to } \frac{1}{B}\,(D - \frac{C}{4}) \right)$

The results of making the above substitutions and performing the integrations of Appendix B yield the following expressions for the hydrodynamic parameters:

$$\bar{x}_o - D = -\bar{c} \left[\frac{2}{5\,(1 + T)} + \frac{7 + 8T}{10\,(5 + 3T)} \text{ AR tan } \lambda \right]$$

$$\bar{x}_1 - D = -\bar{c} \left[\frac{61 + 46T + 21T^2}{10(5 + 3T)\ (1 + T)} + \frac{7 + 8T}{10\,(5 + 3T)} \text{ AR tan } \lambda \right]$$

$$z_o - B = z_1 - B = -\bar{c}\ \frac{7 + 8T}{10\,(5 + 3T)} \text{ AR}$$

$$C_{L\gamma} = 2\pi\eta\ \frac{5 + 3T}{6\,(1 + T)}$$

$$C_{M\dot{\alpha}\dot{\alpha}} = 2\pi\eta\ \frac{26 + 58T + 11T^2}{600(5 + 3T)\ (1 + T)} \text{ AR}^2\, C_t(\bar{k})$$

$$C_{M\alpha\dot{\gamma}} = -2\pi\eta \frac{AR}{4200(5+3T)(1+T)^2} \left[7(26+58T+11T^2)(1+T)\,AR\tan\lambda \right.$$

$$\left. - 2(182+160T-505T^2-117T^3) \right] C_t(\bar{k})$$

$$C_{M\gamma\dot{\alpha}} = -2\pi\eta \frac{AR}{4200(5+3T)(1+T)^2} \left[7(26+58T+11T^2)(1+T)\,AR\tan\lambda \right.$$

$$\left. - 16T(4+T)(2+5T) \right] C_t(\bar{k}) + \frac{\pi}{2}\xi \frac{(26+58T+11T^2)(1-T)}{150(5+3T)} AR$$

$$C_{M\gamma\dot{\gamma}} = \frac{\pi}{4}\xi \frac{2(14+12T+9T^2+5T^3)}{15(1+T)^3} + 2\pi\eta \frac{1}{8400(5+3T)(1+T)^3}$$

$$\left[14(26+58T+11T^2)(1+T)^2 AR^2\tan^2\lambda - 28(26+58T+11T^2) \right.$$

$$\left. (1+T)(1-T)\,AR\tan\lambda - T(1672+1991T-2210T^2-429T^3) \right] C_t(\bar{k})$$

$$-\frac{\pi}{2}\xi \frac{1}{1050(5+3T)(1+T)^3} \left[7(26+58T+11T^2)(1+T)\,AR\tan\lambda \right.$$

$$\left. + 3T(18+18T-T^2)(1-T) \right]$$

$$C_{L\dot{\gamma}} = \frac{\pi}{2}\xi \frac{2(9+7T+4T^2)}{15(1+T)^2}$$

Now $\bar{x}_o$, z_o locate the center of pressure of the trapezoidal rudder and $\bar{x}_1$, z_1 locate the rotation center, in each case relative to the apex 0 of the trapezoid. In the above equations, $\bar{x}_o - D$, $\bar{x}_1 - D$, $z_o - B$, $z_1 - B$ are given instead, so that these points may be loacted with respect to the leading edge of the root chord. This is done to avoid expressions containing $(1 - T)$ in the denominator, which increase without limit when the taper ratio approaches unity.

To recapitualate, if the normalizing factors η, ξ, and ζ are all chosen equal to unity, then the lift coefficients at the root of the rudder are identical to those of the two-dimensional, incompressible-flow case. In the use of the hydrodynamic parameters derived herein, however, the value of η was determined by taking for $C_{L\gamma}$ a value based on wind-tunnel data for rigid lifting surfaces. Here ξ and ζ were assumed equal to η.

APPENDIX D

HYDRODYNAMIC PARAMETERS FOR A TRAPEZOIDAL RUDDER (LIFT COEFFICIENT ASSUMED UNIFORM)

Again the results of Appendix B are applied to a rigid trapezoidal rudder as shown in Figure 92. The origin is taken at the apex 0 of the trapezoid, and the root chord at $z = B$ is assumed to coincide with the horizontal bottom of the hull.

The lift coefficients are assumed *constant* at any spanwise position*

$$c_{L\gamma} = 2\pi\eta$$

$$c_{L\dot{\gamma}} = \frac{\pi}{2}\xi$$

$$c_{M\gamma\dot{\gamma}} = \frac{\pi}{4}\zeta$$

in which η, ξ, ζ are normalizing factors.

The values of x_0 and x_1, which locate the position of the center of pressure and the rotation center, respectively, at any spanwise position, are assumed to be

$$x_0 = \left(D - \frac{1}{4}C\right)\frac{z}{B}$$

$$x_1 = \left(D - \frac{3}{4}C\right)\frac{z}{B}$$

Thus these points lie on the 1/4 chord and 3/4 chord, respectively, as indicated in the figure.

Again the trapezoidal shape gives a local chord of

$$c = \frac{C}{B}z$$

*In Appendix C these coefficients were assumed to drop off progressively with span from root to tip.

and the integrations indicated in Appendix B are performed over the integral

$$b < z < B$$

As in Appendix C, the following substitutions are made:

$$B = \bar{c} \quad \frac{AR}{2(1 - T)}$$

$$b = \bar{c} \quad \frac{T\ AR}{2(1 - T)}$$

$$C = \bar{c} \quad \frac{2}{1 + T}$$

$$D = \bar{c} \left[\frac{AR \tan \lambda}{2(1 - T)} + \frac{1}{2(1 + T)} \right]$$

so that the results again are expressed in terms of mean chord, taper ratio, aspect ratio, and sweepback angle of the rudder planform.

Making the above substitutions and performing the integrations of Appendix B results in the following expressions for the hydrodynamic parameters:

$$\bar{x}_o - D = \bar{c} \quad \frac{1 + 2T}{6(1 + T)} \left[- AR \tan \lambda - \frac{3}{1 + 2T} \right]$$

$$\bar{x}_1 - D = \bar{c} \quad \frac{1 + 2T}{6(1 + T)} \left[- AR \tan \lambda - \frac{7 + 7T + 4T^2}{(1 + T)(1 + 2T)} \right]$$

$$z_o - B = z_1 - B = -\bar{c} \quad \frac{1 + 2T}{6(1 + T)} \quad AR$$

$$C_{L\gamma} = 2\pi\eta$$

$$C_{M\alpha\dot{\alpha}} = 2\pi\eta \frac{1 + 4T + T^2}{72 (1 + T)^2} \quad AR^2 \, C_t(\bar{k})$$

$$C_{M\alpha\dot{\gamma}} = -2\pi\eta \frac{1 + 4T + T^2}{72 (1 + T)^2} \quad AR \quad \left[AR \tan\lambda - 2 \frac{1 - T}{1 + T} \right] \quad C_t(\bar{k})$$

$$C_{M\gamma\dot{\alpha}} = -2\pi\eta \frac{1 + 4T + T^2}{72 (1 + T)^2} \quad AR^2 \tan\lambda C_t(\bar{k}) + \frac{\pi}{2} \xi \frac{(1 + 4T + T^2)(1 - T)}{18 (1 + T)^3} \quad AR$$

$$C_{M\gamma\dot{\gamma}} = \frac{\pi}{4} \zeta \, 2 \frac{1 + T^2}{(1 + T)^2} + 2\pi\eta \frac{1 + 4T + T^2}{72 (1 + T)^2} \quad AR \tan\lambda \quad \left[AR \tan\lambda - 2 \frac{1-T}{1+T} \right] C_t(\bar{k})$$

$$+ \frac{\pi}{2} \xi \frac{(1 + 4T + T^2)(1 - T)}{18(1 + T)^3} \quad AR \tan\lambda$$

$$C_{L\dot{\gamma}} = \frac{\pi}{2} \xi \frac{4(1 + T + T^2)}{3(1 + T)^2}$$

Again, $\bar{x}_o$, z_o locate the center of pressure of the trapezoidal rudder and $\bar{x}_1$, z_1, the rotation center, in each case relative to the apex 0 of the trapezoid. In the above expressions, $\bar{x}_o$ -D, $\bar{x}_1$ - D, z_o - B, z_1 - B are given instead, so that these points may be located with respect to the leading edge of the root chord. This is done to avoid expressions containing (1 - T) in the denominator, which increase without limit when the taper ratio approaches unity.

To recapitulate, if the normalizing factors, η, ξ, and ζ are all chosen equal to unity, then the lift coefficients at the root of the rudder are identical to those

of the two-dimensional, incompressible-flow case. In the use of the hydrodynamic parameters derived herein, however, the value of η was determined by taking for $C_{L\gamma}$ a value based on wind-tunnel data for rigid lifting surfaces. Here ξ and ζ were assumed equal to η.

APPENDIX E

NUMERICAL ANALYTICAL METHODS FOR THREE-AND TWO-DEGREE-OF-FREEDOM SYSTEMS*

In this Appendix, equations for a three-degree-of-freedom system for the rudder and supporting structure are described and reduced to equations for a two-degree-of-freedom system by means of the following procedure:

(a) The three vibration mode frequencies and shapes are determined by equating elastic and inertial forces.

(b) The node lines of the two lowest frequencies are plotted. These node lines intersect at a point $x = x_4$, $z = z_4$. (See Figure 4.)

(c) The constraint $v_4 = 0$ is imposed, thereby eliminating the third vibration mode but not affecting the other two modes.

(d) By means of this constraint, any one of v_2, α, γ may be eliminated. Thus the entire system will have two degrees of freedom.

The method for calculating the flutter modes for the two-degree-of-freedom system is also described.

1. Modes—Three-and Two-Degree-of-Freedom Systems

The elastic properties of the rudder supporting structure are adequately described by specifying a 3 x 3 matrix of influence coefficients** relating the three classes of permitted rudder motion measured at the origin R (Figure 90) to the corresponding

*In Reference 6 an analytical method is developed for determining the flutter of a rudder system with *three*-degrees-of-freedom. The system consists of a rigid foil attached through a flexible stock to a rigid hull. The supporting structure is not included in the analysis.

**Bending and shear strain energy are included; with the exception of $\gamma\dot{\gamma}$ term, which accounts for flexibility of rudder stock in torsion below rudder root R, no γ-moment is transmitted through the bearings.

forces and moments.* It can be shown that the matrix** for the rudder supporting structure of PGM at point R is (this accounts for the flexibility of all the mechanism above R, with the exception noted below):

$$\begin{Bmatrix} v_z \\ \alpha \\ \gamma \end{Bmatrix} = - \begin{bmatrix} +13.59\ \text{ft}^2 & +13.96\ \text{ft} & -16.04\ \text{ft} \\ +13.96\ \text{ft} & +26.68 & -28.89 \\ -16.04\ \text{ft} & -28.89 & +528.15 \end{bmatrix} \cdot 10^{-9} \frac{\text{rad}}{\text{lb ft}} \begin{Bmatrix} F_y \\ M_\alpha \\ M_\gamma \end{Bmatrix} \quad [E\text{-}1]$$

where the minus sign indicates the forces acting on the rudder. (Of the $\gamma\gamma$ term of 528.15, 10.15 represents the torsional flexibility of the portion of the rudder stock below the root chord of the rudder but above the assumed point of attachment of the rudder stock to the rudder hub casting.)

Similarly, it can be shown that the inertial properties (including hydrodynamic or virtual inertias) for the rudder and rudder support structure are represented by the following matrix:

$$\begin{Bmatrix} F_y \\ M_\alpha \\ M_\gamma \end{Bmatrix} = \begin{bmatrix} +156.55 & +273.60\ \text{ft} & -147.33\ \text{ft} \\ +273.60\ \text{ft} & 740.12\ \text{ft}^2 & -282.98\ \text{ft}^2 \\ -147.33\ \text{ft} & -282.98\ \text{ft}^2 & 260.99\ \text{ft}^2 \end{bmatrix} \frac{\text{lb sec}^2}{\text{ft}} \begin{Bmatrix} \ddot{v}_z \\ \ddot{\alpha} \\ \ddot{\gamma} \end{Bmatrix} \quad [E\text{-}2]$$

*In the *analog computer analysis* (discussed in Appendix G), however, the various components of the rudder supporting structure were represented as described there, to (1) be able to determine the effect on flutter of varying portions of the rudder supporting structure, and (2) to permit the addition of more degrees of freedom for later models; for example, the connection of the rudder supporting structure to the hull.

**Any number of well-known advanced calculus texts treat the subject of matrices; e.g., Pipes, L.A., "Matrix Methods for Engineering," Prentice Hall, Inc., New Jersey (1963).

Combining the above equations gives

$$\begin{Bmatrix} v_2 \\ \alpha \\ \gamma \end{Bmatrix} = -\begin{bmatrix} +8,308.7\,\text{ft}^2 & +18,586.1\,\text{ft}^3 & -10,136.9\,\text{ft}^3 \\ +13,741.1\,\text{ft} & +31,740.6\,\text{ft}^2 & -17,146.3\,\text{ft}^2 \\ -88,226.9\,\text{ft} & -175,225.1\,\text{ft}^2 & +148,379.6\,\text{ft}^2 \end{bmatrix} 10^{-9}\,\frac{\text{sec}^2}{\text{ft}^2} \begin{Bmatrix} \ddot{v}_2 \\ \ddot{\alpha} \\ \ddot{\gamma} \end{Bmatrix} \qquad \text{[E-3]}$$

Writing, for sinusoidal motion, $\ddot{v}_2 = -w^2 v_2$, $\ddot{\alpha} = -w^2 \alpha$, $\ddot{\gamma} = -w^2 \gamma$, we have

$$\begin{Bmatrix} v_2 \\ \alpha \\ \gamma \end{Bmatrix} = w^2 \begin{bmatrix} +8.309 & +18.586\,\text{ft} & -10.137\,\text{ft} \\ +13.741\,\text{ft}^{-1} & +31.741 & -17.146 \\ -88.227\,\text{ft}^{-1} & -175.225 & +148.380 \end{bmatrix} 10^{-6}\ \text{sec}^2 \begin{Bmatrix} v_2 \\ \alpha \\ \gamma \end{Bmatrix} \qquad \text{[E-4]}$$

Let $\xi = w^2 10^{-6}\,\text{sec}^2$. Then

$$\begin{bmatrix} +8.309\xi - 1 & +18.586\,\text{ft}\,\xi & -10.137\,\text{ft}\,\xi \\ +13.741\,\text{ft}^{-1}\,\xi & +31.741\,\xi - 1 & -17.146\,\xi \\ -88.227\,\text{ft}^{-1}\,\xi & -175.225\,\xi & +148.380\,\xi - 1 \end{bmatrix} \begin{Bmatrix} v_2 \\ \alpha \\ \gamma \end{Bmatrix} = 0 \qquad \text{[E-5]}$$

The values of ξ permitting nontrivial solutions are obtained by setting the determinant of the matrix to zero. This gives a cubic equation in ξ, with solutions

$$\xi_1 = 0.0056549$$

$$\xi_2 = 0.08778$$

$$\xi_3 = 4.90873$$

Hence

$w_1 = 75.199$ rad/sec or $f_1 = 11.968$ cps

$w_2 = 296.28$ rad/sec or $f_2 = 47.154$ cps

$w_3 = 2215.57$ rad/sec or $f_3 = 352.619$ cps

The results f_1, f_2, f_3 are presented in Table 6.

Mode shapes corresponding to these frequencies can be determined by substituting values of ξ_1, ξ_2, and ξ_3 into the last matrix equation. Thus,

1st Mode ($\xi_1 = 0.0056549$)

$$\begin{bmatrix} +8.309 - \frac{1}{\xi_1} & +18.586 & -10.137 \\ +13.741 & +31.741 - \frac{1}{\xi_1} & -17.146 \\ -88.227 & -175.225 & +148.380 - \frac{1}{\xi_1} \end{bmatrix} \begin{Bmatrix} v_2/\text{ft} \\ \alpha \\ \gamma \end{Bmatrix} =$$

$$\begin{bmatrix} -168.531 & +18.586 & -10.137 \\ +13.741 & -145.099 & -17.146 \\ -88.227 & -175.225 & -28.460 \end{bmatrix} \begin{Bmatrix} v_2/\text{ft} \\ \alpha \\ \gamma \end{Bmatrix} = 0$$

$$\frac{v_2/\text{ft}}{1,125.110} = \frac{\alpha}{1,903.809} = \frac{\gamma}{-15,209.416}$$

$$\frac{v_2}{1\text{ ft}} = \frac{\alpha}{+1.6921} = \frac{\gamma}{-13.518}$$

2nd Mode ($\xi_2 = 0.08778$)

Similarly,

$$\frac{v_2}{1\text{ ft}} = \frac{\alpha}{+1.7045} = \frac{\gamma}{2.8244}$$

3rd Mode ($\xi_3 = 4.90873$)

Similarly,

$$\frac{v_2}{1\text{ ft}} = \frac{\alpha}{-0.31364} = \frac{\gamma}{+0.22453}$$

A summary of the calculated modal results is given in the following chart:

Mode Number		1	2	3
Frequency (cps)		11.968	47.154	352.619
Mode Shape (ft^{-1})	$\frac{\alpha}{v_2}$	+1.6921	+1.7045	-0.31364
	$\frac{\gamma}{v_2}$	-13.518	+2.8244	+0.22453
Node* Lines (ft)	x-intercept	+0.073975	-0.35406	-4.4537
	z-intercept	+0.59098	+0.58668	-3.1184
Intersection of Node Lines** (ft)		x = +0.0004 z = +0.5874		

* Measured relative to origin at point R.
** Calculated below.

For the mode shapes given by $\frac{\alpha}{v_2}$, $\frac{\gamma}{v_2}$, there are node lines such that no deflections occur on these lines. The x and z intercepts for these lines are (see Figure 4)

$$x_n = -\frac{1}{\frac{\gamma}{v_2}} \; ; \qquad z_n = +\frac{1}{\frac{\alpha}{v_2}} \qquad [E\text{-}6a,b]$$

The point of intersection $x = x_4$, $z = z_4$ of the node lines of the first two modes is found as follows:

From Figure 4 it is evident that

$$\frac{x_4}{x_{n1}} = \frac{z_{n1} - z_4}{z_{n1}} \; ; \qquad \frac{x_4}{x_{n2}} = \frac{z_{n2} - z_4}{z_{n2}} \qquad [E\text{-}7a,b]$$

Simultaneous solutions of these equations yields

$$x_4 = \frac{z_{n2} - z_{n1}}{x_{n1}z_{n2} - x_{n2}z_{n1}} \quad x_{n1}x_{n2} \qquad [E\text{-}8a]$$

$$z_4 = \frac{x_{n1} - x_{n2}}{x_{n1}z_{n2} - x_{n2}z_{n1}} \quad z_{n1}z_{n2} \qquad [E\text{-}8b]$$

Substituting the values $x_{n1} = 0.073975$, $x_{n2} = -0.35406$, $z_{n1} = 0.59098$, $z_{n2} = +0.58668$, given in the chart above, we find

$$x_4 = +0.000446 \text{ (approximately zero)}$$

$$z_4 = +0.58742 \text{ above R (or 3.695 above baseline)}$$

as shown on Figure 4. And the constraint is

$$v_4 = v_2 - z_4\,\alpha + x_4\gamma \approx v_2 - z_4\alpha = 0$$

$$\text{or } \frac{\alpha}{v_2} = \frac{1}{z_4} = +1.702 \text{ ft}$$

Thus the third vibration mode is eliminated by means of the constraint $v_4 = 0$. Matrix equations for the constrained two-degree-of-freedom system are now derived.

We first effect a *transformation* of the influence coefficient matrix from Point R to Point 4 ($x = x_4$, $z = z_4$). The transformation is

$$\begin{bmatrix} v_4 \\ \alpha \\ \gamma \end{bmatrix} = \begin{bmatrix} 1 & -z_4 & +x_4 \\ 0 & 1 & 0 \\ 0 & 0 & 1 \end{bmatrix} \begin{bmatrix} v_2 \\ \alpha \\ \gamma \end{bmatrix} \qquad \begin{bmatrix} F_y \\ M_{\alpha 2} \\ M_{\gamma 2} \end{bmatrix} = \begin{bmatrix} 1 & 0 & 0 \\ -z_4 & 1 & 0 \\ +x_4 & 0 & 1 \end{bmatrix} \begin{bmatrix} F_y \\ M_{\alpha 4} \\ M_{\gamma 4} \end{bmatrix} \qquad [E\text{-}9a,b]$$

Thus

$$\begin{bmatrix} v_4 \\ \alpha \\ \gamma \end{bmatrix} = -\begin{bmatrix} C_4 \end{bmatrix} \begin{bmatrix} F_y \\ M_{\alpha 4} \\ M_{\gamma 4} \end{bmatrix} \qquad \text{[E-10]}$$

where

$$\begin{bmatrix} C_4 \end{bmatrix} = \begin{bmatrix} 1 & -z_4 & +x_4 \\ 0 & 1 & 0 \\ 0 & 0 & 1 \end{bmatrix} \begin{bmatrix} C_2 \end{bmatrix} \begin{bmatrix} 1 & 0 & 0 \\ -z_4 & 1 & 0 \\ +x_4 & 0 & 1 \end{bmatrix} \qquad \text{[E-11]}$$

and $\begin{bmatrix} C_2 \end{bmatrix}$ is the matrix in Equation [E-1].

Letting $z_4 = +0.5874$ ft and $x_4 = 0.000$ ft

$$\begin{bmatrix} C_4 \end{bmatrix} = \begin{bmatrix} +6.397 \text{ ft}^2 & -1.714 \text{ ft} & +0.935 \text{ ft} \\ -1.714 \text{ ft} & +26.68 & -28.89 \\ +0.935 \text{ ft} & -28.89 & +528.15 \end{bmatrix} \frac{10^{-9} \text{ rad}}{\text{lb-ft}} \qquad \text{[E-12a]}$$

Writing

$$\begin{bmatrix} C_4 \end{bmatrix} = \begin{bmatrix} a & b & c \\ d & e & f \\ g & h & i \end{bmatrix} \qquad \text{[E-12b]}$$

we have

$$\begin{bmatrix} v_4 \\ \alpha \\ \gamma \end{bmatrix} = - \begin{bmatrix} a & b & c \\ d & e & f \\ g & h & i \end{bmatrix} \begin{bmatrix} F_y \\ M_{\alpha 4} \\ M_{\gamma 4} \end{bmatrix} \qquad \text{[E-13]}$$

Now impose the constraint $v_4 = 0$. We do not retain F_y, but calculate it and substitute for it to express α, γ in terms of $M_{\alpha 4}$, $M_{\gamma 4}$ as follows. With $v_4 = 0$,

$$aF_y + bM_{\alpha 4} + cM_{\gamma 4} = 0$$

or

$$F_y = -\frac{b}{a} M_{\alpha 4} - \frac{c}{a} M_{\gamma 4}$$

Hence the constrained influence coefficient matrix is

$$\begin{bmatrix} \alpha \\ \gamma \end{bmatrix} = -\begin{bmatrix} d \\ g \end{bmatrix} F_y - \begin{bmatrix} e & f \\ h & i \end{bmatrix} \begin{bmatrix} M_{\alpha 4} \\ M_{\gamma 4} \end{bmatrix} = \left(\begin{bmatrix} d \\ g \end{bmatrix} \begin{bmatrix} b & c \\ \bar{a} & \bar{a} \end{bmatrix} - \begin{bmatrix} e & f \\ h & i \end{bmatrix} \right) \begin{bmatrix} M_{\alpha 4} \\ M_{\gamma 4} \end{bmatrix}$$

$$= -\begin{bmatrix} e - \frac{db}{a} & f - \frac{dc}{a} \\ h - \frac{gb}{a} & i - \frac{gc}{a} \end{bmatrix} \begin{bmatrix} M_{\alpha 4} \\ M_{\gamma 4} \end{bmatrix} = -\frac{1}{a} \begin{bmatrix} ae - db & af - dc \\ ah - gb & ai - gc \end{bmatrix} \begin{bmatrix} M_{\alpha 4} \\ M_{\gamma 4} \end{bmatrix} \qquad \text{[E-14]}$$

Substituting the values a ..... i given in Equation [E-12a] into Equation [E-14], we obtain

$$\begin{bmatrix} \alpha \\ \gamma \end{bmatrix} = -\begin{bmatrix} +26.221 & -28.640 \\ -28.640 & +528.013 \end{bmatrix} \frac{10^{-9} \text{ rad}}{\text{lb ft}} \begin{bmatrix} M_{\alpha 4} \\ M_{\gamma 4} \end{bmatrix} \qquad \text{[E-15]}$$

The minus sign means the moments act on the rudder.

It can be shown that the constrained inertia matrix is

$$\begin{bmatrix} M_{\alpha 4} \\ M_{\gamma 4} \end{bmatrix} = -w^2 \begin{bmatrix} 1115.51 & -369.45 \\ -369.45 & +260.99 \end{bmatrix} \text{lb-sec}^2\text{-ft} \begin{bmatrix} \alpha \\ \gamma \end{bmatrix} \qquad \text{[E-16]}$$

The correctness of this expression can be verified by duplicating the first and second normal modes previously obtained, as follows:

$$\begin{bmatrix} \alpha \\ \gamma \end{bmatrix} = w^2 \begin{bmatrix} +26.221 & -28.640 \\ -28.640 & +528.013 \end{bmatrix} \begin{bmatrix} +1115.51 & -369.45 \\ -369.45 & +260.99 \end{bmatrix} 10^{-9} \text{sec}^2 \begin{bmatrix} \alpha \\ \gamma \end{bmatrix} \quad \text{[E-17]}$$

Letting $10^{-6}\,\text{sec}^2\, w^2 = \xi$, we have

$$\begin{bmatrix} +39.830\xi - 1 & -17.162\xi \\ -227.023\xi & +148.387\xi - 1 \end{bmatrix} \begin{bmatrix} \alpha \\ \gamma \end{bmatrix} = 0 \quad \text{[E-18]}$$

The roots of ξ obtained from

$$2014.085\xi^2 - 188.217\xi + 1 = 0 \quad \text{[E-19]}$$

are

$$\xi_1 = 0.0056552$$

$$\xi_2 = 0.087795$$

which checks the previously obtained values for ξ_1, ξ_2.

2. Flutter—Two-Degree-of-Freedom System*

As shown in the previous section, the three-degree-of-freedom system constrained at Point 4 ($v_4 = 0$) reduces to a two-degree-of-freedom system mathematically describable by a 2 x 2 matrix. The general characteristic (frequency quartic) equation for a two-degree-of-freedom system has the form[4]

$$S^4 + A_0 S^3 + A_1 S^2 + A_2 S + A_3 = 0$$

where the coefficients A_i, which are functions of the system parameters and the velocity, are all real and $S = \frac{d}{dt} = \sigma + j\omega$ is a complex operator or complex frequency.

*See footnotes page 34 and 84

For the basic case, in particular, it can be shown that this may be written as

$$\bar{S}^4 + 0.683273\,\bar{S}^3 + (9.344553 - 0.086870\,m^2)\,\bar{S}^2 + (3.300949 - 0.002406\,m^2)\,m\bar{S} + (4.964822 + 0.022639\,m^2) = 0$$

where $\bar{S} = 10^{-2}$ sec S and $m = \frac{V}{V_o}$, the dimensionless velocity.

Note: $\bar{S}$ is dimensionless whereas S is in seconds. For a given velocity (a given value of m) this is a quartic equation with real coefficients.

One way to find the roots of the general equation is to express the equation in terms of its quadratic factors*

$$(S^2 + 2a_1b_1S + b_1^2)\,(S^2 + 2a_2b_2S + b_2^2) = 0$$

The roots are then

$$S = x_1 \pm iy_1,\ x_2 \pm iy_2$$

where

$$x_1 = -a_1b_1, \qquad y_1 = \sqrt{1 - a_1^2}\,b_1$$

$$x_2 = -a_2b_2 \qquad y_2 = \sqrt{1 - a_2^2}\,b_2$$

For the basic case, the solutions of the characteristic equation are presented in Figure 39 which traces points (i.e., roots) located by $x_1, y_1; x_1, -y_1; x_2, y_2; x_2, -y_2$ as the parameter $m = \frac{V}{V_o}$ is varied. Thus, Figure 39 is a plot of the imaginary part of the root versus the real part of S (= 100 $\bar{S}$). This is termed a Nyquist plot

*The reader is referred to page 191 of Reference 25 or page 155 of Reference 26 for methods for obtaining a_1, b_1, a_2, b_2 from $A_0 \ldots\ldots A_3$. In the first reference, let $m = a_1^2$, $\ell = a_1b_1$, $m' = a_2^2$, $\ell' = a_2b_2$ to obtain the form of quadratic factors given here.

and is useful for determining the stable and unstable regions corresponding to a range of values for m. Some numerical values for the solutions of the characteristic equation, for the basic case, are also presented in the following chart (along with values of ζ discussed later):

m	Roots of $\bar{S}$ ($=\frac{S}{100}$)		Values of ζ	
0	0 $\pm$ j 0.7520	0 $\pm$ j 2.968	0	0
1	-0.1818 $\pm$ j 0.7414	-0.1598 $\pm$ j 2.9212	+0.237	+0.0545
2	-0.3931 $\pm$ j 0.6967	-0.2902 $\pm$ j 2.7958	+0.491	+0.1032
3	-0.6781 $\pm$ j 0.5409	-0.3469 $\pm$ j 2.5979	+0.781	+0.1325
4	-1.5775, -0.5824	-0.2866 $\pm$ j 2.3908	----	+0.1192
6.252	-3.9544, -0.3174	0 $\pm$ j 2.1664	----	0
10	-7.2986, -0.2346	+0.3502 $\pm$ j 2.0246	----	-0.1699
20	-15.4958, -0.2585	+1.0445 $\pm$ j 1.5521	----	-0.559
38.26	-30.0522, -0.5693	+0.5693, +3.9102	----	----

Consider the special case $m = \frac{V}{V_o} = 0$; see Figure 39. Then

$$\bar{S}^2 = -0.56531,\ -8.779021$$

and

$$\omega^2 = -S^2 = -10^4 \text{ sec}^{-2}\ \bar{S}^2 = 5655.31 \text{ sec}^{-2};\ 87{,}790.21 \text{ sec}^{-2}$$

which agrees with the solutions of Equations [E-19] and [E-5].

For compatibility with other approaches to flutter, the per unit critical damping parameter ζ (see Appendix F) is shown in most of the curves of flutter characteristics in this report.

The symbols ζ and ω (the "undamped natural frequency" or frequency of the free response when $\zeta = 0$) are defined by expressing each quadratic factor of the characteristic equation as

$$(S^2 + 2\zeta\omega S + \omega^2)$$

Thus ζ is identified as a_1, a_2 and ω is identified as b_1, b_2. Whereas the real part of the roots in Figure 39 represents the damping per unit time, ζ in Figure 40 and elsewhere represents damping per unit cycle. This accounts for the large difference in the magnitudes of damping in these plots.

It can be shown that for a root specified by x, y where x and y are the real and imaginary parts of the root of the characteristic equation in S, ζ may be defined as

$$\zeta = -\sin\theta$$

where

$$\tan\theta = \frac{x}{y}$$

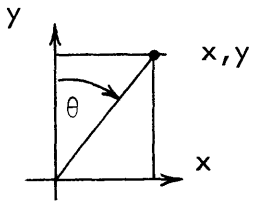

and

$$\zeta \approx -\frac{x}{y} \approx -\theta \text{ (for } \zeta \text{ small)}$$

By eliminating θ from the two equations preceding the last equation, we find

$$\zeta = \frac{-x}{\sqrt{y^2 + x^2}}$$

If $y > 0$, then

$$\zeta = \frac{-x/y}{\sqrt{1 + (\frac{x}{y})^2}}$$

In each case the positive value of the square root is employed. Thus ζ has a sign which is opposite from the sign of x, where x is +, ζ is -, and the solution is unstable.

In this report ζ is the basic flutter damping parameter that is plotted. Its sense in accordance with the foregoing analysis conforms to the following:

Real part of root x	Per unit critical damping ζ	Plotted	Labeled
+	-	up	U (for "Unstable")
-	+	down	S (for "Stable")

The general transient solution of a system whose characteristic equation includes a quadratic term of the form $(S^2 + 2\zeta\omega S + \omega^2)$ is

$$u = u_0 e^{-\zeta\omega t} \sin\left(\sqrt{1 - \zeta^2}\,\omega t + \phi\right)$$

where u is any coordinate describing the behavior of the system and u_0 and ϕ are constants determined by the initial conditions. Since ω is inherently positive, it is apparent that $\zeta > 0$ corresponds to a stable system and $\zeta < 0$ corresponds to an unstable system (additional information on ζ is given in Appendix F).

In Figure 39, at $\frac{V}{V_o} = 1$, the angle $-\theta = \zeta$ is large for the first mode and small for the second mode, indicating greater stability for the first mode than for the second mode at this velocity. As $\frac{V}{V_o}$ is increased, the real part x of the roots of S for the first mode becomes increasingly negative, indicating increasing stability for this mode (since $\zeta = -\theta = -\frac{x}{y}$) ; whereas the real part of the second mode becomes positive, indicating decreasing stability for this mode. Figure 40 illustrates these results in somewhat different form. The curve with the steepest negative slope indicates the rapid increase in stability for the first mode, and any of the remaining curves indicates that although the second mode initially becomes more stable as velocity is increased, eventually the stability decreases and it goes unstable.

APPENDIX F

MEASUREMENT OF DAMPING PARAMETERS

The symbol C is used for a damping constant for a linear or torsional dashpot. For a single mass, dashpot, and spring system, C_c is the critical value of the dashpot constant such that free oscillatory motion is possible only when C is less than C_c. The value of the critical dashpot constant for a single-degree-of-freedom system C_c is equal to $2\,[\,(\text{spring constant})\,(\text{mass})\,]^{\frac{1}{2}}$. Thus for a single-degree-of-freedom system, we define $\zeta = C/C_c \times 100$ percent as the percent of critical damping. In this Appendix, the definition of ζ will be extended to systems with many degrees of freedom.

The extended definition of ζ is chosen such that it has the following properties:

(a) When it is applied to a single-degree-of-freedom system, the value will be that given above.

(b) The value will be based upon some measurement on the system.

(c) The value will depend only upon the system parameters and not upon the particular method of taking the measurement.

(d) For a multi-degree-of-freedom system, a value of ζ will be associated with each mode of response.

(e) For an unstable system, a negative value of ζ will be associated with the unstable mode.

The two methods of measurement of ζ that will be discussed are the free response after some initial excitation and the forced response to a sinusoidal force.

Free Response Method. Due to some initial excitation, let A_o be the measured amplitude at an instant of time and A_n be the amplitude n cycles later. Then, if only one mode of response is present,

$$\zeta = \frac{-\frac{1}{2n\pi} \ell n \frac{A_n}{A_o}}{\sqrt{1 + \left[\frac{1}{2n\pi} \ell n \left(\frac{A_n}{A_o}\right)\right]^2}} \cong -\frac{1}{2n\pi} \ell n \left(\frac{A_n}{A_o}\right)$$

where the last expression is valid for small damping. In actual practice, it is practically impossible, or it is generally difficult, to excite a single mode of response; hence the measured $\frac{A_n}{A_o}$ is only approximate. In this report, when the free response method was used, the value of ζ was calculated as $-\frac{1}{2n\pi} \ell n \left(\frac{A_n}{A_o}\right)$.

Forced Response Method. Here we find the amplitude of the response due to a constant amplitude of excitation. Let the frequency where the response reaches some numerically maximum value be f_o and neighboring frequencies where the amplitude of response differs by a ratio of $\sqrt{2}$ be f_+ and f_-. Then*

$$\zeta \cong \frac{1}{2} \frac{(f_+) - (f_-)}{(f_o)}$$

where the approximation is good for small damping. Since $20 \log \sqrt{2} \cong 3$, this will be called the 3 db method. f_+ and f_- are the frequencies where the response differs from the extreme value by 3 db.

Both methods approximately exhibit properties (a) - (e) above, and give approximately the same value for ζ.

*This equation may be found in many texts on elementary circuit theory.

It is customary in the field of aircraft flutter to use the parameter $g = 2\zeta$.

As defined above, if

$\zeta > 1$ system is stable, damping more than critical

$\zeta = 1$ system is stable, damping critical

$1 > \zeta > 0$ system is stable, damping less than critical

$\zeta = 0$ system is neutral

$0 > \zeta$ system is unstable

If $\zeta^2 < 1$, the free response of the system, with only the one degree of freedom under consideration excited, is given by

$$u = e^{-\zeta \omega_0 t} \left[A \cos \sqrt{1 - \zeta^2}\ \omega_0 t + B \sin \sqrt{1 - \zeta^2}\ \omega_0 t \right]$$

where u is the dependent variable or coordinate,

ω_0 is the natural frequency if damping is removed, and

A, B are arbitrary constants.

The measurement of the damping and frequency of a flutter root by the free response method is illustrated by the photographs of Figure 93. By comparing the first and third traces, the portion of the response occurring while the exciting force is imposed may be distinguished from the portion of the response which is free. The latter portion is used to determine the damping parameter ζ. For Figure 93a, $A_n / A_o = 2.0$ in 2.5 cycles, so $\zeta = -0.044$ (or 0.044 UNSTABLE, as indicated on curves in this report). Similarly, Record 442 is read $\zeta = +0.046$ (STABLE) and Record 443 is read $\zeta = -0.0035$ (UNSTABLE).

The second trace of each record shows a very accurate method of determining the frequency of the flutter root. The response is the ordinate, and a reference sine wave from an audio oscillator is the abscissa. The frequency of the reference is varied until all crossings of the x-axis occur at the same two points, as in the photographs. At this frequency, the phase between reference and response is constant. Therefore, the response has the same frequency as the reference, which is read directly.

APPENDIX G

ELECTRIC ANALOG DEVELOPMENT FOR PGM MOTOR GUNBOAT

The establishment of electrical circuits which are analogous to the mechanical models and hydrodynamic forces outlined in Sections III and IV, respectively, are based on the "mobility" analog,[7,8,23] in which the following quantities are proportional to each other:

Mechanical	Electrical
Force (or Moment)	Current
Velocity (or Angular Velocity)	Voltage
Time	Time
Spring Flexibility	Inductance
Mass	Capacitance
Damping	Resistance

1. Analog Circuits

The electrical circuits by which the analogy is established for the solution of the PGM hull-rudder combination are given in Figures 84 to 87. Figure 84 illustrates the circuit for establishing the mechanical parameters of the rudder. The transformers are drawn in great detail for the purpose of facilitating the many variations in which the center of mass, center of pressure, and rotation center are varied. The circuit of Figure 84 essentially merely represents the three degrees of freedom of the rigid rudder in motion out of its plane. Transformers 471 and 472 represent the coupling

between lateral motion and roll, and different tap locations on the primaries (P471 and P472) represent the v-motion of points with different z-locations. Similarly, Transformers 473 and 474 couple lateral motion and yaw, and taps on P473 and P474 locate points with different x-locations. To establish the two-degree-of-freedom model, Switch 403 is closed. R463, R464, and R465 simulate viscous damping effects.

Figure 85 presents the circuit which represents the elastic properties of the rudder supporting structure. Various portions are identified as representing the rudder stock, the tiller, the connecting rod, the hydraulic system, the upper and lower bearings, the rudder trunk and bearing carrier, and the platform and bottom of the hull. The rudder stock is represented by a three-cell Russell beam (Reference 7) in side bending and a three-cell torsion bar. The rudder trunk and bearing carrier are represented by a two-cell Russell beam and a two-cell torsion bar.

The three capacitors in Figure 85 represent the added masses of the six-degree-of-freedom model. They are set to zero in the models with two, three, and twenty-three degrees of freedom. Switches 401 and 402 are open in the basic case (no yaw moment diverted from the rudder stock through the bearings) and closed in the variation in which bearing friction permits transmission of yaw moment. The four terminals at the right side of Figure 85 are grounded in models with two, three, and six degrees of freedom. They are connected to the corresponding terminals of the hull circuit for the twenty-three-degree-of-freedom model.

Figure 86 illustrates the circuit for hydrodynamic forces (other than virtual mass and viscous damping terms) acting on the rudder. It simulates Equations [B-1] of

Appendix B. Eighteen high-gain amplifiers are employed: one (A061) as an integrator, six (A031, A032, A051, A052, A081, A082) as three current generators, and the remainder as summers or sign changers. Each potentiometer is labeled according to the term it controls. Three hydrodynamic lag functions are employed (R001 to R006).

Figure 87 shows the passive circuit which represents the inertia and elastic properties of the hull as a beam in side bending and torsion. Capacitors R566, R565, R564, R563, and R466 represent mass coupling because of center of mass location above or below the neutral axis,* see Table 4. When the location is above the neutral axis, the capacitor's (-) terminal is connected to the (+) terminal of the transformer in the α-circuit; when below the neutral axis, the capacitor's (-) terminal is connected to the (-) terminal of the transformer.

The four terminals at the left end of Figure 87 are left floating in the twenty-degree-of-freedom model, and are connected to corresponding terminals in the rudder supporting structure circuit in the twenty-three-degree-of-freedom model. Transformers 481, 482, and 483 effect the change in scale factor between hull and rudder circuits. Transformer 482, in addition, establishes, by coupling with the roll coordinate, the different lateral motion of points at different vertical levels in the rudder supporting structure.

*The mass coupling effect (first moment of mass with respect to the neutral axis), is represented by coupling capacitors in the circuit, but because this mass coupling is relatively small, the entire effect is represented by coupling at only five stations: 5, 9, 11, 13, and 17.

2. Scale Factors

The definition of the scale factors employed in this analysis, in relating the physical system to the analog system, is given in Table 14, together with formulas for the use of these scale factors. A listing of the numerical values of the scale factors employed is given in Table 15. It is noted that separate values of the scale factors were used in the rudder and supporting structure as compared with the hull.

Because this entire analysis is based on linear, small-motion theory, the level of vibrations is not significant, and the scale factor defining level K does not enter into any of the formulas.

3. Sample Calculations of Circuit Elements

The calculation of values of circuit elements by means of the formulas and values of Section 2 of this Appendix is presented in Table 16.

REFERENCES

1. Antkowiak, E.T., "Hull Vibration in the DD 931 Class Destroyer," Boston Naval Shipyard Evaluation Report R-10 (20 Aug 1956).
2. McGoldrick, R.T., "Rudder-Excited Hull Vibration on USS FORREST SHERMAN (DD 931)--A Problem in Hydroelasticity," Transactions of Society of Naval Architects and Marine Engineers, Vol. 67 (1959). Also David Taylor Model Basin Report 1431 (Jun 1960).
3. Jewell, D.A. and McCormick, M.E., "Hydroelastic Instability of a Control Surface," David Taylor Model Basin Report 1442 (Dec 1961).
4. Leibowitz, R.C. and Belz, D.J., "Comparison of Theory and Experiment for Marine Control-Surface Flutter," Paper presented at the Fourth Symposium on Naval Hydrodynamics on "Ship Propulsion and Hydroelasticity" at Washington, D.C., 27-31 (Aug 1962), Vol. 3 of ACR-73, Office of Naval Research. Also David Taylor Model Basin Report 1567 (Aug 1962).
5. Ransleben, G.E.,Jr. and Abramson, H.N., "Experimental Determination of Oscillatory Lift and Moment Distributions on Fully Submerged Flexible Hydrofoils," Southwest Research Institute (Nonr-3335(00)) Project 38-1028-2 (1 Nov 1962).
6. Leibowitz, R.C., and Harder, R.L., "Rudder-Diving Plane-Hull Vibration and Flutter Analysis of USS ALBACORE (AGSS 569)," David Taylor Model Basin Report 1961 (Jun 1965).
7. Russell, W.T. and MacNeal, R.H., "An Improved Electrical Analogy for the Analysis of a Beam in Bending," Journal of Applied Mechanics, Vol. 20 (1953), Transactions ASME, Vol. 75 (1953).

8. Leibowitz, R.C. and Kennard, E.H., "Theory of Freely Vibrating Nonuniform Beams, Including Methods of Solution and Application to Ships," David Taylor Model Basin Report 1317 (May 1961). In particular, see pp. 24-26.

9. Whicker, L.F. and Fehlner, L.F., "Free-Stream Characteristics of a Family of Low-Aspect-Ratio, All-Movable Control Surfaces for Application to Ship Design," David Taylor Model Basin Report 933 (Dec 1958).

10. Leibowitz, R.C. and Belz, D.J., "A Procedure for Computing the Hydroelastic Parameters for a Rudder in a Free Stream," David Taylor Model Basin Report 1508 (Apr 1962).

11. Scanlon, R.H. and Rosenbaum, R., "Introduction to the Study of Aircraft Vibration and Flutter," MacMillan Company, New York (1960).

12. Leibowitz, R.C., "USS ALBACORE (AGSS 569) Modes of Rudder Vibration," David Taylor Model Basin Report 1540 (Sep 1961).

13. Bureau of Ships Drawing PGM 84-800-2120672.

14. Bureau of Ships Drawing PGM 84-800-2120669.

15. Bureau of Ships Drawing PGM 84-800-2120668.

16. Bureau of Ships Drawing PGM 84-800-2120666.

17. Gibbs and Cox, Calculation Sheet 15351-8451-206A (28 Feb 1963).

18. Leibowitz, R.C. and Kilcullen, A., "Experimental Determination of Structural and Still Water Damping and Virtual Mass of Control Surfaces," David Taylor Model Basin Report 1836 (May 1965).

19. Leibowitz, R.C. and Kennard, E.H., "Theoretical and Experimental Determination of Damping Constants of One- to Three-Dimensional Vibrating Systems," David Taylor Model Basin Report 1770 (Jun 1964).

20. Dixon, W.J., "Flutter Analysis of Rudders Flexibly Attached to High Speed Ships," Computer Engineering Associates Project ES 206, Contract N600(167)59606(x) (Nov 1963).

21. Kennard, E.H., and Leibowitz, R.C., "Theory of Rudder-Diving Plane-Ship Vibrations and Flutter, Including Methods of Solution," David Taylor Model Basin Report 1507 (Feb 1962).

22. Bisplinghoff, R.L., et al., "Aeroelasticity," Addison-Wesley Publishing Co., Inc., Cambridge, Mass. (1955); (see Chapter 5 and Figures 5-20 and 7-2 and Table 7-1).

23. MacNeal, R.H.,"Electric Circuit Analogies for Elastic Structures," John Wiley and Sons, Inc., New York (1962).

24. Jones, R.T., "Unsteady Lift of Wing of Finite Aspect Ratio," National Advisory Committee for Aeronautics TR 681 (1940).

25. Barnard, S. and Child, J.M., "Higher Algebra," MacMillan and Co., Ltd., London (1952).

26. Zaguskin, V.L., "Handbook of Numerical Methods for the Solution of Algebraic and Transcendental Equations," Pergamon Press, New York (1961).

BIBLIOGRAPHY

1. Kennard, E.H. and Leibowitz, R.C., "Forced Vibration of Beams and Flutter of Beam-Foil Systems," David Taylor Model Basin Report 1848 (Oct 1964).

INITIAL DISTRIBUTION

Copies	
12	CHBUSHIPS 3 Tech Lib (Code 210L) 1 Lab Mgt (Code 320) 1 Applied Res (Code 340) 1 Prelim Des Br (Code 420) 2 Hull Des Br (Code 440) 2 Sci & Res Sec (Code 442) 1 Hull Struc Sec (Code 443) 3 Ship Sil Br (Code 345)
3	CHONR 1 Math Sci Div (Code 430) 1 Fluid Dyn Br (Code 438)
1	CHBUWEPS
1	CO & DIR, USNMEL
1	CO & DIR, USNMDL
1	CDR, USNOL
1	CDR, USNOTS, China Lake
1	CDR, USNOTS, Pasadena
1	DIR, USNRL
1	CO, USNROTC & NAVADMINU MIT
1	Adm, Webb Inst.
1	O in C, PGSCOL, Webb Inst.
1	NAVSHIPYD LBEACH (Code 240)
1	NAVSHIPYD PEARL (Code 240)
1	NAVSHIPYD PUG (Code 240)
1	NAVSHIPYD SFRAN (Code 240)
1	NAVSHIPYD NORVA (Code 240)
1	NAVSHIPYD PHILA (Code 240)
1	NAVSHIPYD BSN (Code 240)
2	NAVSHIPYD NYK 1 Des Supt (Code 240)
1	USNASL
1	CMDT, USCG 1 Secy, Ship Struc Comm
1	DIR, Natl BuStand
1	ADM, MARAD
2	DIR, NASA 1 Ship Struc Comm
20	DDC
1	WHOI
1	St. Anthony Falls Hydrau Lab
5	MIT, Dept of (NAME)
2	New York Univ 1 Dept of Meteorology 1 Fluid Mech Lab
1	Inst of Hydrau Res, Univ of Iowa
1	Sch of Engin & Arch, Catholic Univ

Copies	
2	Inst of Engin Res, Univ of California
1	Head, Dept. of Nav Arch Attn: Prof Schade
3	Univ of Michigan 1 Exper Naval Tank 1 Dept of Engin Mech 1 Dir, Finn Michelson Dept of Naval Arch
1	Hudson Lab, Columbia Univ
1	Univ of Notre Dame Attn: Prof. A. Strandhagen, Head, Dept of Eng Mech
1	APL, JHU
4	Fluid Dyn Res Grp, MIT 1 Mr. John Dugundsi 1 Prof. Holt Ashley 1 Mrs. Sheila E. Widnall 1 Mrs. Nancy Ghareeb
3	Dept of Applied Mech, SWRI 1 Dr. H. Norman Abramson 1 Mr. Wen-Hwa Chu 1 Mr. Jack T. Irick
3	DIR, Davidson Lab, SIT 1 Mr. Charles J. Henry 1 Mr. Raihan Ali
1	NNSB & DD Co. Attn: Mr. Montgomery
1	Gen Dyn, EB Div

Copies	
1	Polytechnic Institute of Bklyn Dept of Aerospace Engineering and Applied Mechanics
2	SNAME 1 Hull Struc Comm
4	Grumman Aircraft Eng Corp. 1 Mr. Eugene F. Baird 1 Mr. Charles E. Squires, Jr. 1 Mr. Renso L. Caporali
2	Technical Research Group 2 Aerial Way, Syosset, N.Y. 1 Mr. Jack Kotik
1	Engineering Index, New York
1	Dr. E.H. Kennard, 4057 Tenango Road, Claremont, Calif
1	Dr. Theodore Theodorsen, Republic Aircraft Corp. Farmingdale, L.I., N.Y.
1	Mr. I.E. Garrick, Langley Res Ctr, NASA, Langley Field, Va.
1	Mr. J.D. Crisp, Aeroelastic & Structures Res Lab, MIT
1	Mr. Maurice Sevik, College of Engin & Arch, ORL Penn State Univ
1	Mr. Alexander H. Flax, Cornell Aero Lab, Inc.

Copies

1 Mr. R.T. McGoldrick,
Box 293, Sheffield, Mass

1 MacNeal Schwendler Corp,
2556 Mission Street
San Marino, Calif

1 Prof.M. Landahl, Dept of Aero
and Astro, MIT,
Cambridge 39, Mass

2 Hydronautics Inc, Pendell School Rd.,
Laurel, Md.

2 President, Oceanics Inc, 114 E 40 St.
New York 16
1 Dr. Paul Kaplan

1 J.G. Eng. Res. Associates
3831 Menlo Drive,
Baltimore, Md.

3 Cornell Aeronautical Lab, Inc
Buffalo 21, New York
1 Mr. Peter Crimi
2 Mr. Irving C. Statler

3 General Dynamics, Convair
P.O. Box 1950, San Diego 12, Calif
1 Mr. Robert C. Peiler
1 Mr. Louis M. Figueron

David Taylor Model Basin. Report 1993.
RUDDER-HULL VIBRATION AND FLUTTER ANALYSIS OF A HIGH-SPEED SHIP (PGM MOTOR GUNBOAT), by Ralph C. Leibowitz. Oct 1965. xvi, 197p. illus., graphs, tables, refs.
UNCLASSIFIED

This report presents the results of a "flutter" analysis for a PGM Motor Gunboat. The results were obtained both by computing the rudder-hull vibrations (including flutter) on an analog computer and by numerical analysis. The analogs are based upon extensions of previously derived theories and methods for representing the vibrating system excited by hydrodynamic forces and for evaluating the rudder-hull structural and hydroelastic parameters and hydrodynamic parameters referenced in this report.

The results indicate that (assuming a minimum conceivable value of damping) for the PGM rudder-hull system, control-surface flutter will occur at approximately 90 knots. Moreover, the flutter

1. Control surface-hull systems--Flutter--Theory
2. Control surface-hull systems--Vibration--Theory
3. Control surface-hull systems--Flutter--Analog computation
4. Control surface systems--Flutter--Analog and digital computation
5. Control surface systems--Vibration--Analog and digital computation
6. Control surface systems--Flutter--Analytical computations

David Taylor Model Basin. Report 1993.
RUDDER-HULL VIBRATION AND FLUTTER ANALYSIS OF A HIGH-SPEED SHIP (PGM MOTOR GUNBOAT), by Ralph C. Leibowitz. Oct 1965. xvi, 197p. illus., graphs, tables, refs.
UNCLASSIFIED

This report presents the results of a "flutter" analysis for a PGM Motor Gunboat. The results were obtained both by computing the rudder-hull vibrations (including flutter) on an analog computer and by numerical analysis. The analogs are based upon extensions of previously derived theories and methods for representing the vibrating system excited by hydrodynamic forces and for evaluating the rudder-hull structural and hydroelastic parameters and hydrodynamic parameters referenced in this report.

The results indicate that (assuming a minimum conceivable value of damping) for the PGM rudder-hull system, control-surface flutter will occur at approximately 90 knots. Moreover, the flutter

1. Control surface-hull systems--Flutter--Theory
2. Control surface-hull systems--Vibration--Theory
3. Control surface-hull systems--Flutter--Analog computation
4. Control surface systems--Flutter--Analog and digital computation
5. Control surface systems--Vibration--Analog and digital computation
6. Control surface systems--Flutter--Analytical computations

David Taylor Model Basin. Report 1993.
RUDDER-HULL VIBRATION AND FLUTTER ANALYSIS OF A HIGH-SPEED SHIP (PGM MOTOR GUNBOAT), by Ralph C. Leibowitz. Oct 1965. xvi, 197p. illus., graphs, tables, refs.
UNCLASSIFIED

This report presents the results of a "flutter" analysis for a PGM Motor Gunboat. The results were obtained both by computing the rudder-hull vibrations (including flutter) on an analog computer and by numerical analysis. The analogs are based upon extensions of previously derived theories and methods for representing the vibrating system excited by hydrodynamic forces and for evaluating the rudder-hull structural and hydroelastic parameters and hydrodynamic parameters referenced in this report.

The results indicate that (assuming a minimum conceivable value of damping) for the PGM rudder-hull system, control-surface flutter will occur at approximately 90 knots. Moreover, the flutter

1. Control surface-hull systems--Flutter--Theory
2. Control surface-hull systems--Vibration--Theory
3. Control surface-hull systems--Flutter--Analog computation
4. Control surface systems--Flutter--Analog and digital computation
5. Control surface systems--Vibration--Analog and digital computation
6. Control surface systems--Flutter--Analytical computations

David Taylor Model Basin. Report 1993.
RUDDER-HULL VIBRATION AND FLUTTER ANALYSIS OF A HIGH-SPEED SHIP (PGM MOTOR GUNBOAT), by Ralph C. Leibowitz. Oct 1965. xvi, 197p. illus., graphs, tables, refs.
UNCLASSIFIED

This report presents the results of a "flutter" analysis for a PGM Motor Gunboat. The results were obtained both by computing the rudder-hull vibrations (including flutter) on an analog computer and by numerical analysis. The analogs are based upon extensions of previously derived theories and methods for representing the vibrating system excited by hydrodynamic forces and for evaluating the rudder-hull structural and hydroelastic parameters and hydrodynamic parameters referenced in this report.

The results indicate that (assuming a minimum conceivable value of damping) for the PGM rudder-hull system, control-surface flutter will occur at approximately 90 knots. Moreover, the flutter

1. Control surface-hull systems--Flutter--Theory
2. Control surface-hull systems--Vibration--Theory
3. Control surface-hull systems--Flutter--Analog computation
4. Control surface systems--Flutter--Analog and digital computation
5. Control surface systems--Vibration--Analog and digital computation
6. Control surface systems--Flutter--Analytical computations

characteristics of the entire rudder-hull system are more complex than classical flutter of simpler systems involving two vibration modes; hence conclusions concerning the classical or binary flutter of a two- or three-degree-of-freedom rudder do not apply to the entire rudder-hull combination.

7. Control surface systems--Flutter--Hydroelastic parameters
8. Control surface systems--Flutter--Hydrodynamic forces
9. Control surface-hull systems--Vibration--Inertial-elastic parameters
10. PGM (U.S. Motor gunboat)
I. Leibowitz, Ralph C.

---

characteristics of the entire rudder-hull system are more complex than classical flutter of simpler systems involving two vibration modes; hence conclusions concerning the classical or binary flutter of a two- or three-degree-of-freedom rudder do not apply to the entire rudder-hull combination.

7. Control surface systems--Flutter--Hydroelastic parameters
8. Control surface systems--Flutter--Hydrodynamic forces
9. Control surface-hull systems--Vibration--Inertial-elastic parameters
10. PGM (U.S. Motor gunboat)
I. Leibowitz, Ralph C.

---

characteristics of the entire rudder-hull system are more complex than classical flutter of simpler systems involving two vibration modes; hence conclusions concerning the classical or binary flutter of a two- or three-degree-of-freedom rudder do not apply to the entire rudder-hull combination.

7. Control surface systems--Flutter--Hydroelastic parameters
8. Control surface systems--Flutter--Hydrodynamic forces
9. Control surface-hull systems--Vibration--Inertial-elastic parameters
10. PGM (U.S. Motor gunboat)
I. Leibowitz, Ralph C.

---

characteristics of the entire rudder-hull system are more complex than classical flutter of simpler systems involving two vibration modes; hence conclusions concerning the classical or binary flutter of a two- or three-degree-of-freedom rudder do not apply to the entire rudder-hull combination.

7. Control surface systems--Flutter--Hydroelastic parameters
8. Control surface systems--Flutter--Hydrodynamic forces
9. Control surface-hull systems--Vibration--Inertial-elastic parameters
10. PGM (U.S. Motor gunboat)
I. Leibowitz, Ralph C.

David Taylor Model Basin. Report 1993.
RUDDER-HULL VIBRATION AND FLUTTER ANALYSIS OF A HIGH-SPEED SHIP (PGM MOTOR GUNBOAT), by Ralph C. Leibowitz. Oct 1965. xvi, 197p. illus., graphs, tables, refs.
UNCLASSIFIED

This report presents the results of a "flutter" analysis for a PGM Motor Gunboat. The results were obtained both by computing the rudder-hull vibrations (including flutter) on an analog computer and by numerical analysis. The analogs are based upon extensions of previously derived theories and methods for representing the vibrating system excited by hydrodynamic forces and for evaluating the rudder-hull structural and hydroelastic parameters and hydrodynamic parameters referenced in this report.

The results indicate that (assuming a minimum conceivable value of damping) for the PGM rudder-hull system, control-surface flutter will occur at approximately 90 knots. Moreover, the flutter

1. Control surface-hull systems--Flutter--Theory
2. Control surface-hull systems--Vibration--Theory
3. Control surface-hull systems--Flutter--Analog computation
4. Control surface systems--Flutter--Analog and digital computation
5. Control surface systems--Vibration--Analog and digital computation
6. Control surface systems--Flutter--Analytical computations

David Taylor Model Basin. Report 1993.
RUDDER-HULL VIBRATION AND FLUTTER ANALYSIS OF A HIGH-SPEED SHIP (PGM MOTOR GUNBOAT), by Ralph C. Leibowitz. Oct 1965. xvi, 197p. illus., graphs, tables, refs.
UNCLASSIFIED

This report presents the results of a "flutter" analysis for a PGM Motor Gunboat. The results were obtained both by computing the rudder-hull vibrations (including flutter) on an analog computer and by numerical analysis. The analogs are based upon extensions of previously derived theories and methods for representing the vibrating system excited by hydrodynamic forces and for evaluating the rudder-hull structural and hydroelastic parameters and hydrodynamic parameters referenced in this report.

The results indicate that (assuming a minimum conceivable value of damping) for the PGM rudder-hull system, control-surface flutter will occur at approximately 90 knots. Moreover, the flutter

1. Control surface-hull systems--Flutter--Theory
2. Control surface-hull systems--Vibration--Theory
3. Control surface-hull systems--Flutter--Analog computation
4. Control surface systems--Flutter--Analog and digital computation
5. Control surface systems--Vibration--Analog and digital computation
6. Control surface systems--Flutter--Analytical computations

David Taylor Model Basin. Report 1993.
RUDDER-HULL VIBRATION AND FLUTTER ANALYSIS OF A HIGH-SPEED SHIP (PGM MOTOR GUNBOAT), by Ralph C. Leibowitz. Oct 1965. xvi, 197p. illus., graphs, tables, refs.
UNCLASSIFIED

This report presents the results of a "flutter" analysis for a PGM Motor Gunboat. The results were obtained both by computing the rudder-hull vibrations (including flutter) on an analog computer and by numerical analysis. The analogs are based upon extensions of previously derived theories and methods for representing the vibrating system excited by hydrodynamic forces and for evaluating the rudder-hull structural and hydroelastic parameters and hydrodynamic parameters referenced in this report.

The results indicate that (assuming a minimum conceivable value of damping) for the PGM rudder-hull system, control-surface flutter will occur at approximately 90 knots. Moreover, the flutter

1. Control surface-hull systems--Flutter--Theory
2. Control surface-hull systems--Vibration--Theory
3. Control surface-hull systems--Flutter--Analog computation
4. Control surface systems--Flutter--Analog and digital computation
5. Control surface systems--Vibration--Analog and digital computation
6. Control surface systems--Flutter--Analytical computations

David Taylor Model Basin. Report 1993.
RUDDER-HULL VIBRATION AND FLUTTER ANALYSIS OF A HIGH-SPEED SHIP (PGM MOTOR GUNBOAT), by Ralph C. Leibowitz. Oct 1965. xvi, 197p. illus., graphs, tables, refs.
UNCLASSIFIED

This report presents the results of a "flutter" analysis for a PGM Motor Gunboat. The results were obtained both by computing the rudder-hull vibrations (including flutter) on an analog computer and by numerical analysis. The analogs are based upon extensions of previously derived theories and methods for representing the vibrating system excited by hydrodynamic forces and for evaluating the rudder-hull structural and hydroelastic parameters and hydrodynamic parameters referenced in this report.

The results indicate that (assuming a minimum conceivable value of damping) for the PGM rudder-hull system, control-surface flutter will occur at approximately 90 knots. Moreover, the flutter

1. Control surface-hull systems--Flutter--Theory
2. Control surface-hull systems--Vibration--Theory
3. Control surface-hull systems--Flutter--Analog computation
4. Control surface systems--Flutter--Analog and digital computation
5. Control surface systems--Vibration--Analog and digital computation
6. Control surface systems--Flutter--Analytical computations

characteristics of the entire rudder-hull system are more complex than classical flutter of simpler systems involving two vibration modes; hence conclusions concerning the classical or binary flutter of a two- or three-degree-of-freedom rudder do not apply to the entire rudder-hull combination.

7. Control surface systems--Flutter--Hydroelastic parameters
8. Control surface systems--Flutter--Hydrodynamic forces
9. Control surface-hull systems--Vibration--Inertial-elastic parameters
10. PGM (U.S. Motor gunboat)
I. Leibowitz, Ralph C.

---

characteristics of the entire rudder-hull system are more complex than classical flutter of simpler systems involving two vibration modes; hence conclusions concerning the classical or binary flutter of a two- or three-degree-of-freedom rudder do not apply to the entire rudder-hull combination.

7. Control surface systems--Flutter--Hydroelastic parameters
8. Control surface systems--Flutter--Hydrodynamic forces
9. Control surface-hull systems--Vibration--Inertial-elastic parameters
10. PGM (U.S. Motor gunboat)
I. Leibowitz, Ralph C.

---

characteristics of the entire rudder-hull system are more complex than classical flutter of simpler systems involving two vibration modes; hence conclusions concerning the classical or binary flutter of a two- or three-degree-of-freedom rudder do not apply to the entire rudder-hull combination.

7. Control surface systems--Flutter--Hydroelastic parameters
8. Control surface systems--Flutter--Hydrodynamic forces
9. Control surface-hull systems--Vibration--Inertial-elastic parameters
10. PGM (U.S. Motor gunboat)
I. Leibowitz, Ralph C.

---

characteristics of the entire rudder-hull system are more complex than classical flutter of simpler systems involving two vibration modes; hence conclusions concerning the classical or binary flutter of a two- or three-degree-of-freedom rudder do not apply to the entire rudder-hull combination.

7. Control surface systems--Flutter--Hydroelastic parameters
8. Control surface systems--Flutter--Hydrodynamic forces
9. Control surface-hull systems--Vibration--Inertial-elastic parameters
10. PGM (U.S. Motor gunboat)
I. Leibowitz, Ralph C.

David Taylor Model Basin. Report 1993.
RUDDER-HULL VIBRATION AND FLUTTER ANALYSIS OF A HIGH-SPEED SHIP (PGM MOTOR GUNBOAT), by Ralph C. Leibowitz. Oct 1965. xvi, 197p. illus., graphs, tables, refs.
UNCLASSIFIED

This report presents the results of a "flutter" analysis for a PGM Motor Gunboat. The results were obtained both by computing the rudder-hull vibrations (including flutter) on an analog computer and by numerical analysis. The analogs are based upon extensions of previously derived theories and methods for representing the vibrating system excited by hydrodynamic forces and for evaluating the rudder-hull structural and hydroelastic parameters and hydrodynamic parameters referenced in this report.

The results indicate that (assuming a minimum conceivable value of damping) for the PGM rudder-hull system, control-surface flutter will occur at approximately 90 knots. Moreover, the flutter

1. Control surface-hull systems--Flutter--Theory
2. Control surface-hull systems--Vibration--Theory
3. Control surface-hull systems--Flutter--Analog computation
4. Control surface systems--Flutter--Analog and digital computation
5. Control surface systems--Vibration--Analog and digital computation
6. Control surface systems--Flutter--Analytical computations

David Taylor Model Basin. Report 1993.
RUDDER-HULL VIBRATION AND FLUTTER ANALYSIS OF A HIGH-SPEED SHIP (PGM MOTOR GUNBOAT), by Ralph C. Leibowitz. Oct 1965. xvi, 197p. illus., graphs, tables, refs.
UNCLASSIFIED

This report presents the results of a "flutter" analysis for a PGM Motor Gunboat. The results were obtained both by computing the rudder-hull vibrations (including flutter) on an analog computer and by numerical analysis. The analogs are based upon extensions of previously derived theories and methods for representing the vibrating system excited by hydrodynamic forces and for evaluating the rudder-hull structural and hydroelastic parameters and hydrodynamic parameters referenced in this report.

The results indicate that (assuming a minimum conceivable value of damping) for the PGM rudder-hull system, control-surface flutter will occur at approximately 90 knots. Moreover, the flutter

1. Control surface-hull systems--Flutter--Theory
2. Control surface-hull systems--Vibration--Theory
3. Control surface-hull systems--Flutter--Analog computation
4. Control surface systems--Flutter--Analog and digital computation
5. Control surface systems--Vibration--Analog and digital computation
6. Control surface systems--Flutter--Analytical computations

David Taylor Model Basin. Report 1993.
RUDDER-HULL VIBRATION AND FLUTTER ANALYSIS OF A HIGH-SPEED SHIP (PGM MOTOR GUNBOAT), by Ralph C. Leibowitz. Oct 1965. xvi, 197p. illus., graphs, tables, refs.
UNCLASSIFIED

This report presents the results of a "flutter" analysis for a PGM Motor Gunboat. The results were obtained both by computing the rudder-hull vibrations (including flutter) on an analog computer and by numerical analysis. The analogs are based upon extensions of previously derived theories and methods for representing the vibrating system excited by hydrodynamic forces and for evaluating the rudder-hull structural and hydroelastic parameters and hydrodynamic parameters referenced in this report.

The results indicate that (assuming a minimum conceivable value of damping) for the PGM rudder-hull system, control-surface flutter will occur at approximately 90 knots. Moreover, the flutter

1. Control surface-hull systems--Flutter--Theory
2. Control surface-hull systems--Vibration--Theory
3. Control surface-hull systems--Flutter--Analog computation
4. Control surface systems--Flutter--Analog and digital computation
5. Control surface systems--Vibration--Analog and digital computation
6. Control surface systems--Flutter--Analytical computations

David Taylor Model Basin. Report 1993.
RUDDER-HULL VIBRATION AND FLUTTER ANALYSIS OF A HIGH-SPEED SHIP (PGM MOTOR GUNBOAT), by Ralph C. Leibowitz. Oct 1965. xvi, 197p. illus., graphs, tables, refs.
UNCLASSIFIED

This report presents the results of a "flutter" analysis for a PGM Motor Gunboat. The results were obtained both by computing the rudder-hull vibrations (including flutter) on an analog computer and by numerical analysis. The analogs are based upon extensions of previously derived theories and methods for representing the vibrating system excited by hydrodynamic forces and for evaluating the rudder-hull structural and hydroelastic parameters and hydrodynamic parameters referenced in this report.

The results indicate that (assuming a minimum conceivable value of damping) for the PGM rudder-hull system, control-surface flutter will occur at approximately 90 knots. Moreover, the flutter

1. Control surface-hull systems--Flutter--Theory
2. Control surface-hull systems--Vibration--Theory
3. Control surface-hull systems--Flutter--Analog computation
4. Control surface systems--Flutter--Analog and digital computation
5. Control surface systems--Vibration--Analog and digital computation
6. Control surface systems--Flutter--Analytical computations

characteristics of the entire rudder-hull system are more complex than classical flutter of simpler systems involving two vibration modes; hence conclusions concerning the classical or binary flutter of a two- or three-degree-of-freedom rudder do not apply to the entire rudder-hull combination.

7. Control surface systems--Flutter--Hydroelastic parameters
8. Control surface systems--Flutter--Hydrodynamic forces
9. Control surface-hull systems--Vibration--Inertial-elastic parameters
10. PGM (U.S. Motor gunboat)
I. Leibowitz, Ralph C.

characteristics of the entire rudder-hull system are more complex than classical flutter of simpler systems involving two vibration modes; hence conclusions concerning the classical or binary flutter of a two- or three-degree-of-freedom rudder do not apply to the entire rudder-hull combination.

7. Control surface systems--Flutter--Hydroelastic parameters
8. Control surface systems--Flutter--Hydrodynamic forces
9. Control surface-hull systems--Vibration--Inertial-elastic parameters
10. PGM (U.S. Motor gunboat)
I. Leibowitz, Ralph C.

characteristics of the entire rudder-hull system are more complex than classical flutter of simpler systems involving two vibration modes; hence conclusions concerning the classical or binary flutter of a two- or three-degree-of-freedom rudder do not apply to the entire rudder-hull combination.

7. Control surface systems--Flutter--Hydroelastic parameters
8. Control surface systems--Flutter--Hydrodynamic forces
9. Control surface-hull systems--Vibration--Inertial-elastic parameters
10. PGM (U.S. Motor gunboat)
I. Leibowitz, Ralph C.

characteristics of the entire rudder-hull system are more complex than classical flutter of simpler systems involving two vibration modes; hence conclusions concerning the classical or binary flutter of a two- or three-degree-of-freedom rudder do not apply to the entire rudder-hull combination.

7. Control surface systems--Flutter--Hydroelastic parameters
8. Control surface systems--Flutter--Hydrodynamic forces
9. Control surface-hull systems--Vibration--Inertial-elastic parameters
10. PGM (U.S. Motor gunboat)
I. Leibowitz, Ralph C.